

SYNTHESIS AND STRUCTURAL CHARACTERIZATION OF
(μ -OXIDO)DIIRON(III)TRIS(2-PYRIDYLMETHYL)AMINE COMPLEXES

A Thesis

Presented to

The Faculty of the Department of Chemistry

Sam Houston State University

In Partial Fulfillment

of the Requirements for the Degree of

Master of Science

by

Codithuwakku Arachchige Upeksha Kawshalya Kumarihami

August, 2022

SYNTHESIS AND STRUCTURAL CHARACTERIZATION OF
(μ -OXIDO)DIIRON(III)TRIS(2-PYRIDYLMETHYL)AMINE COMPLEXES

by

Codithuwakku Arachchige Upeksha Kawshalya Kumarihami

APPROVED:

Dr. Richard E. Norman
Thesis Director

Dr. David E. Thompson
Committee member

Dr. Christopher Zall
Committee Member

Dr. John B. Pascarella
Dean, College of Science and Engineering
Technology

ABSTRACT

Kumariahmi, Codithuwakku Arachchige Upeskha Kawshalya, *Synthesis and structural characterization of (μ -oxido)diiron(III)(tris(2-pyridylmethyl)amine) complexes.* Master of Science (Chemistry), August, 2022, Sam Houston State University, Huntsville, Texas.

Oxido-bridged $[Fe_2(TPA)_2OL]^{3+}$ complexes were synthesized using the tetradeятate ligand TPA (tris(2-pyridylmethyl)amine) (L is defined below) and $[\{Fe(TPA)Br\}_2O]^{2+}$. All structural data were collected at 25 °C. All but one are monoclinic. The anions are perchlorates.

L = OAc•H₂O polymorph 1: P2₁/c with a = 10.532(7) Å, b = 22.572(15) Å, c = 20.758(15) Å, β = 104.711(7)°, V = 4772.8(6) Å³. The structure was determined from 13844 out of a total 39507 reflections with R = 7.76%.

L = OAc•H₂O polymorph 2: P2₁/n with a = 10.601(4) Å, b = 22.529(8) Å, c = 20.923(8) Å, β = 104.192(4)°, V = 4844.3(3) Å³. The structure was determined from 9008 out of a total 24212 reflections with R = 7.25%.

L = 4-hydroxybenzoate: P2₁/c with a = 14.451(6) Å, b = 16.760(7) Å, c = 20.594(7) Å, β = 101.824(4)°, V = 4882.1(3) Å³. The structure was determined from 8582 out of a total 18536 reflections with R = 5.06%.

L = 4-methoxybenzoate: P2₁/c with a = 14.347(9) Å, b = 17.163(13) Å, c = 20.328(11) Å, β = 100.781(6)°, V = 4917.0(6) Å³. The structure was determined from 10168 out of a total of 19784 reflections with R = 6.08%.

L = 4-fluorobenzoate: P2₁/c with a = 14.399(9) Å, b = 17.186(11) Å, c = 20.108(10) Å, β = 101.877(5)°, V = 4869.1(5) Å³. The structure was determined from 10056 out of a total of 21571 reflections with R = 4.50%.

L = 3,5-dihydroxybenzoate•CH₃CN: P2₁/n with a = 13.1877(11) Å, b = 22.2892(12) Å, c = 19.7183(13) Å, β = 95.193(7)°, V = 5772.3(7) Å³. The structure was determined from 9021 out of a total of 18889 reflections with R = 8.34%.

L = 3,5-dimethylbenzoate•0.5H₂O: P-1 with a = 13.362(6) Å, b = 19.053(8) Å, c = 22.057(9) Å and α = 89.650(3)°, β = 74.093(4)°, γ = 84.094(3)°, V = 5370.3(4) Å³. The structure was determined from 19142 out of a total of 30995 reflections with R = 5.30%.

[{Fe(TPA)Br}₂O](ClO₄)₂•H₂O : C2/c with a = 16.148(17) Å, b = 17.204(13) Å, c = 16.852(12) Å, β = 111.204(10)°, V = 4364.6(7) Å³. The structure was determined from 3753 out of a total of 6891 reflections with R = 6.93%.

KEY WORDS: Tris(2-pyridylmethyl)amine, Diiron(III) complexes.

ACKNOWLEDGEMENTS

It is a genuine pleasure to express my deep and sincere gratitude to my mentor, and guide, Dr. Richard E Norman, thesis director, Department of Chemistry, Sam Houston State University. His dedication and patience, and above all, the overwhelming attitude to help his students, has been mainly responsible for me completing my work. His timely advice, meticulous scrutiny, scholarly advice and scientific approach have helped me to a very great extent to accomplish this task. I cannot have imagined having a better advisor and a mentor for my Master's thesis.

I owe a deep sense of gratitude to Dr. Kit Zall, Department of Chemistry, Sam Houston State University for serving on my thesis committee as well as his timely support with my X-ray crystallographic studies. Without his support in X-ray crystallography, things would have been much more difficult.

I profusely thank Dr. David Thompson for serving on my thesis committee and his support in UV-vis spectroscopy studies.

It is my privilege to thank the Department of Chemistry, Sam Houston State University for letting me to start my Master's degree journey with the University. I also thank them for the financial support and research facilities I have used.

Last, but not least, I would like to thank my wonderful family: my parents, my two sisters and my brother for their love and supporting me spiritually throughout my life.

TABLE OF CONTENTS

	Page
ABSTRACT.....	iii
ACKNOWLEDGEMENTS	v
TABLE OF CONTENTS.....	vi
LIST OF TABLES	vii
LIST OF FIGURES	xii
CHAPTER I: INTRODUCTION	1
CHAPTER II: EXPERIMENTAL.....	14
2.1 Materials	14
2.2 Instrumental	14
2.3 Synthesis.....	15
CHAPTER III: RESULTS	33
3.1 Electronic Spectroscopic Results	33
3.2 ^1H NMR Spectroscopic Results	50
3.3 X-ray Crystallographic Results	67
CHAPTER IV: DISCUSSION	221
4.1 Syntheses Discussion	221
4.2 ^1H NMR Spectroscopy Discussion.....	223
4.3 Electronic Spectroscopy Discussion	229
4.4 X-ray Crystallography Discussion	238
REFERENCES	273
VITA	281

LIST OF TABLES

Table	Page
1 Absorption bands of oxido-bridged diiron(III) complexes	48
2 ^1H NMR chemical shift values assignment of TPA•3HClO ₄ in D ₂ O	51
3 ^1H NMR parameters (ppm) for the studied oxo-bridged diiron complexes	65
4 Crystallographic data for [{Fe(TPA)Br} ₂ O](ClO ₄) ₂ •H ₂ O	73
5 Fractional atomic coordinates ($\times 10^4$) and equivalent isotropic displacement parameters ($\text{\AA}^2 \times 10^3$) for [{Fe(TPA)Br} ₂ O](ClO ₄) ₂ •H ₂ O	74
6 Anisotropic displacement parameters ($\text{\AA}^2 \times 10^3$) for [{Fe(TPA)Br} ₂ O](ClO ₄) ₂ •H ₂ O	75
7 Bond lengths for [{Fe(TPA)Br} ₂ O](ClO ₄) ₂ •H ₂ O	77
8 Bond angles for [{Fe(TPA)Br} ₂ O](ClO ₄) ₂ •H ₂ O	78
9 Hydrogen atom coordinates ($\text{\AA} \times 10^4$) and isotropic displacement parameters ($\text{\AA}^2 \times 10^3$) for [{Fe(TPA)Br} ₂ O](ClO ₄) ₂ •H ₂ O	79
10 Partial atomic occupancy for [{Fe(TPA)Br} ₂ O](ClO ₄) ₂ •H ₂ O	80
11 Crystallographic data for [{Fe(TPA)} ₂ O(OAc)](ClO ₄) ₃ •H ₂ O P2 ₁ /c polymorph.	85
12 Fractional atomic coordinates ($\times 10^4$) and equivalent isotropic displacement parameters ($\text{\AA}^2 \times 10^3$) for [{Fe(TPA)} ₂ O(OAc)](ClO ₄) ₃ •H ₂ O P2 ₁ /c polymorph ..	86
13 Anisotropic displacement parameters ($\text{\AA}^2 \times 10^3$) for [{Fe(TPA)} ₂ O(OAc)](ClO ₄) ₃ •H ₂ O P2 ₁ /c polymorph ..	89
14 Bond lengths for [{Fe(TPA)} ₂ O(OAc)](ClO ₄) ₃ •H ₂ O P2 ₁ /c polymorph ..	91
15 Bond angles for [{Fe(TPA)} ₂ O(OAc)](ClO ₄) ₃ •H ₂ O P2 ₁ /c polymorph ..	93

16 Hydrogen atom coordinates ($\text{\AA} \times 10^4$) and isotropic displacement parameters ($\text{\AA}^2 \times 10^3$) for $[\{\text{Fe}(TPA)\}_2\text{O(OAc)}](\text{ClO}_4)_3 \cdot \text{H}_2\text{O}$ P2 ₁ /c polymorph.....	95
17 Crystallographic data for $[\{\text{Fe}(TPA)\}_2\text{O(OAc)}](\text{ClO}_4)_3 \cdot \text{H}_2\text{O}$ P2 ₁ /n polymorph	101
18 Fractional atomic coordinates ($\times 10^4$) and equivalent isotropic displacement parameters ($\text{\AA}^2 \times 10^3$) for $[\{\text{Fe}(TPA)\}_2\text{O(OAc)}](\text{ClO}_4)_3 \cdot \text{H}_2\text{O}$ P2 ₁ /n polymorph	102
19 Anisotropic displacement parameters ($\text{\AA}^2 \times 10^3$) for $[\{\text{Fe}(TPA)\}_2\text{O(OAc)}]$ $(\text{ClO}_4)_3 \cdot \text{H}_2\text{O}$ P2 ₁ /n polymorph.....	105
20 Bond lengths for $[\{\text{Fe}(TPA)\}_2\text{O(OAc)}](\text{ClO}_4)_3 \cdot \text{H}_2\text{O}$ P2 ₁ /n polymorph.....	108
21 Bond angles for $[\{\text{Fe}(TPA)\}_2\text{O(OAc)}](\text{ClO}_4)_3 \cdot \text{H}_2\text{O}$ P2 ₁ /n polymorph	110
22 Hydrogen atom coordinates ($\text{\AA} \times 10^4$) and isotropic displacement parameters ($\text{\AA}^2 \times 10^3$) for $[\{\text{Fe}(TPA)\}_2\text{O(OAc)}](\text{ClO}_4)_3 \cdot \text{H}_2\text{O}$ P2 ₁ /polymorph	113
23 Partial atomic occupancy for $[\{\text{Fe}(TPA)\}_2\text{O(OAc)}](\text{ClO}_4)_3 \cdot \text{H}_2\text{O}$ P2 ₁ /n polymorph.....	114
24 Crystallographic data for $[\{\text{Fe}(TPA)\}_2\text{O(4-hydroxybenzoato)}](\text{ClO}_4)_3$	119
25 Fractional atomic coordinates ($\times 10^4$) and equivalent isotropic displacement parameters ($\text{\AA}^2 \times 10^3$) for $[\{\text{Fe}(TPA)\}_2\text{O(4-hydroxybenzoato)}](\text{ClO}_4)_3$	120
26 Anisotropic displacement parameters ($\text{\AA}^2 \times 10^3$) for $[\{\text{Fe}(TPA)\}_2\text{O(4-hydroxy-}$ $\text{benzoato)}](\text{ClO}_4)_3$	123
27 Bond lengths for $[\{\text{Fe}(TPA)\}_2\text{O(4-hydroxybenzoato)}](\text{ClO}_4)_3$	126
28 Bond angles for $[\{\text{Fe}(TPA)\}_2\text{O(4-hydroxybenzoato)}](\text{ClO}_4)_3$	128
29 Hydrogen atom coordinates ($\text{\AA} \times 10^4$) and isotropic displacement parameters ($\text{\AA}^2 \times 10^3$) for $[\{\text{Fe}(TPA)\}_2\text{O(4-hydroxybenzoato)}](\text{ClO}_4)_3$	131

30 Partial atomic occupancy for [{Fe(TPA)} ₂ O(4-hydroxybenzoato)](ClO ₄) ₃	132
31 Crystallographic data for [{Fe (TPA)} ₂ O(4-methoxybenzoato)](ClO ₄) ₃	137
32 Fractional atomic coordinates ($\times 10^4$) and equivalent Isotropic displacement parameters ($\text{\AA}^2 \times 10^3$) for [{Fe(TPA)} ₂ O(4-methoxybenzoato)](ClO ₄) ₃	138
33 Anisotropic displacement parameters ($\text{\AA}^2 \times 10^3$) for [{Fe(TPA)} ₂ O(4-methoxy- benzoato)](ClO ₄) ₃	141
34 Bond lengths for [{Fe(TPA)} ₂ O(4-methoxybenzoato)](ClO ₄) ₃	145
35 Bond angles for [{Fe(TPA)} ₂ O(4-methoxybenzoato)](ClO ₄) ₃	147
36 Hydrogen atom coordinates ($\text{\AA} \times 10^4$) and isotropic displacement parameters ($\text{\AA}^2 \times 10^3$) for [{Fe(TPA)} ₂ O(4-methoxybenzoato)](ClO ₄) ₃	150
37 Partial atomic occupancy for [{Fe(TPA)} ₂ O(4-methoxybenzoato)](ClO ₄) ₃	152
38 Crystallographic data for [{Fe (TPA)} ₂ O(4-fluorobenzoato)](ClO ₄) ₃	157
39 Fractional atomic coordinates ($\times 10^4$) and equivalent isotropic displacement parameters ($\text{\AA}^2 \times 10^3$) for [{Fe(TPA)} ₂ O(4-fluorobenzoato)](ClO ₄) ₃	158
40 Anisotropic displacement parameters ($\text{\AA}^2 \times 10^3$) for [{Fe(TPA)} ₂ O(4-fluoro- benzoato)](ClO ₄) ₃	161
41 Bond lengths for [{Fe(TPA)} ₂ O(4-fluorobenzoato)](ClO ₄) ₃	164
42 Bond angles for [{Fe(TPA)} ₂ O(4-fluorobenzoato)](ClO ₄) ₃	166
43 Hydrogen atom coordinates ($\text{\AA} \times 10^4$) and isotropic displacement parameters ($\text{\AA}^2 \times 10^3$) for [{Fe(TPA)} ₂ O(4-fluorobenzoato)](ClO ₄) ₃	169
44 Partial atomic occupancy for [{Fe(TPA)} ₂ O(4-fluorobenzoato)](ClO ₄) ₃	171
45 Crystallographic data for [Fe(TPA) ₂ O(3,5-dimethylbenzoato)](ClO ₄) ₃ • 0.5H ₂ O	175

46 Fractional atomic coordinates ($\times 10^4$) and equivalent isotropic displacement parameters ($\text{\AA}^2 \times 10^3$) for [Fe(TPA) ₂ O(3,5-dimethylbenzoato)](ClO ₄) ₃ •0.5H ₂ O.	176
47 Anisotropic displacement parameters ($\text{\AA}^2 \times 10^3$) for [Fe(TPA) ₂ O(3,5-dimethylbenzoato)](ClO ₄) ₃ •0.5H ₂ O.....	182
48 Bond lengths for [Fe(TPA) ₂ O(3,5-dimethylbenzoato)](ClO ₄) ₃ •0.5H ₂ O.	188
49 Bond angles for [Fe(TPA) ₂ O(3,5-dimethylbenzoato)](ClO ₄) ₃ •0.5H ₂ O.....	191
50 Hydrogen atom coordinates ($\text{\AA} \times 10^4$) and isotropic displacement parameters ($\text{\AA}^2 \times 10^3$) for [Fe(TPA) ₂ O(3,5-dimethylbenzoato)](ClO ₄) ₃ •0.5H ₂ O.....	197
51 Partial atomic occupancy for [Fe(TPA) ₂ O(3,5-dimethylbenzoato)](ClO ₄) ₃ •0.5H ₂ O.....	201
52 Crystallographic data for [{Fe(TPA)} ₂ O(3,5-dihydroxybenzoato)](ClO ₄) ₃ •CH ₃ CN.....	206
53 Fractional atomic coordinates ($\times 10^4$) and equivalent isotropic displacement parameters ($\text{\AA}^2 \times 10^3$) for [{Fe(TPA)} ₂ O(3,5-dihydroxybenzoato)](ClO ₄) ₃ •CH ₃ CN.....	207
54 Anisotropic displacement parameters ($\text{\AA}^2 \times 10^3$) for [{Fe(TPA)} ₂ O(3,5-dihydroxybenzoato)](ClO ₄) ₃ •CH ₃ CN.....	210
55 Bond lengths for [{Fe(TPA)} ₂ O(3,5-dihydroxybenzoato)](ClO ₄) ₃ •CH ₃ CN....	213
56 Bond angles for [{Fe(TPA)} ₂ O(3,5-dihydroxybenzoato)](ClO ₄) ₃ •CH ₃ CN....	215
57 Hydrogen atom coordinates ($\text{\AA} \times 10^4$) and isotropic displacement parameters ($\text{\AA}^2 \times 10^3$) for [{Fe(TPA)} ₂ O(3,5-dihydroxybenzoato)]ClO ₄) ₃ •CH ₃ CN.....	218

58 Partial atomic occupancy for [{Fe(TPA)} ₂ O(3,5-dihydroxybenzoato)] (ClO ₄) ₃ ·CH ₃ CN.....	220
59 Comparison and assignments of ¹ H NMR chemical shifts for symmetric (μ -oxido)diiron(III)TPA	225
60 Comparison and assignment of ¹ H NMR chemical shifts for bent oxido-bridged dinuclear complexes.	227
61 Comparison of the absorption bands of the oxido-bridged diiron complexes with some previously reported complexes.....	233
62 Comparison of Fe-O-Fe angle vs 490 nm feature.....	236
63 Comparison of relevant distances and angles of some symmetrical oxido-bridged dinuclear Fe(III)-TPA and the mononuclear [Fe(TPA)Br ₂] ⁺	242
64 Comparison of pertinent bond distances and angles of (μ -oxido)(μ -carboxylato)diiron(III)TPA complexes.	246
65 Comparison of pertinent bond distances and angles of previously studied (μ -oxido)(μ -carboxylato)diiron(III)TPA complexes along with linear (μ -oxido)(4-nitrobenzoate) ₂ diiron(III)TPA complex.	247
66 The comparison of (μ -oxido)(μ -OAc)diiron(III)TPA polymorphs with previous acetate bridged diiron(III) complexes.....	256
67 Comparison of Fe-pyridine bonds for asymmetric Fe(III)-TPA complexes.	262
68 Bond lengths (Å), bond angles (°) of (μ -oxido)(μ -carboxylato)diiron(III)TPA complexes and pK _a of the acid form of the bridging carboxylates.	263
69 Bond lengths and bond angles of relevant (μ -oxido)diiron(III)TPA complexes and pK _a of the acid form of the bridging carboxylates.	264

LIST OF FIGURES

Figure	Page
1 Pervasive Fe-S motifs in biology.....	3
2 The proposed oxygen activation mechanism of MMO.....	6
3 Common tridentate ligands used in synthesis of (μ -oxo)bis(μ -carboxylato) diiron complexes.....	9
4 Tris(2-pyridylmethyl)amine.....	10
5 UV-Visible spectrum of TPA•3HClO ₄	34
6 Electronic spectrum of [{Fe(TPA)Br ₂ O}(ClO ₄) ₂ •H ₂ O (Concentrated).....	35
7 Electronic spectrum of [{Fe(TPA)Br ₂ O}(ClO ₄) ₂ •H ₂ O (Diluted).....	35
8 Electronic spectrum of [Fe ₂ (TPA) ₂ O(OAc)](ClO ₄) ₃ (Concentrated).	36
9 Electronic spectrum of [Fe ₂ (TPA) ₂ O(OAc)](ClO ₄) ₃ (Diluted).....	36
10 Electronic spectrum of [Fe ₂ (TPA) ₂ O(OAc)](ClO ₄) ₃ •H ₂ O (Concentrated).	37
11 Electronic spectrum of [Fe ₂ (TPA) ₂ O(OAc)](ClO ₄) ₃ •H ₂ O (Diluted).	37
12 Electronic spectrum of [Fe ₂ (TPA) ₂ O(4-hydroxybenzoato)](ClO ₄) ₃ (Concentrated).....	38
13 Electronic spectrum of [Fe ₂ (TPA) ₂ O(4-hydroxybenzoato)](ClO ₄) ₃ (Diluted).	38
14 Electronic spectrum of [Fe ₂ (TPA) ₂ O(4-methoxybenzoato)](ClO ₄) ₃ (Concentrated).....	39
15 Electronic spectrum of [Fe ₂ (TPA) ₂ O(4-methoxybenzoato)](ClO ₄) ₃ (Diluted)....	39
16 Electronic spectrum of [Fe ₂ (TPA) ₂ O(4-fluorobenzoato)](ClO ₄) ₃ (Concentrated).....	40
17 Electronic spectrum of [Fe ₂ (TPA) ₂ O(4-fluorobenzoato)](ClO ₄) ₃ (Diluted).....	40

18 Electronic spectrum of $[\text{Fe}_2(\text{TPA})_2\text{O}(4\text{-cyanobenzoato})](\text{ClO}_4)_3$ (Concentrated).....	41
19 Electronic spectrum of $[\text{Fe}_2(\text{TPA})_2\text{O}(4\text{-cyanobenzoato})](\text{ClO}_4)_3$ (Diluted).	41
20 Electronic spectrum of $[\text{Fe}_2(\text{TPA})_2\text{O}(3,5\text{-dimethylbenzoato})](\text{ClO}_4)_3 \bullet 0.5\text{H}_2\text{O}$ (Concentrated).....	42
21 Electronic spectrum of $[\text{Fe}_2(\text{TPA})_2\text{O}(3,5\text{-dimethylbenzoato})](\text{ClO}_4)_3 \bullet 0.5\text{H}_2\text{O}$ (Diluted).....	42
22 Electronic spectrum of $[\text{Fe}_2(\text{TPA})_2\text{O}(3,5\text{-dihydroxybenzoato})](\text{ClO}_4)_3$ $\bullet \text{CH}_3\text{CN}$ (Concentrated).....	43
23 Electronic spectrum of $[\text{Fe}_2(\text{TPA})_2\text{O}(3,5\text{-dihydroxybenzoato})](\text{ClO}_4)_3$ $\bullet \text{CH}_3\text{CN}$ (Diluted).....	43
24 Electronic spectrum of $[\text{Fe}_2(\text{TPA})_2\text{O}(3,5\text{-dimethoxybenzoato})](\text{ClO}_4)_3$ (Concentrated).....	44
25 Electronic spectrum of $[\text{Fe}_2(\text{TPA})_2\text{O}(3,5\text{-dimethoxybenzoato})](\text{ClO}_4)_3$ (Diluted).....	44
26 Electronic spectrum of $[\text{Fe}_2(\text{TPA})_2\text{O}(3,5\text{-dichlorobenzoato})](\text{ClO}_4)_3$ (Concentrated).....	45
27 Electronic spectrum of $[\text{Fe}_2(\text{TPA})_2\text{O}(3,5\text{-dichlorobenzoato})](\text{ClO}_4)_3$ (Diluted).....	45
28 Electronic spectrum of $[\text{Fe}_2(\text{TPA})_2\text{O}(3,5\text{-dibromobenzoato})](\text{ClO}_4)_3$ (Concentrated).....	46
29 Electronic spectrum of $[\text{Fe}_2(\text{TPA})_2\text{O}(3,5\text{-dibromobenzoato})](\text{ClO}_4)_3$ (Diluted).....	46

30 Electronic spectrum of $[\text{Fe}_2(\text{TPA})_2\text{O}(3,5\text{-dinitrobenzoato})](\text{ClO}_4)_3$ (Concentrated).....	47
31 Electronic spectrum of $[\text{Fe}_2(\text{TPA})_2\text{O}(3,5\text{-dinitrobenzoato})](\text{ClO}_4)_3$ (Diluted)....	47
32 ^1H NMR spectrum of $\text{TPA}\bullet 3\text{HClO}_4$	51
33 ^1H NMR spectrum of $[\{\text{Fe}(\text{TPA})\text{Br}_2\text{O}\}(\text{ClO}_4)_2\bullet \text{H}_2\text{O}$	52
34 ^1H NMR spectrum of $[\text{Fe}_2(\text{TPA})_2\text{O}(\text{OAc})](\text{ClO}_4)_3$	53
35 ^1H NMR spectrum of $[\text{Fe}_2(\text{TPA})_2\text{O}(\text{OAc})](\text{ClO}_4)_3\bullet \text{H}_2\text{O}$	54
36 ^1H NMR spectrum of $[\text{Fe}_2(\text{TPA})_2\text{O}(4\text{-hydroxybenzoato})](\text{ClO}_4)_3$	55
37 ^1H NMR spectrum of $[\text{Fe}_2(\text{TPA})_2\text{O}(4\text{-methoxybenzoato})](\text{ClO}_4)_3$	56
38 ^1H NMR spectrum of $[\text{Fe}_2(\text{TPA})_2\text{O}(4\text{-fluorobenzoato})](\text{ClO}_4)_3$	57
39 ^1H NMR spectrum of $[\text{Fe}_2(\text{TPA})_2\text{O}(4\text{-cyanobenzoato})](\text{ClO}_4)_3$	58
40 ^1H NMR spectrum of $[\text{Fe}_2(\text{TPA})_2\text{O}(3,5\text{-dimethylbenzoato})](\text{ClO}_4)_3\bullet 0.5\text{H}_2\text{O}$	59
41 ^1H NMR spectrum of $[\text{Fe}_2(\text{TPA})_2\text{O}(3,5\text{-dihydroxybenzoato})](\text{ClO}_4)_3\bullet \text{CH}_3\text{CN}$..	60
42 ^1H NMR spectrum of $[\text{Fe}_2(\text{TPA})_2\text{O}(3,5\text{-dimethoxybenzoato})](\text{ClO}_4)_3$	61
43 ^1H NMR spectrum of $[\text{Fe}_2(\text{TPA})_2\text{O}(3,5\text{-dichlorobenzoato})](\text{ClO}_4)_3$	62
44 ^1H NMR spectrum of $[\text{Fe}_2(\text{TPA})_2\text{O}(3,5\text{-dibromobenzoato})](\text{ClO}_4)_3$	63
45 ^1H NMR spectrum of $[\text{Fe}_2(\text{TPA})_2\text{O}(3,5\text{-dinitrobenzoato})](\text{ClO}_4)_3$	64
46 Numbering scheme for TPA in $[\{\text{Fe}(\text{TPA})\text{Br}\}_2\text{O}](\text{ClO}_4)_2\bullet \text{H}_2\text{O}$	67
47 Numbering scheme for TPA bound to Fe1 in carboxylato-bridged complexes. ..	68
48 Numbering scheme for TPA bound to Fe2 in carboxylato-bridged complexes. ..	69
49 A view of the asymmetric unit of $[\{\text{Fe}(\text{TPA})\text{Br}\}_2\text{O}](\text{ClO}_4)_2\bullet \text{H}_2\text{O}$	71
50 A view of the cationic portion of $[\{\text{Fe}(\text{TPA})\text{Br}\}_2\text{O}](\text{ClO}_4)_2\bullet \text{H}_2\text{O}$. Hydrogen atoms are omitted.....	72

51 A view of the asymmetric unit of [{Fe(TPA)} ₂ O(OAc)](ClO ₄) ₃ •H ₂ O P2 ₁ /c polymorph.....	83
52 A view of the cationic portion of [{Fe(TPA)} ₂ O(OAc)](ClO ₄) ₃ •H ₂ O P2 ₁ /c polymorph. Hydrogen atoms are omitted.	84
53 A view of the asymmetric unit of [{Fe(TPA)} ₂ O(OAc)](ClO ₄) ₃ •H ₂ O P2 ₁ /n polymorph.....	99
54 A view of the cationic portion of [{Fe(TPA)} ₂ O(OAc)](ClO ₄) ₃ •H ₂ O P2 ₁ /n polymorph. Hydrogen atoms are omitted.	100
55 A view of the asymmetric unit of [{Fe(TPA)} ₂ O(4-hydroxybenzoato)](ClO ₄) ₃	116
56 A view of the cationic portion of [{Fe(TPA)} ₂ O(4-hydroxybenzoato)](ClO ₄) ₃ . Hydrogen atoms are omitted.	117
57 Numbering scheme for 4-hydroxybenzoate.....	118
58 A view of the asymmetric unit of [{Fe (TPA)} ₂ O(4-methoxybenzoato)](ClO ₄) ₃	134
59 A view of the cationic portion of [{Fe (TPA)} ₂ O(4-methoxybenzoato)](ClO ₄) ₃ . Hydrogen atoms are omitted.	135
60 Numbering scheme for 4-methoxybenzoate.	136
61 A view of the asymmetric unit of [{Fe (TPA)} ₂ O(4-fluorobenzoato)](ClO ₄) ₃ ..	154
62 A view of the cationic portion of [{Fe (TPA)} ₂ O(4-fluorobenzoato)](ClO ₄) ₃ . Hydrogen atoms are omitted.	155
63 Numbering scheme for 4-fluorobenzoate.	156

64 A view of the asymmetric unit of [Fe (TPA) ₂ O(3,5-dimethylbenzoato)] (ClO ₄) ₃ •0.5H ₂ O.....	172
65 A view of the cationic portion of [Fe ₂ (TPA) ₂ O(3,5-dimethylbenzoato)] (ClO ₄) ₃ •0.5H ₂ O. Hydrogen atoms are omitted.	173
66 Numbering scheme for 3,5-dimethylbenzoate.....	174
67 A view of the asymmetric unit of [{Fe(TPA)} ₂ O(3,5-dihydroxybenzoato)] (ClO ₄) ₃ •CH ₃ CN.....	203
68 A view of the cationic portion of [{Fe(TPA)} ₂ O(3,5-dihydroxybenzoato)] (ClO ₄) ₃ •CH ₃ CN. Hydrogen atoms are omitted.	204
69 Numbering scheme for dihydroxybenzoate.	205
70 Different environment of 3,5-H's in symmetric TPA orientation.	226
71 Near-UV features for para substituted-benzoate ligands.	235
72 Near-UV features for meta disubstituted-benzoate ligands.....	235
73 Graph of Fe-O-Fe bond angle vs 490 nm feature.	237
74 A view of the asymmetric unit of [{Fe(TPA)Br} ₂ O](ClO ₄) ₂ •H ₂ O.....	239
75 A view of the cationic portion of [{Fe(TPA)Br} ₂ O](ClO ₄) ₂ •H ₂ O. Hydrogen atoms are omitted.	240
76 A view of the cationic portion of [{Fe(TPA)} ₂ O(OAc)](ClO ₄) ₃ •H ₂ O P2 ₁ /c polymorph. Hydrogen atoms are omitted.	249
77 A view of the cationic portion of [{Fe(TPA)} ₂ O(OAc)](ClO ₄) ₃ •H ₂ O P2 ₁ /n polymorph. Hydrogen atoms are omitted.	250
78 A view of the cationic portion of [{Fe(TPA)} ₂ O(4-hydroxybenzoato)] (ClO ₄) ₃ . Hydrogen atoms are omitted.	251

79 A view of the cationic portion of [{Fe (TPA)} ₂ O(4-methoxybenzoato)] (ClO ₄) ₃ . Hydrogen atoms are omitted.....	252
80 A view of the cationic portion of [{Fe (TPA)} ₂ O(4-fluorobenzoato)](ClO ₄) ₃ . Hydrogen atoms are omitted.....	253
81 A view of the cationic portion of [Fe (TPA) ₂ O(3,5-dimethylbenzoato)] (ClO ₄) ₃ •0.5H ₂ O. Hydrogen atoms are omitted.	254
82 A view of the cationic portion of [{Fe(TPA)} ₂ O(3,5-dihydroxybenzoato)] (ClO ₄) ₃ •CH ₃ CN. Hydrogen atoms are omitted.	255
83 Graph of Fe-O(carboxylate) vs pK _a in current (μ -oxido)(μ -modified-benzoato) diiron(III)TPA structures.	265
84 Graph of Fe-O(carboxylate) vs pK _a for previously reported (μ -oxido)(μ -modified-benzoato)diiron(III) TPA complexes.	265
85 Graph of Fe-O(carboxylate) vs pK _a for current and previously reported (μ -oxido)(μ -modified-benzoato)diiron(III) TPA complexes.....	266
86 Graph of Fe-O(carboxylate) vs pK _a in current (μ -oxido)(μ -modified-benzoato)diiron(III)TPA structures.	267
87 Graph of Fe-O(carboxylate) vs pK _a for previously reported (μ -oxido)(μ -modified-benzoato)diiron(III) TPA complexes.	267
88 Graph of Fe-O(carboxylate) vs pK _a for current and previously reported (μ -oxido)(μ -modified-benzoato)diiron(III) TPA complexes.....	268
89 Plot of Fe1-N _{3°} bond distance vs pK _a for (μ -oxido)(μ -modifiedbenzoato) diiron(III)TPA of the current study.....	269

90 Plot of Fe1-N _{3°} bond distance vs pK _a for previously reported (μ -oxido)(μ -modifiedbenzoato)diiron(III) TPA complexes. ⁴²	269
91 Plot of Fe1-N _{3°} bond distance vs pK _a for current and previously reported (μ -oxido)(μ -modifiedbenzoato)diiron(III) TPA complexes.	270
92 Plot of Fe-N _{pyr} bond distance vs pK _a for current (μ -oxido)(μ -modifiedbenzoato)diiron(III) TPA.	271
93 Plot of Fe-N _{pyr} bond distance vs pK _a for previously reported (μ -oxido) (μ -modifiedbenzoato) diiron(III) TPA complexes.	271
94 Plot of Fe1-N _{pyr} bond distance vs pK _a for current and previously reported (μ -oxido)(μ -modified-benzoato)diiron(III) TPA complexes.....	272

CHAPTER I

Introduction

Iron is the earth's fourth most abundant element which is 62000 ppm in the crust.

It comprises nearly 5% of the present-day crust.¹ Iron plays a paramount role in cell survival and function such as respiration, central metabolism, nitrogen fixation and photosynthesis.² Iron has various oxidation states and the energy associated with its valance state transformations is widely used by biological systems. Thus, electron flow of the oxidation or reduction of the iron is tied to reaction with redox sensitive elements such as carbon, oxygen, nitrogen, and sulfur.¹

Iron containing proteins are involved in many redox-related functions in cells. As a first-row transition element, iron has partially filled *d* orbitals and can form a range of oxidation states. The most common oxidation states for iron in proteins are III (d^5) and II (d^6), but less common intermediate states like IV (d^4) and V (d^5) can be seen as catalytic reaction intermediates in reactions catalyzed by iron proteins.

Iron proteins can be categorized as heme proteins and non-heme proteins. These heme and non-heme proteins are well known primarily for their reactivities toward O₂. Most of the reactions that involve dioxygen activation, such as alkane hydroxylation, are challenging in the laboratory due to high activation energies. In heme proteins, iron is chelated by porphyrin. Proteins in this class transport (hemoglobin) and store (myoglobin) O₂,³ and activate O₂ to oxidize a variety of substances, as in cytochrome P-450, for example.⁴ Non-heme proteins are further subdivided into iron sulfur proteins and diiron carboxylate bridged proteins.³

Iron-sulfur proteins contain Fe-S clusters that are typically bound to cysteinyl ligands and are generally considered to be inorganic cofactors. Approximately 1% of the iron content in mammals exists as Fe-S proteins.⁵ Fe-S proteins are involved primarily in redox electron-transfer reactions. These proteins are important in fundamental biological functions such as mitochondrial respiration, hydroxylation reactions, photosynthesis and nitrogen fixation.^{6,7} The ability of Fe-S centers to participate in electron transfer results from blending partially filled iron *d* orbitals with the sulfur orbitals.⁸ More importantly, the Fe-S units that have more than one iron center gain additional stabilization through electron delocalization. This means that the Fe-S cofactor does not need to undergo significant reorganization of its internal geometry during electron transfer reactions.⁸

Figure 1 shows the three major types of Fe-S clusters found in nature. The highly pervasive 2Fe-2S cluster is rhombic Fe₂S₂ which is also the building block for other higher order Fe-S proteins. This unit consists of two irons and two inorganic sulfides. The 4Fe-4S cubane Fe₄S₄, is considered to be a coalescence of two rhombic units.^{7,8} The third type is more complicated and higher order stoichiometric clusters that are found in hydrogenases and the p-cluster of nitrogenase. These complex units are also often associated with other metals such as molybdenum.⁸ Additionally, there are two other common Fe-S entities. In rubredoxin, a single iron is bound to four cysteine residues from the protein. 3Fe-4S clusters are also known.⁹

The second class of non-heme iron enzymes, the diiron carboxylato bridged proteins, possess a (μ -oxido)diiron center (Fe-O-Fe). This Fe-O-Fe unit exists in almost every species on earth and is included in proteins such as hemerythrin (Hr- invertebrate oxygen storage), methane monooxygenase (MMO- hydroxylation of alkanes), purple acid

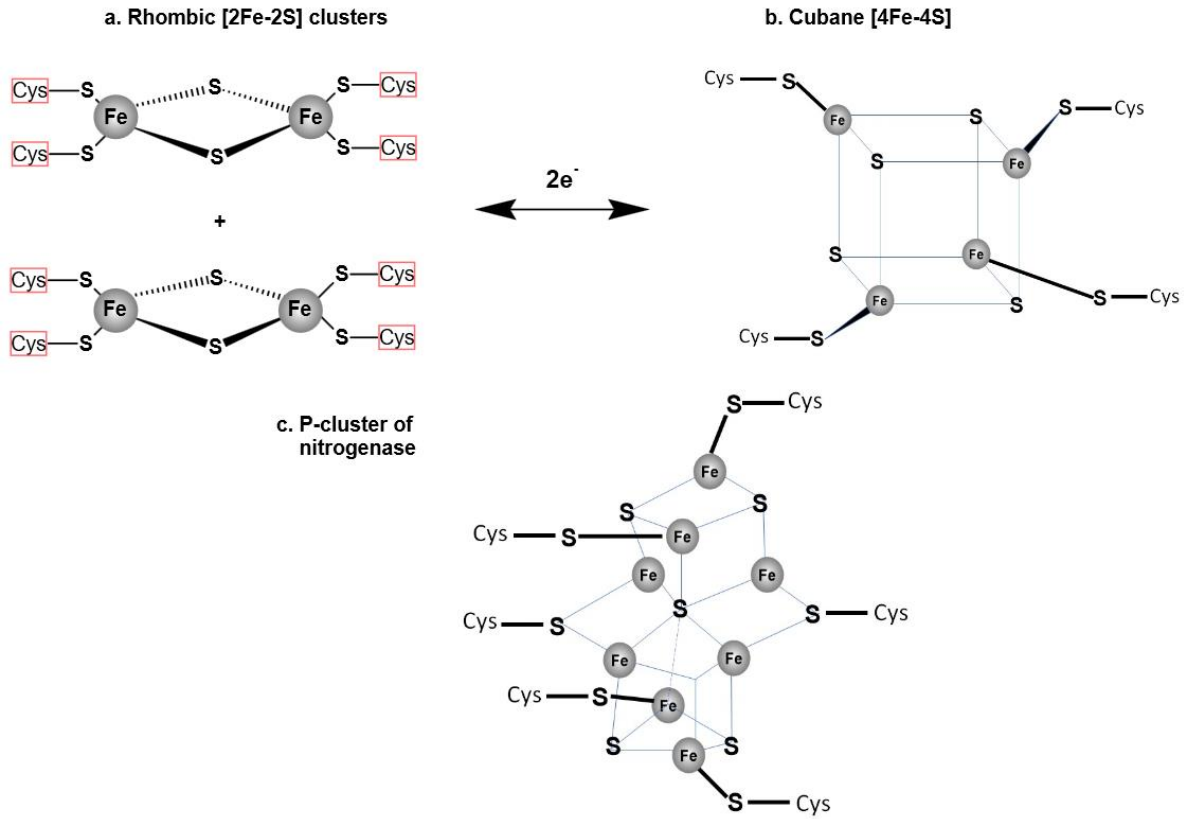


Figure 1. Pervasive Fe-S motifs in biology.

(a) rhombic 2Fe-2S. (b) cubane 4Fe-4S cluster (c) magnificent p cluster in nitrogenase.

phosphatases (PAP's- phosphate ester hydrolysis), and ribonucleotide reductase (RR-DNA synthesis). The spectroscopic data suggest that stearoyl-acyl carrier protein Δ^9 desaturase,¹⁰ and rubrerythrin¹¹ belong in this class as well. The inherent diverse and intense nature of the reactivity of this unit comes with its stability in the diferric form and its magnetic behavior.^{12,13}

Though the study of the Fe-O-Fe unit dates back to the early 1970's, a renaissance in this area began in 1983.¹² Pioneering contributions for this renaissance were the establishment of two independent (μ -oxido)bis(μ -carboxylato)diiron(III) "hemerythrin active site" models.^{14,15} In 1984, Stenkamp *et al.* were able to X-ray characterize methemerythrin and found the presence of a (μ -oxido)bis(μ -carboxylato)diiron(III) unit

in its active site.¹⁶ The interest in (μ -oxido)(μ -carboxylato)diiron(III) units escalated further with the discovery of this structure in ribonucleotide reductase from *Escherichia coli*.^{17,18} Also, methane monooxygenase contains a (μ -hydroxo)(μ -hydroxo /aqua)(μ -carboxylato)diiron(III) center in its active site.¹⁹

Oxido-bridged carboxylate non-heme iron protein centers have been known for years. Yet there are no known native proteins that have a carboxylate bridge and that carry a sulfido bridge instead of an oxido bridge. The first structurally authenticated Fe(III)-S-Fe(III) singly bridged compound, (μ -sulfido) bis [(*N,N'*-ethylenebis(salicylaldiminato)) iron(III)], was synthesized by Dorfman *et al.* in 1984.²⁰ The overall configuration in this [Fe(salen)]₂S was comparable to [Fe(salen)]₂O. However, the Fe-S-Fe angle (121.8°) was considerably smaller than the Fe-O-Fe analog (145°) and Fe-S average bond distance 2.17 Å is 0.37 Å longer than the Fe-O distance in its oxido bridge analog.²⁰ In a separate study, Kurtz *et al.* synthesized and spectroscopically characterized the non-native (sulfido)methemerythrin analog to metHr (which has an oxido bridge instead of the sulfido bridge). It was calculated that the Fe-S had a comparable bond length of 2.18 Å to the [Fe(salen)]₂S.²¹

The primary goal of the present study originally was to synthesize and structurally characterize (μ -sulfido)(μ -carboxylato)diiron(III)TPA complexes, using acetate and benzoate as the carboxylate source, where TPA is the tetradeятate tris(2-pyridylmethyl) amine ligand. In the past, thesis director Richard E. Norman and graduate student Yelda Hangun at Duquesne University attempted to produce (μ -sulfido)(μ -carboxylato)diiron(III)TPA and obtained dark green cubes that did not diffract X-rays cleanly. That project was not completed in the 1990s. The complete absence of synthetic models for

the (μ -sulfido)(μ -carboxylato) diiron(III)TPA unit motivated this attempt. The attempts made in the current research project to repeat the previous procedure were not able to reproduce the results and instead ended up forming oxido-bridged diiron complexes. Thus the current study has focused on another less addressed topic that will be discussed below.

Industrial methanol production from simple hydrocarbons incorporates oxidants such as H_2O_2 , which is not economical, so instead attempts have been made to incorporate normal air, which has O_2 and is more economical.²² Methane monooxygenase (MMO) is a fascinating catalyst found in biology, that converts methane to methanol in methanotrophs using dioxygen.



Figure 2 illustrates the proposed O_2 activation mechanism for MMO for methane hydroxylation.

The alkane hydroxylation mechanism is initiated by interaction of the diiron complex with O_2 or H_2O_2 . As seen in **Figure 2**, the diiron(II) site is oxidized to form a diiron(III) peroxide intermediate (by interacting with dioxygen) which is immediately converted to a high valent oxodiiron(IV). This involves loss of a water molecule. The generated oxodiiron(IV) species has resonance forms: that is, oxoiron(IV) paired with iron(IV) and oxoiron(V) paired with iron(III). This generated high valent oxodiiron(IV) species is capable of abstracting a hydrogen atom from methane (RH). The diiron intermediate returns to the diiron(III) stage by giving up the ·OH radical to the methyl radical ($R\cdot$) to form methanol (ROH).

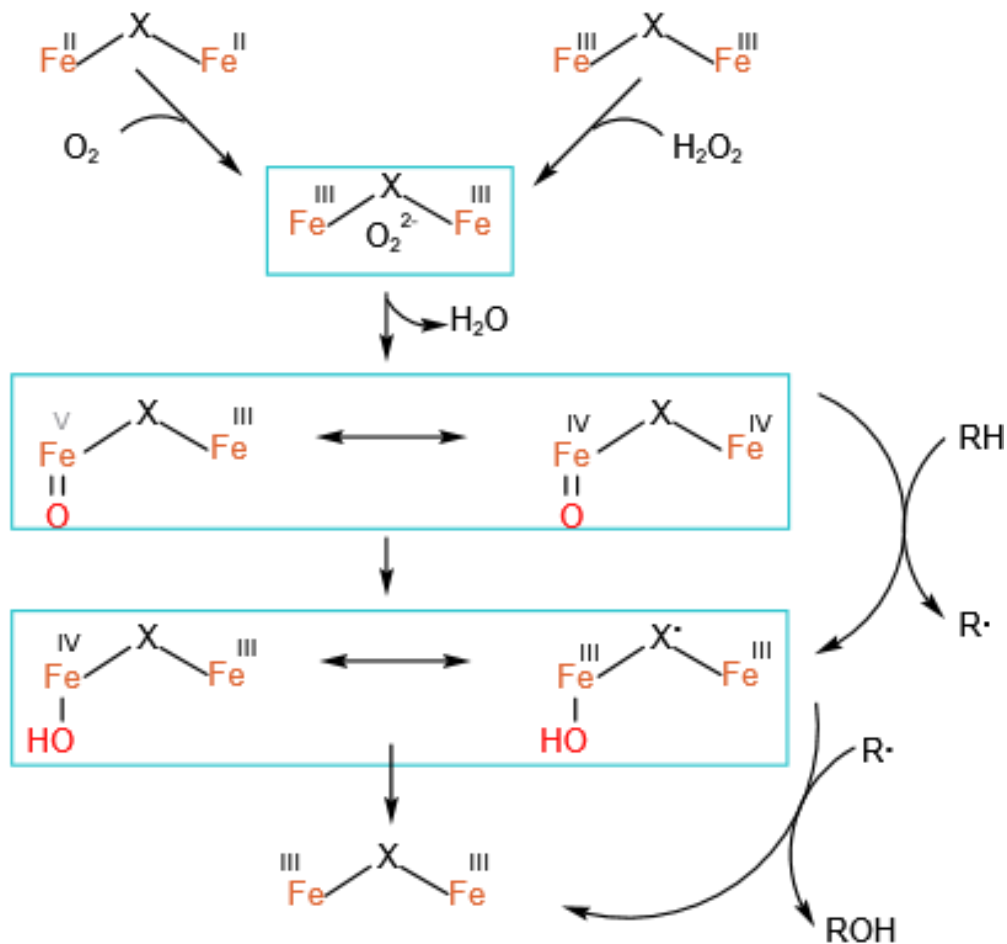


Figure 2. The proposed oxygen activation mechanism of MMO.

The unique structural and spectroscopic nature of diiron carboxylato units have drawn the attention of scientists for many years.^{23,24,25,26} These units are capable of small molecule activation such as O_2 , CO_2 , H_2 , and CH_4 as in the case of MMO. These small molecules are present in the atmosphere, and some are generated as industrial by-products and involved in elemental cycles and metabolic processes in biology. They are relatively cheap, and their high abundance has made them attractive in a variety of industrially important reactions such as alkane functionalization.

Alkanes are a huge reservoir of carbon, mainly existing in natural gases and crude oil.^{22,27} The possibility of using alkanes as a chemical feedstock for chemical synthesis remained unexplored for a long time. Hence alkanes were only used as an energy source through combustion which is an unsustainable, non-green approach that leads to greenhouse gas emission.²² Continued combustion of alkanes will exhaust these non-renewable fossil fuels. Recently, scientists are investigating the catalytic functionalization of alkanes into value-added products, such as alcohols, ketones, carboxylic acids, amides, and amines. These functionalized organic chemicals can then act as starting materials, or as the final targets, of many industrial processes, hence they act as chemical and industrial feedstocks. The interest in alkane functionalization intensified with the discovery of new natural gas and shale gas deposits which are promising candidates for lightweight alkanes.²²

However, alkane functionalization under mild conditions is a tantalizing challenge due to the inertness of hydrocarbons toward chemical conversion. Alkanes are extremely difficult to oxidize selectively.²⁸ While industrial alkane oxidation requires high pressure and high temperatures, Nature has evolved numerous enzymes that can functionalize these hydrocarbons selectively under mild, ambient conditions.²⁹

Scientists initially built catalytic models for metalloporphyrin proteins such as cytochrome P450 for selective hydrocarbon oxidation.³⁰ Cytochrome P450 performs a broad range of biological oxidations including epoxidation, hydroxylation and heteroatom oxidation.³¹ Although much research effort has been made on these heme enzymes, there is significant interest in studying iron proteins which have the diiron centers bridged by oxide and carboxylate (Fe-O-Fe unit) as an important group of

catalysts useful in a variety of activities such as monofunctionalization or deoxygenation of organic compounds.³² Therefore, numerous diiron oxido complexes with mono- and di-carboxylate bridges have been synthesized.^{12,13,25}

Before 1983, the majority of these models synthesized were monobridged or tribridged, while the dibridged complexes evolved subsequently.¹² Early studies used various tridentate ligands, such as tris(*N*-methylimidazol-2-yl)-phosphine (tmip), hydrotris(1-pyrazolyl)borate (HBpz₃⁻), and *N,N*-bis(2-ethyl-5-methylimidazol-4-ylmethyl)aminopropane (biap), to synthesize diiron centers bridged by oxido and carboxylate groups.^{12,33} For instance, Armstrong *et al.* prepared a series of (μ -oxido) bis(μ -carboxylato)diiron(III) complexes; [(Fe(HBpz₃))₂O(O₂CR)₂] where R= (H, CH₃, C₆H₅) to mimic the tribridged methemerythrin protein active site. These complexes possessed average Fe-O_(oxo) bond lengths of 1.783 Å and an average Fe-O-Fe bond angle of 124.6°.³⁴ Another tribridged diiron(III) series were synthesized in the form of [(Fe(biap))₂O(O₂CR)₂]²⁺ where R=C₆H₅, CH(C₆H₅)₂, CH₂C(C₆H₅)₃. These structures had two-fold rotation and both amine nitrogens were *trans* to the oxo bridge. The Fe-N_(amine) bond length is 0.16 Å longer than the average imidazole Fe-N distance of 2.188 Å. The Fe-O-Fe bond angle is 122.1°.³⁵ **Figure 3** shows several tridentate ligands that have been used to model non-heme protein active sites.

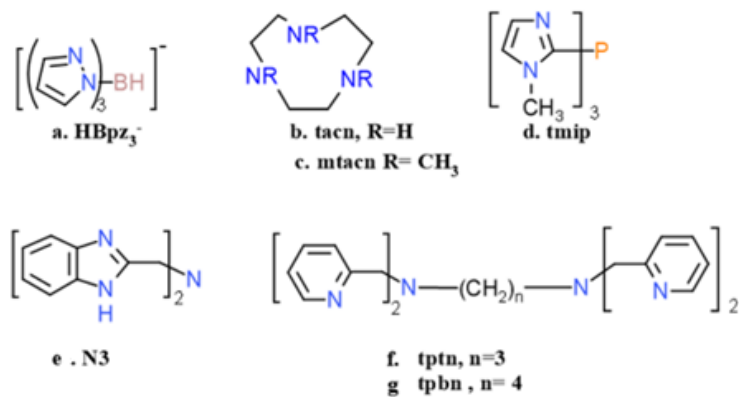


Figure 3. Common tridentate ligands used in synthesis of (μ -oxido)(μ -carboxylato) diiron complexes.(a). hydrotris(1-pyrazolyl)borate (b). 1,4,7-triazacyclononane (c). N,N',N'' -trimethyl-1,4,7-triazacyclononane (d). tris(N -methylimidazol-2-yl-phosphine (e). bis(2-benzimidazolylmethyl)amine (f). tetrakis(2-pyridylmethyl)-1,3-propanediamine (g). tetrakis(2-pyridylmethyl)-1,4-butanediamine.

Spectroscopic studies of the (μ -oxido)(μ -carboxylato) units in ribonucleotide reductase and purple acid phosphatases revealed that the diiron centers are distinct.^{36,37} The (μ -oxido)bis(μ -carboxylato) analogs that were synthesized using the tridentate capping ligands were useful for modeling the UV-vis and Raman spectroscopy in methemerythrin and ribonucleotide reductase and produced comparable antiferromagnetic coupling constants. The biggest drawback was that the tridentate ligand based (μ -oxido)(μ -carboxylato) complexes failed to model the asymmetric nature of the diiron centers.³³ So a new family of (μ -oxo)(μ -carboxylato)diiron(III) complexes using the tripodal ligand, tris(2-pyridylmethyl)amine (TPA) was synthesized.²⁵

Tetradentate tripodal ligands are extensively used in synthesizing (μ -oxido)diiron(III) complexes with distinct iron sites.³³ These ligands fix four coordination sites for an iron ion.²⁹ The popular tetrapodal ligand TPA is an excellent ligand to model the metal coordination environment due to its ability to form stable and catalytically

active metal complexes and to bind to a wide variety of metal ions.³⁸ TPA containing metal complexes are proven to be among the best catalysts for alkane hydroxylation, olefin oxidation and radical reactions including additions, cyclization, and polymerizations.^{39,40} **Figure 4** shows the chemical structure of TPA.

Unlike the tridentate ligands mentioned above, tetradeятate ligands such as TPA favor the formation of dibridged (μ -oxido)(μ -carboxylato) complexes over tribridged {(μ -oxido)bis(μ -carboxylato)} analogs. Further, TPA complexes mimic the spectral and electronic properties of proteins similar to hemerythrin and ribonucleotide reductase.²⁵

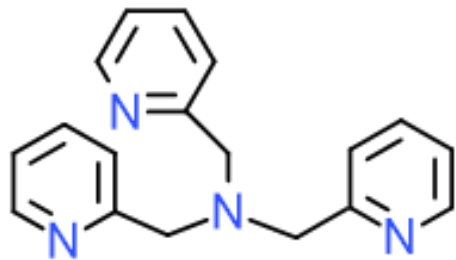


Figure 4. *Tris(2-pyridylmethyl)amine.*

Several mononuclear Fe(III) TPA complexes with the formula [Fe(III)(TPA)X₂](ClO₄) (X = Cl⁻, Br⁻, N₃⁻) and two oxido-bridged dinuclear Fe(III)TPA complexes with the general formula [{Fe(III)(TPA)X}₂O](ClO₄)₂ (X = Cl⁻ and Br⁻) were synthesized by Larry Que's group.²⁹ In their catalytic investigations, a 70-80% catalytic efficiency for the formation of cyclohexane halides in the presence of a 1:1 mixture of the alkyl peroxide and the Fe(TPA) complexes was observed.

The first dibridged (μ -oxido)(μ -carboxylato)diiron(III): [Fe₂L₂O(OBz)]⁺ where L = tetrapodal ligand HDP, was reported by the Que group in an attempt to model the

purple acid phosphatase active site in 1988.⁴¹ Both irons have the same coordination environment and the structure has both tertiary amine nitrogens *trans* to the oxido bridge. The first (μ -oxido)(μ -carboxylato)diiron(III)TPA complex, $[Fe_2(TPA)_2O(OBz)](ClO_4)_3$ was prepared by substituting the HDP ligands by TPA. Surprisingly, the two iron centers were distinct.²⁵

In another study, (μ -oxido)(μ -L)diiron(III)-TPA complexes were synthesized where L= benzoate, acetate, diphenyl phosphate, carbonate, H-maleate and phthalate, and were characterized by X-ray crystallography.^{24,25} These studies have shown that the Fe-O-Fe bond angle is affected by the bite angle of the bridging carboxylate/phosphate source. The study showed that for the bridging ligand with an ascending order of bite angle, (carbonate, acetate, hydrogen-maleate, diphenyl phosphate and phthalate) have Fe-O-Fe angles of 125.4°, 129.2°, 131.0°, 138.1° and 143.4°, respectively.^{25,24} Further, they discovered that the magnetic properties are independent of the Fe-O-Fe angle by showing that there is no clear dependence of the antiferromagnetic coupling constant (J) on the Fe-O-Fe angle. All of the (μ -oxido)(μ -L)diiron(III)TPA complexes which have been structurally characterized have distinct iron sites except for $[Fe_2(TPA)_2O(phthalate)]^{2+}$. In the $[Fe_2(TPA)_2O(phthalate)]^{2+}$ complex, the two carboxylate groups of the phthalate ring coordinate in a monodentate fashion and the complex has 2-fold symmetry about the Fe-O-Fe unit bisecting the phthalate ring.²⁴ Therefore, unlike other dibridged complexes that have only one tertiary amine nitrogen *trans* to the oxo bridge, while on the other iron atom, a pyridine ring nitrogen is *trans* to the oxo bridge, $[Fe_2(TPA)_2O(phthalate)]^{2+}$ has both tertiary amine nitrogens *cis* to the oxo bridge.²⁴ In general, these (μ -oxido)(μ -

carboxylato)diiron(III) complexes have Fe-O-Fe angles of $120 \pm 5^\circ$ and the Fe—Fe separation is $3.1 \pm 0.1 \text{ \AA}$.²⁵

While a variety of diiron TPA complexes have been synthesized and their structural, UV-vis and magnetic properties were well studied, there is a lack of systematic study of carboxylate bridged iron complexes where the carboxylate group is a benzoic acid derivative. In a recent master's research study, Harshani Arachchilage synthesized several (μ -oxido)(μ -carboxylato)diiron(III)TPA with *para*-substituted benzoates to assess the *trans* influence of modified benzoates.⁴² In that study, three complexes with formula $[\text{Fe}_2(\text{TPA})_2\text{O}(\mu\text{-R})]^{3+}$ where R = 4-chlorobenzoate, 4-methylbenzoate and 4-ethylbenzoate were reported. Crystal structures revealed that all three of these have distinct iron sites. These complexes have Fe-O-Fe bond angles, Fe-Fe separations and Fe-O_{bridge} bond distances comparable to previously reported (μ -oxido)(μ -carboxylato)diiron(III)TPA complexes. The Fe-O-Fe bond angles were 129.1° , 130.1° , 128.9° , respectively, and the average Fe-O_{bridge} distance was 1.80 \AA . According to that study, there is no definite relationship between substituted benzoate p*K*_a and the *trans* influence.⁴² However, more examples are needed to properly assess the interplay of p*K*_a and *trans* influence. Thus, as a secondary focus, this research will report the synthesis, electronic spectra, NMR spectra and structure of several dibridged oxido iron complexes with various benzoate derivatives with the general formula of $[\text{Fe}_2(\text{TPA})_2\text{O}(\mu\text{-modified-benzoato})]^{3+}$. During this research study, several *para*- and *di-meta*- substituted benzoic acid derivatives were used for this purpose to assess any structural and spectral variations associated with the modified carboxylate ligands.

In 2015, during an attempt to make $[\text{Fe}_2(\text{TPA})_2\text{O} \text{ (modifiedbenzoato)}_2]^{2+}$, Arachchilage synthesized (and structurally characterized) $[\{\text{Fe}(\text{TPA})(4\text{-nitrobenzoato})\}_2\text{O}](\text{ClO}_4)_2 \bullet 2\text{CH}_3\text{CN}$ accidentally.⁴² This is the only X-ray characterized $[\text{Fe}_2(\text{TPA})_2\text{O} \text{ (modifiedbenzoato)}_2]^{2+}$ complex reported to date.

The bridging oxide sits on a two-fold axis, so the two iron sites are symmetry related. The tertiary amine is *cis* to the oxido bridge, and the 4-nitrobenzoate is *trans* to the tertiary amine. The relative orientation of the two 4-nitrobenzoates is *anti*.

The above mentioned thesis project involved the synthesis and characterization of a variety of $[\{\text{Fe}(\text{TPA})\}_2\text{O}(\mu\text{-carboxylato})]^{3+}$ complexes varying the basicity of the bridging carboxylate. 4-Nitrobenzoate was the least basic carboxylate and the only carboxylate that gave a linear Fe-O-Fe core with two non-bridging carboxylates. A tertiary focus of the current research project is the attempted synthesis of other examples of a $[\{\text{Fe}(\text{TPA})\}_2\text{O}(\text{carboxylato})_2]^{2+}$ unit using 3,5-disubstituted benzoates.

CHAPTER II

Experimental

2.1 Materials

Acetone (HPLC grade), acetonitrile (HPLC grade), activated charcoal, 4-cyano-benzoic acid, 3,5-dibromobenzoic acid, 3,5-dichlorobenzoic acid, 3,5-dimethoxy-benzoic acid, 3,5-dimethylbenzoic acid, 3,5-dinitrobenzoic acid, 4-fluorobenzoic acid, 4-hydroxy-benzoic acid, iron(III) perchlorate decahydrate, methanol (HPLC grade), 4-methoxy-benzoic acid, concentrated perchloric acid (70 % W/W), 2-picollylamine, 2-picollyl chloride hydrochloride, potassium cyanate, 4-pyridinecarboxylic acid, sodium acetate, sodium benzoate, sodium bromide, sodium chloride, sodium cyanate, sodium hydroxide, sodium sulfide nonahydrate and triethylamine (99.5% W/W) were purchased and used without further purification.

2.2 Instrumental

2.2.1 Electronic Spectroscopy

All of the UV-Visible spectra were recorded on *Jasco* model V-750 double-beam spectrophotometer with a photomultiplier detector located in the Department of Chemistry. Data were collected using 1.0 nm bandwidth, 0.06 sec response time, 1.0 nm data intervals continuous spectrum at 1000 nm/min. Samples for electronic spectroscopy were prepared by using HPLC grade acetonitrile (99%), and 1 cm path length cuvettes.

2.2.2 ^1H NMR Spectroscopy

A *JEOL* Eclipse+ 300 FT-NMR, located in the Department of Chemistry, was used to collect the NMR spectra. Outer diameter 5 mm NMR tubes were used. The chemical shift reference value for diamagnetic ^1H NMR was the residual proton signal of D_2O which was assigned a chemical shift δ value of 4.79 ppm. The acquisition conditions for “normal/diamagnetic” ^1H NMR were 5.4 μsec pulses, 16384 data points, 4 sec relaxation delay, and the number of scans was 8. The acquisition conditions for “paramagnetic” ^1H NMR were 5.4 μsec pulses, 16384 data points, 0.03 sec relaxation delay, x-offset 50 ppm, x-sweep 300 ppm and the number of scans was 5000. The chemical shift reference for paramagnetic ^1H NMR was the residual proton signal of CD_3CN (99.9%), which was assigned a chemical shift δ value of 1.94 ppm.

2.2.3 X-ray crystallography

X-ray crystallographic data were collected using a *Rigaku* XtaLAB mini diffractometer equipped with a CCD detector and graphite monochromated Mo $\text{K}\alpha$ radiation ($\lambda = 0.71075 \text{ \AA}$). Data were collected at room temperature (298 K). Cell constants were determined by least-squares refinement of a variable large number of reflections. The resultant data were used to solve and refine the structures.

2.3 Synthesis

2.3.1 Preparation of $\text{TPA}\cdot 3\text{HClO}_4$

2-Picolylchloride hydrochloride (13.0 g, 79.2 mmol) was dissolved in 5.0 mL of deionized water at 0 °C in a 200 mL round bottom flask equipped with a magnetic stirrer.

Aqueous NaOH (14.0 mL of 5.40 M NaOH) was added to the flask while stirring. 2-Picolylamine (4.07 mL, 41.6 mmol) was slowly added dropwise and formed a light-red emulsion. Throughout the above addition steps, the flask was kept in an ice bath at 0 °C. Over the next four days, at room temperature, the pH was maintained between 7 and 9.5 by adding 11.0 mL of 5.40 M NaOH to the mixture. The pH of the mixture was checked using pH papers during the four days. One hour after the final addition of NaOH, concentrated (70% w/w, approximately 11.6 M) perchloric acid (20.0 mL) was added to the flask. Brown-red crystals formed immediately. These crystals were removed and washed with ice-cold water.

The brown-red crystals (21.08 g) were dissolved in deionized water (80.0 mL) and heated to 35 °C. Activated charcoal (2.00 g) was added and the mixture was filtered. Then 15.0 mL of concentrated HClO₄ was added to the filtrate and the solution was set aside to form crystals. Two distinctly different colored crystal layers formed over 2 days. The top light-yellow crystal layer was manually separated, dried, and saved. The orange bottom layer of formed crystals was dissolved in distilled water (50.0 mL) and heated to 35 °C. Activated charcoal (1.00 g) was added and the mixture was filtered. Then concentrated HClO₄ (10.0 mL) was added to the filtrate and the solution was set aside to form crystals. Again, two distinctly different colored crystal layers formed. Again, the top layer was light-yellow, and the bottom layer was orange. The top crystal layer was separated, dried, and saved. The orange layer was dissolved in deionized water (50.0 mL) and heated to 35 °C. Activated charcoal (0.50 g) was added and the mixture was filtered. Then concentrated HClO₄ (4.0 mL) was added to the filtrate and the solution was set aside to form crystals.

The crystals obtained were recrystallized 2-3 times from DI water giving light-yellow crystals. The identity and purity of the crystals were determined using ^1H NMR spectroscopy. UV-visible spectroscopy was also performed.

2.3.2 Attempted synthesis of (μ -sulfido)(μ -carboxylato)düiron(III) complexes

2.3.2.1 Attempted synthesis of $[\text{Fe}_2(\text{TPA})_2\text{S}(\text{OAc})](\text{ClO}_4)_3$

A mixture of TPA·3HClO₄ (0.590 g, 1.00 mmol) and triethylamine (0.56 mL, 4.0 mmol) was added to 40.0 mL methanol and stirred for several minutes with slight heating (30 °C). Ferric perchlorate decahydrate (0.54 g, 1.0 mmol) was dissolved in 2.0 mL methanol by mixing with a disposable Pasteur pipette in a small vial. In a separate vial, sodium acetate trihydrate (0.068g, 0.50 mmol) was dissolved in 2.0 mL of methanol. The iron solution was added to the TPA solution and mixed well. This was followed by the carboxylate solution. Finally, solid sodium sulfide nonahydrate (0.12 g, 0.50 mmol) was added. Most of the Na₂S·9H₂O dissolved, but not all. After stirring for 30 minutes, the solution was gravity filtered to another flask giving a dark-brown solution, which was allowed to sit to form crystals. After several days, needle shaped dark greenish-black crystals were formed. The ^1H NMR and UV-visible spectra of the crystals were consistent with $[\text{Fe}_2(\text{TPA})_2\text{O}(\text{OAc})](\text{ClO}_4)_3$ which has been previously synthesized and characterized.²⁵

2.3.2.2 Attempted preparation of $[Fe_2(TPA)_2S(OBz)](ClO_4)_3$

Method 1

A mixture of TPA·3HClO₄ (0.591 g, 0.999 mmol) and triethylamine (0.56 mL, 4.0 mmol) was added to 40.0 mL methanol and stirred for several minutes with slight heating (30 °C). Ferric perchlorate decahydrate (0.549 g, 1.03 mmol) was dissolved in 2.0 mL methanol by mixing with a disposable Pasteur pipette in a small vial. In a separate vial, sodium benzoate (0.076 g, 0.53 mmol) was dissolved in 2.0 mL of methanol. The iron solution was added to the TPA solution and mixed well. This was followed by the addition of carboxylate solution. Finally, solid sodium sulfide nonahydrate (0.12 g, 0.50 mmol) was added. Most of the Na₂S·9H₂O dissolved, but not all. After stirring for 30 minutes, the solution was gravity filtered to another flask giving a dark-brown solution, which was allowed to sit to form crystals. After several days, dark-brown needle shaped crystals were formed. X-ray crystallographic studies indicated that this compound is [Fe₂(TPA)₂O(OAc)](ClO₄)₃ which has been previously synthesized and characterized.²⁵

Method 2

A mixture of TPA·3HClO₄ (0.593 g, 1.00 mmol) and triethylamine (0.56 mL, 4.0 mmol) was added to 40.0 mL methanol and stirred for several minutes with slight heating (30 °C). A solution of ferric perchlorate decahydrate (0.545 g, 1.02 mmol) and sodium benzoate (0.072 g, 0.50 mmol) in 4.0 mL of methanol was added to the TPA·3HClO₄ solution. This was followed by the addition of sodium sulfide nonahydrate (0.129 g, 0.537 mmol). Most of the Na₂S·9H₂O dissolved, but not all. After stirring for 30 minutes, the solution was gravity filtered to another flask giving a dark-green solution, which was

allowed to sit to form crystals. After about two weeks, brown crystals formed. The ^1H NMR and UV-visible spectra of the crystals were consistent with the $[\text{Fe}_2(\text{TPA})_2\text{O}(\text{OAc})](\text{ClO}_4)_3$ which has been previously synthesized and characterized.²⁵

2.3.3 Preparation of mononuclear iron(III) complexes

2.3.3.1 Synthesis of $[\text{Fe}(\text{TPA})(\text{NCO})_2](\text{ClO}_4)$

Method 1

$\text{TPA}\bullet 3\text{HClO}_4$ (0.2955 g, 0.4994 mmol) and triethylamine (0.0695 mL, 0.498 mmol) were added to 20 mL methanol and stirred to effect solution. A solution of ferric perchlorate decahydrate (0.2670 g, 0.4997 mmol) in 2 mL of methanol was added. This was followed by the addition of NaOCN (0.065 g, 1.0 mmol). After stirring for 30 minutes, the solution turned cloudy reddish-orange. A drop of HClO_4 was added to the mixture. The solution was gravity filtered to another flask producing a bright-orange solution, which was allowed to sit to form crystals. One month later, no crystals had formed.

Method 2

$\text{TPA}\bullet 3\text{HClO}_4$ (0.2955 g, 0.4994 mmol) and triethylamine (0.0695 mL, 0.498 mmol) were added to 20 mL methanol and stirred to effect solution. A solution of ferric perchlorate decahydrate (0.2670 g, 0.4997 mmol) in 2 mL of methanol was added. This was followed by the addition of KOCN (0.0810 g, 0.999 mmol). After stirring for 30 minutes the solution turned cloudy reddish-orange. A drop of HClO_4 was added to the mixture. The solution was gravity filtered to another flask producing a bright-orange

solution, which was allowed to stand to form crystals. One month later, no crystals had formed.

All of the amounts were doubled, but still no crystals formed.

2.3.4 Preparation of oxido-bridged diiron(III) complexes (singly bridged)

2.3.4.1 Attempted preparation of $[Fe_2(TPA)_2O(3,5\text{-dinitrobenzoato})_2](ClO_4)_2$

TPA•3HClO₄ (0.592 g, 1.00 mmol) and triethylamine (0.56 mL, 4.0 mmol) were added to 40.0 mL methanol and stirred for several minutes with slight heating (30 °C). Ferric perchlorate decahydrate (0.549 g, 1.03 mmol) was dissolved in 2.0 mL methanol by mixing with a disposable Pasteur pipette in a small vial. In a separate vial, 3,5-dinitrobenzoic acid (0.216 g, 1.02 mmol) was dissolved in 2.0 mL of methanol followed by triethylamine (0.14 mL, 1.0 mmol). The iron solution was added to the TPA solution and mixed well. This was followed by addition of the carboxylate solution. A yellowish-brown solution was observed. After stirring for 30 minutes, the solution was gravity filtered. The filtrate was allowed to sit to form crystals. After several days, powdery light-brown crystals formed. These crystals were dissolved in a minimum volume of acetonitrile and placed inside an ethyl acetate vapor bath in an attempt to form X-ray quality single crystals. X-ray crystallographic studies indicated that the crystals formed were $[Fe_2(TPA)_2O(OAc)](ClO_4)_3$ which has been previously synthesized and characterized.²⁵

2.3.4.2 Attempted preparation of $[Fe_2(TPA)_2O(3,5\text{-dimethoxybenzoato})_2](ClO_4)_2$

TPA \cdot 3HClO₄ (0.592 g, 1.00 mmol) and triethylamine (0.56 mL, 4.0 mmol) were added to 40.0 mL methanol and stirred for several minutes with slight heating (30 °C). Ferric perchlorate decahydrate (0.549 g, 1.03 mmol) was dissolved in 2.0 mL methanol by mixing with a disposable Pasteur pipette in a small vial. In a separate vial, 3,5-dimethoxybenzoic acid (0.1860 g, 1.021 mmol) was dissolved in 2.0 mL of methanol followed by triethylamine (0.14 mL, 1.0 mmol). The iron solution was added to the TPA solution and mixed well. This was followed by addition of the carboxylate solution. A light-green solution was observed. After stirring for 30 minutes, the solution was gravity filtered. The filtrate was allowed to sit to form crystals. The obtained crystals were dissolved in a minimum volume of acetonitrile and placed inside an ethyl acetate vapor bath in an attempt to form X-ray quality single crystals. The resultant powdery dark-brown crystals were not suitable for X-ray diffraction. However, the ¹H NMR and UV-visible spectra of the crystals were consistent with a dibridged complex instead of the desired singly-bridged complex.

2.3.4.3 Attempted preparation of $[Fe_2(TPA)_2O(3,5\text{-dimethylbenzoato})_2](ClO_4)_2$

TPA \cdot 3HClO₄ (0.592 g, 1.00 mmol) and triethylamine (0.56 mL, 4.0 mmol) were added to 40.0 mL methanol and stirred for several minutes with slight heating (30 °C). Ferric perchlorate decahydrate (0.549 g, 1.03 mmol) was dissolved in 2.0 mL methanol by mixing with a disposable Pasteur pipette in a small vial. In a separate vial, 3,5-dimethylbenzoic acid (0.1540 g, 1.026 mmol) was dissolved in 2.0 mL of methanol followed by triethylamine (0.14 mL, 1.0 mmol). The iron solution was added to the TPA

solution and mixed well. This was followed by addition of the carboxylate solution. A light-brown solution was observed. After stirring for 30 minutes, the solution was gravity filtered. The filtrate was allowed to sit to form crystals. After several days, needle shaped brown crystals formed. X-ray diffraction analysis indicated that instead of the desired singly-bridged compound, dibridged $[Fe_2(TPA)_2O(3,5\text{-dimethylbenzoato})](ClO_4)_3$ had formed. The structure will be discussed subsequently in section 3.3.6 below.

2.3.4.4 Attempted preparation of $[Fe_2(TPA)_2O(3,5\text{-dihydroxidobenzoato})_2](ClO_4)_2$

TPA•3HClO₄ (0.592 g, 1.00 mmol) and triethylamine (4.0 mmol, 0.56 mL) were added to 40.0 mL methanol and stirred for several minutes with slight heating (30 °C). Ferric perchlorate decahydrate (0.549 g, 1.03 mmol) was dissolved in 2.0 mL methanol by mixing with a disposable Pasteur pipette in a small vial. In a separate vial, 3,5-dihydroxybenzoic acid (0.158 g, 1.03 mmol) was dissolved in 2.0 mL of methanol followed by triethylamine (0.14 mL, 1.0 mmol). The iron solution was added to the TPA solution and mixed well. This was followed by addition of the carboxylate solution. A yellowish-brown solution was observed. After stirring for 30 minutes, the solution was gravity filtered. The filtrate was allowed to sit to form crystals. After several days, dark-brown rectangular crystals formed. X-ray diffraction analysis indicated that instead of the desired singly-bridged compound, dibridged $[Fe_2(TPA)_2O(3,5\text{-dihydroxybenzoato})](ClO_4)_3$ had formed. The structure will be discussed subsequently in section 3.3.7 below.

2.3.4.5 Attempted preparation of $[Fe_2(TPA)_2O(3,5\text{-dibromobenzoato})_2](ClO_4)_2$

TPA•3HClO₄ (0.592 g, 1.00 mmol) and triethylamine (0.56 mL, 4.0 mmol)

were added to 40.0 mL methanol and stirred for several minutes with slight heating (30 °C). Ferric perchlorate decahydrate (0.549 g, 1.03 mmol) was dissolved in 2.0 mL methanol by mixing with a disposable Pasteur pipette in a small vial. In a separate vial, 3,5-dibromobenzoic acid (0.2820 g, 1.007 mmol) was dissolved in 2.0 mL of methanol followed by triethylamine (0.14 mL, 1.0 mmol). The iron solution was added to the TPA solution and mixed well. This was followed by addition of the carboxylate solution. A brownish-yellow solution was observed. After stirring for 30 minutes, the solution was gravity filtered. The filtrate was allowed to sit to form crystals. After several days, powdery reddish-brown crystals formed. These crystals were dissolved in a minimum volume of acetonitrile and placed inside an ethyl acetate vapor bath in an attempt to form X-ray quality single crystals. However, the crystals were too small and not suitable for X-ray crystallography. The ¹H NMR and UV-visible spectra of the solids were consistent with a dibridged complex instead of a singly-bridged complex.

2.3.4.6 Attempted preparation of $[Fe_2(TPA)_2O(3,5\text{-dichlorobenzoato})_2](ClO_4)_3$

TPA•3HClO₄ (0.592 g, 1.00 mmol) and triethylamine (0.56 mL, 4.0 mmol)

were added to 40.0 mL methanol and stirred for several minutes with slight heating (30 °C). Ferric perchlorate decahydrate (0.549 g, 1.03 mmol) was dissolved in 2.0 mL methanol by mixing with a disposable Pasteur pipette in a small vial. In a separate vial, 3,5-dichlorobenzoic acid (0.194 g, 1.02 mmol) was dissolved in 2.0 mL of methanol followed by triethylamine (0.14 mL, 1.0 mmol). The iron solution was added to the TPA

solution and mixed well. This was followed by addition of the carboxylate solution. A light-brown solution was observed. After stirring for 30 minutes, the solution was gravity filtered. The filtrate was allowed to sit to form crystals. After several days, brown powdery crystals had formed and were not suitable for X-ray crystallography. The ^1H NMR and UV-visible spectra of the solids were consistent with a dibridged complex instead of a singly-bridged complex.

2.3.4.7 Preparation of $[\{\text{Fe}(\text{TPA})\text{Br}\}_2\text{O}](\text{ClO}_4)_2$

$\text{TPA}\cdot 3\text{HClO}_4$ (0.1480 g, 0.2501 mmol) and triethylamine (160 μl , 1.15 mmol) were added to 20 mL of methanol and warmed to nearly 60 °C with stirring to dissolve all of the ligand. When the solution was cooled to room temperature, NaBr (0.0302 g, 0.294 mmol) was added and the system was mixed well. Ferric perchlorate decahydrate (0.1336 g, 0.2500 mmol) dissolved in methanol (2.0 mL) was added to the above mixture and stirred for 30 min. A dark brownish-red solution resulted. After stirring, the solution was gravity filtered. One day later, small dark greenish-brown color crystals were observed. Those crystals were too small for X-ray crystallographic analysis. Therefore, the crystals were recrystallized using acetonitrile (99%) and kept in an ethyl acetate vapor bath. After a few days, dark-brown rectangular shaped crystals formed. X-ray diffraction analysis indicated that this complex was $[\{\text{Fe}(\text{TPA})\text{Br}\}_2\text{O}](\text{ClO}_4)_2\cdot \text{H}_2\text{O}$ and its structure will be discussed subsequently in section 3.3.1 below.

2.3.5 Preparation of (μ -oxido)(μ -carboxylato)diiron(III) complexes

2.3.5.1 Attempted preparation of $[\text{Fe}_2(\text{TPA})_2\text{O}(3,5\text{-dinitrobenzoato})](\text{ClO}_4)_3$

TPA•3HClO₄ (0.592 g, 1.00 mmol) and triethylamine (0.56 mL, 4.0 mmol) were added to 40.0 mL methanol and stirred for several minutes with slight heating (30 °C). Ferric perchlorate decahydrate (0.549 g, 1.03 mmol) was dissolved in 2.0 mL methanol by mixing with a disposable Pasteur pipette in a small vial. In a separate vial, 3,5-dinitrobenzoic acid (0.1080 g, 0.5092 mmol) was dissolved in 2.0 mL of methanol followed by triethylamine (0.07 mL, 0.5 mmol). The iron solution was added to the TPA solution and mixed well. This was followed by addition of the carboxylate solution. A light-green-yellow solution was observed. After stirring for 30 minutes, the solution was gravity filtered. The filtrate was allowed to sit to form crystals. After several days, small dark-brown irregular crystals formed. These crystals were unsuitable for X-ray crystallographic analysis and were recrystallized from acetonitrile (99%) and kept in an ethyl acetate vapor bath. After a few days, brown short needle crystals were formed. These crystals diffracted X-rays very poorly and a structure determination was not possible. However, the ¹H NMR and UV-visible spectra of the crystals were consistent with a dibridged complex.

2.3.5.2 Preparation of $[\text{Fe}_2(\text{TPA})_2\text{O}(3,5\text{-dimethoxybenzoato})](\text{ClO}_4)_3$

TPA•3HClO₄ (0.592 g, 1.00 mmol) and triethylamine (0.56 mL, 4.0 mmol) were added to 40.0 mL methanol and stirred for several minutes with slight heating (30 °C). Ferric perchlorate decahydrate (0.549 g, 1.03 mmol) was dissolved in 2.0 mL methanol by mixing with a disposable Pasteur pipette in a small vial. In a separate vial,

3,5-dimethoxybenzoic acid (0.093 g, 0.51 mmol) was dissolved in 2.0 mL of methanol followed by triethylamine (0.07 mL, 0.5 mmol). The iron solution was added to the TPA solution and mixed well. This was followed by addition of the carboxylate solution. A light-green solution was observed. After stirring for 30 minutes, the solution was gravity filtered. The filtrate was allowed to sit to form crystals. After several days, yellowish-brown crystals had formed. Those crystals were recrystallized using acetonitrile (99%) and kept in an ethyl acetate vapor bath. The resultant small brown crystals were not suitable for X-ray crystallography. However, the ^1H NMR and UV-visible spectra of the crystals were consistent with a dibridged complex.

2.3.5.3 Preparation of $[\text{Fe}_2(\text{TPA})_2\text{O}(3,5\text{-dimethylbenzoato})](\text{ClO}_4)_3$

TPA•3HClO₄ (0.592 g, 1.00 mmol) and triethylamine (0.56 mL, 4.0 mmol) were added to 40.0 mL methanol and stirred for several minutes with slight heating (30 °C). Ferric perchlorate decahydrate (0.549 g, 1.03 mmol) was dissolved in 2.0 mL methanol by mixing with a disposable Pasteur pipette in a small vial. In a separate vial, 3,5-dimethylbenzoic acid (0.077 g, 0.51 mmol) was dissolved in 2.0 mL of methanol followed by triethylamine (0.07 mL, 0.5 mmol). The iron solution was added to the TPA solution and mixed well. This was followed by addition of the carboxylate solution. A light-brown solution was observed. After stirring for 30 minutes, the solution was gravity filtered. The filtrate was allowed to sit to form crystals. The resultant dark brown crystals were recrystallized using acetonitrile (99%) and kept in an ethyl acetate vapor bath. The resultant brown needle-shaped crystals were not suitable for X-ray crystallography.

However, the ^1H NMR and UV-visible spectra of the crystals were consistent with a dibridged complex.

2.3.5.4 Preparation of $[\text{Fe}_2(\text{TPA})_2\text{O}(3,5\text{-dihydroxybenzoato})](\text{ClO}_4)_3$

$\text{TPA}\cdot 3\text{HClO}_4$ (0.592 g, 1.00 mmol) and triethylamine (0.56 mL, 4.0 mmol) were added to 40.0 mL methanol and stirred for several minutes with slight heating (30 °C). Ferric perchlorate decahydrate (0.549 g, 1.03 mmol) was dissolved in 2.0 mL methanol by mixing with a disposable Pasteur pipette in a small vial. In a separate vial, 3,5-dihydroxybenzoic acid (0.079 g, 0.51 mmol) was dissolved in 2.0 mL of methanol followed by triethylamine (0.07 mL, 0.5 mmol). The iron solution was added to the TPA solution and mixed well. This was followed by addition of the carboxylate solution. A dark-green solution was observed. After stirring for 30 minutes, the solution was gravity filtered. The filtrate was allowed to sit to form crystals. The resultant brown crystals were recrystallized using acetonitrile (99%) and kept in an ethyl acetate vapor bath. After a few days, shiny reddish-brown rectangular crystals were formed. X-ray diffraction analysis indicated that this complex is $[\{\text{Fe}(\text{TPA})\}_2\text{O}(3,5\text{-dihydroxybenzoato})](\text{ClO}_4)_3 \cdot \text{CH}_3\text{CN}$ and its structure will be discussed in section 3.3.7 below.

2.3.5.5 Attempted preparation of $[\text{Fe}_2(\text{TPA})_2\text{O}(3,5\text{-dibromobenzoato})](\text{ClO}_4)_3$

$\text{TPA}\cdot 3\text{HClO}_4$ (0.592 g, 1.00 mmol) and triethylamine (0.56 mL, 4.0 mmol) were added to 40.0 mL methanol and stirred for several minutes with slight heating (30 °C). Ferric perchlorate decahydrate (0.549 g, 1.03 mmol) was dissolved in 2.0 mL methanol by mixing with a disposable Pasteur pipette in a small vial. In a separate vial,

3,5-dibromobenzoic acid (0.1410 g, 0.5037 mmol) was dissolved in 2.0 mL of methanol followed by triethylamine (0.14 mL, 1.0 mmol). The iron solution was added to the TPA solution and mixed well. This was followed by addition of the carboxylate solution. A dark-brown solution was observed. After stirring for 30 minutes, the solution was gravity filtered. The filtrate was allowed to sit to form crystals. The resultant brown crystals were recrystallized using acetonitrile (99%) and kept in an ethyl acetate vapor bath. After a few days, dark-brown rectangular shaped crystals were formed. X-ray crystallographic studies showed that the desired compound was not formed, but instead proved to be $[\text{Fe}_2(\text{TPA})_2\text{O}(\text{OAc})](\text{ClO}_4)_3 \cdot \text{H}_2\text{O}$ and its structure will be discussed in section 3.3.2.1 below.

2.3.5.6 Attempted preparation of $[\text{Fe}_2(\text{TPA})_2\text{O}(3,5\text{-dichlorobenzoato})](\text{ClO}_4)_3$

TPA•3HClO₄ (0.592 g, 1.00 mmol) and triethylamine (0.56 mL, 4.0 mmol) were added to 40.0 mL methanol and stirred for several minutes with slight heating (30 °C). Ferric perchlorate decahydrate (0.549 g, 1.03 mmol) was dissolved in 2.0 mL methanol by mixing with a disposable Pasteur pipette in a small vial. In a separate vial, 3,5-dichlorobenzoic acid (0.097 g, 0.51 mmol) was dissolved in 2.0 mL of methanol followed by triethylamine (0.14 mL, 1.0 mmol). The iron solution was added to the TPA solution and mixed well. This was followed by addition of the carboxylate solution. A light-brown solution was observed. After stirring for 30 minutes, the solution was gravity filtered. The filtrate was allowed to sit to form crystals. After several days, light-brown short needle-shaped crystals were formed. These crystals diffracted X-rays poorly, hence

X-ray crystallographic characterization could not be done. However, the ^1H NMR and UV-visible spectra of the crystals were consistent with a dibridged complex.

2.3.5.7 Preparation of $[\text{Fe}_2(\text{TPA})_2\text{O}(4\text{-fluorobenzoato})](\text{ClO}_4)_3$

TPA•3HClO₄ (0.591 g, 0.999 mmol) and triethylamine (0.56 mL, 4.0 mmol) were added to 40.0 mL methanol and stirred for several minutes with slight heating (30 °C). Ferric perchlorate decahydrate (0.549 g, 1.03 mmol) was dissolved in 2.0 mL methanol by mixing with a disposable Pasteur pipette in a small vial. In a separate vial, 4-fluorobenzoic acid (0.075 g, 0.54 mmol) was dissolved in 2.0 mL of methanol followed by triethylamine (0.07 mL, 0.5 mmol). The iron solution was added to the TPA solution and mixed well. This was followed by the addition of the carboxylate solution. A brownish-green solution was observed. After stirring for 30 minutes, the solution was gravity filtered. The filtrate was allowed to sit to form crystals. After several days, brown-black rectangular prisms were formed. X-ray crystallographic studies showed that the compound was $[\text{Fe}_2(\text{TPA})_2\text{O}(4\text{-fluorobenzoato})](\text{ClO}_4)_3$ and structure will be discussed in the section 3.3.5 below.

2.3.5.8 Preparation of $[\text{Fe}_2(\text{TPA})_2\text{O}(4\text{-methoxybenzoato})](\text{ClO}_4)_3$

TPA•3HClO₄ (0.591 g, 0.999 mmol) and triethylamine (0.56 mL, 4.0 mmol) were added to 40.0 mL methanol and stirred for several minutes with slight heating (30 °C). Ferric perchlorate decahydrate (0.549 g, 1.03 mmol) was dissolved in 2.0 mL methanol by mixing with a disposable Pasteur pipette in a small vial. In a separate vial, 4-methoxybenzoic acid (0.50 mmol, 0.076 g) was dissolved in 2.0 mL of methanol

followed by triethylamine (0.07 mL, 0.5 mmol). The iron solution was added to the TPA solution and mixed well. This was followed by the addition of the carboxylate solution. A light-green solution was observed. After stirring for 30 minutes, the solution was gravity filtered. The filtrate was allowed to sit to form crystals. After several days, maroon rectangular prisms were formed. X-ray crystallographic studies showed that the compound was $[Fe_2(TPA)_2O(4\text{-methoxybenzoato})](ClO_4)_3$ and its structure will be discussed in section 3.3.4 below.

2.3.5.9 Attempted preparation of $[Fe_2(TPA)_2O(4\text{-pyridinecarboxylato})](ClO_4)_3$

$TPA \cdot 3HClO_4$ (0.592 g, 1.00 mmol) and triethylamine (0.56 mL, 4.0 mmol) were added to 40.0 mL methanol and stirred for several minutes with slight heating (30 °C). Ferric perchlorate decahydrate (0.549 g, 1.03 mmol) was dissolved in 2.0 mL methanol by mixing with a disposable Pasteur pipette in a small vial. In a separate vial, 4-pyridinecarboxylic acid (0.062 g, 0.50 mmol) was dissolved in 2.0 mL of methanol followed by triethylamine (0.07 mL, 0.5 mmol). The iron solution was added to the TPA solution and mixed well. This was followed by the addition of the carboxylate solution. A greenish-yellow solution was observed. After stirring for 30 minutes, a drop of $HClO_4$ was added to the solution and gravity filtered. The filtrate was allowed to sit to form crystals. The crystals that formed were dissolved in minimum amount of acetonitrile and kept in an ethyl acetate vapor bath. After several days, dark-brown rectangular prisms were formed. X-ray crystallographic studies showed that the desired compound was not formed, but instead proved to be $[Fe_2(TPA)_2O(OAc)](ClO_4)_3 \cdot H_2O$ and the structure will be discussed in section 3.3.2.2 below.

2.3.5.10 Attempted preparation of $[Fe_2(TPA)_2O(4\text{-cyanobenzoato})](ClO_4)_3$

TPA•3HClO₄ (0.592 g, 1.00 mmol) and triethylamine (0.56 mL, 4.0 mmol) were added to 40.0 mL methanol and stirred for several minutes with slight heating (30 °C). Ferric perchlorate decahydrate (0.549 g, 1.03 mmol) was dissolved in 2.0 mL methanol by mixing with a disposable Pasteur pipette in a small vial. In a separate vial, 4-cyanobenzoic acid (0.075 g, 0.51 mmol) was dissolved in 2.0 mL of methanol followed by triethylamine (0.07 mL, 0.5 mmol). The iron solution was added to the TPA solution and mixed well. This was followed by the addition of the carboxylate solution. A light-green solution was observed. After stirring for 30 minutes, the solution was gravity filtered. The filtrate was allowed to sit to form crystals. The resultant light-brown powdery crystals were recrystallized using acetonitrile (99%) and kept in an ethyl acetate vapor bath. The crystals formed were not suitable for X-ray crystallography. However, the ¹H NMR and UV-visible spectra of the crystals were consistent with a dibridged complex.

2.3.5.11 Preparation of $[Fe_2(TPA)_2O(4\text{-hydroxybenzoato})](ClO_4)_3$

TPA•3HClO₄ (0.592 g, 1.00 mmol) and triethylamine (0.56 mL, 4.0 mmol) were added to 40.0 mL methanol and stirred for several minutes with slight heating (30 °C). Ferric perchlorate decahydrate (0.549 g, 1.03 mmol) was dissolved in 2.0 mL methanol by mixing with a disposable Pasteur pipette in a small vial. In a separate vial, 4-hydroxybenzoic acid (0.070 g, 0.51 mmol) was dissolved in 2.0 mL of methanol followed by triethylamine (0.07 mL, 0.5 mmol). The iron solution was added to the TPA solution and

mixed well. This was followed by the addition of the carboxylate solution. A light-brown solution was observed. After stirring for 30 minutes, the solution was gravity filtered. The filtrate was allowed to sit to form crystals. The resultant light-brown powdery crystals were recrystallized using acetonitrile (99%) and kept in an ethyl acetate vapor bath. After several days, brown rectangular prisms were formed. X-ray crystallographic studies showed that the compound was $[\text{Fe}_2(\text{TPA})_2\text{O}(4\text{-hydroxy-benzoato})](\text{ClO}_4)_3$ and its structure will be discussed in section 3.3.3 below.

CHAPTER III

Results

3.1 Electronic Spectroscopic Results

Electronic spectra of the synthesized complexes were recorded in the 250-900 nm region. Spectra of both diluted and concentrated samples were analyzed. All of the samples were prepared using 99% acetonitrile. The UV-visible spectrum of the primary ligand of this study, tris(2-pyridylmethyl)amine ($\text{TPA}\bullet\text{3HClO}_4$), is shown in **Figure 5**. The spectrum has a strong single absorption feature at 270 nm. Electronic spectral data are collected in **Table 1**.

The electronic spectra of the single oxido-bridged diiron complex $[\{\text{Fe}(\text{TPA})\text{Br}\}_2\text{O}](\text{ClO}_4)_2\bullet\text{H}_2\text{O}$ are shown in **Figure 6** and **Figure 7**. The electronic spectra of $[\text{Fe}_2(\text{TPA})_2\text{O}(\text{OAc})](\text{ClO}_4)_3$ are shown in **Figure 8** and **Figure 9**. The electronic spectra of $[\text{Fe}_2(\text{TPA})_2\text{O}(\text{OAc})](\text{ClO}_4)_3\bullet\text{H}_2\text{O}$ are shown in **Figure 10** and **Figure 11**. The electronic spectra of $[\text{Fe}_2(\text{TPA})_2\text{O}(4\text{-hydroxybenzoato})](\text{ClO}_4)_3$ are shown in **Figure 12** and **Figure 13**. The electronic spectra of $[\text{Fe}_2(\text{TPA})_2\text{O}(4\text{-methoxybenzoato})](\text{ClO}_4)_3$ are shown in **Figure 14** and **Figure 15**. The electronic spectra of $[\text{Fe}_2(\text{TPA})_2\text{O}(4\text{-fluorobenzoato})](\text{ClO}_4)_3$ are shown in **Figure 16** and **Figure 17**. The electronic spectra of $[\text{Fe}_2(\text{TPA})_2\text{O}(4\text{-cyanobenzoato})](\text{ClO}_4)_3$ are shown in **Figure 18** and **Figure 19**. The electronic spectra of $[\text{Fe}_2(\text{TPA})_2\text{O}(3,5\text{-dimethylbenzoato})(\text{ClO}_4)_3\bullet0.5\text{H}_2\text{O}$ are shown in **Figure 20** and **Figure 21**. The electronic spectra of $[\text{Fe}_2(\text{TPA})_2\text{O}(3,5\text{-dihydroxybenzoato})](\text{ClO}_4)_3\bullet\text{CH}_3\text{CN}$ are shown in **Figure 22** and **Figure 23**. The electronic spectra of $[\text{Fe}_2(\text{TPA})_2\text{O}(3,5\text{-dimethoxybenzoato})](\text{ClO}_4)_3$ are shown in **Figure 24** and **Figure 25**. The electronic spectra of $[\text{Fe}_2(\text{TPA})_2\text{O}(3,5\text{-dichlorobenzoato})](\text{ClO}_4)_3$

are shown in **Figure 26** and **Figure 27**. The electronic spectra of $[Fe_2(TPA)_2O(3,5\text{-dibromobenzoato})](ClO_4)_3$ are shown in **Figure 28** and **Figure 29**. The electronic spectra of $[Fe_2(TPA)_2O(3,5\text{-dinitrobenzoato})](ClO_4)_3$ are shown in **Figure 30** and **Figure 31**.

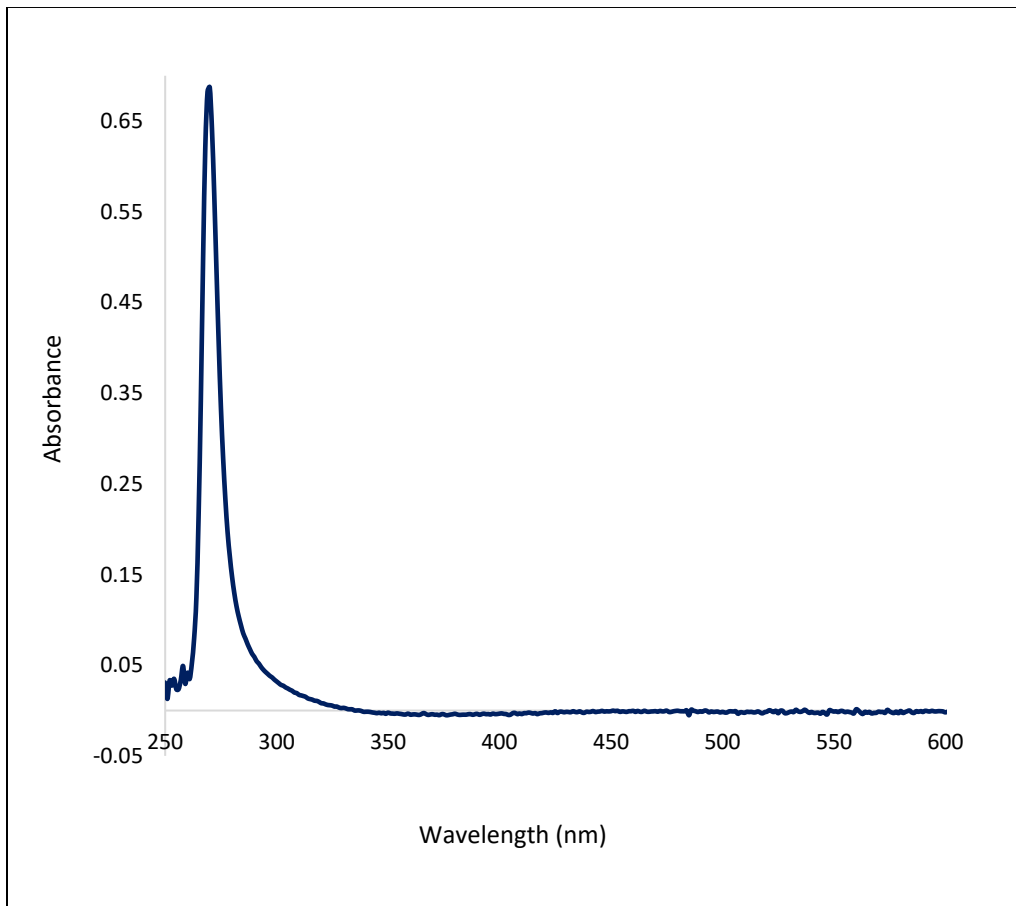


Figure 5. UV-Visible spectrum of $TPA \bullet 3HClO_4$.

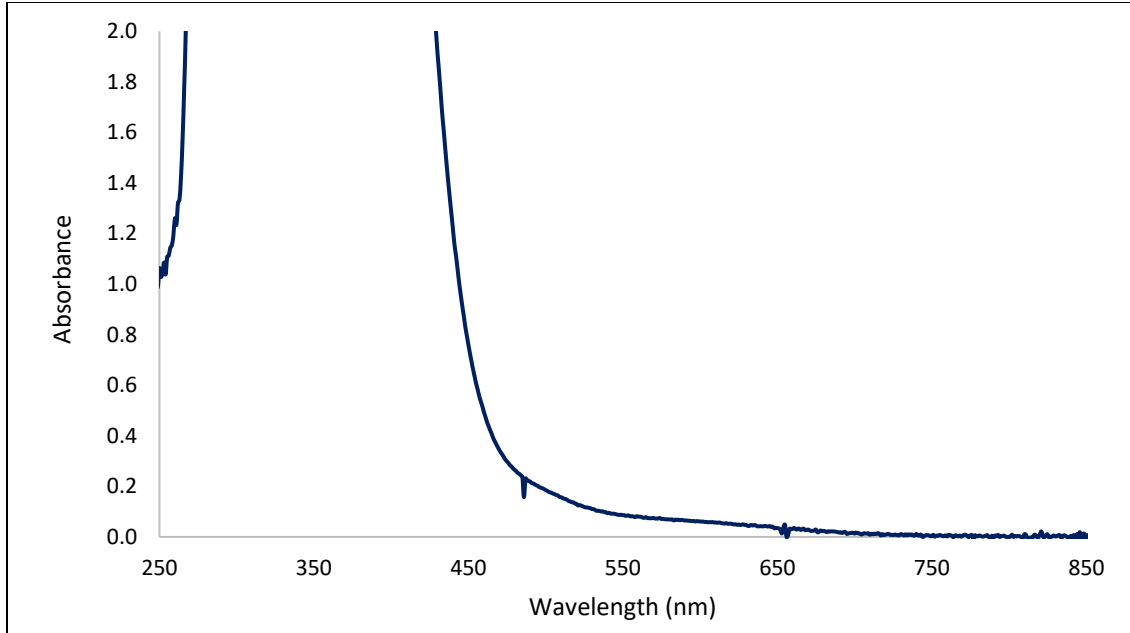


Figure 6. Electronic spectrum of $[Fe(TPA)Br_2O](ClO_4)_2 \bullet H_2O$ (Concentrated).

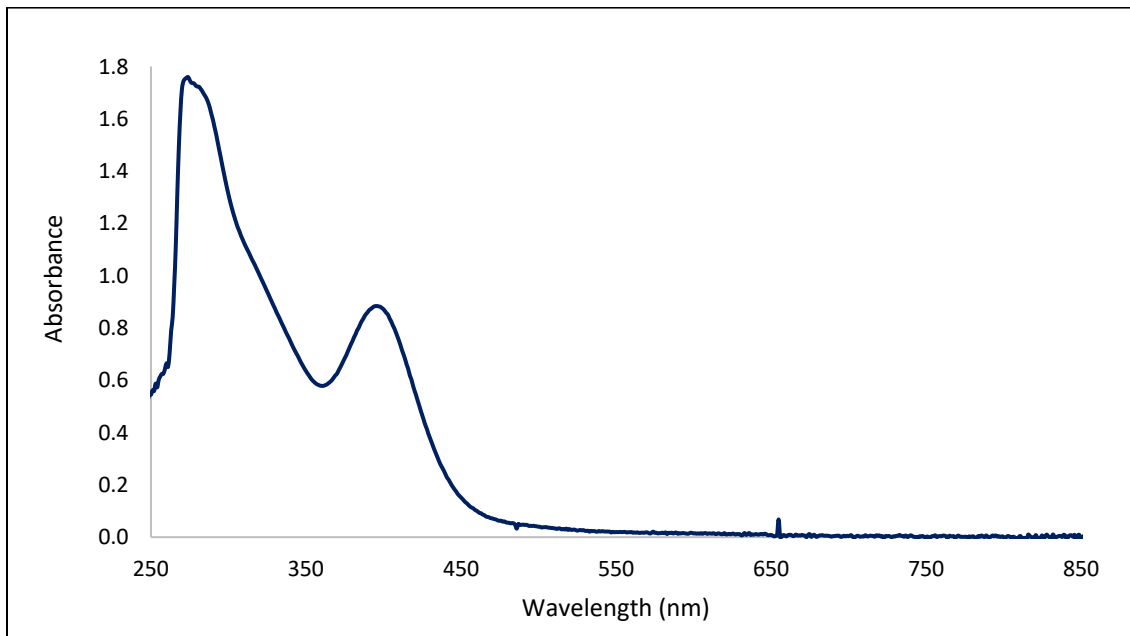


Figure 7. Electronic spectrum of $[Fe(TPA)Br_2O](ClO_4)_2 \bullet H_2O$ (Diluted).

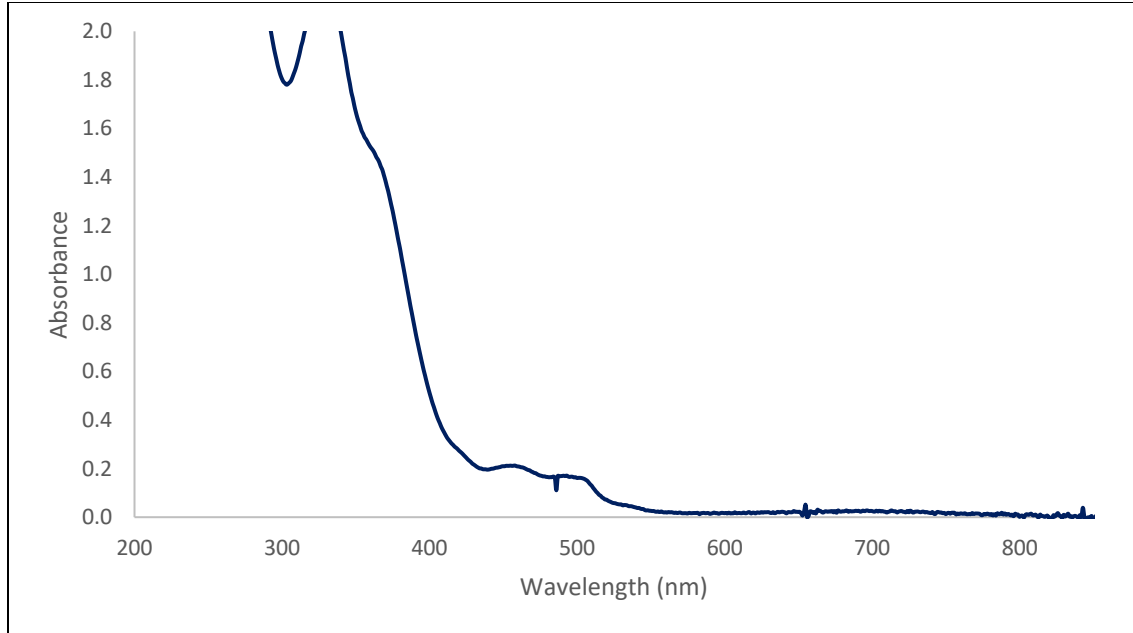


Figure 8. Electronic spectrum of $[Fe_2(TPA)_2O(OAc)](ClO_4)_3$ (Concentrated).

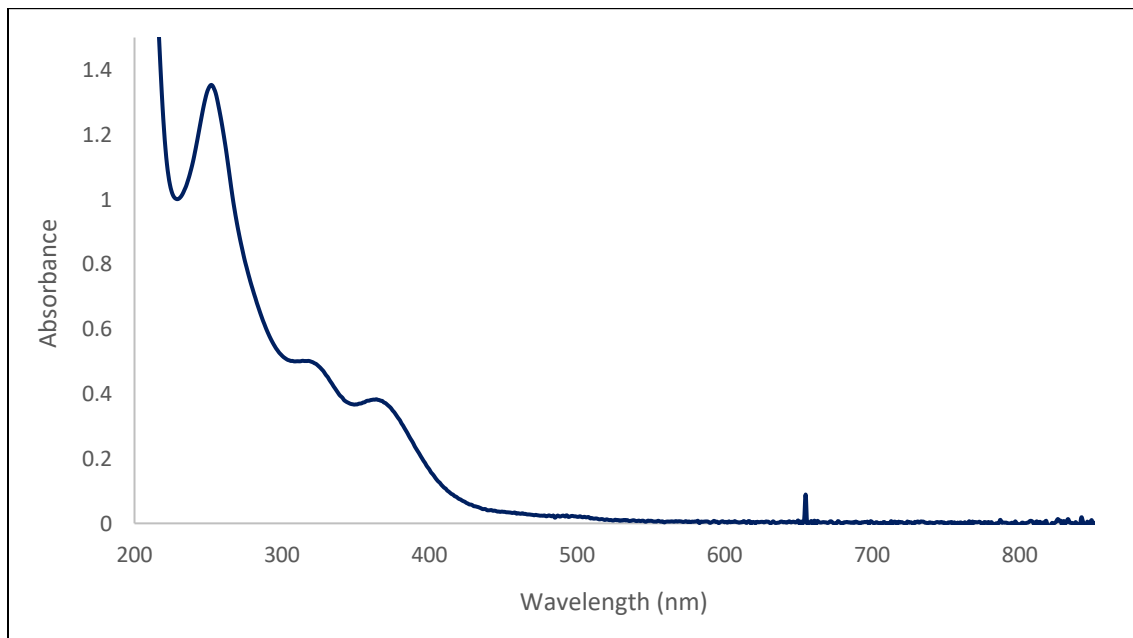


Figure 9. Electronic spectrum of $[Fe_2(TPA)_2O(OAc)](ClO_4)_3$ (Diluted).

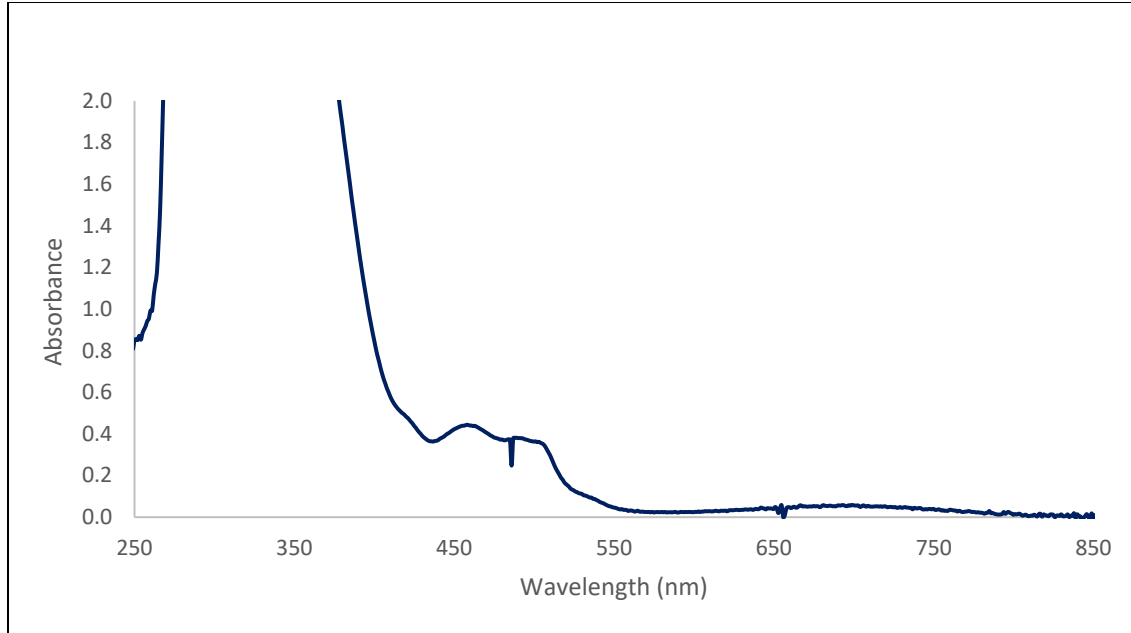


Figure 10. Electronic spectrum of $[Fe_2(TPA)_2O(OAc)](ClO_4)_3 \cdot H_2O$ (Concentrated).

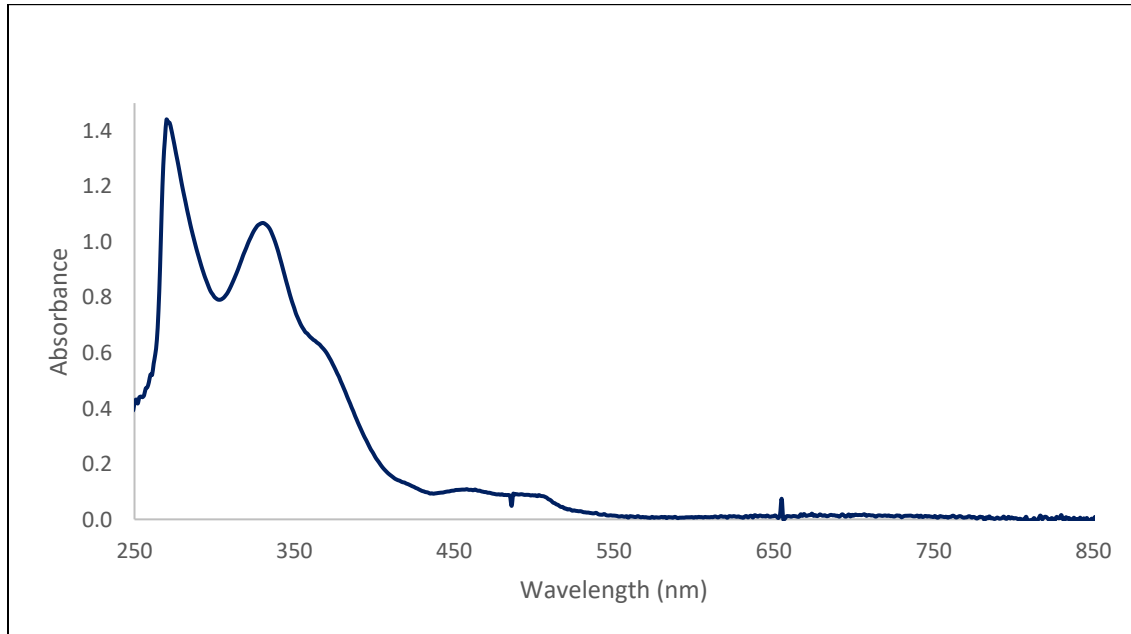


Figure 11. Electronic spectrum of $[Fe_2(TPA)_2O(OAc)](ClO_4)_3 \cdot H_2O$ (Diluted).

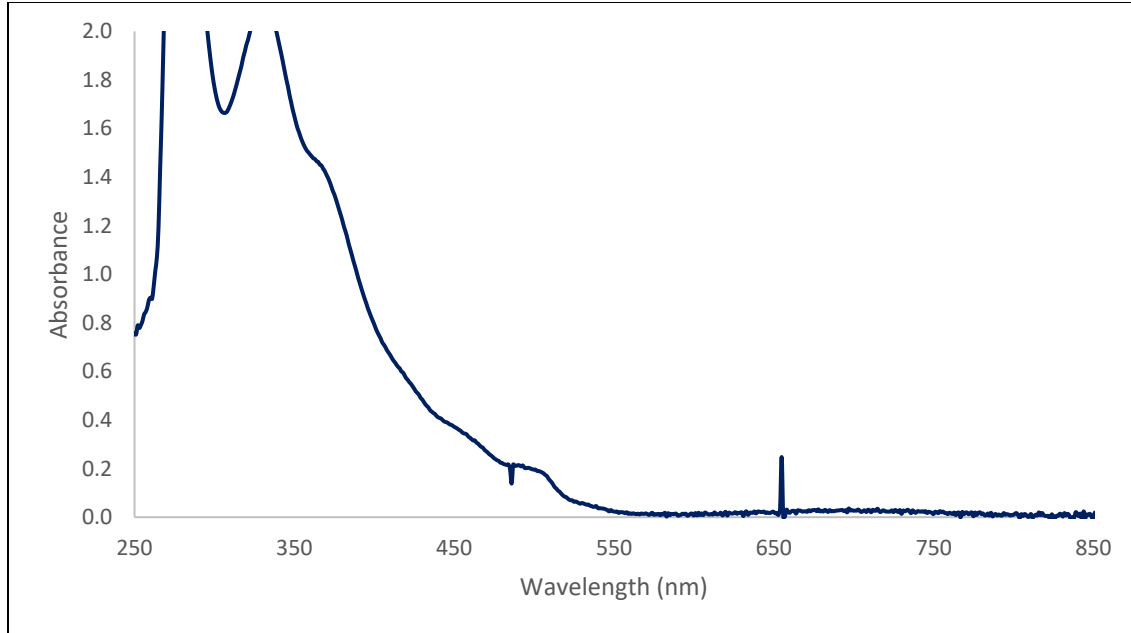


Figure 12. Electronic spectrum of $[Fe_2(TPA)_2O(4\text{-hydroxybenzoato})](ClO_4)_3$ (Concentrated).

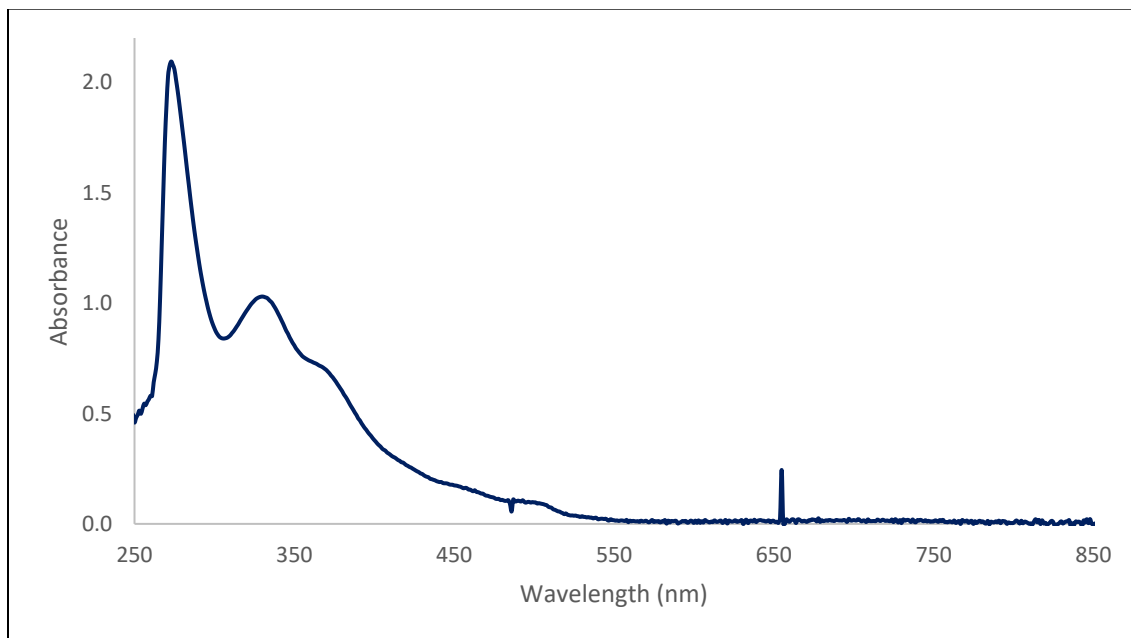


Figure 13. Electronic spectrum of $[Fe_2(TPA)_2O(4\text{-hydroxybenzoato})](ClO_4)_3$ (Diluted).

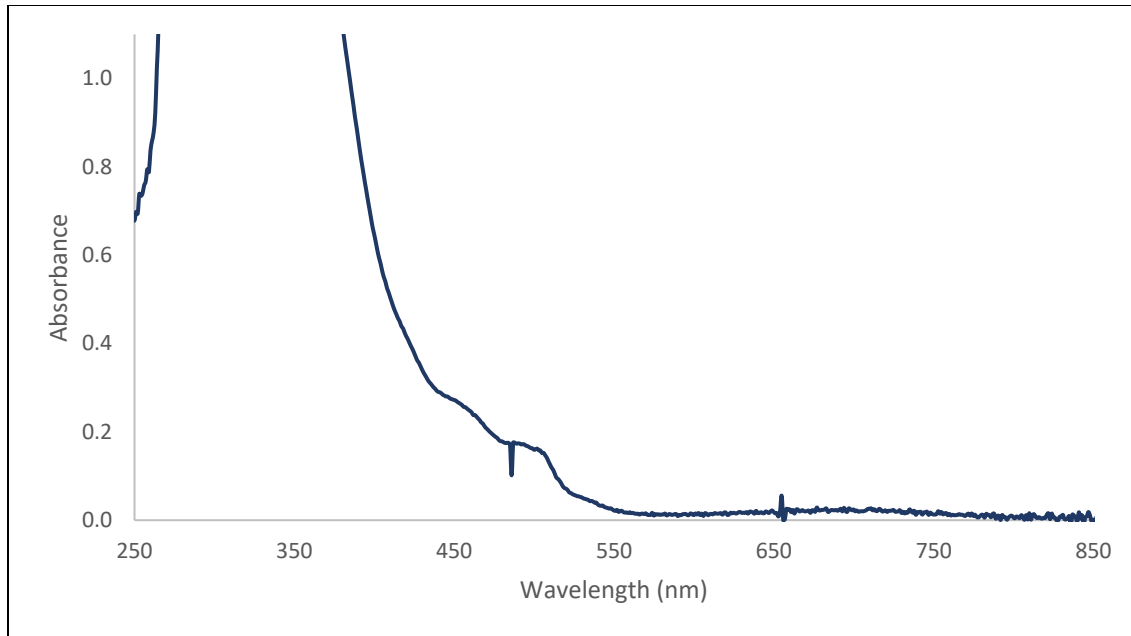


Figure 14. Electronic spectrum of $[Fe_2(TPA)_2O(4\text{-methoxybenzoato})](ClO_4)_3$ (Concentrated).

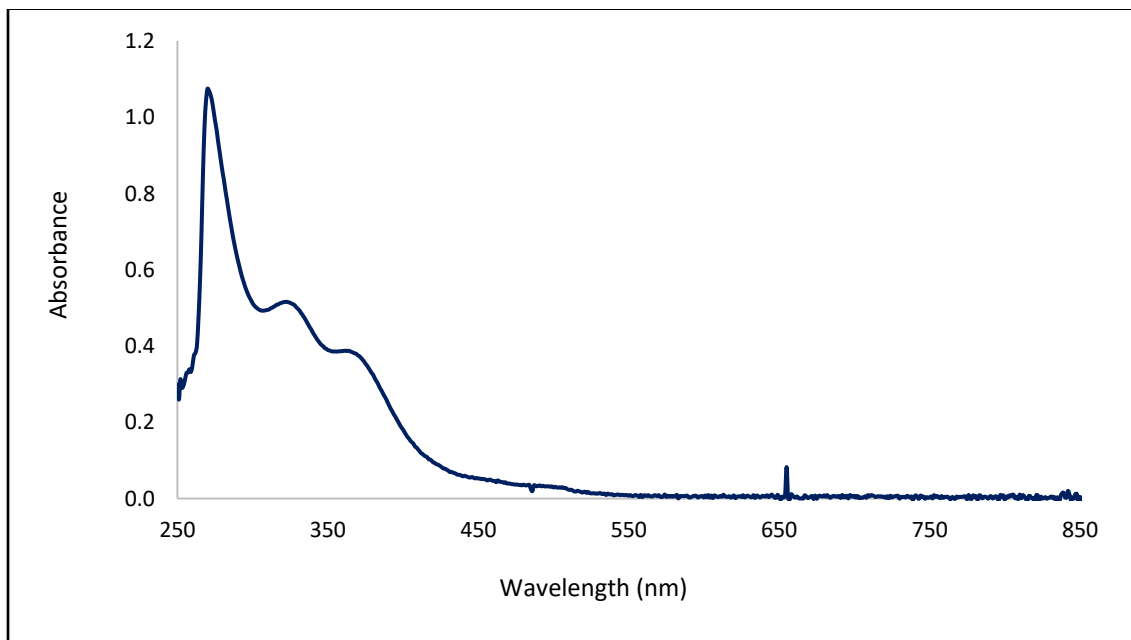


Figure 15. Electronic spectrum of $[Fe_2(TPA)_2O(4\text{-methoxybenzoato})](ClO_4)_3$ (Diluted).

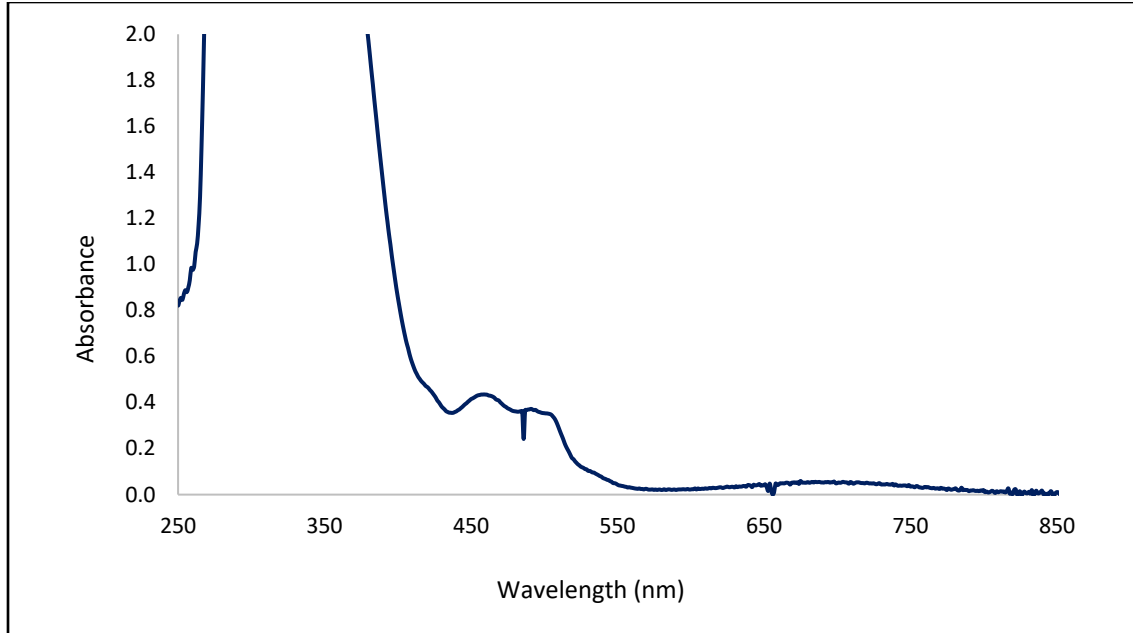


Figure 16. Electronic spectrum of $[Fe_2(TPA)_2O(4\text{-fluorobenzoato})](ClO_4)_3$ (Concentrated).

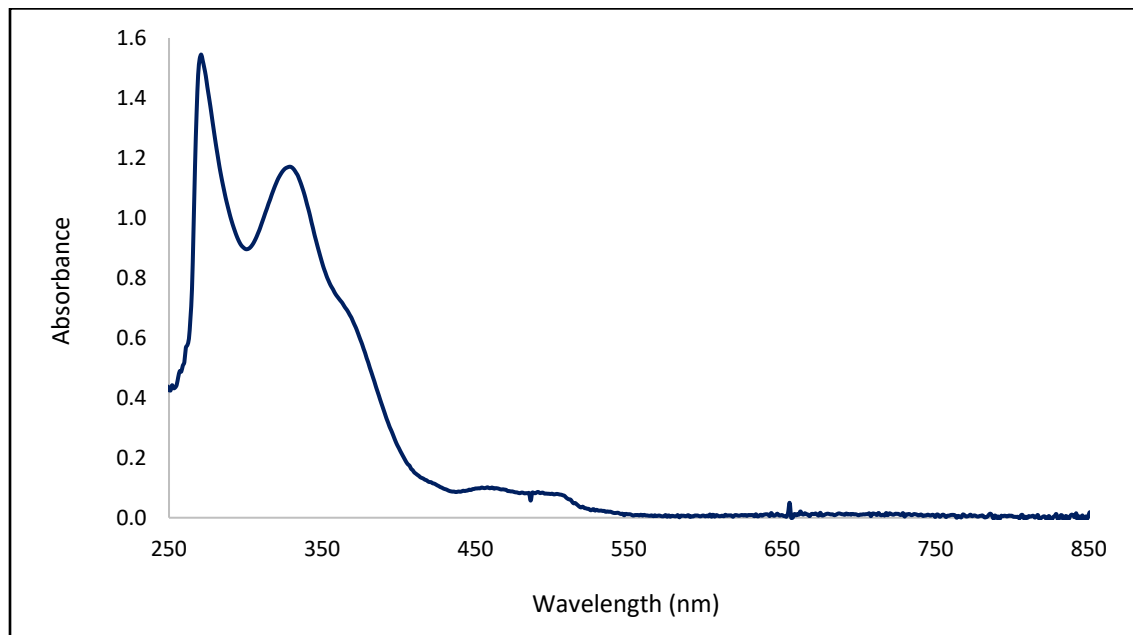


Figure 17. Electronic spectrum of $[Fe_2(TPA)_2O(4\text{-fluorobenzoato})](ClO_4)_3$ (Diluted).

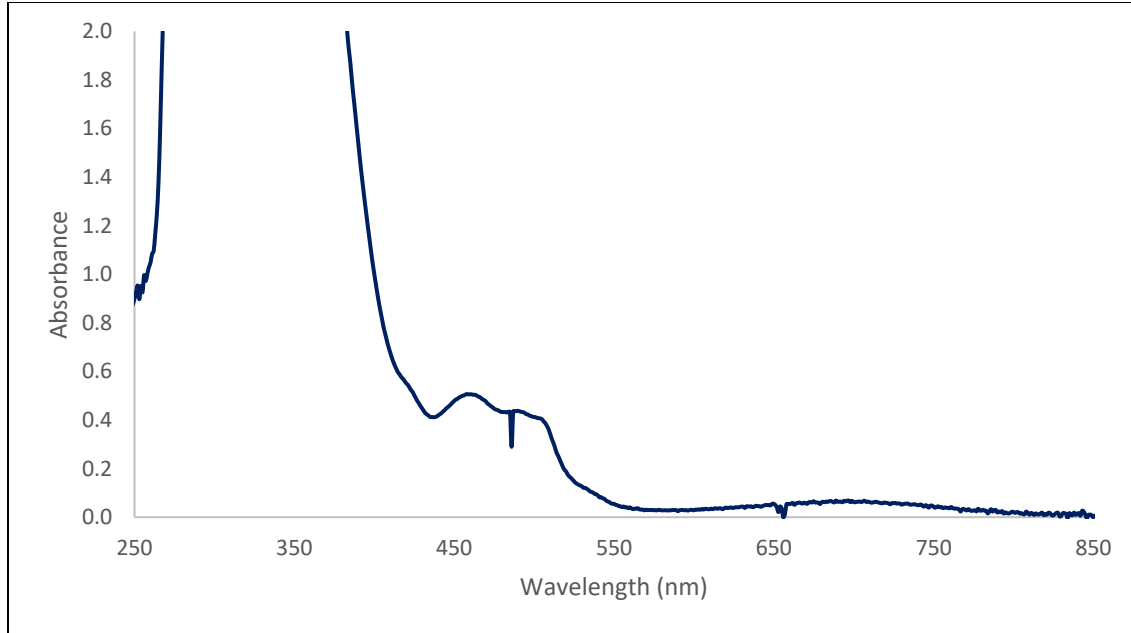


Figure 18. Electronic spectrum of $[Fe_2(TPA)_2O(4\text{-cyanobenzoato})](ClO_4)_3$ (Concentrated).

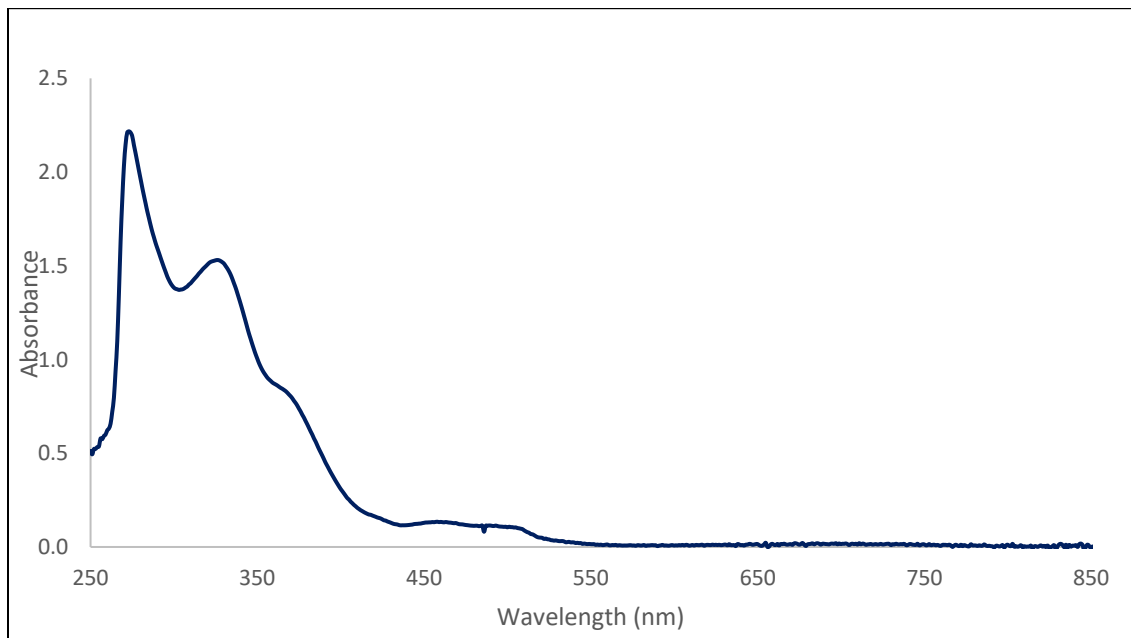


Figure 19. Electronic spectrum of $[Fe_2(TPA)_2O(4\text{-cyanobenzoato})](ClO_4)_3$ (Diluted).

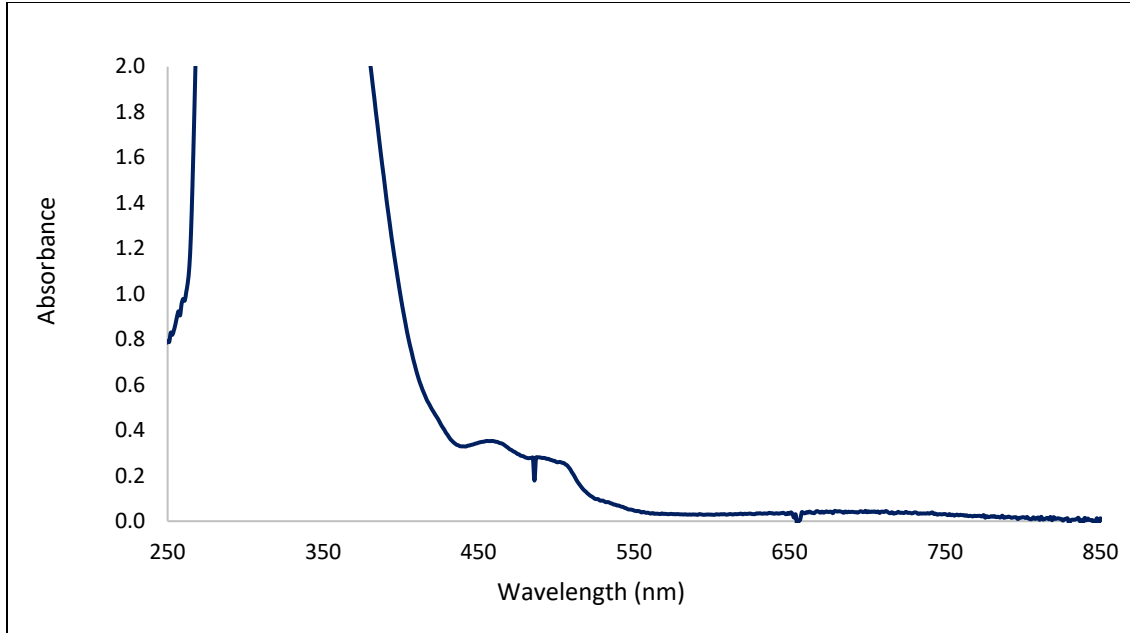


Figure 20. Electronic spectrum of $[Fe_2(TPA)_2O(3,5\text{-dimethylbenzoato})](ClO_4)_3 \bullet 0.5H_2O$ (Concentrated).

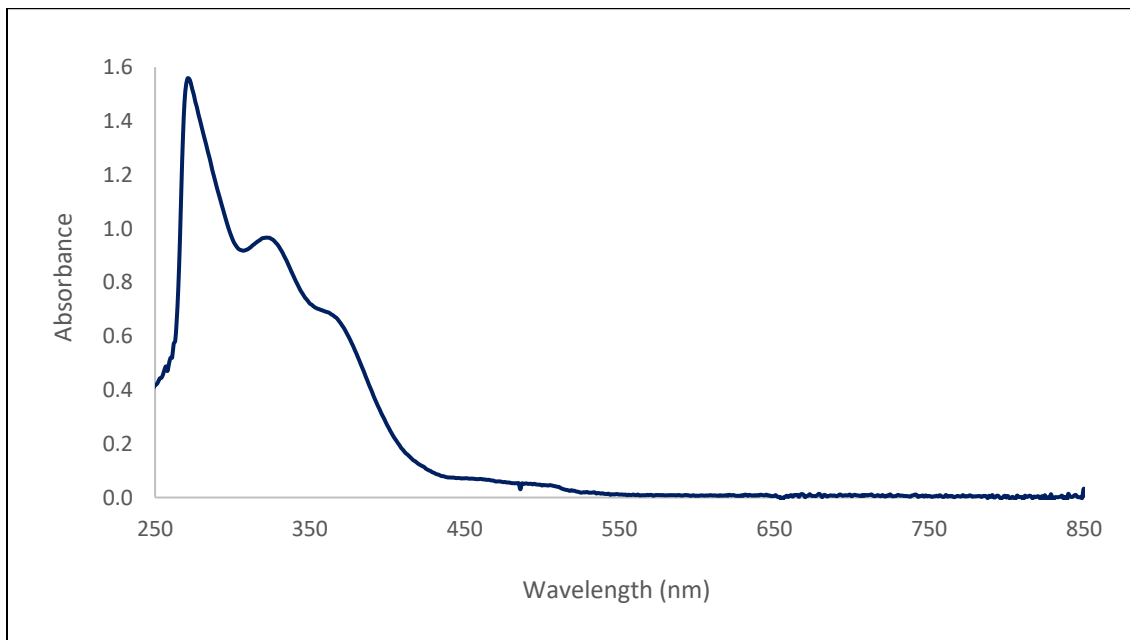


Figure 21. Electronic spectrum of $[Fe_2(TPA)_2O(3,5\text{-dimethylbenzoato})](ClO_4)_3 \bullet 0.5H_2O$ (Diluted).

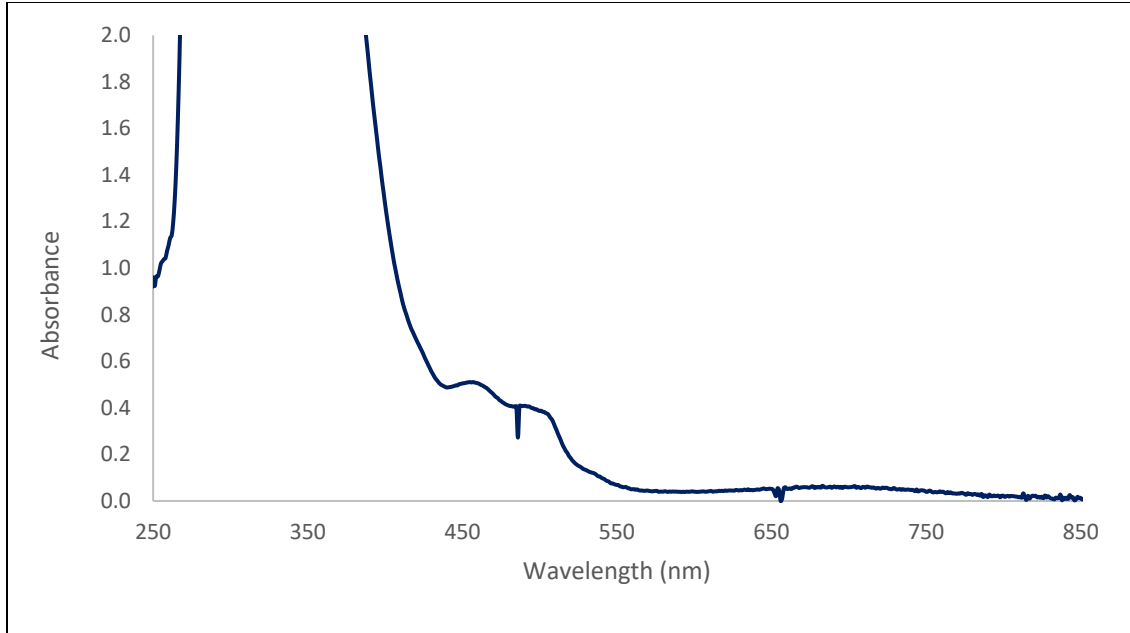


Figure 22. Electronic spectrum of $[Fe_2(TPA)_2O(3,5\text{-dihydroxybenzoato})](ClO_4)_3$ • CH_3CN (Concentrated).

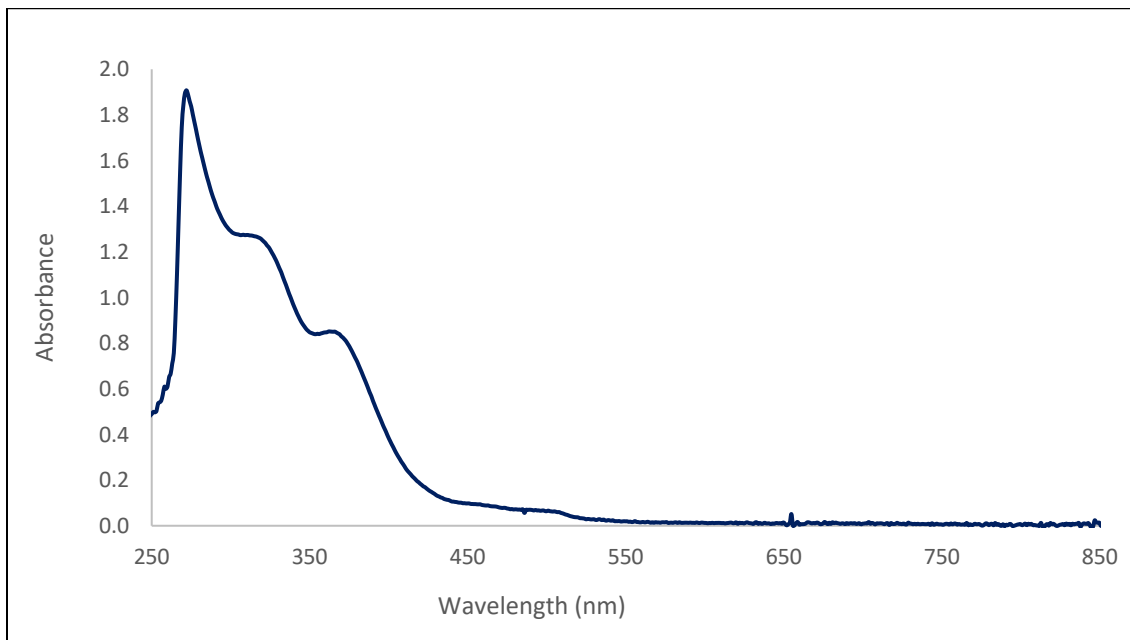


Figure 23. Electronic spectrum of $[Fe_2(TPA)_2O(3,5\text{-dihydroxybenzoato})](ClO_4)_3$ • CH_3CN (Diluted).

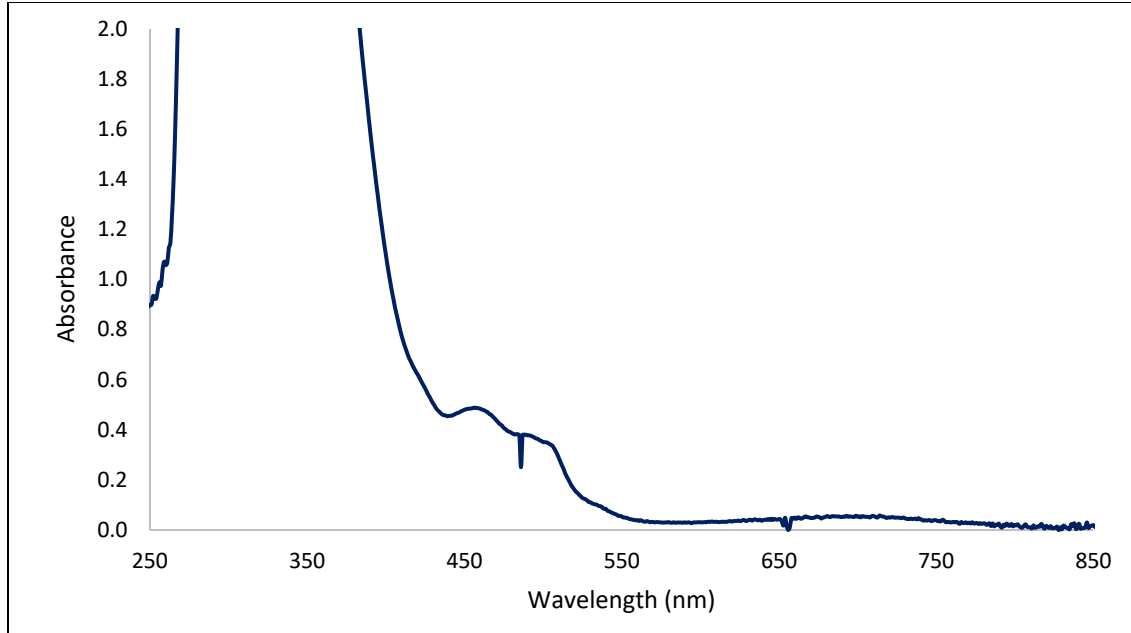


Figure 24. Electronic spectrum of $[Fe_2(TPA)_2O(3,5\text{-dimethoxybenzoato})](ClO_4)_3$ (Concentrated).

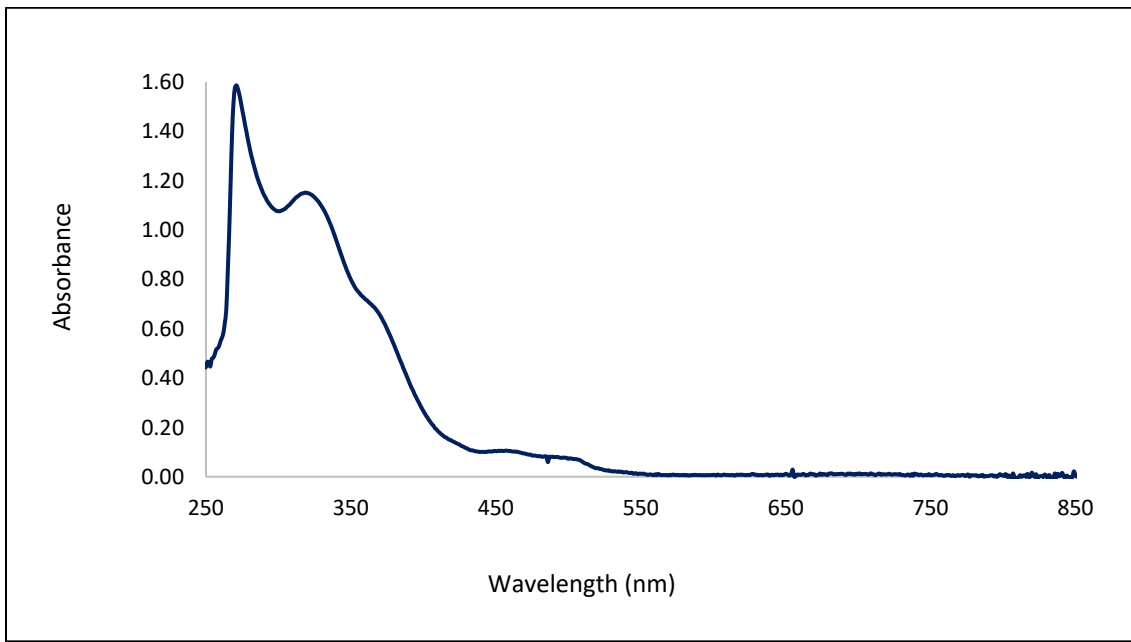


Figure 25. Electronic spectrum of $[Fe_2(TPA)_2O(3,5\text{-dimethoxybenzoato})](ClO_4)_3$ (Diluted).

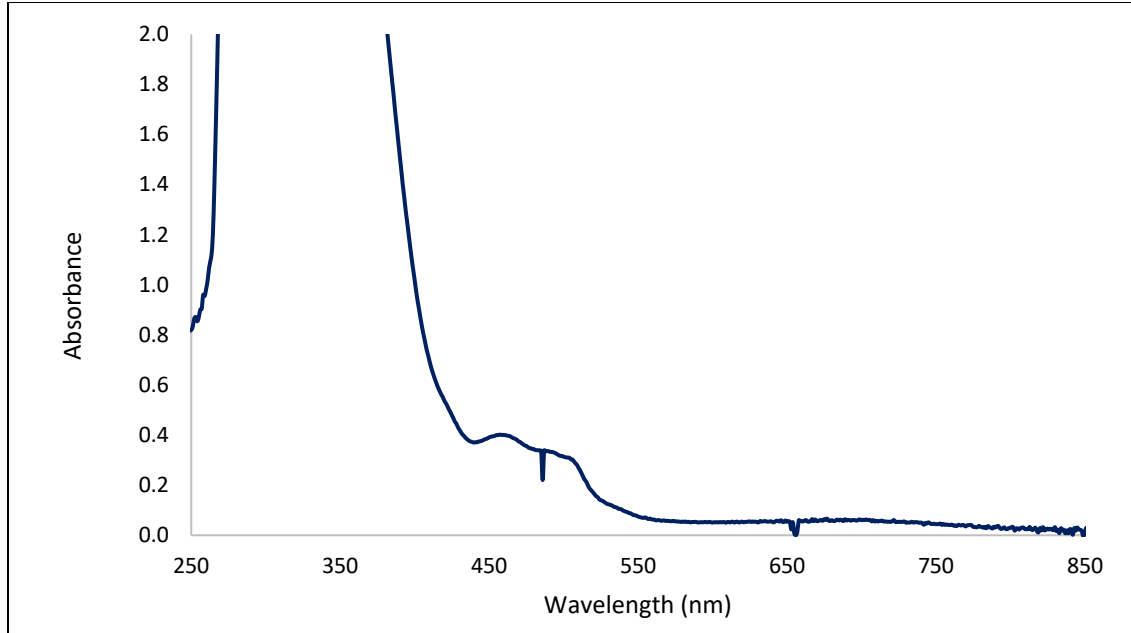


Figure 26. Electronic spectrum of $[Fe_2(TPA)_2O(3,5\text{-dichlorobenzoato})](ClO_4)_3$ (Concentrated).

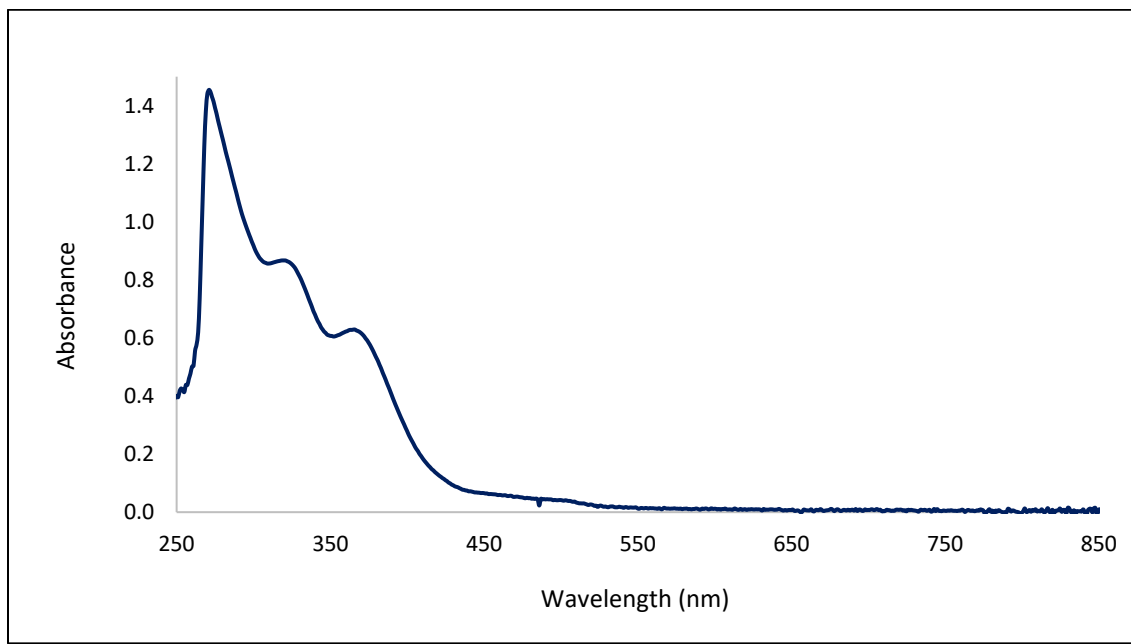


Figure 27. Electronic spectrum of $[Fe_2(TPA)_2O(3,5\text{-dichlorobenzoato})](ClO_4)_3$ (Diluted).

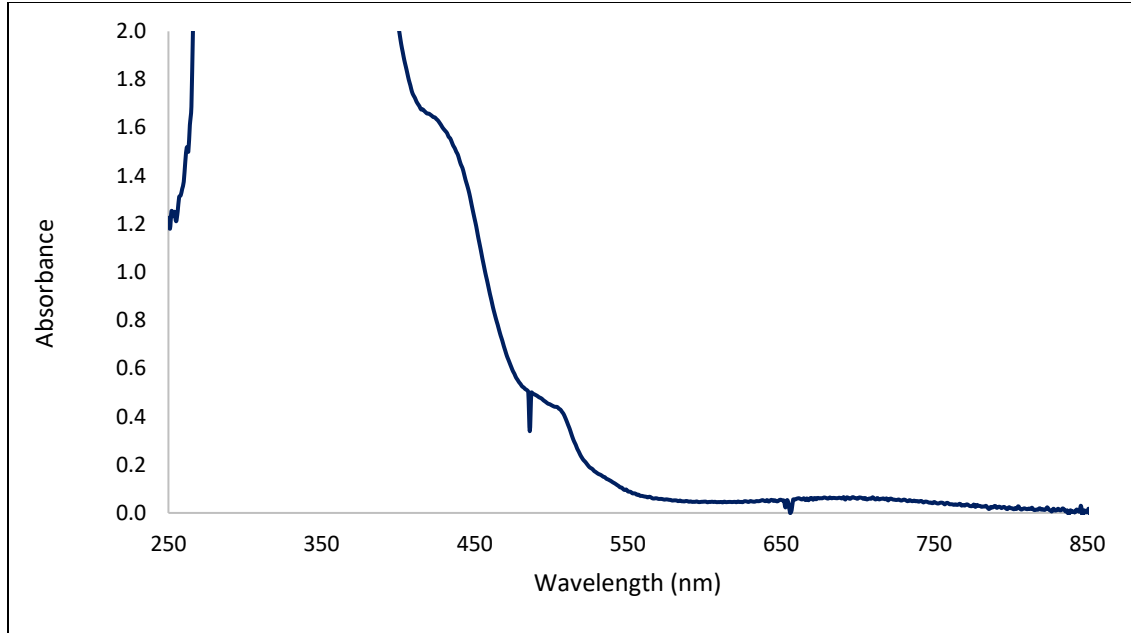


Figure 28. Electronic spectrum of $[Fe_2(TPA)_2O(3,5\text{-dibromobenzoato})](ClO_4)_3$ (Concentrated).

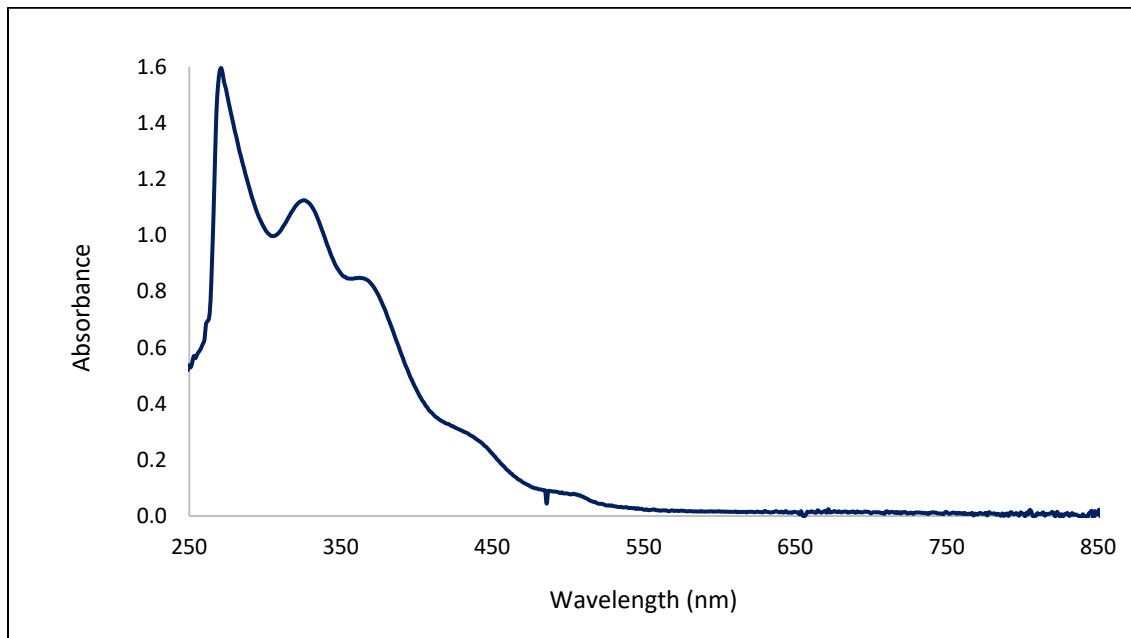


Figure 29. Electronic spectrum of $[Fe_2(TPA)_2O(3,5\text{-dibromobenzoato})](ClO_4)_3$ (Diluted).

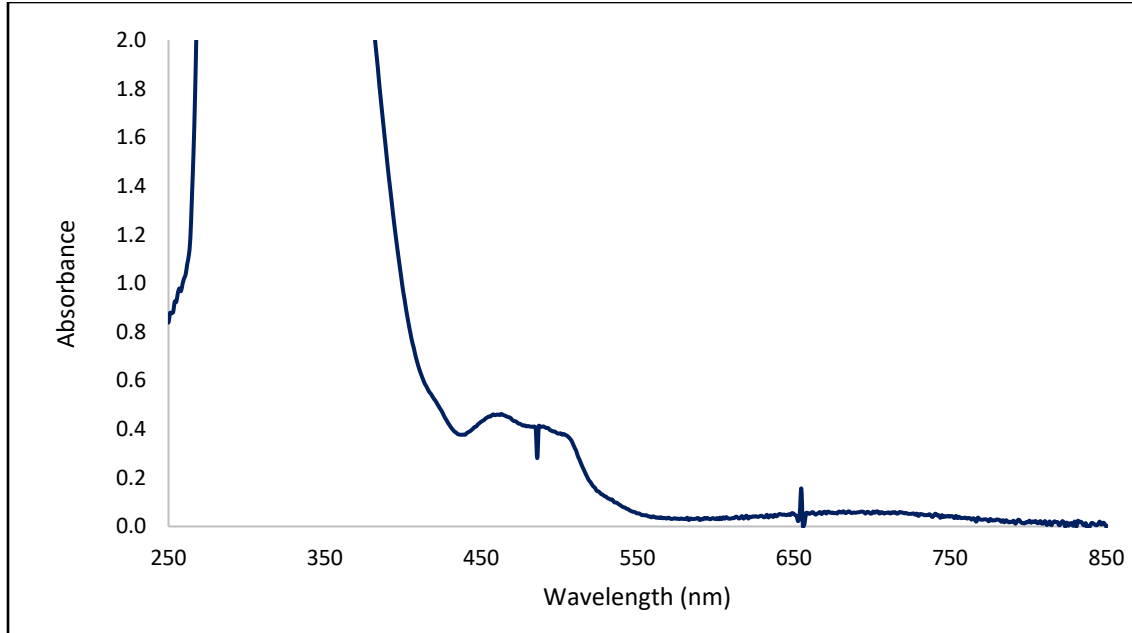


Figure 30. Electronic spectrum of $[Fe_2(TPA)_2O(3,5\text{-dinitrobenzoato})](ClO_4)_3$ (Concentrated).

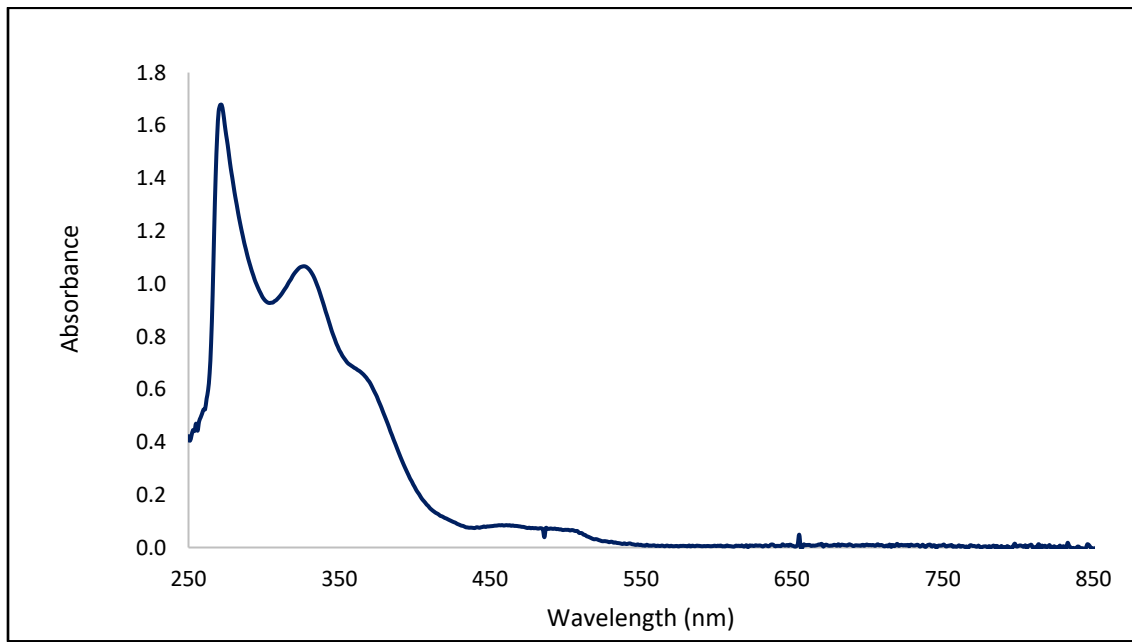


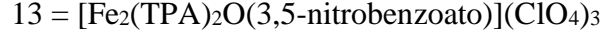
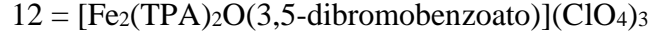
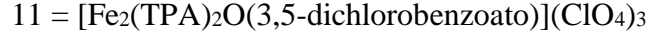
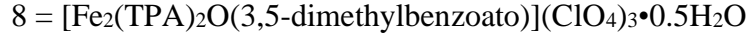
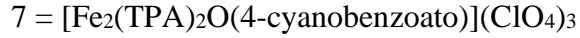
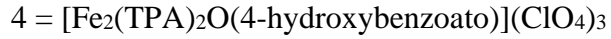
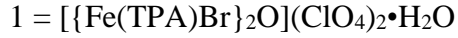
Figure 31. Electronic spectrum of $[Fe_2(TPA)_2O(3,5\text{-dinitrobenzoato})](ClO_4)_3$ (Diluted).

Table 1. Absorption bands of oxido-bridged diiron(III) complexes

1	2	3	4	5	6	7	8	9	10	11	12	13
274 (19.95)	252 (20.83)	270 (13.15)	273 (24.92)	270 (35.81)	271 (16.26)	273 (19.98)	271 (17.61)	272 (19.27)	271 (15.47)	271 (16.53)	270 (18.61)	272 (18.63)
304 (sh)	320 (7.67)	330 (9.75)	330 (12.25)	322 (17.19)	333 (12.10)	326 (13.79)	323 (10.91)	306 (sh)	319 (11.23)	319 (9.85)	327 (13.20)	327 (11.84)
396 (10.04)	364 (sh)	366 (sh)	370 (sh)	364 (11.48)	365 (sh)	358 (sh)	350 (sh)	362 (8.60)	358 (sh)	366 (7.15)	367 (9.90)	354 (sh)
	417 (sh)	420 (sh)	422 (sh)	435 (sh)	422 (sh)	423 (sh)	416 (sh)	421 (sh)	417 (sh)	420 (sh)	423 (3.73)	418 (sh)
	458 (0.93)	460 (1.01)	466 (sh)	449 (sh)	459 (1.14)	458 (1.14)	458 (1.00)	457 (1.29)	456 (1.91)	460 (1.01)	430 (3.61)	463 (1.16)
	496 (0.73)	489 (0.871)	487 (sh)	490 (sh)	494 (0.97)	490 (sh)	493 (sh)	490 (1.03)	491 (0.92)	489 (0.85)		490 (1.15)
			507 (sh)	498 (sh)		508 (sh)				496 (sh)	508 (sh)	503 (sh)
		535 (sh)		534 (sh)	525 (sh)	539 (sh)	530 (sh)	524 (sh)		525 (sh)		
	703 (0.12)	699 (0.14)	697 (0.21)	677 (0.24)	675 (0.16)	689 (0.15)	699 (0.13)	683 (0.07)	714 (0.141)	677 (0.17)	697 (0.15)	682 (0.16)

Note: Data are given in the format – Wavelength λ in nm (ϵ in $\text{mM}^{-1}\text{cm}^{-1}$)

Where,



3.2 ^1H NMR Spectroscopic Results

In this section the ^1H NMR spectra for the TPA ligand followed by various oxido-bridged diiron(III) complexes are presented. The NMR spectrum of TPA•3HClO₄ in D₂O is shown in **Figure 32** followed by **Table 2** which lists the relevant NMR peak assignments for this compound.

The ^1H NMR of [{Fe(TPA)Br₂O}](ClO₄)₂•H₂O in 99% CD₃CN is shown in **Figure 33**. The ^1H NMR of [Fe₂(TPA)₂O(OAc)](ClO₄)₃ in 99% CD₃CN is shown in **Figure 34**. The ^1H NMR of [Fe₂(TPA)₂O(OAc)](ClO₄)₃•H₂O in 99% CD₃CN is shown in **Figure 35**. The ^1H NMR of [Fe₂(TPA)₂O(4-hydroxybenzoato)](ClO₄)₃ in 99% CD₃CN is shown in **Figure 36**. The ^1H NMR of [Fe₂(TPA)₂O(4-methoxybenzoato)](ClO₄)₃ in 99% CD₃CN is shown in **Figure 37**. The ^1H NMR of [Fe₂(TPA)₂O(4-fluorobenzoato)](ClO₄)₃ in 99% CD₃CN is shown in **Figure 38**. The ^1H NMR of [Fe₂(TPA)₂O(4-cyanobenzoato)](ClO₄)₃ in 99% CD₃CN is shown in **Figure 39**. The ^1H NMR of [Fe₂(TPA)₂O(3,5-dimethylbenzoato)](ClO₄)₃•0.5H₂O in 99% CD₃CN is shown in **Figure 40**. The ^1H NMR of [Fe₂(TPA)₂O(3,5-dihydroxybenzoato)](ClO₄)₃•CH₃CN in 99% CD₃CN is shown in **Figure 41**. The ^1H NMR of [Fe₂(TPA)₂O(3,5-dimethoxybenzoato)](ClO₄)₃ in 99% CD₃CN is shown in **Figure 42**. The ^1H NMR of [Fe₂(TPA)₂O(3,5-dichlorobenzoato)](ClO₄)₃ in 99% CD₃CN is shown in **Figure 43**. The ^1H NMR of [Fe₂(TPA)₂O(3,5-dibromobenzoato)](ClO₄)₃ in 99% CD₃CN is shown in **Figure 44**. The ^1H NMR of [Fe₂(TPA)₂O(3,5-dinitrobenzoato)](ClO₄)₃ in 99% CD₃CN is shown in **Figure 45**. All of the peak assignments for the metal complexes are listed in **Table 3**.

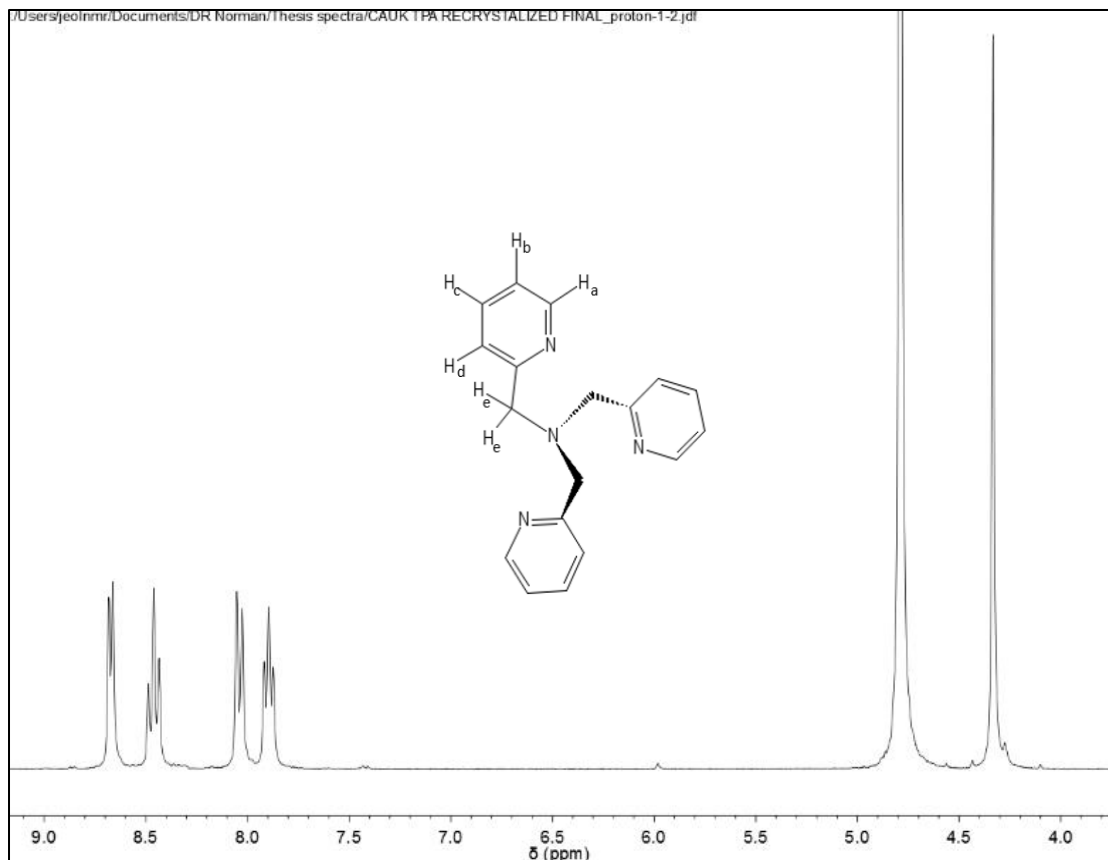


Figure 32. ^1H NMR spectrum of TPA•3HClO₄.

Table 2. ^1H NMR chemical shift values assignment of TPA•3HClO₄ in D_2O

<i>Chemical shift (ppm)</i>	<i>Multiplicity</i>	<i>Assignment</i>
8.67	Doublet	H _a
8.46	Triplet	H _c
8.04	Doublet	H _d
7.89	Triplet	H _b
4.33	Singlet	H _e

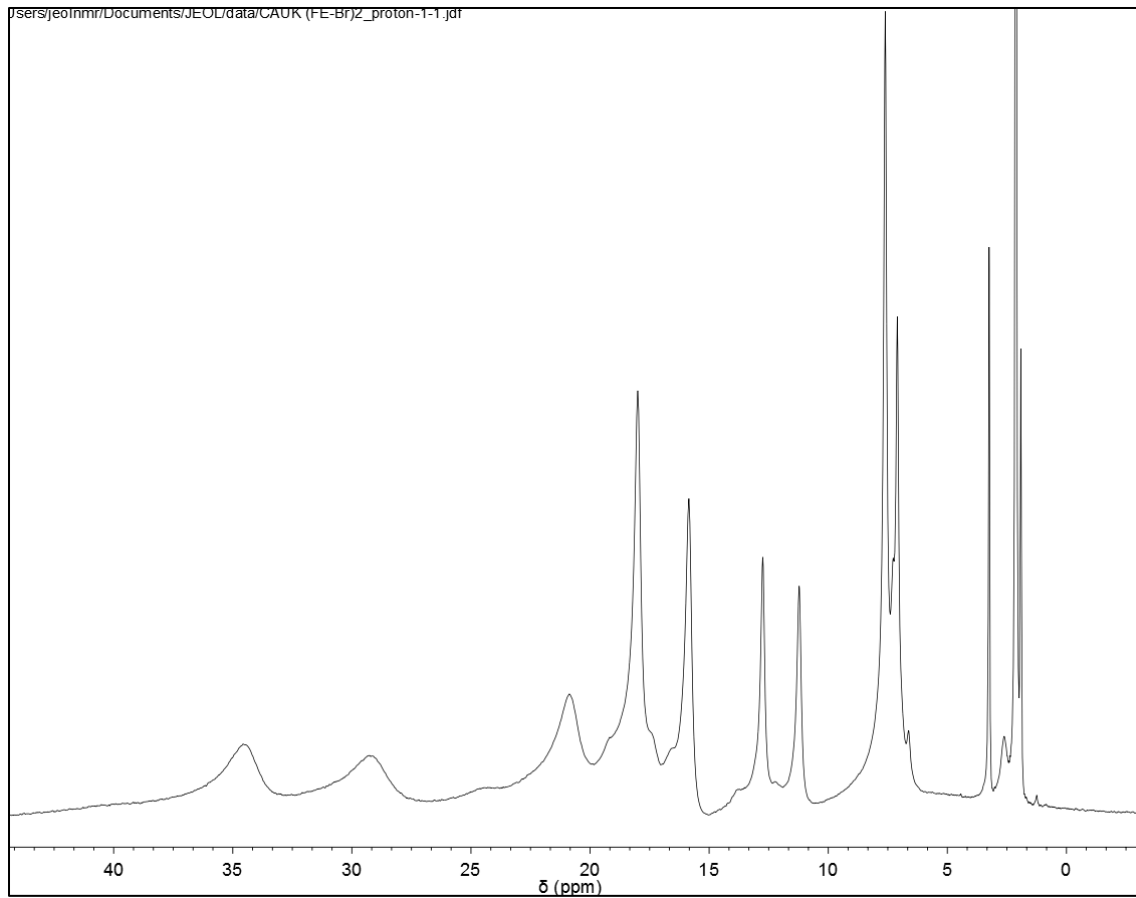


Figure 33. ^1H NMR spectrum of $\left[\{\text{Fe}(\text{TPA})\text{Br}_2\text{O}\}\right](\text{ClO}_4)_2 \cdot \text{H}_2\text{O}$.

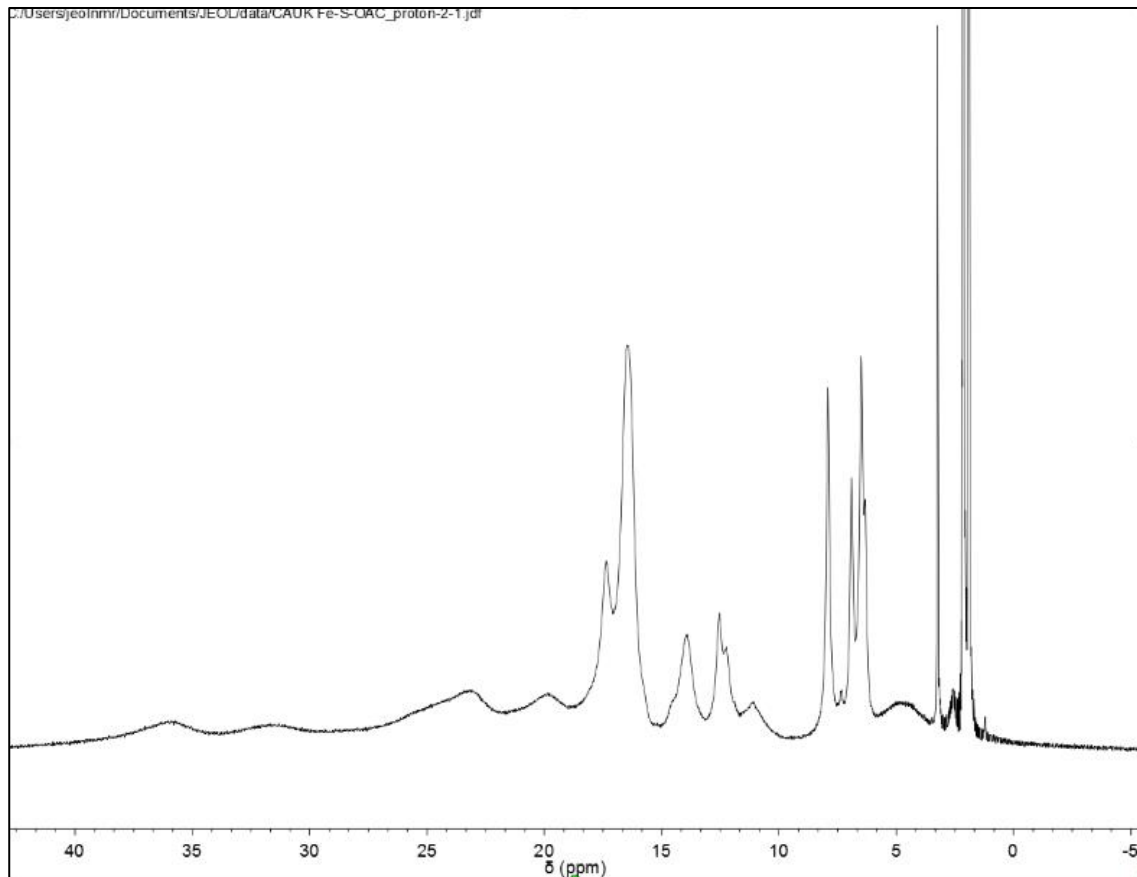


Figure 34. ^1H NMR spectrum of $[\text{Fe}_2(\text{TPA})_2\text{O}(\text{OAc})](\text{ClO}_4)_3$.

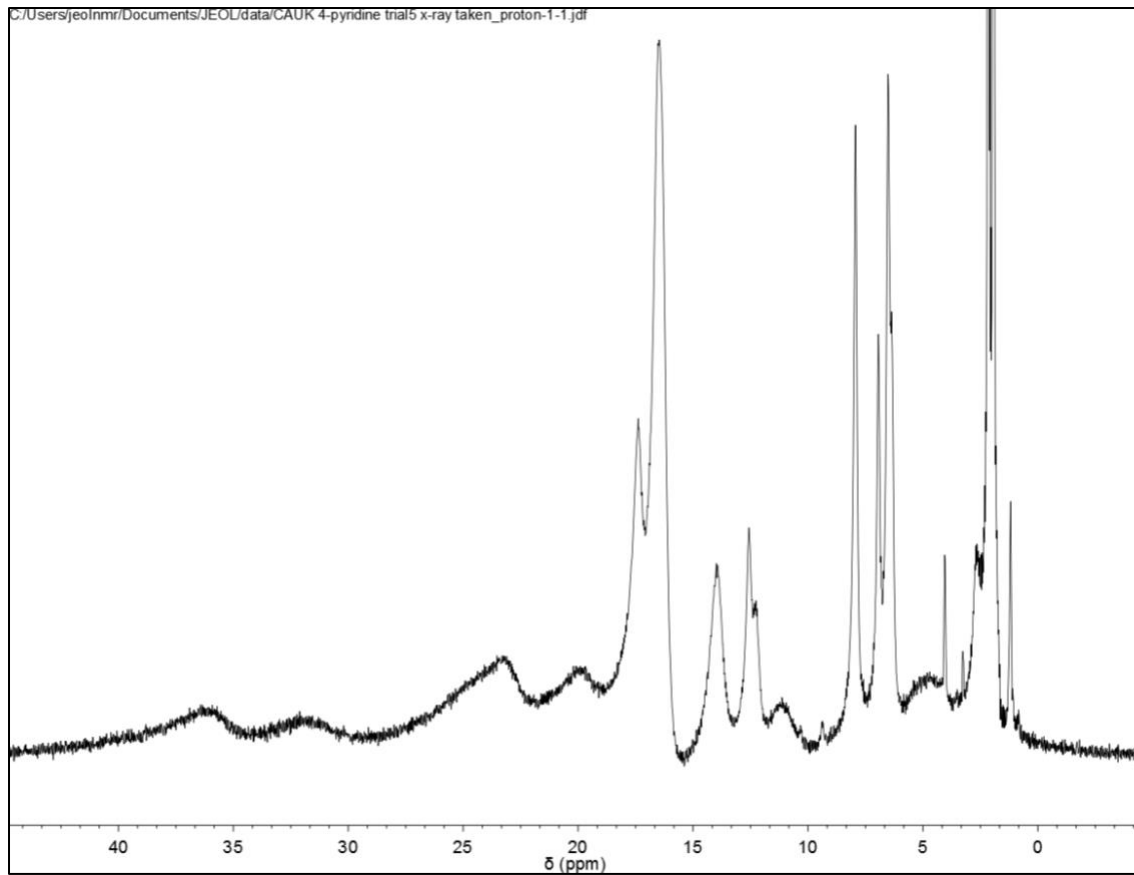


Figure 35. ¹H NMR spectrum of [Fe₂(TPA)₂O(OAc)](ClO₄)₃•H₂O.

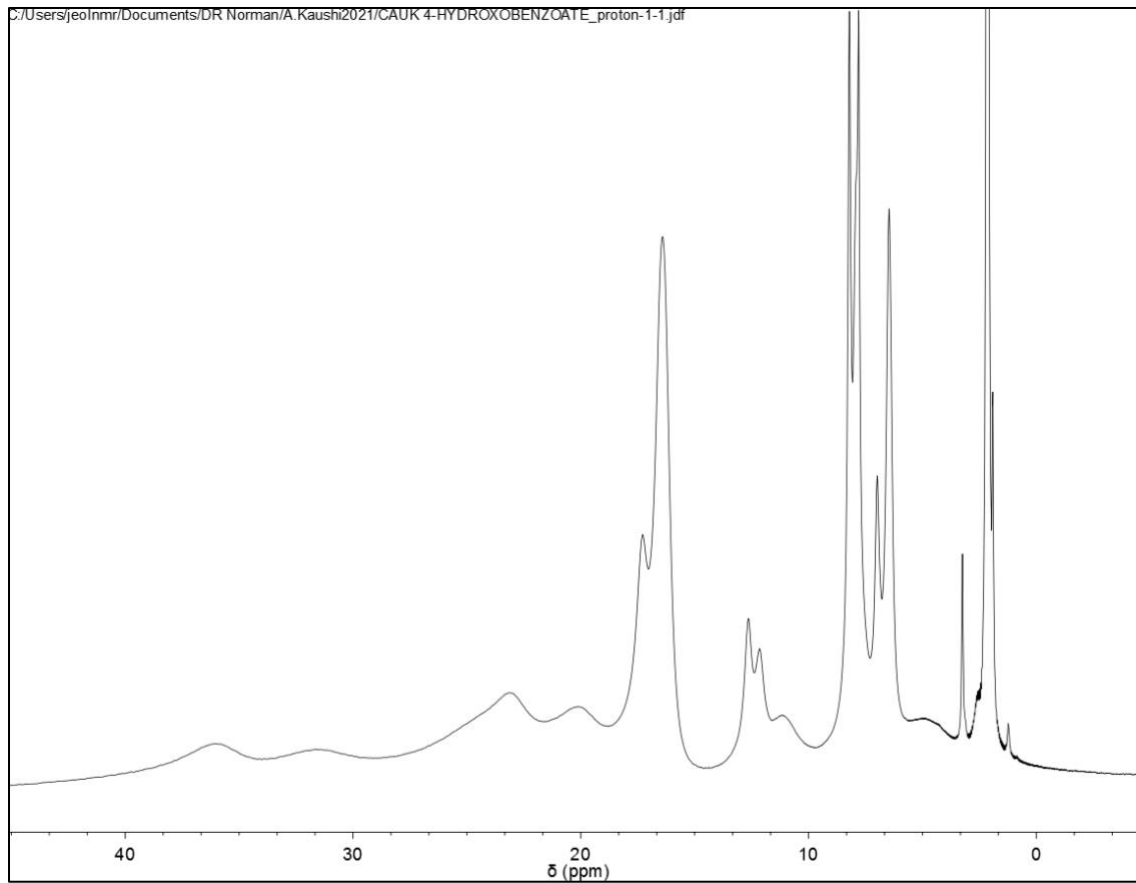


Figure 36. ^1H NMR spectrum of $[\text{Fe}_2(\text{TPA})_2\text{O}(4\text{-hydroxybenzoato})](\text{ClO}_4)_3$.

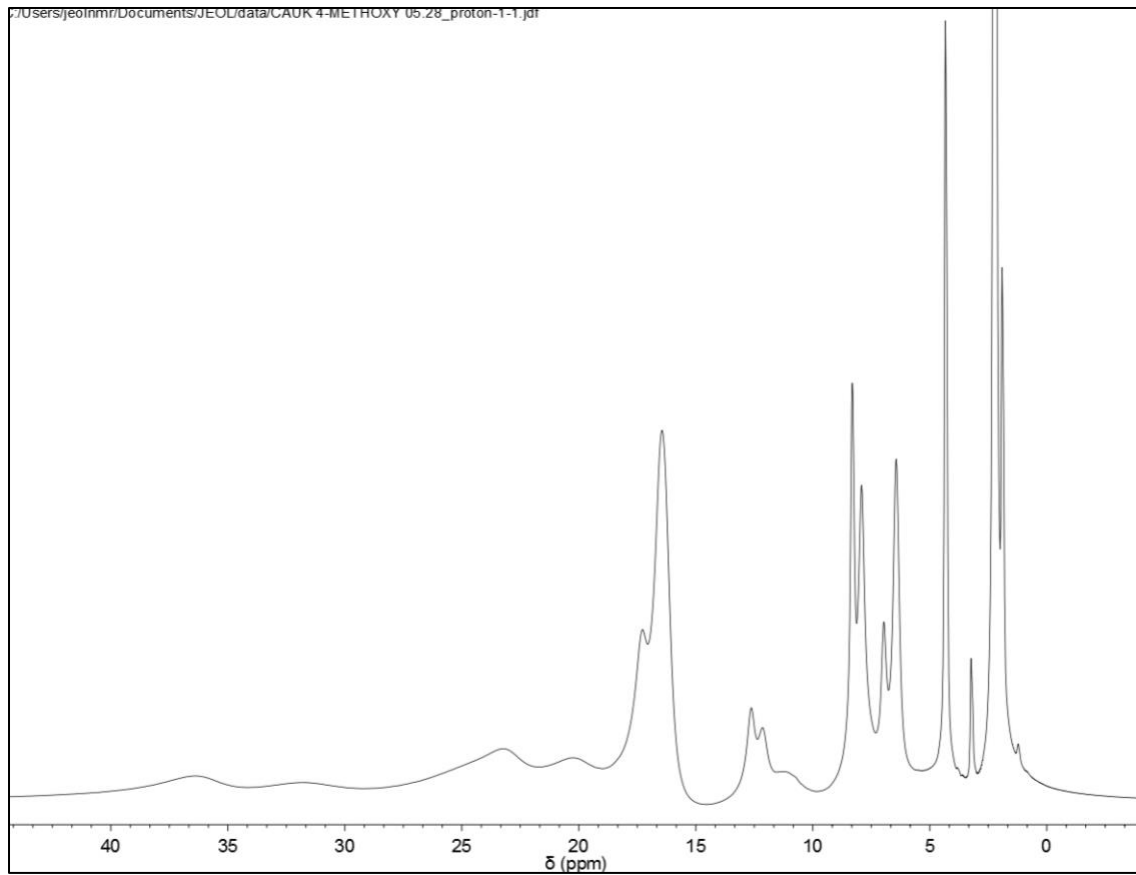


Figure 37. ^1H NMR spectrum of $[\text{Fe}_2(\text{TPA})_2\text{O}(4\text{-methoxybenzoato})](\text{ClO}_4)_3$.

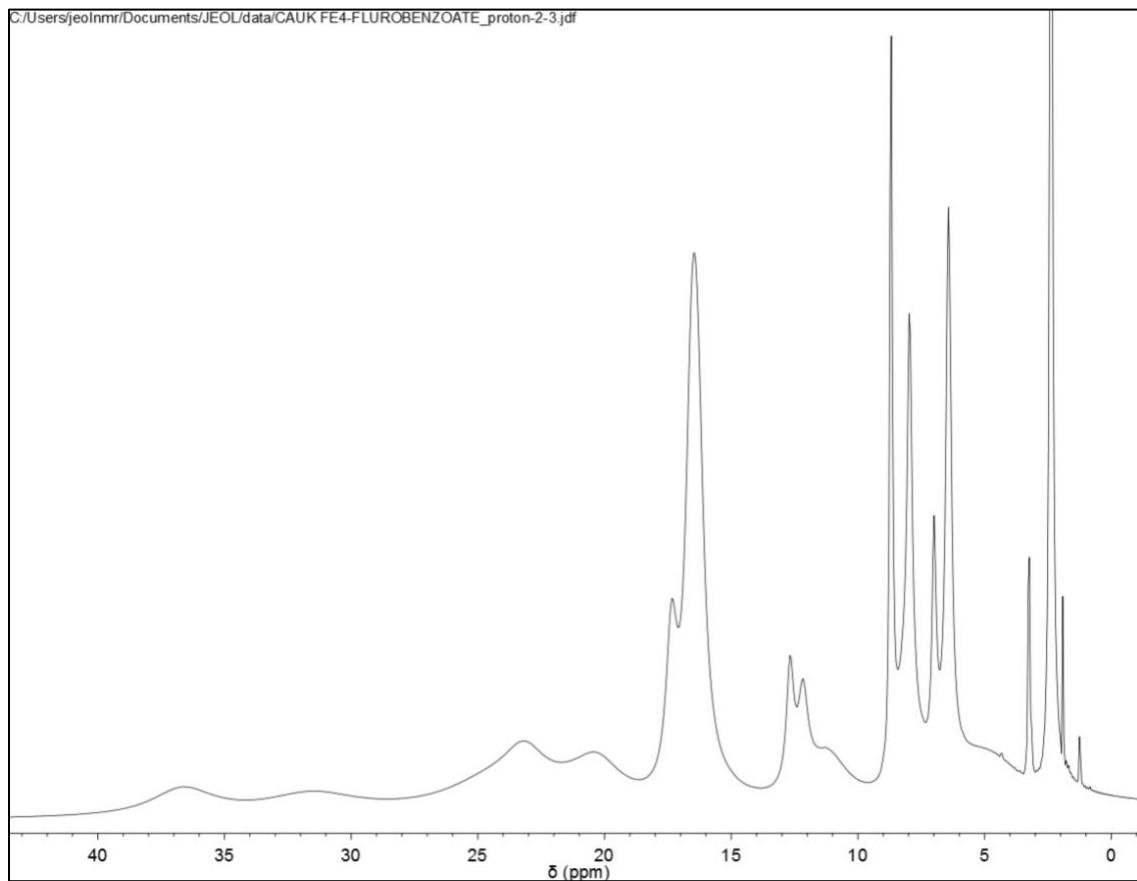


Figure 38. ^1H NMR spectrum of $[\text{Fe}_2(\text{TPA})_2\text{O}(4\text{-fluorobenzoato})](\text{ClO}_4)_3$.

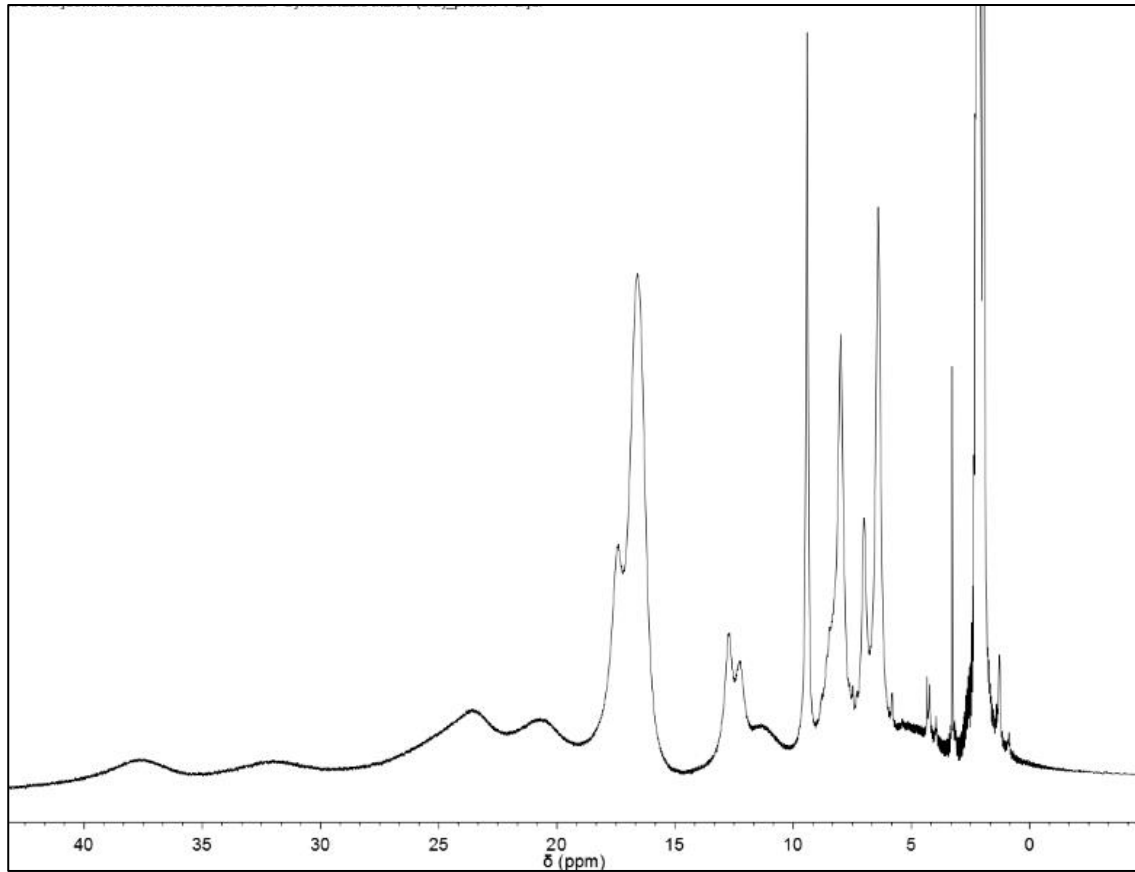


Figure 39. ^1H NMR spectrum of $[\text{Fe}_2(\text{TPA})_2\text{O}(4\text{-cyanobenzoato})](\text{ClO}_4)_3$.

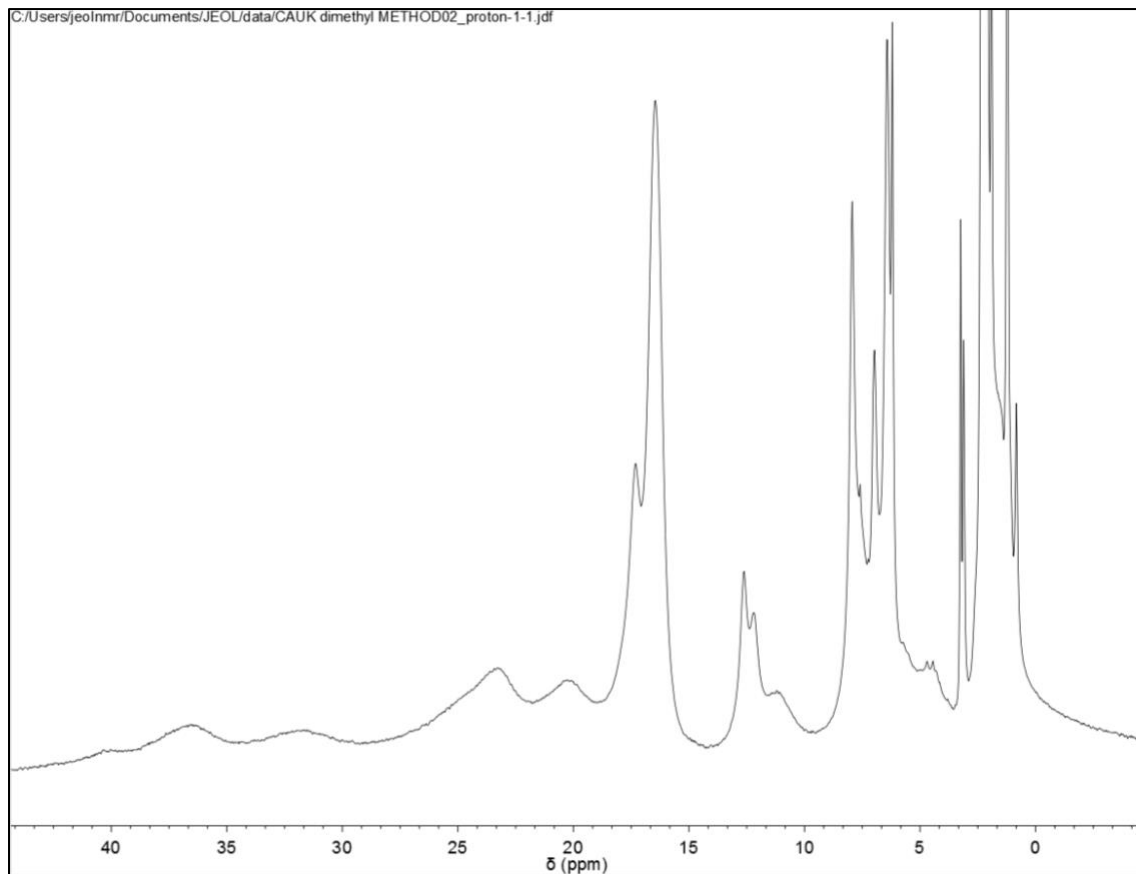


Figure 40. ^1H NMR spectrum of $[\text{Fe}_2(\text{TPA})_2\text{O}(3,5\text{-dimethylbenzoato})](\text{ClO}_4)_3 \bullet 0.5\text{H}_2\text{O}$.

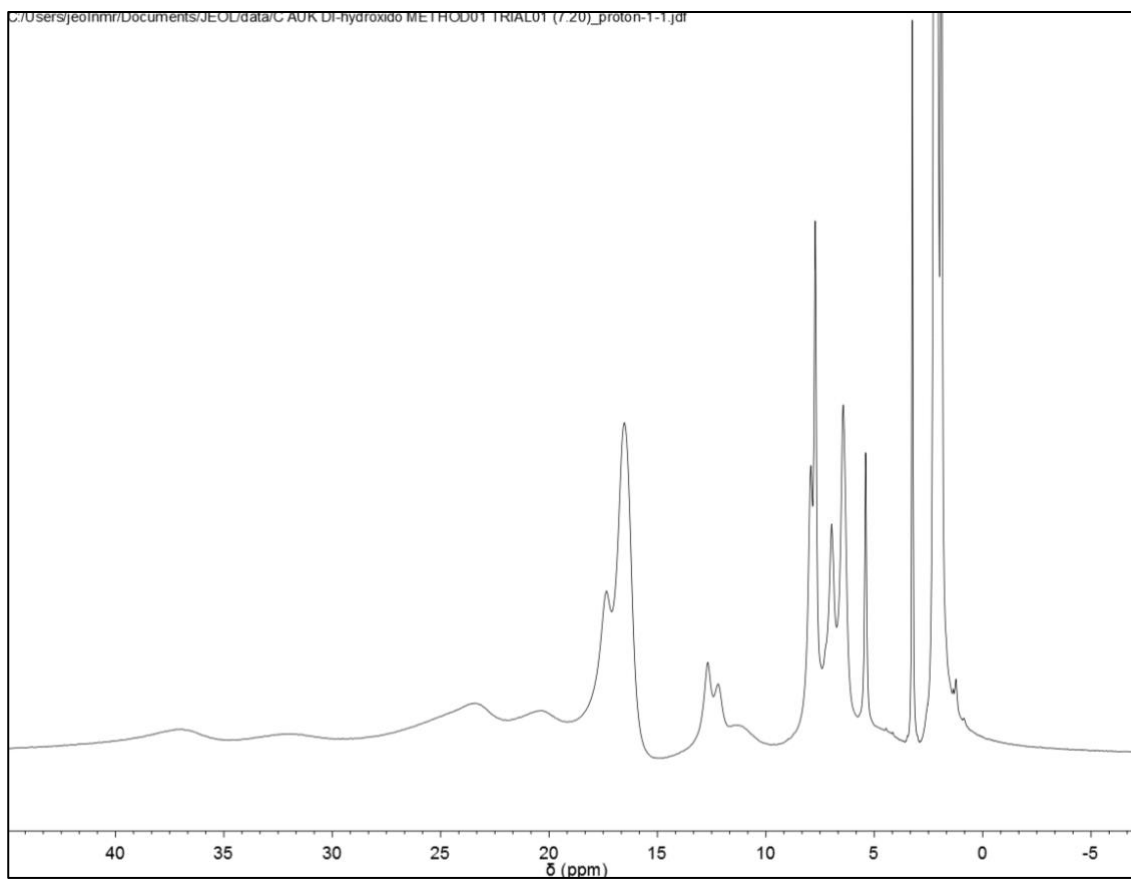


Figure 41. 1H NMR spectrum of $[Fe_2(TPA)_2O(3,5\text{-dihydroxybenzoato})](ClO_4)_3 \bullet CH_3CN$.

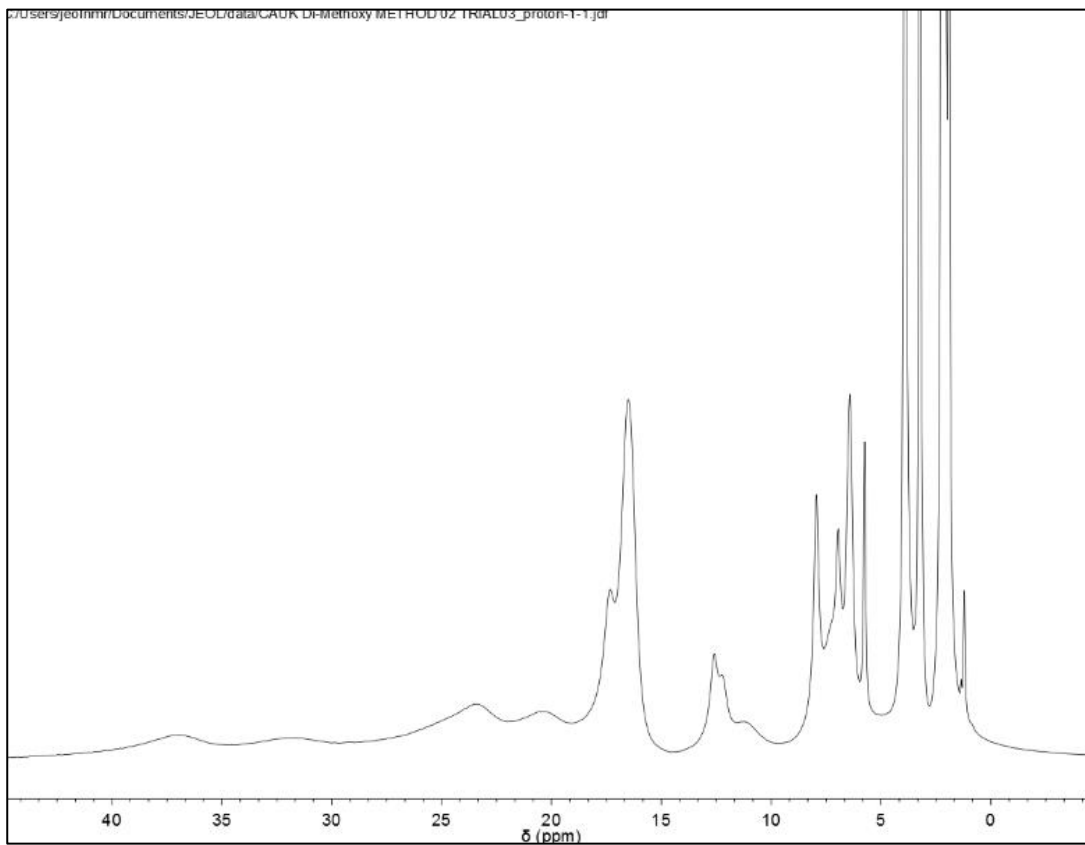


Figure 42. ^1H NMR spectrum of $[\text{Fe}_2(\text{TPA})_2\text{O}(3,5\text{-dimethoxybenzoato})](\text{ClO}_4)_3$.

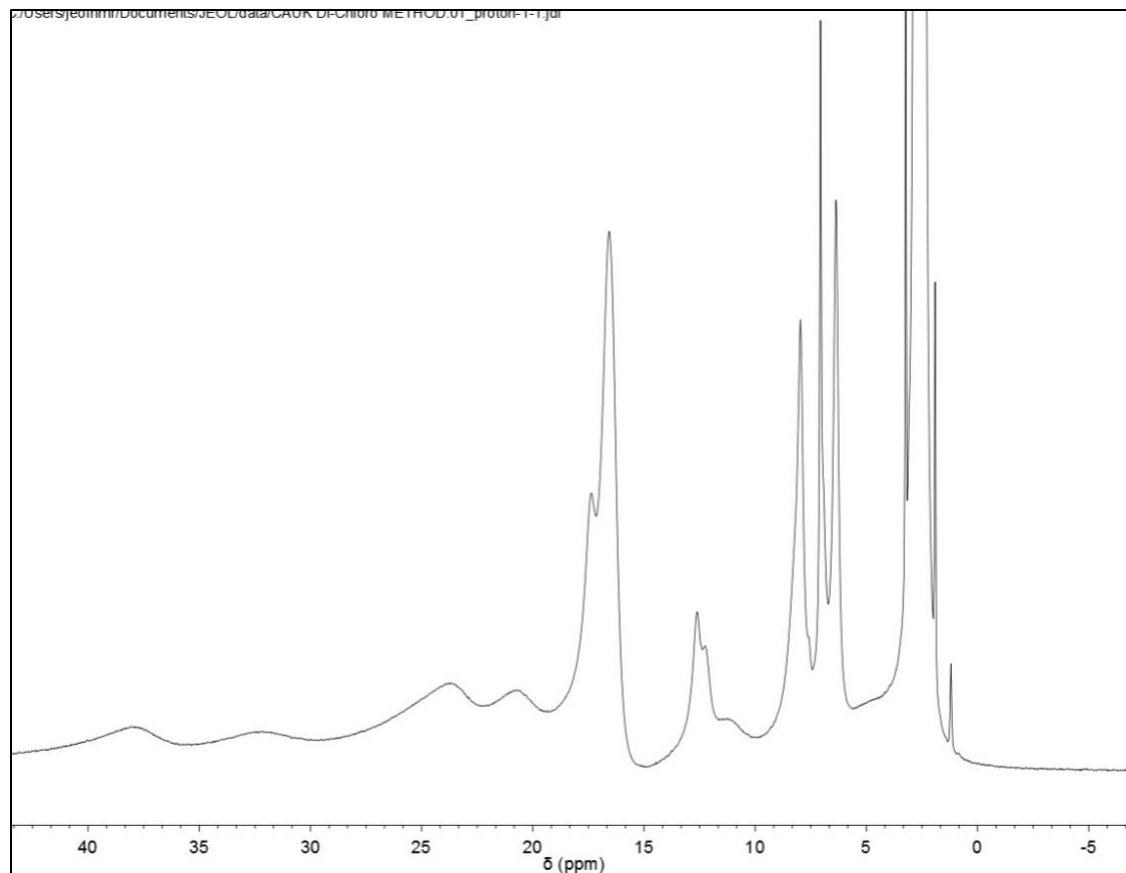


Figure 43. 1H NMR spectrum of $[Fe_2(TPA)_2O(3,5\text{-dichlorobenzoato})](ClO_4)_3$.

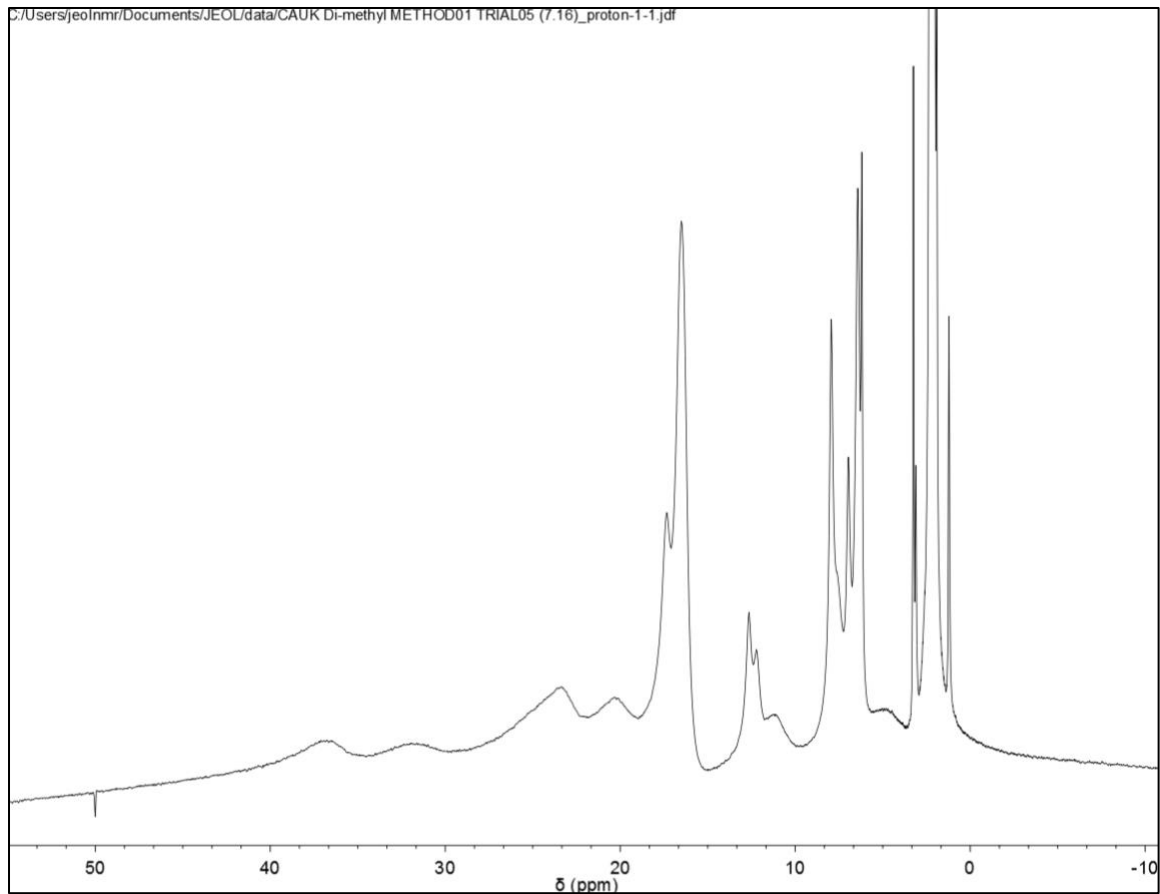


Figure 44. ^1H NMR spectrum of $[\text{Fe}_2(\text{TPA})_2\text{O}(3,5\text{-dibromobenzoato})](\text{ClO}_4)_3$.

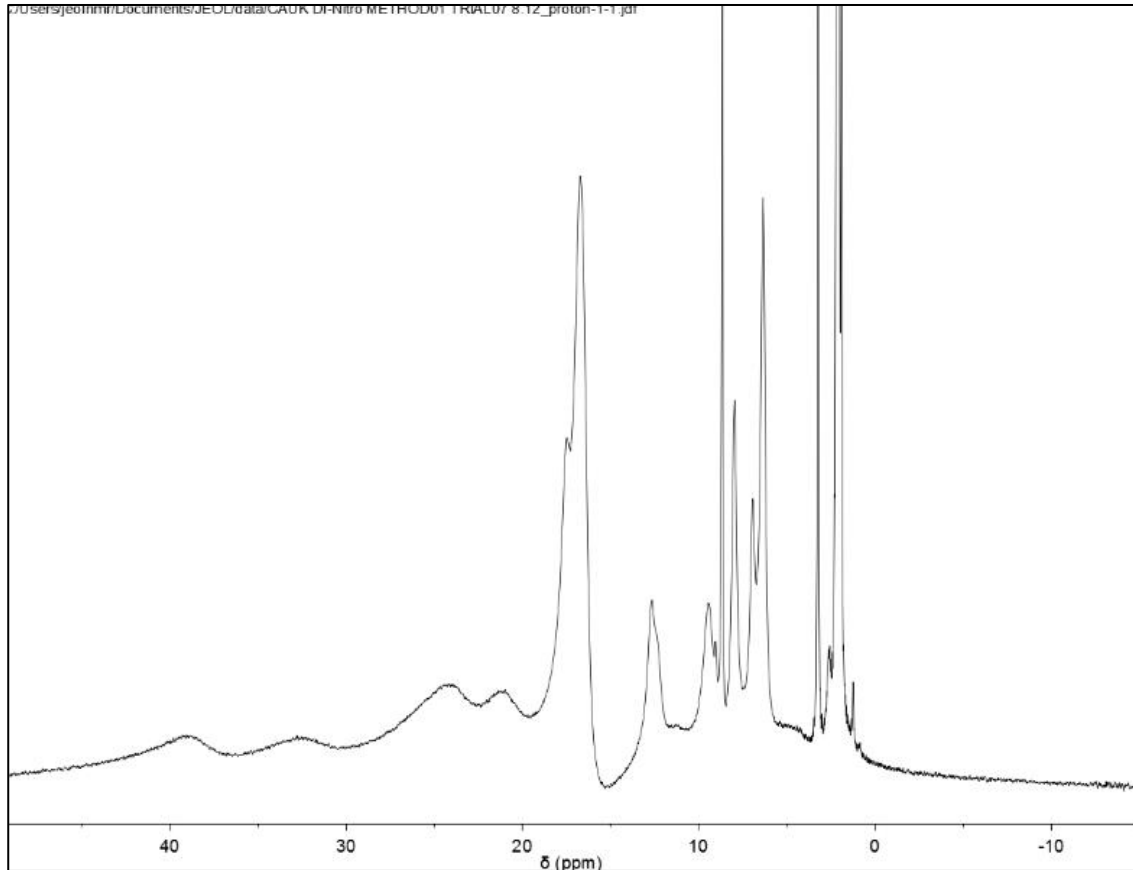


Figure 45. ^1H NMR spectrum of $[\text{Fe}_2(\text{TPA})_2\text{O}(3,5\text{-dinitrobenzoato})](\text{ClO}_4)_3$.

Table 3. ^1H NMR parameters (ppm) for the studied oxo-bridged diiron complexes

1	2	3	4	5	6	7	Assignment
7.1	6.3	6.4	6.5	6.4	6.4	6.4	
7.6	6.5	6.5					
	6.9	6.9	7.0	7.0	7.0	7.0	para-py-4-H
	7.9	7.9	7.8	7.9	8.0	8.0	
	11.0	11.1	11.1	11.1	11.3	11.2	
11.2	12.3	12.3	12.2	12.1	12.3	12.2	
12.8	12.5	12.6	12.6	12.6	12.7	12.7	meta-py-
15.9	16.5	16.5	16.4	16.4	16.5	16.6	3,5-H
18.0	17.3	17.4	17.3	17.3	17.3	17.4	
20.9	19.8	20.0	20.3	20.1	20.5	20.6	
24.3	23.2	23.7	23.3	23.2	23.2	23.6	ortho-py-
29.3	31.6	32.1	31.4	31.7	31.5	32.0	2,6-H or
34.6	36.1	35.9	36.2	36.2	36.6	37.7	CH ₂
	13.9(OAc)	13.9(OAc)		4.3 (OCH ₃)			
							para-OBz
			8.2	8.3	8.7	9.4	meta-OBz

Note: 1 = Br⁻, 2 = OAc⁻, 3 = *OAc⁻, 4 = 4-hydroxybenzoato, 5 = 4-methoxybenzoato, 6 = 4-fluorobenzoato, 7 = 4-cyanobenzoato.

*OAc = [Fe₂(TPA)₂O(OAc)](ClO₄)₃•H₂O from section 2.3.5.5. and 2.3.5.9.

8	9	10	11	12	13	Assignment
6.4	6.4	6.4		6.4	6.4	
7.0	7.0	7.0	7.0	7.0	6.9	<i>para</i> -py-4-H
7.9	7.7	7.9	8.0	7.9	8.0	
	7.9				9.5	
10.9	11.1	11.2	11.1	11.2		
12.2	12.2	12.2	12.2	12.2	12.3	<i>meta</i> -py-
12.6	12.7	12.6	12.6	12.6	12.7	3,5-H
16.5	16.5	16.5	16.6	16.5	16.7	
17.3	17.4	17.3	17.4	17.3	17.4	
20.2	20.4	20.3	20.6	20.3	21.0	
23.3	23.5	23.7	23.8	23.5	23.9	
32.2	31.9	31.7	32.3	31.5	32.4	<i>ortho</i> -py-
36.3	37.0	37.2	37.8	36.5	38.5	2,6-H or
40.4						CH ₂
1.2 (CH ₃)		3.9 (OCH ₃)				
6.2	5.4	5.8	6.4	6.2	8.7	<i>para</i> -OBz
						<i>meta</i> -OBz

Note: 8 = 3,5-dimethylbenzoato, 9 = 3,5-dihydroxybenzoato, 10 = 3,5-dimethoxybenzoato, 11 = 3,5-dichlorobenzoato, 12 = 3,5-dibromobenzoato, 13 = 3,5-dinitrobenzoato.

3.3 X-ray Crystallographic Results

X-ray structures for several (μ -oxido)(TPA)diiron(III) complexes were solved and refined. The X-ray structure of singly bridged $[\{\text{Fe}(\text{TPA})\text{Br}\}_2\text{O}](\text{ClO}_4)_2 \cdot \text{H}_2\text{O}$ is reported. The X-ray structures of two polymorphs of $[\{\text{Fe}(\text{TPA})\}_2\text{O}(\text{OAc})](\text{ClO}_4)_3 \cdot \text{H}_2\text{O}$ are reported. X-ray structures of $[\{\text{Fe}(\text{TPA})\}_2\text{O}(4\text{-hydroxybenzoato})](\text{ClO}_4)_3$, $[\{\text{Fe}(\text{TPA})\}_2\text{O}(4\text{-methoxybenzoato})](\text{ClO}_4)_3$, $[\{\text{Fe}(\text{TPA})\}_2\text{O}(4\text{-fluorobenzoato})](\text{ClO}_4)_3$, $[\{\text{Fe}(\text{TPA})\}_2\text{O}(3,5\text{-dimethylbenzoato})](\text{ClO}_4)_3 \cdot 0.5\text{H}_2\text{O}$ and $[\{\text{Fe}(\text{TPA})\}_2\text{O}(3,5\text{-dihydroxybenzoato})](\text{ClO}_4) \cdot \text{CH}_3\text{CN}$ are reported in this section.

The numbering scheme for TPA in $[\{\text{Fe}(\text{TPA})\text{Br}\}_2\text{O}](\text{ClO}_4)_2 \cdot \text{H}_2\text{O}$ is shown in

Figure 46. N2 is in the Fe1-O1-N4 (tertiary amine) plane, and it is *trans* to the oxido bridge.

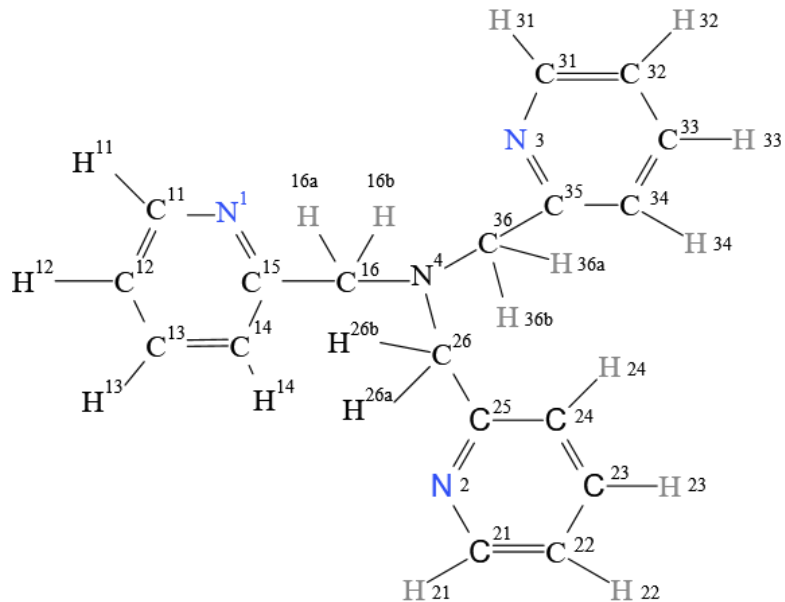


Figure 46. Numbering scheme for TPA in $[\{\text{Fe}(\text{TPA})\text{Br}\}_2\text{O}](\text{ClO}_4)_2 \cdot \text{H}_2\text{O}$.

All of the (μ -oxido)(μ -carboxylato)diiron(III)TPA complexes have the same core structure. Each Fe is 6-coordinate pseudo octahedral. O1 is the oxide ion that bridges the two iron centers. Fe1 is always bound to O2 of the bridging carboxylate and has the tertiary amine of TPA bound *cis* to the oxido bridge. This places a pyridyl arm of TPA at Fe1 *trans* to the oxido bridge. Fe2 is always bound to O3 of the bridging carboxylate and has the tertiary amine of TPA bound *trans* to the oxido bridge. This places a pyridyl arm of TPA at Fe2 *cis* to the oxido bridge.

The numbering scheme for TPA bound to Fe1 in carboxylato-bridged diiron(III) complexes is shown in **Figure 47**. The tertiary amine nitrogen bound to Fe1 is denoted as N14. The pyridine nitrogen N12 is *trans* to the oxido-bridge for the TPA bound to Fe1.

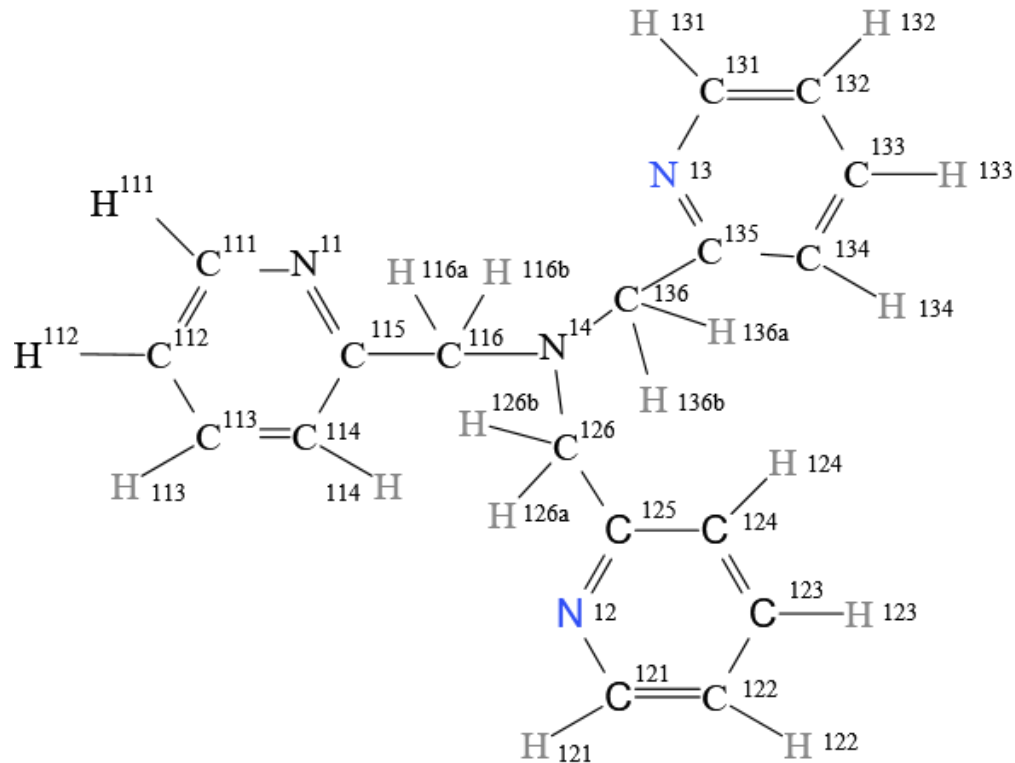


Figure 47. Numbering scheme for TPA bound to Fe1 in carboxylato-bridged complexes.

The numbering scheme for TPA bound to Fe2 in carboxylato-bridged diiron(III) complexes is shown in **Figure 48**. The tertiary amine nitrogen bound to Fe2 is denoted as N24 and is *trans* to the oxido bridge. The pyridine nitrogen N22 is coplanar with N24-Fe2-O1.

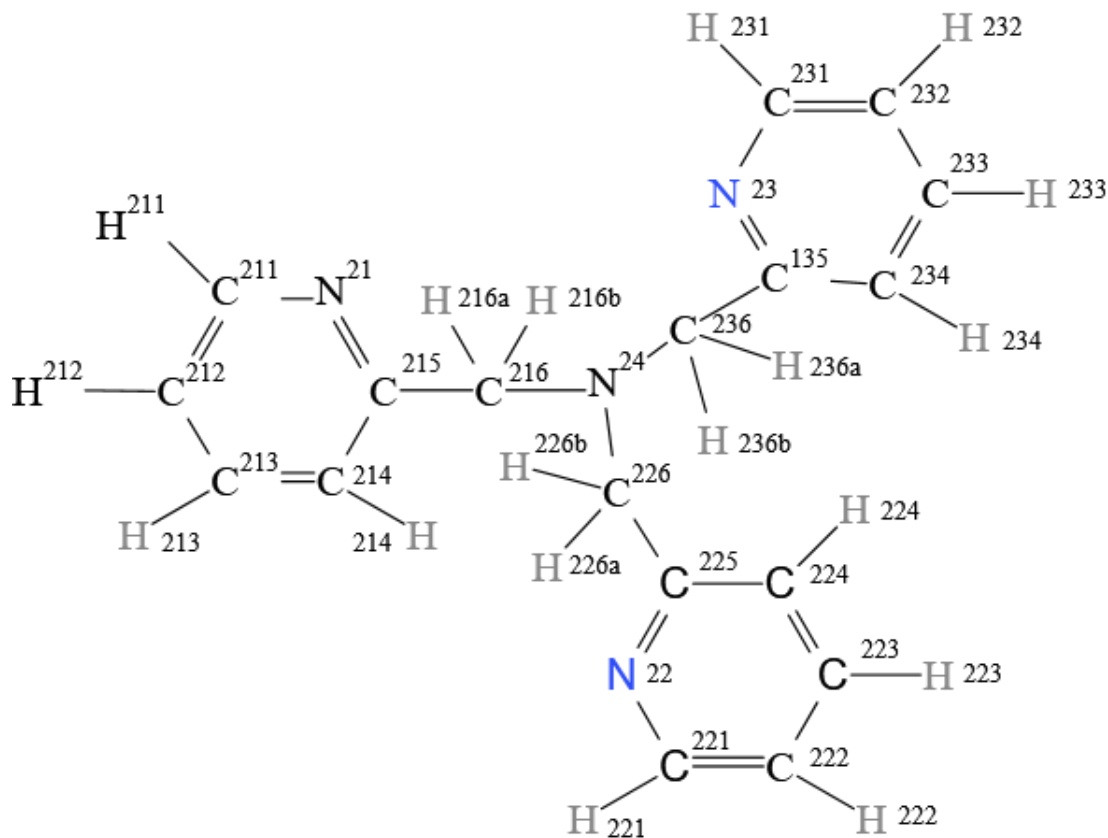


Figure 48. Numbering scheme for TPA bound to Fe2 in carboxylato-bridged complexes.

3.3.1 [{Fe(TPA)Br}₂O](ClO₄)₂•H₂O

Figure 49 shows the asymmetric unit of [{Fe(TPA)Br}₂O](ClO₄)₂•H₂O. **Figure 50** shows the cationic portion of [{Fe(TPA)Br}₂O](ClO₄)₂•H₂O. Crystallographic details for [{Fe(TPA)Br}₂O](ClO₄)₂•H₂O are listed in **Table 4**. Fractional atomic coordinates, anisotropic displacement parameters, bond lengths and bond angles involving the non-hydrogen atoms and hydrogen atom coordinates, atomic occupancy for disordered atoms are listed in **Table 5**, **Table 6**, **Table 7**, **Table 8**, **Table 9** and **Table 10**, respectively.

The asymmetric unit was found to contain one half of a single [{Fe(TPA)Br}₂O] unit with one perchlorate iron and a water molecule which has an occupancy of 0.5. O1, the bridging oxide, sits on a two-fold symmetry axis. Br1 coordinates to Fe1 and is *trans* to the tertiary amine (N4). O2 is the oxygen atom of the water molecule. The perchlorate ion is disordered about the Cl1-O14 axis and is modeled with two sets of oxygen atoms with occupancies of 0.65 and 0.35, respectively.

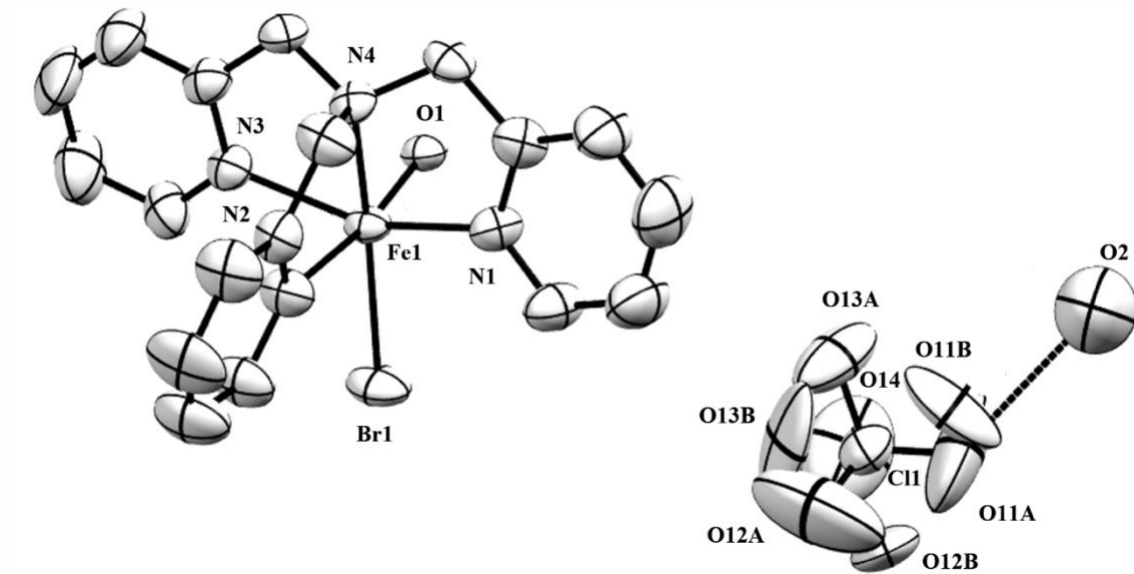


Figure 49. A view of the asymmetric unit of $\{[Fe(TPA)Br]_2O\}(ClO_4)_2 \cdot H_2O$.

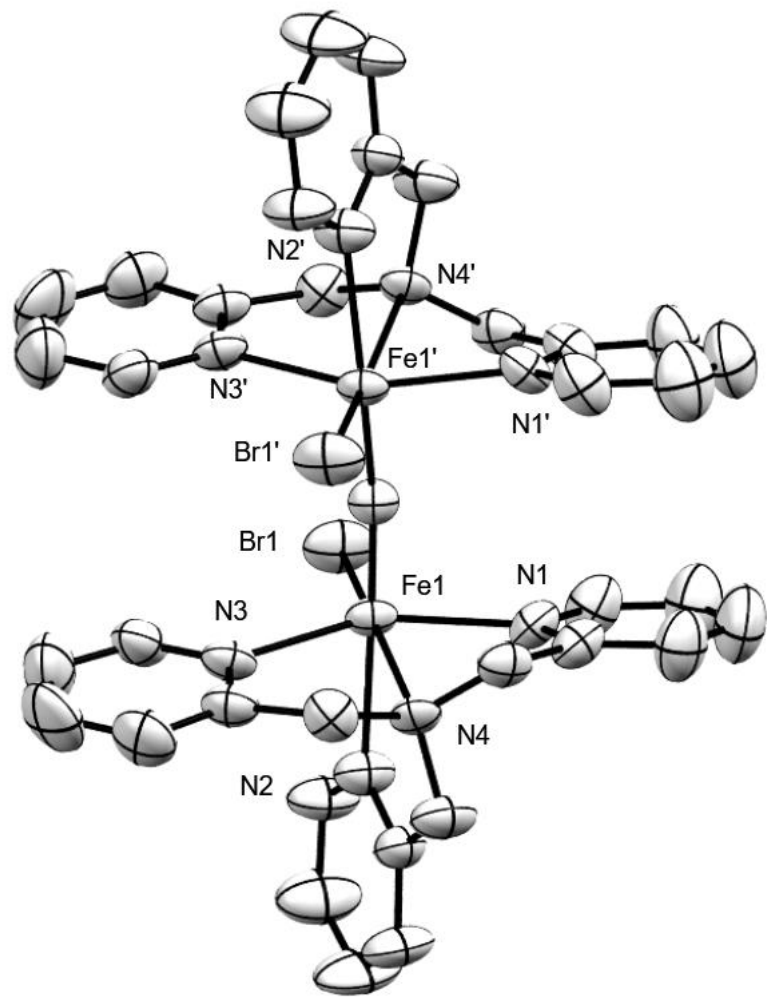


Figure 50. A view of the cationic portion of $\{[Fe(TPA)Br]_2O\}(ClO_4)_2 \bullet H_2O$. Hydrogen atoms are omitted.

Table 4. Crystallographic data for $\{Fe(TPA)Br\}_2O](ClO_4)_2 \bullet H_2O$

Crystallographic data	
Empirical formula	C ₃₆ H ₃₈ Br ₂ Cl ₂ Fe ₂ N ₈ O ₁₀
Formula weight	1085.16
Temperature/K	298
Crystal system	monoclinic
Space group	C2/c
a/Å	16.1480(17)
b/Å	17.2036(13)
c/Å	16.8521(12)
α/°	90
β/°	111.204(10)
γ/°	90
Volume/Å ³	4364.6(7)
Z	4
ρ _{calc} /g cm ⁻³	1.651
μ/mm ⁻¹	2.681
F(000)	2184
Crystal size/mm ³	4.2 × 3.2 × 1
Radiation	MoKα ($\lambda = 0.71073$)
2θ range for data collection/°	5.186 to 50
Index ranges	-19 ≤ h ≤ 17, -20 ≤ k ≤ 19, -10 ≤ l ≤ 20

Crystallographic data	
Reflections collected	6891
Independent reflections	3753 [$R_{\text{int}} = 0.0520$, $R_{\text{sigma}} = 0.0665$]
Data/restraints/parameters	3753/0/312
Goodness-of-fit on F^2	1.068
Final R indexes [$I \geq 2\sigma (I)$]	$R_1 = 0.0693$, $wR_2 = 0.1511$
Final R indexes [all data]	$R_1 = 0.1220$, $wR_2 = 0.1824$
Largest diff. peak/hole / e Å ⁻³	1.00/-0.91

Table 5. Fractional atomic coordinates ($\times 10^4$) and equivalent isotropic displacement parameters ($\text{\AA}^2 \times 10^3$) for $[\{\text{Fe}(TPA)\text{Br}\}_2\text{O}](\text{ClO}_4)_2 \cdot \text{H}_2\text{O}$

Atom	x	y	z	U(eq)
Br1	6422.2(6)	8589.4(6)	4400.1(5)	60.2(3)
Fe1	6183.9(7)	8335.2(7)	2904.3(6)	34.7(3)
Cl1	6940.5(19)	3964.8(16)	4993.5(15)	62.2(7)
O1	5000	8286(4)	2500	36.3(17)
O2	5910(20)	2012(17)	3951(17)	164(10)
O11A	6740(30)	3240(15)	5110(20)	174(17)
O12A	7818(18)	4080(30)	5380(20)	233(19)
O13A	6824(17)	4044(11)	4143(9)	115(6)
O11B	6600(40)	3230(30)	4690(30)	150(30)
O12B	7360(40)	3850(30)	5861(17)	180(20)
O13B	7520(30)	4330(30)	4760(40)	150(20)
O14	6378(10)	4474(7)	5146(9)	167(5)
N1	6308(4)	7084(4)	2941(4)	42.0(16)

Atom	x	y	z	U(eq)
N2	7647(4)	8432(4)	3202(4)	49.6(18)
N3	6192(4)	9432(4)	2324(4)	42.3(16)
N4	6341(4)	8002(4)	1694(4)	37.4(15)
C11	6565(7)	6639(6)	3649(6)	60(3)
C12	6550(9)	5857(7)	3614(8)	83(4)
C13	6282(9)	5507(7)	2824(8)	89(4)
C14	6043(8)	5954(6)	2101(7)	70(3)
C15	6052(6)	6746(5)	2180(6)	49(2)
C16	5795(6)	7300(5)	1438(5)	44(2)
C21	8242(6)	8764(6)	3913(6)	62(3)
C22	9127(7)	8825(8)	4033(7)	84(4)
C23	9422(7)	8536(8)	3432(8)	90(4)
C24	8823(6)	8210(7)	2704(7)	69(3)
C25	7937(5)	8170(5)	2597(5)	46(2)
C26	7270(6)	7815(6)	1825(6)	57(2)
C31	6237(6)	10120(5)	2710(6)	54(2)
C32	6199(8)	10812(6)	2292(8)	82(4)
C33	6138(9)	10782(7)	1460(8)	86(4)
C34	6113(7)	10082(6)	1067(6)	67(3)
C35	6112(5)	9420(5)	1507(5)	45(2)
C36	5986(6)	8644(5)	1091(5)	46(2)

Table 6. Anisotropic displacement parameters ($\text{\AA}^2 \times 10^3$) for $\{[\text{Fe}(TPA)\text{Br}]_2\text{O}\}(\text{ClO}_4)_2 \cdot \text{H}_2\text{O}$

Atom	U₁₁	U₂₂	U₃₃	U₂₃	U₁₃	U₁₂
Br1	57.8(6)	94.1(8)	30.9(5)	-15.4(5)	18.6(4)	-6.0(5)
Fe1	32.6(6)	49.6(7)	24.7(5)	-3.0(5)	13.7(4)	-0.2(5)

Atom	U₁₁	U₂₂	U₃₃	U₂₃	U₁₃	U₁₂
Cl1	73.7(18)	69.9(17)	50.0(14)	3.7(12)	30.8(13)	-5.4(14)
O1	37(4)	46(4)	24(4)	0	9(3)	0
O2	180(30)	150(20)	150(20)	10(18)	42(19)	-20(20)
O11A	280(40)	100(20)	220(30)	60(20)	190(40)	20(20)
O12A	120(20)	380(60)	170(30)	-120(30)	10(20)	-40(30)
O13A	200(20)	100(12)	70(9)	20(8)	79(12)	51(13)
O11B	120(30)	150(50)	160(40)	-120(40)	30(30)	-20(30)
O12B	270(50)	180(40)	39(15)	40(20)	-10(20)	-110(40)
O13B	100(30)	140(30)	260(60)	100(40)	120(40)	0(30)
O14	224(14)	137(9)	204(13)	-9(9)	155(12)	47(10)
N1	44(4)	47(4)	37(4)	1(3)	16(3)	14(3)
N2	39(4)	69(5)	44(4)	-7(4)	18(3)	-2(4)
N3	41(4)	56(4)	37(4)	0(3)	23(3)	-5(3)
N4	41(4)	48(4)	32(3)	-1(3)	23(3)	2(3)
C11	76(7)	60(6)	43(5)	1(5)	19(5)	16(5)
C12	112(10)	69(8)	58(7)	9(6)	19(7)	13(7)
C13	115(11)	50(6)	100(10)	10(7)	38(8)	17(7)
C14	100(9)	53(6)	56(6)	-10(5)	27(6)	6(6)
C15	44(5)	52(5)	50(5)	-6(4)	17(4)	10(4)
C16	46(5)	55(5)	36(4)	-14(4)	20(4)	-4(4)
C21	35(5)	96(8)	55(6)	-13(5)	17(4)	-9(5)
C22	48(6)	133(11)	67(7)	-23(7)	15(5)	-9(7)
C23	28(5)	142(12)	94(9)	-26(8)	16(5)	-2(6)
C24	37(5)	98(8)	80(7)	-7(6)	30(5)	8(5)
C25	41(5)	51(5)	53(5)	1(4)	25(4)	4(4)
C26	44(5)	81(7)	54(6)	-16(5)	27(4)	-3(5)

Atom	U₁₁	U₂₂	U₃₃	U₂₃	U₁₃	U₁₂
C31	57(6)	58(6)	59(6)	-8(5)	35(5)	-13(5)
C32	116(10)	47(6)	97(9)	-10(6)	55(8)	-8(6)
C33	118(11)	74(8)	82(8)	24(7)	55(8)	-18(7)
C34	82(8)	74(7)	57(6)	15(6)	38(6)	-4(6)
C35	43(5)	60(6)	40(5)	5(4)	22(4)	-2(4)
C36	54(5)	54(5)	29(4)	-1(4)	14(4)	-4(4)

Table 7. Bond lengths for $\{\text{Fe}(TPA)\text{Br}\}_2\text{O}\}(\text{ClO}_4)_2 \bullet \text{H}_2\text{O}$

Atom	Atom	Length/Å
Br1	Fe1	2.4477(13)
Fe1	O1	1.7844(11)
Fe1	N1	2.160(7)
Fe1	N2	2.237(7)
Fe1	N3	2.127(7)
Fe1	N4	2.220(6)
Cl1	O11A	1.32(2)
Cl1	O12A	1.34(3)
Cl1	O13A	1.383(13)
Cl1	O11B	1.39(5)
Cl1	O12B	1.38(3)
Cl1	O13B	1.29(3)
Cl1	O14	1.352(10)
N1	C11	1.350(11)
N1	C15	1.331(10)
N2	C21	1.361(11)
N2	C25	1.343(10)

Atom	Atom2	Length/Å
N4	C16	1.465(10)
N4	C26	1.470(10)
N4	C36	1.470(10)
C11	C12	1.347(15)
C12	C13	1.380(16)
C13	C14	1.374(14)
C14	C15	1.369(13)
C15	C16	1.506(12)
C21	C22	1.373(13)
C22	C23	1.359(15)
C23	C24	1.378(15)
C24	C25	1.378(12)
C25	C26	1.488(12)
C31	C32	1.373(14)
C32	C33	1.371(15)
C33	C34	1.368(15)
C34	C35	1.360(12)

Atom	Atom	Length/Å
N3	C31	1.341(11)
N3	C35	1.335(10)

Atom	Atom	Length/Å
C35	C36	1.487(12)

Table 8. Bond angles for $[\{Fe(TPA)Br\}_2O](ClO_4)_2 \bullet H_2O$

Atom1	Atom	Atom2	Angle/°	Atom	Atom2	Atom3	Angle/°
Br1	Fe1	O1	98.58(6)	Fe1	N3	C35	116.5(6)
Br1	Fe1	N1	99.77(18)	C31	N3	C35	118.8(7)
Br1	Fe1	N2	89.78(18)	Fe1	N4	C16	103.1(4)
Br1	Fe1	N3	106.87(18)	Fe1	N4	C26	111.6(5)
Br1	Fe1	N4	164.72(17)	Fe1	N4	C36	107.2(4)
O1	Fe1	N1	92.3(3)	C16	N4	C36	111.9(6)
O1	Fe1	N2	171.08(19)	C16	N4	C26	109.7(7)
O1	Fe1	N3	92.9(3)	C26	N4	C36	112.9(7)
O1	Fe1	N4	95.73(18)	N1	C11	C12	122.2(10)
N1	Fe1	N2	89.3(3)	C11	C12	C13	118.2(11)
N1	Fe1	N3	151.8(2)	C12	C13	C14	120.1(11)
N1	Fe1	N4	74.3(2)	C13	C14	C15	118.8(10)
N2	Fe1	N3	81.7(3)	N1	C15	C14	121.1(9)
N2	Fe1	N4	76.3(2)	N1	C15	C16	114.9(7)
N3	Fe1	N4	77.6(2)	C14	C15	C16	124.0(8)
O11A	Cl1	O12A	110(3)	N4	C16	C15	108.7(6)
O11A	Cl1	O13A	107.0(15)	N2	C21	C22	121.8(9)
O12A	Cl1	O13A	102.5(17)	C21	C22	C23	119.2(10)
O11B	Cl1	O12B	104(3)	C22	C23	C24	119.4(10)
O11B	Cl1	O13B	124(4)	C23	C24	C25	119.8(10)
O12B	Cl1	O13B	105(3)	N2	C25	C26	117.4(7)

Atom1	Atom	Atom2	Angle/$^{\circ}$	Atom	Atom2	Atom3	Angle/$^{\circ}$
O14	Cl1	O11A	111.9(17)	N2	C25	C24	121.0(8)
O14	Cl1	O12A	118.2(17)	C24	C25	C26	121.6(8)
O14	Cl1	O13A	106.5(9)	N4	C26	C25	114.7(7)
O14	Cl1	O11B	117(3)	N3	C31	C32	122.2(9)
O14	Cl1	O12B	90(3)	C31	C32	C33	117.7(10)
O14	Cl1	O13B	111(2)	C32	C33	C34	120.5(10)
Fe1	O1	Fe1 ¹	174.6(5)	C33	C34	C35	118.6(9)
Fe1	N1	C11	125.9(6)	N3	C35	C34	122.1(9)
Fe1	N1	C15	114.4(5)	N3	C35	C36	116.5(7)
C11	N1	C15	119.6(8)	C34	C35	C36	121.4(8)
Fe1	N2	C21	125.4(6)	N4	C36	C35	113.3(6)
Fe1	N2	C25	115.8(5)				
C21	N2	C25	118.7(7)				
Fe1	N3	C31	124.6(6)				

¹1-X,+Y,1/2-Z

Table 9. Hydrogen atom coordinates ($\text{\AA} \times 10^4$) and isotropic displacement parameters ($\text{\AA}^2 \times 10^3$) for $[\{Fe(TPA)Br\}_2O](ClO_4)_2 \bullet H_2O$

Atom	x	y	z	U(eq)
H11	6610(60)	6870(60)	4200(60)	72
H12	6730(80)	5600(70)	4180(80)	99
H13	6264.26	4967.95	2781.98	106
H14	5877.18	5722.98	1567.03	84
H21	8043.27	8954.21	4329.04	74
H22	9520.08	9062.41	4519.58	101
H23	10022.6	8557.73	3512.8	107
H24	9016.56	8018.03	2284.51	83

Atom	x	y	z	U(eq)
H31	6295.56	10129.4	3279.61	65
H32	6213.24	11285	2564.21	98
H33	6114.07	11240.6	1160.41	103
H34	6096.28	10059	509.92	81
H2A	6077.01	1587.82	4219.49	246
H16A	5889.12	7057.55	957.71	53
H26A	7392.12	7987.2	1330.11	69
H36A	5357.08	8558.24	785.93	55
H2B	6110.76	2391.72	4286.97	246
H16B	5171.29	7434.44	1267.33	53
H26B	7341.82	7255.18	1862.26	69
H36B	6276.81	8641.24	677.85	55

Table 10. Partial atomic occupancy for $\{Fe(TPA)Br\}_2O](ClO_4)_2 \bullet H_2O$

Atom	<i>Occupancy</i>		Atom	<i>Occupancy</i>		Atom	<i>Occupancy</i>
O11A	0.65		O11B	0.35		H2A	0.5
O12A	0.65		O12B	0.35		H2B	0.5
O13A	0.65		O13B	0.35		O2	0.5

3.3.2. [{Fe(TPA)}₂O(OAc)](ClO₄)₃•H₂O

Two polymorphic structures of [{Fe(TPA)}₂O(OAc)](ClO₄)₃•H₂O are reported in this section. One polymorph is P2₁/c and the other polymorph is P2₁/n. The packing arrangement of the cations with counter ions and the solvate water molecule is different between these two structures which makes these two polymorphs and not identical structures. In P2₁/c, the acetate carbon (C2) is near O14 and O22 with the distances 3.87501(19) Å and 3.7248(3) Å, respectively. In P2₁/n, the acetate carbon (C2) is near O21 and O22 with the distances 3.71531(13) Å and 3.60228(9) Å, respectively. Therefore, when compared to P2₁/c, the perchlorate oxygens are packed more closer in the P2₁/n polymorph. The organization about the water molecule is also different in these two structures. In P2₁/c, the oxygen of water (O4) is only hydrogen bonded to one O32 with the O-O separation of 3.1282(2) Å. In contrast, in P2₁/n the oxygen of water (O4) is 2.85054(8) Å from O33B indicative of a stronger hydrogen bond than the P2₁/c case and is also hydrogen bound to a second oxygen (O31A) of a symmetry related perchlorate.

3.3.2.1. [{Fe(TPA)}₂O(OAc)](ClO₄)₃•H₂O P2₁/c polymorph

Figure 51 shows the asymmetric unit of [{Fe(TPA)}₂O(OAc)](ClO₄)₃•H₂O P2₁/c polymorph. The cationic portion of [{Fe(TPA)}₂O(OAc)](ClO₄)₃•H₂O is shown in **Figure 52**. Crystallographic details for the [{Fe(TPA)}₂O(OAc)](ClO₄)₃•H₂O P2₁/c polymorph are listed in **Table 11**. Fractional atomic coordinates, anisotropic displacement parameters, bond lengths and bond angles involving the non-hydrogen atoms and hydrogen atom coordinates are listed in **Table 12**, **Table 13**, **Table 14**, **Table 15**, and **Table 16**, respectively.

The O1 is the bridging oxygen for the Fe1-O1-Fe2 unit in the dimer. The coordinated acetate unit is labeled C1, C2, O2, and O3. C1 is bonded to O2 and O3. O2 and O3 coordinate to the Fe1 and Fe2, respectively. For the non-coordinated perchlorate ions, the first perchlorate is labeled Cl1, O11, O12, O13, and O14. The second perchlorate is labeled Cl2, O21, O22, O23 and O24. The third perchlorate is labeled Cl3, O31, O32, O33 and O34. The oxygen atom of the water molecule is O4, and it is hydrogen bonded to O32.

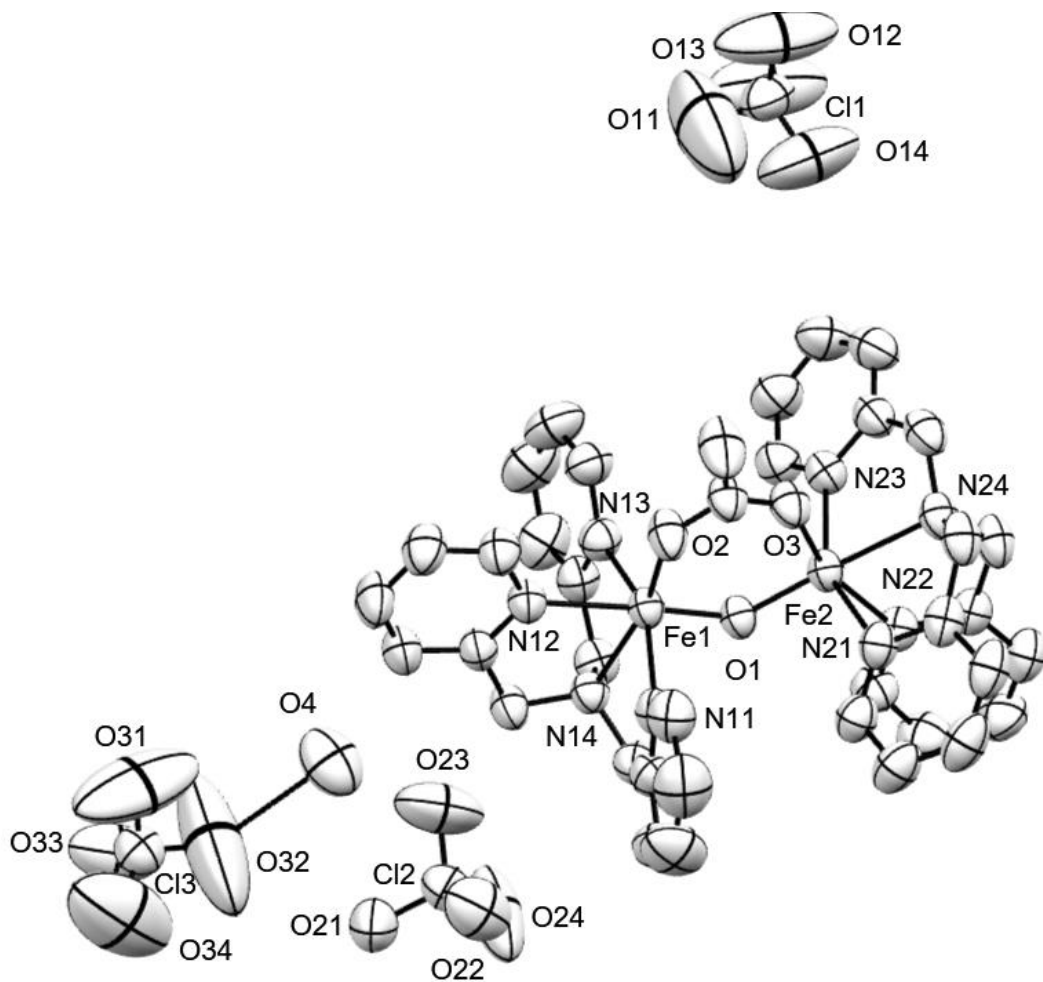


Figure 51. A view of the asymmetric unit of $\{Fe(TPA)\}_2O(OAc)\}](ClO_4)_3 \cdot H_2O$ P2₁/c polymorph.

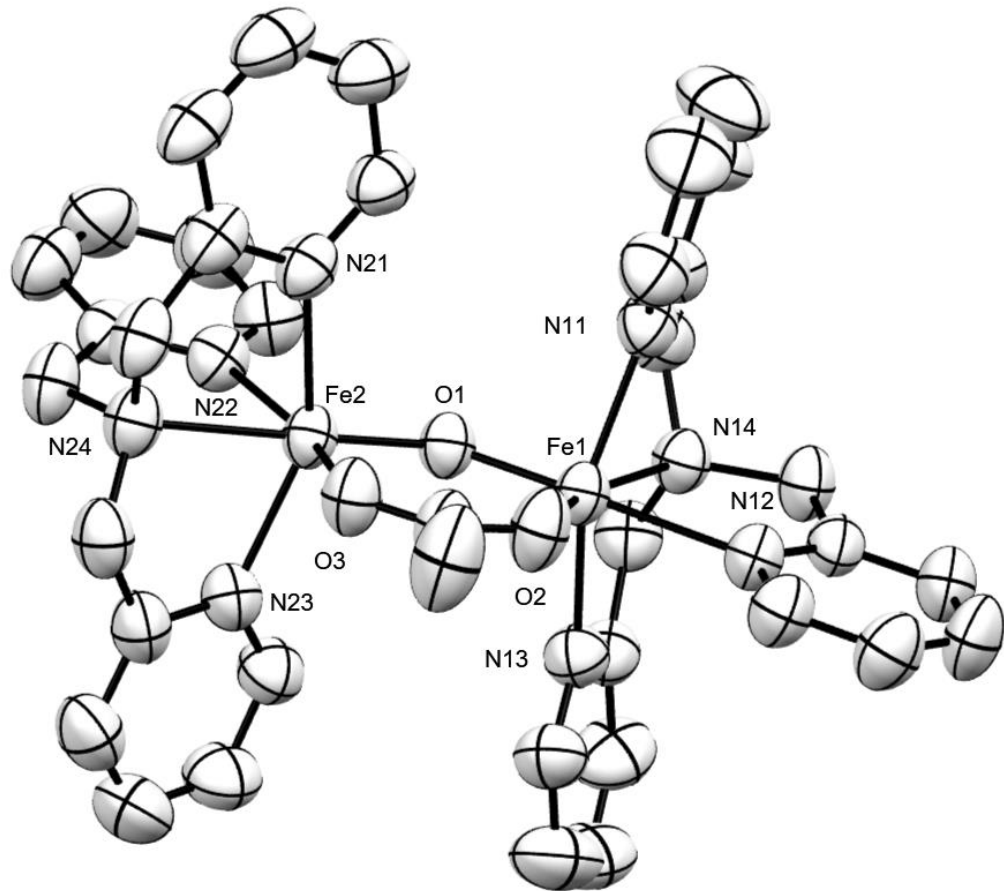


Figure 52. A view of the cationic portion of $\{Fe(TPA)\}_2O(OAc)\}(ClO_4)_3 \cdot H_2O$ P2₁/c polymorph. Hydrogen atoms are omitted.

Table 11. Crystallographic data for $\left[\{Fe(TPA)\}_2O(OAc)\right](ClO_4)_3 \cdot H_2O$ P2₁/c polymorph

Crystallographic data	
Empirical formula	C ₃₈ H ₄₁ Cl ₃ Fe ₂ N ₈ O ₁₆
Formula weight	1083.84
Temperature/K	298
Crystal system	monoclinic
Space group	P2 ₁ /c
a/Å	10.5315(7)
b/Å	22.5724(15)
c/Å	20.7577(15)
α/°	90
β/°	104.711(7)
γ/°	90
Volume/Å ³	4772.8(6)
Z	4
ρ _{calc} /g cm ⁻³	1.508
μ/mm ⁻¹	0.851
F(000)	2224
Crystal size/mm ³	6.1 × 3 × 2.3
Radiation	MoKα ($\lambda = 0.71073$)
2θ range for data collection/°	5.242 to 60
Index ranges	-14 ≤ h ≤ 13, -31 ≤ k ≤ 31, -26 ≤ l ≤ 29

Crystallographic data	
Reflections collected	39507
Independent reflections	13844 [$R_{\text{int}} = 0.0219$, $R_{\text{sigma}} = 0.0221$]
Data/restraints/parameters	13844/0/608
Goodness-of-fit on F^2	1.061
Final R indexes [$I \geq 2\sigma (I)$]	$R_1 = 0.0776$, $wR_2 = 0.2369$
Final R indexes [all data]	$R_1 = 0.0938$, $wR_2 = 0.2685$
Largest diff. peak/hole / e Å ⁻³	1.66/-0.47

Table 12. Fractional atomic coordinates ($\times 10^4$) and equivalent isotropic displacement parameters ($\text{\AA}^2 \times 10^3$) for $[\{\text{Fe}(TPA)\}_2\text{O(OAc)}](\text{ClO}_4)_3 \cdot \text{H}_2\text{O}$ P2₁/c polymorph

Atom	x	y	z	U(eq)
Fe1	3281.3(4)	7893.4(2)	3238.9(2)	50.37(14)
Fe2	5418.2(4)	6835.0(2)	3636.5(2)	49.90(14)
Cl1	11943.6(15)	9038.1(6)	5922.6(6)	91.3(3)
Cl2	-2662.1(11)	8146.9(6)	1631.6(6)	79.9(3)
Cl3	1918.0(11)	9016.7(5)	98.8(6)	80.9(3)
O1	4374(2)	7330.9(9)	3078.2(10)	52.3(4)
O2	3500(3)	7798.6(12)	4194.1(13)	70.3(7)
O3	5015(3)	7093.2(12)	4493.4(12)	64.1(6)
O11	10954(16)	9323(8)	5718(7)	344(9)
O12	12285(11)	9077(5)	6577(3)	256(6)
O13	12833(10)	9243(5)	5590(3)	242(6)
O14	11384(11)	8530(4)	5676(4)	221(4)
O21	-3604(4)	8551.5(16)	1223(2)	98.3(10)
O22	-3348(5)	7726(3)	1905(3)	132.9(18)

Atom	x	y	z	U(eq)
O23	-1823(6)	8447(4)	2163(3)	172(3)
O24	-1991(8)	7852(3)	1226(3)	192(4)
O31	1553(17)	8867(5)	-520(4)	309(8)
O32	1222(16)	9500(8)	-43(7)	392(12)
O33	1427(6)	8697(3)	533(3)	158(3)
O34	3180(10)	9162(6)	356(7)	281(7)
O4	10(5)	9806(3)	1145(3)	129.1(16)
N11	1563(3)	7374.8(13)	2878.8(15)	59.7(6)
N12	1964(3)	8636.1(12)	3326.5(14)	56.3(6)
N13	4556(3)	8609.7(13)	3171.3(15)	60.0(6)
N14	2552(3)	8169.9(12)	2201.2(13)	53.7(5)
N21	4213(3)	6072.2(12)	3623.6(15)	58.2(6)
N22	6123(3)	6336.2(13)	2922.2(14)	57.3(6)
N23	7241(3)	7290.0(13)	3927.0(14)	58.7(6)
N24	6776(3)	6188.2(13)	4282.7(14)	58.7(6)
C1	4240(4)	7465.5(16)	4624.1(16)	61.9(7)
C2	4090(6)	7511(3)	5321(2)	100.4(18)
C111	898(4)	7091.2(19)	3268(3)	75.4(10)
C112	-133(6)	6728(3)	2984(4)	107.2(19)
C113	-543(6)	6679(3)	2324(4)	113(2)
C114	140(5)	6954(2)	1917(3)	88.7(13)
C115	1195(3)	7305.1(16)	2222(2)	64.2(8)
C116	2034(4)	7623.4(17)	1842.9(18)	63.4(7)
C121	1810(4)	8867.3(17)	3894.0(19)	67.0(8)
C122	1007(5)	9341.0(19)	3910(2)	77.9(10)
C123	345(5)	9596(2)	3319(3)	83.0(12)
C124	517(4)	9368.3(17)	2734(2)	68.7(8)

Atom	x	y	z	U(eq)
C125	1337(3)	8890.2(14)	2754.6(17)	55.3(6)
C126	1496(4)	8625.4(16)	2114.1(17)	63.0(8)
C131	5303(4)	8913.5(19)	3681(2)	72.8(9)
C132	6038(6)	9392(3)	3584(3)	97.9(15)
C133	6003(6)	9564(2)	2950(3)	99.4(16)
C134	5267(5)	9248(2)	2434(3)	86.3(12)
C135	4527(3)	8768.7(15)	2546.7(19)	61.3(7)
C136	3730(4)	8385.9(17)	2008.6(17)	62.6(7)
C211	3076(4)	5970.3(16)	3163(2)	65.2(8)
C212	2403(5)	5446.8(19)	3129(3)	80.6(11)
C213	2949(5)	4993.9(18)	3557(3)	85.3(13)
C214	4129(5)	5087.2(16)	4012(2)	75.0(11)
C215	4727(4)	5635.9(15)	4047.5(18)	62.1(7)
C216	5944(4)	5799.2(17)	4567.0(18)	67.2(8)
C221	5640(4)	6393.3(19)	2268.4(19)	69.8(8)
C222	5913(5)	6000(2)	1816(2)	82.9(11)
C223	6738(5)	5522(2)	2065(3)	86.9(13)
C224	7253(5)	5468.8(19)	2725(2)	78.3(11)
C225	6924(3)	5883.5(15)	3152.7(18)	59.2(7)
C226	7517(4)	5852.2(17)	3885.5(19)	67.0(8)
C231	7541(4)	7770.2(17)	3613(2)	66.5(8)
C232	8684(5)	8071(2)	3851(3)	81.5(11)
C233	9536(5)	7889(2)	4418(3)	90.9(14)
C234	9254(4)	7386(2)	4737(2)	80.4(11)
C235	8098(3)	7095.1(17)	4480.9(18)	64.0(8)
C236	7677(4)	6550.4(19)	4797.9(18)	69.0(9)

Table 13. Anisotropic displacement parameters ($\text{\AA}^2 \times 10^3$) for $[\{\text{Fe}(TPA)\}_2\text{O(OAc)}] (\text{ClO}_4)_3 \cdot \text{H}_2\text{O}$ $P2_1/c$ polymorph

Atom	U₁₁	U₂₂	U₃₃	U₂₃	U₁₃	U₁₂
Fe1	52.9(2)	49.4(2)	49.1(2)	6.55(15)	13.53(17)	6.00(15)
Fe2	52.0(2)	48.8(2)	50.4(2)	6.95(15)	15.75(17)	5.69(15)
Cl1	113.9(9)	82.0(7)	73.2(6)	-12.0(5)	14.9(6)	-10.3(6)
Cl2	75.3(6)	92.3(7)	70.8(6)	4.1(5)	16.1(4)	-0.4(5)
Cl3	81.1(6)	87.5(7)	75.4(6)	3.6(5)	22.2(5)	1.8(5)
O1	54(1)	52.9(10)	50.8(10)	7.6(8)	14.9(8)	6.6(8)
O2	87.5(17)	72.2(15)	55.2(12)	10.9(11)	25.3(12)	28.3(13)
O3	71.4(14)	72.0(15)	50.5(11)	7.2(10)	18.3(10)	19.3(11)
O11	333(15)	430(20)	258(13)	44(14)	60(11)	243(16)
O12	343(12)	323(12)	93(4)	-33(5)	42(5)	-207(10)
O13	300(11)	316(11)	106(4)	1(5)	46(5)	-186(10)
O14	297(11)	211(8)	159(6)	-80(6)	66(6)	-124(8)
O21	110(3)	81(2)	98(2)	-0.4(18)	14(2)	14.0(18)
O22	124(3)	138(4)	130(4)	42(3)	19(3)	-29(3)
O23	133(4)	234(7)	124(4)	-9(5)	-13(3)	-63(5)
O24	248(7)	233(7)	119(4)	63(4)	89(5)	160(6)
O31	550(20)	282(11)	104(4)	-49(6)	108(8)	-211(14)
O32	470(20)	480(20)	274(14)	184(14)	181(14)	361(19)
O33	144(4)	232(7)	97(3)	23(4)	26(3)	-85(4)
O34	210(8)	293(12)	299(13)	136(10)	-12(8)	-121(9)
O4	122(3)	166(5)	105(3)	34(3)	40(3)	25(3)
N11	55.9(13)	56.5(13)	70.1(16)	6.2(12)	22.6(12)	3.2(11)
N12	59.1(13)	52.7(13)	58.0(14)	3.4(11)	16.6(11)	7.9(10)
N13	61.3(14)	56.8(14)	62.2(15)	1.5(12)	16.4(12)	-1.9(11)
N14	56.9(13)	54.1(13)	50.4(12)	3.9(10)	14.3(10)	4.8(10)

Atom	U₁₁	U₂₂	U₃₃	U₂₃	U₁₃	U₁₂
N21	65.8(15)	50.5(12)	63.6(15)	7.3(11)	26.3(12)	3.4(11)
N22	60.2(14)	58.4(14)	57.4(14)	1.9(11)	22.4(11)	1.7(11)
N23	55.3(13)	62.0(14)	58.0(14)	4.0(12)	13.1(11)	4.6(11)
N24	65.4(15)	60.5(14)	53.0(13)	9.4(11)	20.1(11)	12.3(12)
C1	73.7(19)	63.8(17)	50.7(15)	9.0(13)	20.5(14)	15.3(15)
C2	141(4)	109(4)	58(2)	17(2)	38(3)	54(3)
C111	68(2)	79(2)	87(3)	5(2)	35(2)	0.2(17)
C112	84(3)	102(4)	148(6)	18(4)	52(4)	-17(3)
C113	79(3)	123(4)	129(5)	8(4)	12(3)	-40(3)
C114	70(2)	86(3)	102(3)	-1(2)	7(2)	-17(2)
C115	53.9(16)	60.3(17)	75(2)	0.4(15)	11.0(15)	2.8(13)
C116	69.2(18)	63.0(18)	56.5(16)	-1.1(14)	13.7(14)	2.0(14)
C121	77(2)	65.2(18)	60.9(18)	3.6(15)	21.8(16)	10.4(16)
C122	93(3)	71(2)	75(2)	-6.0(19)	32(2)	14(2)
C123	93(3)	70(2)	89(3)	2(2)	30(2)	32(2)
C124	66.5(19)	63.7(19)	75(2)	8.0(16)	16.8(16)	16.0(15)
C125	51.3(14)	50.7(14)	63.0(16)	5.6(12)	13.0(12)	3.7(11)
C126	66.1(18)	65.1(18)	56.8(16)	10.6(14)	14.0(14)	17.3(14)
C131	75(2)	69(2)	72(2)	-7.2(17)	14.3(18)	-8.2(17)
C132	96(3)	92(3)	107(4)	-30(3)	27(3)	-32(3)
C133	102(3)	81(3)	125(4)	-10(3)	47(3)	-33(3)
C134	96(3)	75(2)	101(3)	7(2)	48(3)	-16(2)
C135	58.6(16)	59.4(16)	68.6(19)	7.2(14)	21.4(14)	-0.3(13)
C136	66.5(18)	67.4(18)	58.1(17)	8.5(14)	23.7(14)	0.8(14)
C211	66.7(18)	55.7(17)	78(2)	-0.3(15)	27.7(16)	-2.3(13)
C212	83(3)	64(2)	103(3)	-11(2)	39(2)	-13.6(18)
C213	103(3)	55.8(19)	114(4)	-6(2)	58(3)	-12.3(19)

Atom	U₁₁	U₂₂	U₃₃	U₂₃	U₁₃	U₁₂
C214	100(3)	52.6(16)	88(3)	12.7(17)	54(2)	5.7(17)
C215	76(2)	53.6(15)	66.5(18)	7.2(13)	36.3(16)	6.3(14)
C216	82(2)	63.7(18)	62.6(18)	20.9(15)	31.4(17)	16.6(16)
C221	72(2)	78(2)	61.0(18)	1.8(16)	19.8(16)	4.1(17)
C222	86(3)	101(3)	63(2)	-13(2)	22.0(19)	-1(2)
C223	87(3)	91(3)	85(3)	-31(2)	27(2)	1(2)
C224	84(3)	65(2)	92(3)	-3.4(19)	35(2)	12.4(18)
C225	62.5(17)	54.8(15)	65.4(17)	2.4(13)	25.8(14)	1.3(12)
C226	69.6(19)	68.5(19)	69.7(19)	13.2(16)	30.2(16)	23.7(16)
C231	59.6(17)	68.2(19)	72(2)	4.4(16)	16.7(15)	-2.9(14)
C232	75(2)	76(2)	93(3)	3(2)	22(2)	-16.8(19)
C233	72(3)	97(3)	95(3)	-11(3)	6(2)	-15(2)
C234	64(2)	99(3)	71(2)	-3(2)	3.6(17)	4(2)
C235	59.0(17)	74(2)	56.8(17)	0.6(15)	10.7(13)	12.2(14)
C236	68.1(19)	83(2)	52.9(16)	8.5(16)	9.8(14)	17.2(17)

Table 14. Bond lengths for $[\{Fe(TPA)\}_2O(OAc)](ClO_4)_3 \cdot H_2O$ P2₁/c polymorph

Atom	Atom	Length/Å	Atom	Atom	Length/Å
Fe1	O1	1.800(2)	N22	C225	1.334(4)
Fe1	O2	1.949(3)	N23	C231	1.343(5)
Fe1	N11	2.125(3)	N23	C235	1.342(4)
Fe1	N12	2.213(3)	N24	C216	1.467(5)
Fe1	N13	2.129(3)	N24	C226	1.480(4)
Fe1	N14	2.186(3)	N24	C236	1.482(5)
Fe2	O1	1.777(2)	C1	C2	1.497(5)
Fe2	O3	2.017(2)	C111	C112	1.368(8)
Fe2	N21	2.135(3)	C112	C113	1.332(10)

Atom	Atom	Length/Å
Fe2	N22	2.139(3)
Fe2	N23	2.125(3)
Fe2	N24	2.237(3)
Cl1	O11	1.206(11)
Cl1	O12	1.316(6)
Cl1	O13	1.378(8)
Cl1	O14	1.332(7)
Cl2	O21	1.453(4)
Cl2	O22	1.397(5)
Cl2	O23	1.400(6)
Cl2	O24	1.398(5)
Cl3	O31	1.289(7)
Cl3	O32	1.306(11)
Cl3	O33	1.355(5)
Cl3	O34	1.341(9)
O2	C1	1.271(4)
O3	C1	1.249(4)
N11	C111	1.357(5)
N11	C115	1.329(5)
N12	C121	1.336(5)
N12	C125	1.333(4)
N13	C131	1.336(5)
N13	C35	1.338(5)
N14	C116	1.472(5)
N14	C126	1.492(4)
N14	C136	1.479(4)

Atom	Atom	Length/Å
C113	C114	1.387(9)
C114	C115	1.380(6)
C115	C116	1.507(5)
C121	C122	1.369(5)
C122	C123	1.375(7)
C123	C124	1.371(6)
C125	C126	1.505(5)
C124	C125	1.376(5)
C131	C132	1.373(7)
C132	C133	1.364(9)
C133	C134	1.355(8)
C135	C136	1.491(5)
C134	C135	1.386(5)
C211	C212	1.371(5)
C212	C213	1.380(7)
C213	C214	1.373(8)
C214	C215	1.383(5)
C215	C216	1.496(6)
C221	C222	1.375(6)
C222	C223	1.400(7)
C223	C224	1.344(7)
C225	C226	1.492(5)
C224	C225	1.393(5)
C231	C232	1.362(6)
C232	C233	1.351(7)
C233	C234	1.385(7)

Atom	Atom	Length/Å
N21	C211	1.348(5)
N21	C215	1.340(4)
N22	C221	1.329(5)

Atom	Atom	Length/Å
C235	C236	1.513(6)
C234	C235	1.367(6)

Table 15. Bond angles for $[\{Fe(TPA)\}_2O(OAc)](ClO_4)_3 \cdot H_2O$ P2 $_1$ /c polymorph

Atom	Atom	Atom	Angle/ $^{\circ}$	Atom	Atom	Atom	Angle/ $^{\circ}$
O1	Fe1	O2	101.25(10)	Fe2	N21	C211	124.4(2)
O1	Fe1	N11	94.20(11)	Fe2	N21	C215	116.4(2)
O1	Fe1	N12	173.19(10)	C211	N21	C215	118.6(3)
O1	Fe1	N13	94.59(11)	Fe2	N22	C221	123.1(2)
O1	Fe1	N14	95.73(10)	Fe2	N22	C225	117.0(2)
O2	Fe1	N11	99.63(13)	C225	N22	C221	118.9(3)
O2	Fe1	N12	85.07(10)	Fe2	N23	C231	124.0(2)
O2	Fe1	N13	103.71(13)	Fe2	N23	C235	116.5(2)
O2	Fe1	N14	162.74(10)	C231	N23	C235	119.4(3)
N11	Fe1	N12	87.17(11)	Fe2	N24	C216	106.0(2)
N11	Fe1	N13	152.89(11)	Fe2	N24	C226	110.3(2)
N11	Fe1	N14	75.89(11)	Fe2	N24	C236	105.5(2)
N12	Fe1	N13	81.32(11)	C216	N24	C226	111.8(3)
N12	Fe1	N14	78.12(10)	C216	N24	C236	112.2(3)
N13	Fe1	N14	77.75(11)	C226	N24	C236	110.7(3)
O1	Fe2	O3	99.15(10)	O2	C1	O3	124.3(3)
O1	Fe2	N21	103.42(11)	O2	C1	C2	116.2(3)
O1	Fe2	N22	98.38(10)	O3	C1	C2	119.4(3)
O1	Fe2	N23	104.22(11)	N11	C111	C112	119.9(5)
O1	Fe2	N24	176.27(10)	C111	C112	C113	120.5(5)

Atom	Atom	Atom	Angle/[°]	Atom	Atom	Atom	Angle/[°]
O3	Fe2	N21	89.22(11)	C112	C113	C114	120.4(5)
O3	Fe2	N22	162.03(10)	C113	C114	C115	117.4(5)
O3	Fe2	N23	89.29(12)	N11	C115	C114	122.0(4)
O3	Fe2	N24	84.58(10)	N11	C115	C116	115.0(3)
N21	Fe2	N22	82.92(11)	C114	C115	C116	123.1(4)
N21	Fe2	N23	152.20(11)	N14	C116	C115	109.1(3)
N21	Fe2	N24	76.63(11)	N12	C121	C122	122.8(4)
N22	Fe2	N23	90.20(11)	C121	C122	C123	118.7(4)
N22	Fe2	N24	77.90(11)	C122	C123	C124	118.9(4)
N23	Fe2	N24	75.59(11)	C123	C124	C125	119.3(4)
O11	Cl1	O12	108.2(9)	N12	C125	C124	122.0(3)
O11	Cl1	O13	106.4(10)	N12	C125	C126	118.4(3)
O11	Cl1	O14	93.7(10)	C124	C125	C126	119.6(3)
O12	Cl1	O13	116.9(5)	N14	C126	C125	114.4(3)
O12	Cl1	O14	115.7(6)	N13	C131	C132	121.8(4)
O13	Cl1	O14	112.8(6)	C131	C132	C133	119.3(5)
O21	Cl2	O22	108.5(3)	C132	C133	C134	118.7(4)
O21	Cl2	O23	110.9(4)	C133	C134	C135	120.8(5)
O21	Cl2	O24	108.8(3)	N13	C135	C134	119.8(4)
O22	Cl2	O23	107.3(4)	N13	C135	C136	116.1(3)
O22	Cl2	O24	108.3(5)	C134	C135	C136	124.0(4)
O23	Cl2	O24	113.0(5)	N14	C136	C135	109.9(3)
O31	Cl3	O32	89.3(9)	N21	C211	C212	122.6(4)
O31	Cl3	O33	117.1(5)	C211	C212	C213	118.7(5)
O31	Cl3	O34	118.4(10)	C212	C213	C214	119.1(4)
O32	Cl3	O33	107.9(7)	C213	C214	C215	119.6(4)
O32	Cl3	O34	109.1(11)	N21	C215	C214	121.4(4)

Atom	Atom	Atom	Angle/$^{\circ}$	Atom	Atom	Atom	Angle/$^{\circ}$
O33	Cl3	O34	111.9(5)	N21	C215	C216	114.9(3)
Fe1	O1	Fe2	129.95(12)	C214	C215	C216	123.6(4)
Fe1	O2	C1	132.2(2)	N24	C216	C215	110.4(3)
Fe2	O3	C1	133.0(2)	N22	C221	C222	122.8(4)
Fe1	N11	C111	124.9(3)	C221	C222	C223	117.7(4)
Fe1	N11	C115	115.3(2)	C222	C223	C224	119.8(4)
C111	N11	C115	119.7(3)	C223	C224	C225	119.3(4)
Fe1	N12	C121	126.0(2)	N22	C225	C224	121.5(4)
Fe1	N12	C125	115.6(2)	N22	C225	C226	117.7(3)
C121	N12	C125	118.3(3)	C224	C225	C226	120.7(3)
Fe1	N13	C131	126.3(3)	N24	C226	C225	113.6(3)
Fe1	N13	C135	114.1(2)	N23	C231	C232	121.4(4)
C135	N13	C131	119.6(3)	C231	C232	C233	119.7(4)
Fe1	N14	C116	104.5(2)	C232	C233	C234	119.4(4)
Fe1	N14	C126	112.4(2)	C233	C234	C235	119.1(4)
Fe1	N14	C136	104.6(2)	N23	C235	C234	120.9(4)
C116	N14	C126	110.3(3)	N23	C235	C236	115.6(3)
C116	N14	C136	111.6(3)	C234	C235	C236	123.5(4)
C126	N14	C136	113.0(3)	N24	C236	C235	109.8(3)

Table 16. Hydrogen atom coordinates ($\text{\AA} \times 10^4$) and isotropic displacement parameters ($\text{\AA}^2 \times 10^3$) for $[\{\text{Fe}(TPA)\}_2\text{O(OAc)}](\text{ClO}_4)_3 \bullet \text{H}_2\text{O}$ P2₁/c polymorph

Atom	x	y	z	U(eq)
H111	1142.44	7143.27	3727.59	90
H112	-550.38	6514.51	3253.51	129
H113	-1292	6459.35	2135.35	135
H114	-103.79	6904.04	1457.67	106

Atom	x	y	z	U(eq)
H121	2266.51	8699.31	4295.05	80
H122	911.39	9487.85	4314.1	93
H123	-209.82	9916.69	3314.82	100
H124	84.67	9535.43	2328.45	82
H131	5325.03	8797.73	4113.78	87
H132	6553.52	9595.68	3946.08	117
H133	6475.98	9893.27	2873.13	119
H134	5257.26	9352.78	2000.1	104
H211	2735.98	6266.81	2856.71	78
H212	1594.84	5397.69	2823.07	97
H213	2523.91	4630.64	3536.51	102
H214	4523.09	4783.23	4295.39	90
H221	5092.75	6713.23	2110.03	84
H222	5561.63	6049.72	1361.01	100
H223	6930.29	5241.96	1774.63	104
H224	7821.95	5158.85	2893.66	94
H231	6954.27	7899.7	3224	80
H232	8877.1	8400.87	3623.95	98
H233	10304.2	8100.44	4593.44	109
H234	9844.6	7246.8	5119.53	97
H2A	3218.26	7643.2	5309.9	151
H4A	429.99	9538	998.79	194
H11A	2754.34	7370.26	1802.45	76
H12A	669.45	8446.15	1881	76
H13A	3465.35	8610.47	1597.82	75
H21A	5706.07	5999.64	4932.87	81

Atom	x	y	z	U(eq)
H22A	7565.66	5440.39	4023.23	80
H23A	8442.48	6317.95	5011.73	83
H2B	4717.22	7788.95	5567.68	151
H4B	-789.64	9802.77	921.91	194
H11B	1515.33	7719.69	1398.53	76
H12B	1683.62	8941.4	1835.42	76
H13B	4252.63	8051.73	1932.9	75
H21B	6425.95	5443.02	4740.34	81
H22B	8406.18	6004.73	3980.61	80
H23B	7236.74	6668.38	5135.26	83
H2C	4237.53	7129.45	5531.12	151

3.3.2.2. [{Fe(TPA)}₂O(OAc)][ClO₄)₃•H₂O P2₁/n polymorph

Figure 53 shows the structure of the asymmetric unit of [{Fe(TPA)}₂O(OAc)][ClO₄)₃•H₂O P2₁/n polymorph. The cationic portion of [{Fe(TPA)}₂O(OAc)][ClO₄)₃•H₂O is shown in **Figure 54**. Crystallographic details for the [{Fe(TPA)}₂O(OAc)][ClO₄)₃•H₂O are listed in **Table 17**. Fractional atomic coordinates, anisotropic displacement parameters, bond lengths and bond angles involving the non-hydrogen atoms, hydrogen atom coordinates and atomic occupancies for the disordered perchlorate molecule are listed in **Table 18**, **Table 19**, **Table 20**, **Table 21**, **Table 22** and **Table 23**, respectively.

The O1 is the bridging oxygen for Fe1-O1-Fe2 unit in the dimer. The coordinated acetate unit is labeled C1, C2, O2, and O3. C1 is bonded to O2 and O3. O2 and O3 coordinate to the Fe1 and Fe2 respectively. The oxygen atom of the water molecule is O4, and it is hydrogen bonded O33 of a disordered perchlorate ion. The first perchlorate is labeled Cl1, O11, O12, O13 and O14. The second perchlorate is labeled C21, O21, O22, O23 and O24. Unlike the P2₁/c polymorph, the P2₁/n polymorph has the third perchlorate disordered and is modeled with two sets of oxygen atoms with occupancies of 0.55 and 0.45.

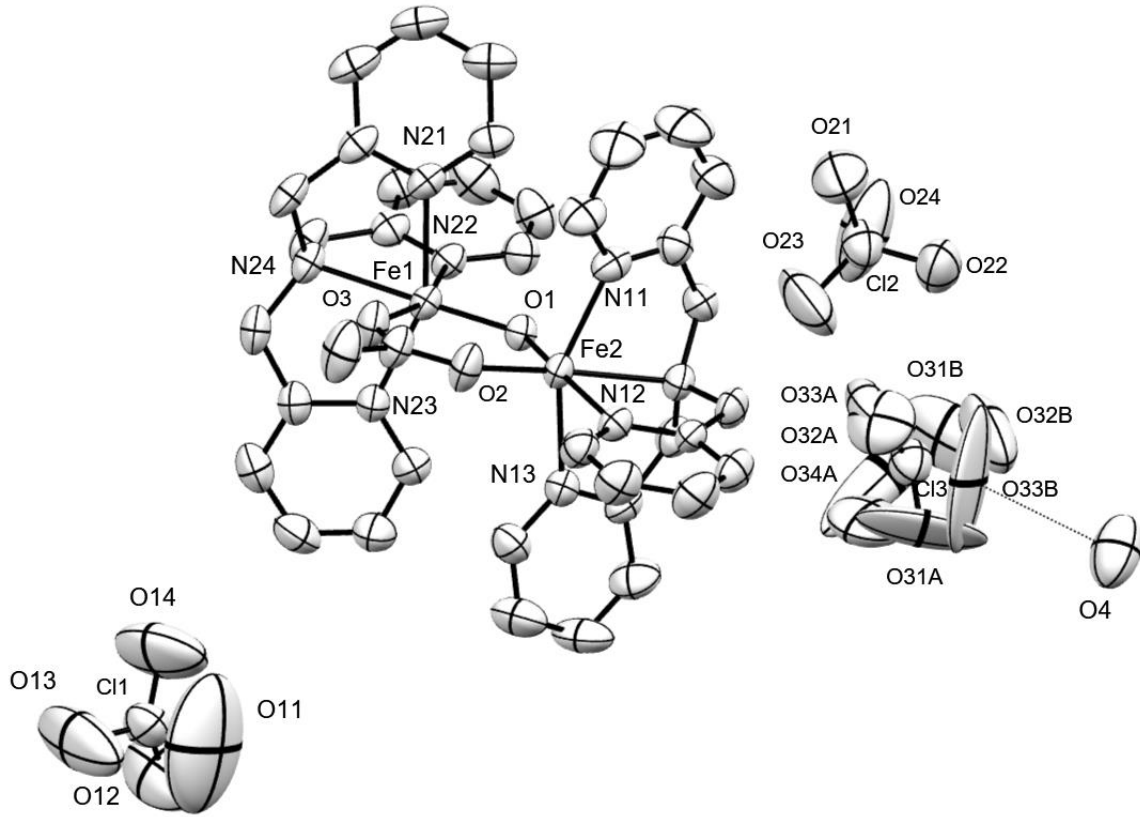


Figure 53. A view of the asymmetric unit of $\left[\{Fe(TPA)\}_2O(OAc)\right](ClO_4)_3 \cdot H_2O$ $P2_1/n$ polymorph.

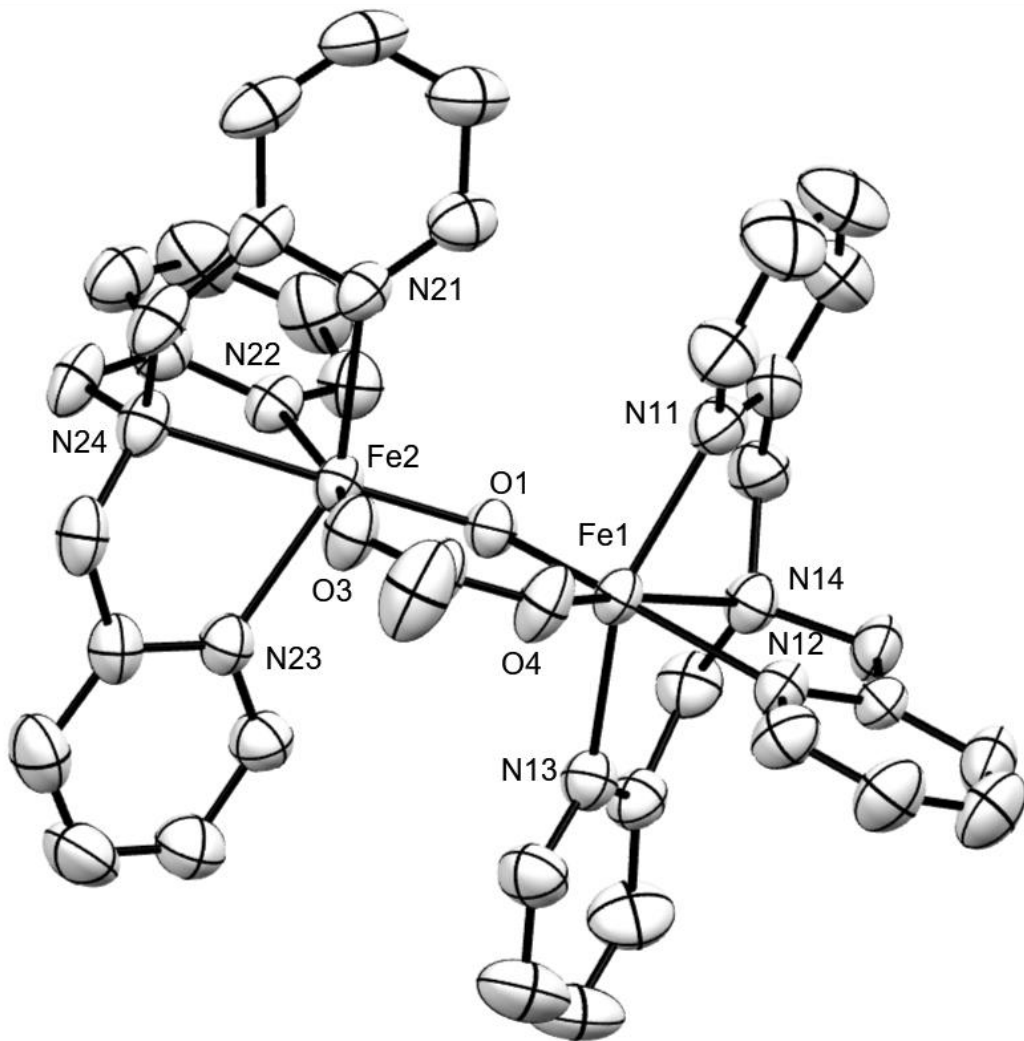


Figure 54. A view of the cationic portion of $\{[Fe(TPA)]_2O(OAc)\}[ClO_4]_3 \cdot H_2O$ P2₁/n polymorph. Hydrogen atoms are omitted.

Table 17. Crystallographic data for $\left[\{Fe(TPA)\}_2O(OAc)\right](ClO_4)_3 \bullet H_2O$ P2₁/n polymorph

Crystallographic data	
Empirical formula	C ₃₈ H ₄₁ Cl ₃ Fe ₂ N ₈ O ₁₆
Formula weight	1083.84
Temperature/K	298
Crystal system	monoclinic
Space group	P2 ₁ /n
a/Å	10.6005(4)
b/Å	22.5290(8)
c/Å	20.9229(8)
α/°	90
β/°	104.192(4)
γ/°	90
Volume/Å ³	4844.3(3)
Z	4
ρ _{calc} /g cm ⁻³	1.486
μ/mm ⁻¹	0.838
F(000)	2224
Crystal size/mm ³	7 × 3.7 × 1.7
Radiation	MoKα ($\lambda = 0.71073$)
2θ range for data collection/°	5.366 to 50.998
Index ranges	-12 ≤ h ≤ 12, -25 ≤ k ≤ 27, -25 ≤ l ≤ 25

Crystallographic data	
Reflections collected	24212
Independent reflections	9008 [$R_{\text{int}} = 0.0474$, $R_{\text{sigma}} = 0.0463$]
Data/restraints/parameters	9008/0/644
Goodness-of-fit on F^2	1.084
Final R indexes [$I \geq 2\sigma (I)$]	$R_1 = 0.0725$, $wR_2 = 0.2089$
Final R indexes [all data]	$R_1 = 0.1024$, $wR_2 = 0.2495$
Largest diff. peak/hole / e Å ⁻³	1.96/-0.51

Table 18. Fractional atomic coordinates ($\times 10^4$) and equivalent isotropic displacement parameters ($\text{\AA}^2 \times 10^3$) for $[\{\text{Fe}(TPA)\}_2\text{O(OAc)}](\text{ClO}_4)_3 \cdot \text{H}_2\text{O}$ P2₁/n polymorph

Atom	x	y	z	U(eq)
Fe1	4926.7(7)	7088.1(3)	3248.7(3)	35.5(2)
Fe2	3190.2(7)	8147.0(3)	3651.4(3)	35.2(2)
Cl1	-1010(2)	5982.3(9)	5940.8(9)	73.8(5)
Cl2	9283.4(18)	6840.8(9)	1641.7(9)	67.8(5)
Cl3	3177.9(17)	5991.6(8)	109.8(9)	66.3(5)
O1	3681(3)	7656.0(15)	3093.2(16)	36.5(8)
O2	5639(4)	7173.9(18)	4205.6(19)	54.4(11)
O3	4427(4)	7877.5(18)	4504.3(18)	49.7(10)
O4	3857(7)	4801(4)	-1136(4)	122(3)
O11	-314(19)	5624(10)	5725(9)	341(13)
O12	-762(14)	5938(7)	6599(4)	244(8)
O13	-2214(11)	5759(6)	5593(5)	206(6)
O14	-692(12)	6494(5)	5700(5)	195(5)

Atom	x	y	z	U(eq)
O21	10253(8)	7264(4)	1911(4)	124(3)
O22	9789(7)	6450(3)	1219(3)	90.7(17)
O23	8996(10)	6532(5)	2172(4)	166(4)
O24	8180(9)	7120(5)	1263(4)	176(5)
O31A	3300(30)	5431(14)	240(30)	260(20)
O32A	4200(40)	6196(18)	529(17)	127(14)
O33A	3960(30)	6420(16)	535(13)	105(12)
O34A	1895(19)	6140(20)	-10(40)	390(50)
O31B	2550(30)	6236(14)	-446(11)	202(14)
O32B	3530(30)	6020(17)	-510(10)	183(13)
O33B	3960(40)	5630(20)	-99(17)	330(30)
O34B	2370(30)	5733(12)	410(15)	182(11)
N11	6301(4)	7615(2)	2908(2)	45.2(11)
N12	6323(4)	6344.0(19)	3333(2)	39.8(10)
N13	3580(4)	6370(2)	3164(2)	41.8(10)
N14	4657(4)	6821(2)	2214(2)	39.6(10)
N21	4395(4)	8911.8(19)	3648(2)	41.9(10)
N22	1793(4)	8653(2)	2944(2)	40.8(10)
N23	1649(4)	7691(2)	3928(2)	41.5(10)
N24	2472(4)	8790(2)	4301(2)	42.2(10)
C1	5342(5)	7511(3)	4634(3)	45.4(13)
C2	6141(8)	7451(4)	5327(3)	78(2)
C111	7333(6)	7895(3)	3300(4)	59.2(16)
C112	8107(8)	8257(4)	3037(5)	87(3)
C113	7856(9)	8326(5)	2360(6)	100(3)
C114	6796(8)	8037(3)	1963(4)	75(2)

Atom	x	y	z	U(eq)
C115	6039(5)	7688(3)	2255(3)	47.8(13)
C116	4844(6)	7378(3)	1864(3)	46.8(13)
C121	7026(6)	6107(3)	3899(3)	51.4(14)
C122	7844(7)	5636(3)	3910(4)	62.7(17)
C123	7917(7)	5381(3)	3329(4)	67.1(18)
C124	7201(6)	5618(3)	2740(3)	55.8(15)
C125	6409(5)	6095(2)	2769(3)	39.1(11)
C126	5614(6)	6366(3)	2127(3)	48.7(13)
C131	3317(6)	6063(3)	3670(3)	55.6(15)
C132	2482(8)	5599(4)	3569(4)	80(2)
C133	1891(8)	5429(4)	2926(5)	86(2)
C134	2157(7)	5742(3)	2415(4)	68.0(19)
C135	2997(5)	6216(2)	2540(3)	45.2(12)
C136	3284(6)	6613(3)	2012(3)	49.7(14)
C211	5060(5)	9016(3)	3187(3)	50.2(14)
C212	5694(6)	9538(3)	3159(4)	64.2(17)
C213	5575(7)	9989(3)	3594(4)	66.0(19)
C214	4859(6)	9895(3)	4040(4)	59.0(17)
C215	4283(5)	9351(2)	4072(3)	46.2(13)
C216	3587(6)	9183(3)	4585(3)	51.4(15)
C221	1647(6)	8601(3)	2287(3)	51.3(14)
C222	942(7)	9001(4)	1853(3)	67.0(18)
C223	353(7)	9470(4)	2088(4)	72(2)
C224	489(6)	9524(3)	2759(3)	58.0(16)
C225	1225(5)	9108(3)	3173(3)	45.4(13)
C226	1360(5)	9134(3)	3916(3)	50.8(14)

Atom	x	y	z	U(eq)
C231	1032(6)	7219(3)	3611(3)	48.6(13)
C232	121(7)	6911(3)	3842(4)	61.8(17)
C233	-174(7)	7090(3)	4400(4)	71(2)
C234	421(7)	7591(3)	4734(3)	62.8(17)
C235	1342(5)	7884(3)	4484(3)	46.7(13)
C236	2063(6)	8421(3)	4806(3)	52.6(15)

Table 19. Anisotropic displacement parameters ($\text{\AA}^2 \times 10^3$) for $[\{Fe(TPA)\}_2O(OAc)](ClO_4)_3 \cdot H_2O$ P2₁/n polymorph

Atom	U ₁₁	U ₂₂	U ₃₃	U ₂₃	U ₁₃	U ₁₂
Fe1	39.8(4)	33.9(4)	32.9(4)	-6.1(3)	9.3(3)	2.5(3)
Fe2	36.4(4)	33.6(4)	35.0(4)	-7.0(3)	7.5(3)	1.5(3)
Cl1	96.3(14)	66.5(11)	58.1(10)	11.4(8)	18.2(9)	-4.5(10)
Cl2	67.3(10)	80.7(12)	55.6(9)	-5.2(8)	15.7(8)	-2.8(9)
Cl3	67.1(10)	71.3(11)	59.6(9)	-4.4(8)	14.1(8)	-2.7(8)
O1	36.8(17)	38.5(19)	33.5(17)	-2.4(15)	7.5(14)	1.7(15)
O2	67(3)	52(2)	40(2)	-11.1(18)	5.0(19)	20(2)
O3	57(2)	55(2)	35.1(19)	-5.6(17)	6.7(17)	16.9(19)
O4	100(5)	158(7)	102(5)	-51(5)	10(4)	-1(5)
O11	330(20)	410(30)	277(19)	-58(18)	68(16)	250(20)
O12	307(15)	322(17)	80(5)	31(8)	2(7)	-193(14)
O13	185(10)	287(15)	118(7)	1(8)	-18(6)	-122(11)
O14	239(12)	156(9)	171(9)	86(8)	12(8)	-54(9)
O21	137(6)	130(6)	113(5)	-39(5)	44(5)	-62(5)
O22	129(5)	73(4)	76(4)	-3(3)	37(3)	16(3)
O23	202(9)	222(11)	99(5)	15(6)	83(6)	-69(8)

Atom	U₁₁	U₂₂	U₃₃	U₂₃	U₁₃	U₁₂
O24	163(8)	218(10)	112(6)	-67(6)	-32(5)	109(8)
O31A	200(30)	130(20)	440(60)	200(30)	40(30)	-20(20)
O32A	102(14)	150(30)	102(18)	-9(16)	-26(13)	-28(16)
O33A	130(20)	140(20)	58(11)	-40(12)	45(14)	-90(20)
O34A	40(9)	310(40)	770(100)	-400(60)	-20(20)	24(17)
O31B	150(20)	290(30)	115(15)	110(20)	-48(14)	-40(20)
O32B	190(20)	290(30)	75(10)	-17(14)	49(15)	-90(30)
O33B	350(40)	460(50)	170(20)	-140(30)	60(20)	250(40)
O34B	170(20)	150(20)	270(30)	-28(19)	130(20)	-85(16)
N11	39(2)	38(2)	58(3)	-7(2)	10(2)	-0.4(19)
N12	42(2)	35(2)	43(2)	-3.5(19)	11.0(19)	3.2(18)
N13	46(2)	41(2)	40(2)	-3.6(19)	12.1(19)	-0.4(19)
N14	44(2)	41(2)	33(2)	-5.8(18)	8.4(18)	1.2(19)
N21	41(2)	35(2)	47(2)	-7(2)	6(2)	0.4(18)
N22	40(2)	40(2)	40(2)	-4.1(19)	4.9(19)	1.1(18)
N23	45(2)	43(2)	38(2)	-4(2)	12.3(19)	1(2)
N24	41(2)	44(2)	39(2)	-13(2)	3.4(19)	3.2(19)
C1	49(3)	47(3)	37(3)	-9(2)	2(2)	9(3)
C2	89(5)	87(5)	44(3)	-11(4)	-9(3)	36(4)
C111	41(3)	64(4)	69(4)	-6(3)	6(3)	-6(3)
C112	57(4)	98(6)	108(7)	-21(5)	21(4)	-31(4)
C113	82(6)	97(7)	135(9)	-2(6)	52(6)	-39(5)
C114	76(5)	74(5)	85(5)	3(4)	42(4)	-10(4)
C115	48(3)	48(3)	53(3)	-1(3)	21(3)	6(3)
C116	56(3)	47(3)	40(3)	2(2)	15(2)	-3(3)
C121	63(4)	45(3)	42(3)	-3(3)	6(3)	1(3)

Atom	U₁₁	U₂₂	U₃₃	U₂₃	U₁₃	U₁₂
C122	65(4)	53(4)	65(4)	7(3)	6(3)	18(3)
C123	67(4)	52(4)	79(5)	-4(4)	10(4)	21(3)
C124	54(3)	50(3)	65(4)	-12(3)	19(3)	9(3)
C125	45(3)	32(3)	43(3)	-8(2)	16(2)	-4(2)
C126	61(3)	41(3)	49(3)	-8(3)	22(3)	10(3)
C131	65(4)	56(4)	48(3)	6(3)	17(3)	-5(3)
C132	82(5)	69(5)	89(6)	21(4)	22(4)	-19(4)
C133	82(5)	64(5)	108(7)	13(5)	18(5)	-33(4)
C134	61(4)	63(4)	71(4)	-9(4)	-2(3)	-18(3)
C135	41(3)	41(3)	52(3)	-8(3)	8(2)	-2(2)
C136	48(3)	53(3)	44(3)	-8(3)	4(2)	-4(3)
C211	44(3)	44(3)	58(3)	2(3)	5(3)	-2(2)
C212	58(4)	50(4)	81(5)	10(3)	10(3)	-10(3)
C213	62(4)	38(3)	89(5)	7(3)	0(4)	-11(3)
C214	55(4)	37(3)	71(4)	-8(3)	-11(3)	-2(3)
C215	40(3)	40(3)	50(3)	-10(2)	-5(2)	4(2)
C216	51(3)	44(3)	51(3)	-23(3)	-2(3)	3(3)
C221	54(3)	56(4)	42(3)	-2(3)	9(3)	0(3)
C222	68(4)	86(5)	47(3)	14(3)	12(3)	9(4)
C223	67(4)	81(5)	62(4)	27(4)	8(3)	13(4)
C224	55(3)	48(3)	68(4)	3(3)	10(3)	11(3)
C225	40(3)	43(3)	50(3)	-3(2)	6(2)	0(2)
C226	41(3)	47(3)	60(3)	-14(3)	3(3)	16(2)
C231	52(3)	46(3)	48(3)	-3(3)	13(3)	-5(3)
C232	62(4)	58(4)	70(4)	-5(3)	24(3)	-12(3)
C233	72(5)	72(5)	75(5)	13(4)	33(4)	-12(4)

Atom	U₁₁	U₂₂	U₃₃	U₂₃	U₁₃	U₁₂
C234	65(4)	80(5)	50(4)	5(3)	27(3)	7(4)
C235	45(3)	55(3)	40(3)	-2(3)	12(2)	8(3)
C236	57(3)	65(4)	38(3)	-13(3)	15(3)	11(3)

Table 20. Bond lengths for [{Fe(TPA)}₂O(OAc)](ClO₄)₃•H₂O P2₁/n polymorph

Atom	Atom	Length/Å	Atom	Atom	Length/Å
Fe1	O1	1.810(3)	N14	C136	1.488(7)
Fe1	O2	1.968(4)	N21	C211	1.346(8)
Fe1	N11	2.133(5)	N21	C215	1.355(7)
Fe1	N12	2.214(4)	N22	C221	1.349(7)
Fe1	N13	2.135(5)	N22	C225	1.335(7)
Fe1	N14	2.196(4)	N23	C231	1.336(7)
Fe2	O1	1.777(3)	N23	C235	1.353(7)
Fe2	O3	2.031(4)	N24	C216	1.480(7)
Fe2	N21	2.146(5)	N24	C226	1.475(7)
Fe2	N22	2.147(4)	N24	C236	1.490(8)
Fe2	N23	2.126(5)	C1	C2	1.496(8)
Fe2	N24	2.243(4)	C111	C112	1.365(11)
Cl1	O11	1.251(13)	C112	C113	1.384(14)
Cl1	O12	1.342(9)	C113	C114	1.385(12)
Cl1	O13	1.399(9)	C114	C115	1.370(9)

Atom	Atom	Length/Å
Cl1	O14	1.333(9)
Cl2	O21	1.414(7)
Cl2	O22	1.440(6)
Cl2	O23	1.405(7)
Cl2	O24	1.391(8)
Cl3	O31A	1.29(2)
Cl3	O32A	1.30(3)
Cl3	O33A	1.43(3)
Cl3	O34A	1.363(18)
Cl3	O31B	1.310(16)
Cl3	O32B	1.435(17)
Cl3	O33B	1.308(19)
Cl3	O34B	1.319(16)
O2	C1	1.271(6)
O3	C1	1.252(6)
O32A	O33A	0.57(7)
O31B	O32B	1.18(4)
O32B	O33B	1.23(4)
N11	C111	1.352(8)
N11	C115	1.337(8)
N12	C121	1.345(7)
N12	C125	1.331(7)

Atom	Atom	Length/Å
C115	C116	1.501(8)
C121	C122	1.368(9)
C122	C123	1.364(10)
C123	C124	1.385(10)
C124	C125	1.374(8)
C125	C126	1.526(8)
C131	C132	1.352(10)
C132	C133	1.390(12)
C133	C134	1.366(11)
C134	C135	1.375(8)
C135	C136	1.510(8)
C211	C212	1.365(9)
C212	C213	1.389(10)
C213	C214	1.355(10)
C214	C215	1.377(8)
C215	C216	1.492(9)
C221	C222	1.365(9)
C222	C223	1.377(11)
C223	C224	1.381(10)
C224	C225	1.380(8)
C225	C226	1.527(8)
C231	C232	1.371(9)

Atom	Atom	Length/Å	Atom	Atom	Length/Å
N13	C131	1.349(7)	C232	C233	1.341(10)
N13	C135	1.346(7)	C233	C234	1.394(10)
N14	C116	1.489(7)	C234	C235	1.383(9)
N14	C126	1.485(7)	C235	C236	1.500(9)

Table 21. Bond angles for $\left[\{Fe(TPA)\}_2O(OAc)\right](ClO_4)_3 \cdot H_2O$ P2₁/n polymorph

Atom	Atom	Atom2	Angle/°	Atom	Atom	Atom	Angle/°
O1	Fe1	O2	101.21(16)	C116	N14	C126	110.1(4)
O1	Fe1	N11	94.29(17)	C116	N14	C136	111.4(4)
O1	Fe1	N12	173.41(16)	C126	N14	C136	113.4(4)
O1	Fe1	N13	94.41(17)	Fe2	N21	C211	124.0(4)
O1	Fe1	N14	95.93(16)	Fe2	N21	C215	115.9(4)
O2	Fe1	N11	99.32(19)	C215	N21	C211	119.2(5)
O2	Fe1	N12	84.88(16)	Fe2	N22	C221	122.9(4)
O2	Fe1	N13	103.92(18)	Fe2	N22	C225	117.1(4)
O2	Fe1	N14	162.54(17)	C221	N22	C225	118.8(5)
N11	Fe1	N12	87.12(17)	Fe2	N23	C231	124.4(4)
N11	Fe1	N13	153.04(17)	Fe2	N23	C235	116.2(4)
N11	Fe1	N14	75.95(17)	C231	N23	C235	119.3(5)
N12	Fe1	N13	81.58(17)	Fe2	N24	C216	105.8(3)
N12	Fe1	N14	78.15(16)	Fe2	N24	C226	110.7(3)
N13	Fe1	N14	77.80(17)	Fe2	N24	C236	105.7(3)
O1	Fe2	O3	99.28(15)	C216	N24	C226	110.9(5)
O1	Fe2	N21	103.12(17)	C216	N24	C236	113.1(4)
O1	Fe2	N22	98.12(16)	C226	N24	C236	110.4(5)
O1	Fe2	N23	104.28(17)	O2	C1	C2	116.8(5)

Atom	Atom	Atom2	Angle/$^{\circ}$	Atom	Atom	Atom	Angle/$^{\circ}$
O1	Fe2	N24	176.30(16)	O2	C1	O3	123.6(5)
O3	Fe2	N21	89.22(17)	O3	C1	C2	119.5(5)
O3	Fe2	N22	162.20(16)	N11	C111	C112	120.8(7)
O3	Fe2	N23	89.45(17)	C111	C112	C113	119.7(7)
O3	Fe2	N24	84.42(15)	C112	C113	C114	119.0(8)
N21	Fe2	N22	83.20(17)	C113	C114	C115	118.7(8)
N21	Fe2	N23	152.42(17)	N11	C115	C116	115.8(5)
N21	Fe2	N24	76.99(17)	N11	C115	C114	121.9(6)
N22	Fe2	N23	89.88(17)	C114	C115	C116	122.3(6)
N22	Fe2	N24	78.20(16)	N14	C116	C115	108.7(5)
N23	Fe2	N24	75.46(17)	N12	C121	C122	122.3(6)
O11	Cl1	O12	109.8(12)	C121	C122	C123	119.1(6)
O11	Cl1	O13	97.1(12)	C122	C123	C124	119.5(6)
O11	Cl1	O14	101.3(13)	C123	C124	C125	118.0(6)
O12	Cl1	O13	115.6(7)	N12	C125	C126	118.0(4)
O12	Cl1	O14	116.6(8)	N12	C125	C124	123.0(5)
O13	Cl1	O14	113.4(7)	C124	C125	C126	119.0(5)
O21	Cl2	O22	108.3(4)	N14	C126	C125	114.5(4)
O21	Cl2	O23	107.2(5)	N13	C131	C132	121.9(6)
O21	Cl2	O24	110.5(7)	C131	C132	C133	119.1(7)
O22	Cl2	O23	111.6(6)	C132	C133	C134	119.0(7)
O22	Cl2	O24	108.2(4)	C133	C134	C135	120.0(7)
O23	Cl2	O24	111.0(7)	N13	C135	C136	115.5(5)
O31A	Cl3	O32A	101(3)	N13	C135	C134	120.5(6)
O31A	Cl3	O33A	121(2)	C134	C135	C136	124.0(6)
O31A	Cl3	O34A	109(3)	N14	C136	C135	109.7(4)

Atom	Atom	Atom2	Angle/[°]	Atom	Atom	Atom	Angle/[°]
O32A	Cl3	O33A	23(3)	N21	C211	C212	122.1(6)
O32A	Cl3	O34A	132(2)	C211	C212	C213	118.4(7)
O33A	Cl3	O34A	110.2(19)	C212	C213	C214	119.6(6)
O31B	Cl3	O32B	50.7(15)	C213	C214	C215	120.2(6)
O31B	Cl3	O33B	101(2)	N21	C215	C216	115.1(5)
O31B	Cl3	O34B	111.2(19)	N21	C215	C214	120.4(6)
O32B	Cl3	O33B	53.0(19)	C214	C215	C216	124.4(6)
O32B	Cl3	O34B	142.5(15)	N24	C216	C215	110.6(4)
O33B	Cl3	O34B	115(3)	N22	C221	C222	121.9(6)
Fe1	O1	Fe2	129.82(19)	C221	C222	C223	119.3(6)
Fe1	O2	C1	132.5(4)	C222	C223	C224	119.1(6)
Fe2	O3	C1	133.3(3)	C223	C224	C225	118.7(6)
C111	N11	C115	119.8(5)	N22	C225	C226	117.2(5)
Fe1	N11	C111	125.1(4)	N22	C225	C224	122.1(6)
Fe1	N11	C115	115.0(4)	C224	C225	C226	120.6(5)
Fe1	N12	C121	125.9(4)	N24	C226	C225	113.5(4)
Fe1	N12	C125	116.0(3)	N23	C231	C232	122.0(6)
C121	N12	C125	118.1(5)	C231	C232	C233	119.3(7)
Fe1	N13	C131	125.9(4)	C232	C233	C234	120.4(6)
Fe1	N13	C135	114.5(4)	C233	C234	C235	118.1(6)
C131	N13	C135	119.5(5)	N23	C235	C234	120.9(6)
Fe1	N14	C116	104.7(3)	N23	C235	C236	116.2(5)
Fe1	N14	C126	112.5(3)	C234	C235	C236	123.0(5)
Fe1	N14	C136	104.4(3)	N24	C236	C235	109.6(4)

Table 22. Hydrogen atom coordinates ($\text{\AA} \times 10^4$) and isotropic displacement parameters ($\text{\AA}^2 \times 10^3$) for $[\{Fe(TPA)\}_2O(OAc)](ClO_4)_3 \cdot H_2O$ P2₁/polymorph

Atom	x	y	z	U(eq)
H111	7517.98	7840.29	3754.1	71
H112	8800.38	8456.84	3311.47	105
H113	8390.26	8563.48	2174.55	120
H114	6602.12	8079.42	1506.92	89
H121	6952.51	6269.76	4297.1	62
H122	8344.31	5491.58	4307.81	75
H123	8443	5051.31	3327.54	81
H124	7255	5458.98	2337.35	67
H131	3721.89	6172.62	4099.32	67
H132	2305.18	5396.32	3924.12	96
H133	1324.28	5107.6	2845.68	103
H134	1769.08	5633.7	1982.87	82
H211	5088.2	8721.84	2879.08	60
H212	6194.44	9592.22	2855.28	77
H213	5982.91	10352	3579.79	79
H214	4757.68	10197.6	4325.14	71
H221	2037.91	8284.19	2126.26	62
H222	859.42	8957.33	1402.22	80
H223	-129.57	9746.49	1798.26	86
H224	93.02	9834.02	2928.33	70
H231	1225.81	7096.49	3221.55	58
H232	-288.17	6581.07	3615.5	74
H233	-779.13	6878.51	4564.43	85
H234	204.94	7724.31	5113.74	75
H2A	5952.41	7775.53	5586.61	116

Atom	x	y	z	U(eq)
H4A	3604.99	5138.53	-1033.8	183
H11A	4090.68	7632.96	1819.39	56
H12A	6206.72	6544.9	1895.78	58
H13A	3143.79	6396.43	1600.31	60
H21A	4182.72	8980.56	4944.54	62
H22A	1460.28	9545.59	4056.62	61
H23A	1506.44	8651.9	5016.55	63
H2B	7047.8	7456.16	5330.68	116
H4B	3201.49	4572.97	-1255.9	183
H11B	4944	7284.54	1426.71	56
H12B	5151.87	6050.14	1851.18	58
H13B	2701.02	6951.75	1944.45	60
H21B	3277.11	9537.97	4759.68	62
H22B	566.15	8985.55	4009.7	61
H23B	2822.57	8298.47	5141.62	63
H2C	5934.08	7083.18	5509.88	116

Table 23. Partial atomic occupancy for $\left[\{Fe(TPA)\}_2O(OAc)\right](ClO_4)_3 \bullet H_2O$ P2₁/n polymorph

Atom	Occupancy	Atom	Occupancy	Atom	Occupancy
O31A	0.45	O34A	0.45	O33B	0.55
O32A	0.45	O31B	0.55	O34B	0.55
O33A	0.45	O32B	0.55		

3.3.3. $[\{Fe(TPA)\}_2O(4\text{-hydroxybenzoato})](ClO_4)_3$

Figure 55 shows the asymmetric unit of $[\{Fe(TPA)\}_2O(4\text{-hydroxybenzoato})](ClO_4)_3$. The cationic portion of $[\{Fe(TPA)\}_2O(4\text{-hydroxybenzoato})](ClO_4)_3$ is shown in **Figure 56**. Crystallographic details for $[\{Fe(TPA)\}_2O(4\text{-hydroxybenzoato})](ClO_4)_3$ are listed in **Table 24**. Fractional atomic coordinates, anisotropic displacement parameters, bond lengths and bond angles involving the non-hydrogen atoms and hydrogen atom coordinates and atomic occupancies for the disordered atoms are listed in **Table 25**, **Table 26**, **Table 27**, **Table 28**, **Table 29** and **Table 30**, respectively.

Figure 57 shows the numbering system for 4-hydroxybenzoate. C1 is bonded to O2 and O3. O2 and O3 coordinate to the Fe1 and Fe2, respectively. O1 is the bridging oxygen for Fe1-O1-Fe2 unit in the dimer. O4 bonds to C5 and is hydrogen bonded to O13 of a perchlorate. The first perchlorate is labeled Cl1, O11, O12, O13, and O14. The second perchlorate is labeled Cl2, O21, O22, O23 and O24. The third perchlorate is disordered and is modeled with two set of oxygen atoms with half occupancy.

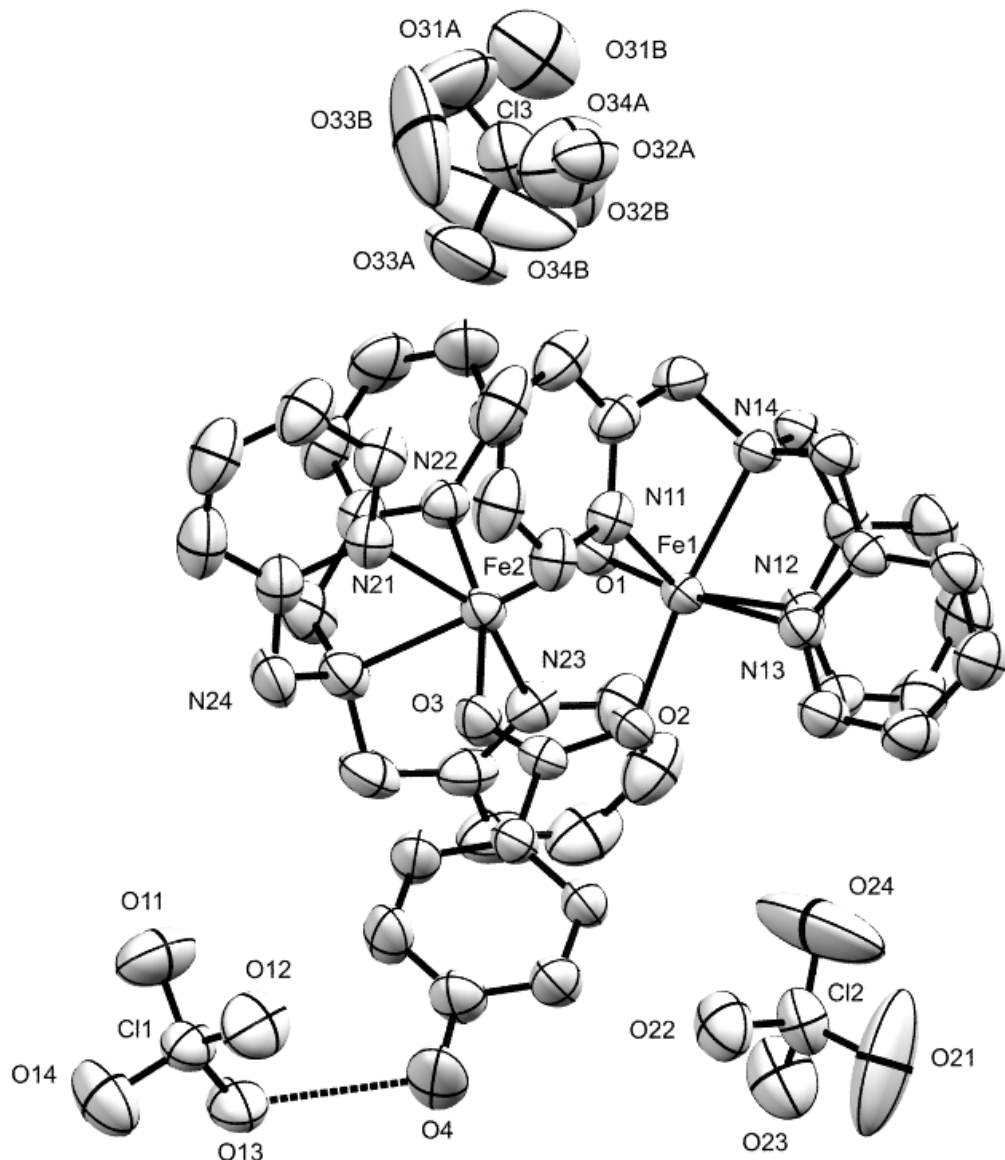


Figure 55. A view of the asymmetric unit of $\left[\{\text{Fe}(\text{TPA})\}_2\text{O}(4\text{-hydroxybenzoato})\right](\text{ClO}_4)_3$.

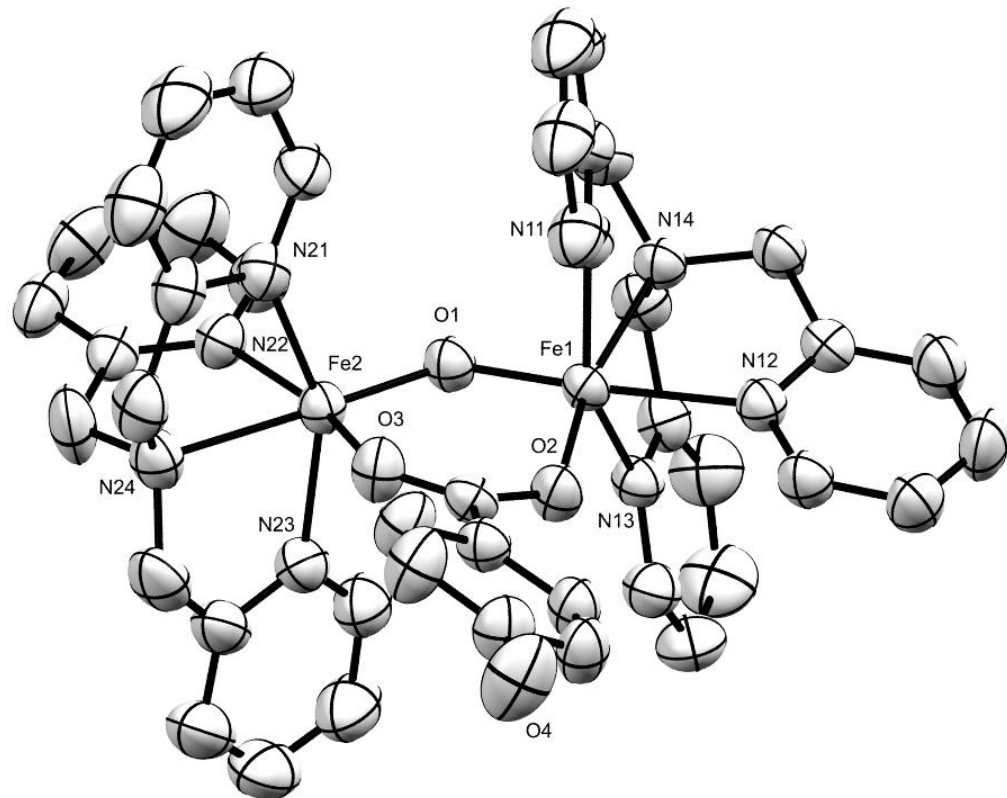


Figure 56. A view of the cationic portion of $\{Fe(TPA)\}_2O(4\text{-hydroxybenzoato})](ClO_4)_3$. Hydrogen atoms are omitted.

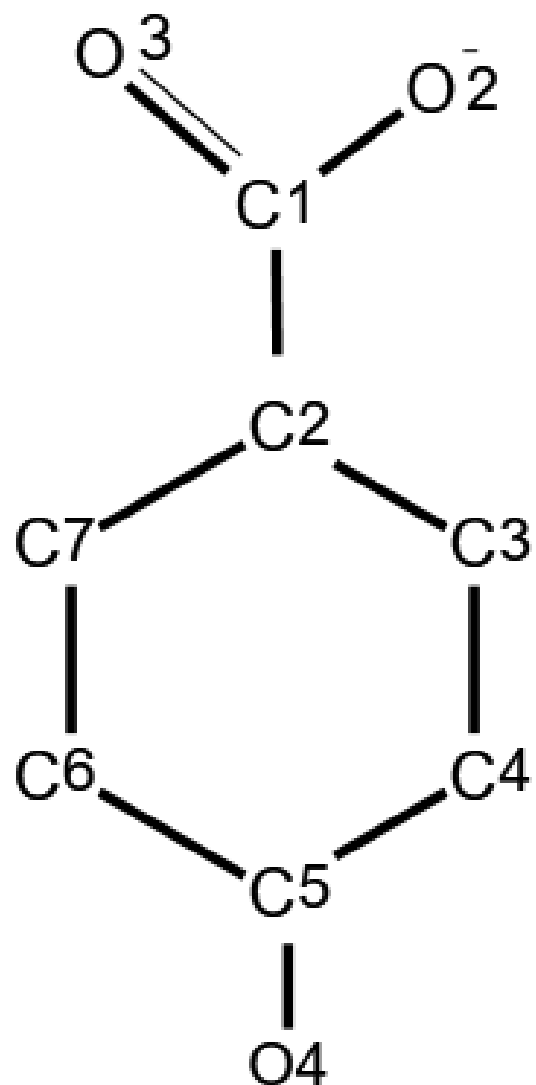


Figure 57. Numbering scheme for 4-hydroxybenzoate.

Table 24. Crystallographic data for $[\{Fe(TPA)\}_2O(4\text{-hydroxybenzoato})](ClO_4)_3$

Crystallographic data	
Empirical formula	C ₄₃ H ₄₁ Cl ₃ Fe ₂ N ₈ O ₁₆
Formula weight	1143.89
Temperature/K	298
Crystal system	monoclinic
Space group	P2 ₁ /c
a/Å	14.4510(6)
b/Å	16.7603(7)
c/Å	20.5942(7)
α/°	90
β/°	101.824(4)
γ/°	90
Volume/Å ³	4882.1(3)
Z	4
ρ _{calc} /g cm ⁻³	1.556
μ/mm ⁻¹	0.837
F(000)	2344
Crystal size/mm ³	0.25 × 0.18 × 0.15
Radiation	MoKα ($\lambda = 0.71073$)
2θ range for data collection/°	5.076 to 49.998

Crystallographic data

Index ranges	-17 ≤ h ≤ 14, -19 ≤ k ≤ 19, -24 ≤ l ≤ 23
Reflections collected	18536
Independent reflections	8582 [R _{int} = 0.0367, R _{sigma} = 0.0464]
Data/restraints/parameters	8582/0/686
Goodness-of-fit on F ²	1.115
Final R indexes [I≥2σ (I)]	R ₁ = 0.0506, wR ₂ = 0.1306
Final R indexes [all data]	R ₁ = 0.0729, wR ₂ = 0.1583
Largest diff. peak/hole / e Å ⁻³	0.55/-0.46

Table 25. Fractional atomic coordinates ($\times 10^4$) and equivalent isotropic displacement parameters ($\text{\AA}^2 \times 10^3$) for $\{[\text{Fe}(TPA)]_2\text{O(4-hydroxybenzoato)}\}(\text{ClO}_4)_3$

Atom	x	y	z	U(eq)
Fe1	6664.3(4)	4795.1(3)	8022.4(2)	37.63(16)
Fe2	8381.0(4)	5268.9(3)	7292.1(2)	40.26(17)
Cl1	3990.4(8)	8389.4(7)	3961.4(5)	56.6(3)
Cl2	1921.0(9)	4552.1(8)	5879.0(6)	65.9(3)
Cl3	9730.9(12)	6706.7(10)	10164.0(8)	86.3(4)
O1	7881.2(18)	4957.6(16)	7977.3(12)	44.6(6)
O2	6060.2(19)	4884.9(17)	7068.1(12)	49.0(7)
O3	7163(2)	5517.9(18)	6643.9(13)	51.9(7)
O4	3548(3)	6325(3)	4458.6(18)	86.5(12)
O11	4859(3)	8583(3)	4392(2)	100.0(13)
O12	3239(3)	8434(3)	4308.1(19)	92.7(12)
O13	4044(3)	7586(2)	3721.6(15)	72.7(9)

Atom	x	y	z	U(eq)
O14	3832(3)	8925(2)	3417.7(19)	98.6(13)
O21	1054(4)	4200(3)	5880(5)	202(4)
O22	1749(3)	5339(2)	5641.7(19)	81.6(11)
O23	2372(3)	4106(2)	5447(2)	100.6(14)
O24	2460(7)	4559(5)	6487(2)	213(4)
O31A	10373(10)	7179(12)	10420(9)	160(6)
O32A	8780(12)	6693(10)	10408(7)	78(3)
O33A	9448(8)	6718(10)	9440(4)	131(4)
O34A	10026(10)	5851(8)	10199(8)	135(5)
O31B	10361(8)	6636(11)	10834(6)	144(5)
O32B	8973(17)	6690(20)	10310(12)	165(11)
O33B	9833(18)	7522(9)	10035(12)	227(10)
O34B	10136(18)	6289(16)	9827(9)	278(15)
N11	6461(2)	5999(2)	8310.1(16)	48.2(8)
N12	5230(2)	4542.1(19)	8199.8(15)	43.2(7)
N13	6827(2)	3536.5(19)	8235.3(14)	43.3(7)
N14	6937(2)	4761.3(19)	9106.5(14)	43.6(7)
N21	8575(2)	6529(2)	7409.4(16)	49.1(8)
N22	9821(2)	5223(2)	7789.0(16)	46.2(8)
N23	8546(2)	4177(2)	6811.0(17)	52.7(8)
N24	9111(3)	5625(2)	6478.4(16)	53.9(9)
C1	6325(3)	5316(2)	6623.6(17)	42.6(9)
C2	5592(3)	5593(2)	6057.9(18)	45.8(9)
C3	4717(3)	5225(3)	5896.7(19)	50.9(10)
C4	4053(3)	5483(3)	5358(2)	59.7(12)
C5	4245(3)	6123(3)	4989(2)	59.5(11)

Atom	x	y	z	U(eq)
C6	5095(3)	6511(3)	5154(2)	66.7(13)
C7	5774(3)	6239(3)	5680(2)	60.4(12)
C111	6001(3)	6576(3)	7916(2)	58.8(11)
C112	6008(4)	7358(3)	8112(3)	73.6(14)
C113	6496(4)	7557(3)	8732(3)	82.1(17)
C114	6960(3)	6980(3)	9146(3)	66.4(13)
C115	6927(3)	6201(3)	8925(2)	51.4(10)
C116	7416(3)	5521(3)	9331(2)	54.8(11)
C121	4454(3)	4381(3)	7746.5(19)	51.6(10)
C122	3651(3)	4057(3)	7892(2)	62.5(12)
C123	3647(3)	3874(3)	8547(2)	71.6(14)
C124	4444(3)	4048(3)	9024(2)	61.4(12)
C125	5213(3)	4403(2)	8838.9(18)	45.0(9)
C126	6033(3)	4693(3)	9348.3(19)	50.7(10)
C131	6527(3)	2942(3)	7806(2)	52.9(10)
C132	6610(4)	2155(3)	7993(3)	71.5(14)
C133	7001(5)	1981(3)	8647(3)	83.4(16)
C134	7287(4)	2584(3)	9091(2)	72.0(14)
C135	7205(3)	3364(3)	8870.9(19)	49.3(10)
C136	7556(3)	4058(3)	9306.5(18)	51.8(10)
C211	8564(3)	6918(3)	7972(2)	58.5(11)
C212	8728(4)	7720(3)	8043(3)	74.7(14)
C213	8911(4)	8136(3)	7513(3)	87.6(17)
C214	8938(4)	7745(3)	6937(3)	80.5(16)
C215	8779(3)	6931(3)	6887(2)	57.7(11)
C216	8788(4)	6446(3)	6280(2)	64.4(12)

Atom	x	y	z	U(eq)
C221	10097(3)	5061(3)	8442(2)	61.2(12)
C222	11010(4)	5108(4)	8773(3)	80.9(16)
C223	11684(4)	5314(3)	8414(3)	77.6(15)
C224	11419(3)	5487(3)	7750(3)	62.9(12)
C225	10477(3)	5434(2)	7449(2)	48.0(9)
C226	10150(3)	5590(4)	6721(2)	75.3(15)
C231	8463(3)	3457(3)	7070(3)	64.0(12)
C232	8565(4)	2761(3)	6744(3)	82.5(16)
C233	8810(4)	2818(4)	6135(3)	86.9(18)
C234	8917(4)	3534(4)	5870(3)	78.6(15)
C235	8773(3)	4219(3)	6209(2)	59.0(11)
C236	8807(4)	5045(3)	5933(2)	66.7(13)

Table 26. Anisotropic displacement parameters ($\text{\AA}^2 \times 10^3$) for $[\{Fe(TPA)\}_2O(4\text{-hydroxybenzoato})](ClO_4)_3$

Atom	U ₁₁	U ₂₂	U ₃₃	U ₂₃	U ₁₃	U ₁₂
Fe1	40.5(3)	41.1(3)	31.1(3)	2.6(2)	6.8(2)	-0.8(2)
Fe2	37.9(3)	45.8(3)	37.6(3)	3.1(2)	9.0(2)	0.3(2)
Cl1	58.9(7)	60.3(7)	52.2(5)	-6.2(5)	15.3(5)	-0.7(5)
Cl2	66.0(7)	67.7(8)	69.6(7)	18.9(6)	27.1(6)	7.8(6)
Cl3	82.5(11)	89.8(11)	88.6(9)	11.8(9)	22.4(8)	2.2(8)
O1	42.4(15)	53.3(16)	38.0(13)	3.2(12)	7.6(11)	0.0(12)
O2	48.3(16)	63.1(18)	34.1(13)	7.8(12)	4.8(11)	-7.7(13)
O3	42.9(17)	64.8(19)	46.5(15)	14.4(13)	5.4(12)	-1.1(13)
O4	64(2)	100(3)	81(2)	38(2)	-18.8(18)	-6(2)
O11	74(3)	120(4)	100(3)	-34(3)	2(2)	-16(2)
O12	82(3)	119(3)	89(2)	-25(2)	47(2)	-10(2)

Atom	U₁₁	U₂₂	U₃₃	U₂₃	U₁₃	U₁₂
O13	102(3)	59(2)	58.6(18)	-9.3(16)	20.6(17)	-3.2(18)
O14	140(4)	79(3)	83(2)	25(2)	36(2)	27(3)
O21	116(5)	100(4)	430(12)	33(6)	151(6)	-8(3)
O22	106(3)	55(2)	86(2)	8.0(18)	27(2)	6.1(19)
O23	129(4)	76(3)	110(3)	8(2)	54(3)	32(2)
O24	323(11)	220(8)	64(3)	2(4)	-31(4)	96(7)
O31A	108(10)	194(18)	158(14)	-41(13)	-20(9)	-61(11)
O32A	60(8)	110(8)	65(5)	-17(5)	13(5)	-10(6)
O33A	121(8)	223(14)	48(4)	12(6)	12(5)	-17(8)
O34A	146(10)	111(9)	165(13)	60(9)	67(9)	33(7)
O31B	74(7)	226(16)	135(10)	19(11)	30(7)	28(8)
O32B	76(10)	260(20)	178(18)	-50(14)	69(9)	-35(10)
O33B	340(30)	117(11)	280(20)	104(14)	180(20)	21(14)
O34B	370(30)	320(30)	140(14)	-50(16)	47(17)	230(30)
N11	45.8(19)	42.7(19)	57.3(19)	0.5(16)	13.2(15)	-0.8(15)
N12	41.8(18)	48.2(19)	40.0(16)	2.1(14)	9.5(13)	0.1(14)
N13	49.1(19)	42.0(18)	40.0(16)	2.0(14)	11.7(14)	0.8(14)
N14	44.0(19)	52(2)	34.8(15)	-1.2(14)	6.9(13)	-1.8(15)
N21	47(2)	47(2)	54.7(19)	3.9(16)	12.9(15)	-1.0(15)
N22	40.1(18)	49(2)	49.0(18)	0.4(15)	7.2(14)	-1.4(14)
N23	47(2)	55(2)	58(2)	-9.0(17)	13.4(15)	-1.2(16)
N24	55(2)	65(2)	43.7(17)	5.3(17)	14.5(15)	0.2(17)
C1	47(2)	47(2)	33.5(18)	-0.9(16)	6.7(16)	2.4(17)
C2	46(2)	52(2)	38.4(18)	1.7(17)	7.0(16)	0.0(18)
C3	50(2)	62(3)	41(2)	8.8(18)	8.0(17)	-6(2)
C4	42(2)	84(3)	51(2)	7(2)	4.8(18)	-11(2)

Atom	U₁₁	U₂₂	U₃₃	U₂₃	U₁₃	U₁₂
C5	48(3)	73(3)	53(2)	11(2)	-0.7(19)	3(2)
C6	60(3)	67(3)	67(3)	28(2)	-1(2)	-6(2)
C7	53(3)	65(3)	58(2)	15(2)	-2(2)	-10(2)
C111	58(3)	46(3)	75(3)	8(2)	20(2)	0(2)
C112	66(3)	47(3)	112(4)	10(3)	28(3)	4(2)
C113	75(4)	47(3)	133(5)	-13(3)	40(4)	-8(3)
C114	58(3)	58(3)	87(3)	-22(3)	23(2)	-10(2)
C115	48(2)	53(3)	56(2)	-10(2)	16.9(18)	-8.3(19)
C116	59(3)	58(3)	46(2)	-12(2)	6.6(19)	-9(2)
C121	49(2)	63(3)	42(2)	0.3(19)	7.9(18)	0(2)
C122	47(3)	83(3)	57(2)	-7(2)	7.6(19)	-8(2)
C123	45(3)	100(4)	72(3)	0(3)	18(2)	-22(3)
C124	57(3)	85(3)	45(2)	5(2)	17.2(19)	-6(2)
C125	48(2)	46(2)	42.7(19)	-0.6(17)	11.9(16)	3.1(18)
C126	51(2)	65(3)	37.6(19)	-2.5(18)	11.7(17)	-2(2)
C131	59(3)	50(3)	51(2)	-3(2)	13.5(19)	0(2)
C132	83(4)	51(3)	81(3)	-13(3)	20(3)	-7(2)
C133	106(5)	45(3)	98(4)	14(3)	19(3)	10(3)
C134	92(4)	56(3)	65(3)	20(3)	8(3)	7(3)
C135	51(2)	52(2)	46(2)	8.5(18)	10.7(18)	4.9(19)
C136	50(2)	64(3)	39.3(19)	4.5(19)	4.0(17)	5(2)
C211	59(3)	50(3)	73(3)	-6(2)	27(2)	-1(2)
C212	71(3)	57(3)	101(4)	-16(3)	29(3)	-6(2)
C213	93(4)	47(3)	126(5)	0(3)	30(4)	-11(3)
C214	80(4)	63(3)	101(4)	23(3)	24(3)	-8(3)
C215	54(3)	54(3)	66(3)	13(2)	15(2)	-3(2)

Atom	U₁₁	U₂₂	U₃₃	U₂₃	U₁₃	U₁₂
C216	71(3)	71(3)	53(2)	22(2)	17(2)	-7(2)
C221	56(3)	70(3)	55(2)	11(2)	4(2)	-5(2)
C222	63(3)	99(4)	69(3)	14(3)	-13(3)	-11(3)
C223	43(3)	85(4)	93(4)	5(3)	-14(3)	-7(2)
C224	41(2)	59(3)	90(3)	-1(3)	16(2)	-7(2)
C225	42(2)	40(2)	62(2)	0.7(19)	13.2(18)	1.7(17)
C226	46(3)	123(5)	63(3)	9(3)	26(2)	-5(3)
C231	57(3)	61(3)	78(3)	-5(3)	22(2)	-2(2)
C232	74(4)	61(3)	117(5)	-15(3)	31(3)	-7(3)
C233	74(4)	86(4)	104(4)	-40(4)	26(3)	2(3)
C234	72(4)	92(4)	73(3)	-30(3)	18(3)	-3(3)
C235	51(3)	74(3)	52(2)	-17(2)	9.9(19)	-2(2)
C236	72(3)	91(4)	39(2)	-2(2)	14(2)	2(3)

Table 27. Bond lengths for $\left[\{Fe(TPA)\}_2O(4\text{-hydroxybenzoato})\right](ClO_4)_3$

Atom	Atom	Length/Å	Atom	Atom	Length/Å
Fe1	O1	1.801(3)	N22	C225	1.336(5)
Fe1	O2	1.986(2)	N23	C231	1.334(6)
Fe1	N11	2.140(3)	N23	C235	1.348(5)
Fe1	N12	2.218(3)	N24	C216	1.483(6)
Fe1	N13	2.158(3)	N24	C226	1.483(6)
Fe1	N14	2.187(3)	N24	C236	1.483(6)
Fe2	O1	1.790(2)	C1	C2	1.480(5)
Fe2	O3	2.023(3)	C2	C3	1.384(6)
Fe2	N21	2.138(3)	C2	C7	1.389(6)
Fe2	N22	2.123(3)	C3	C4	1.380(6)
Fe2	N23	2.117(3)	C4	C5	1.376(6)

Atom	Atom	Length/Å
Fe2	N24	2.237(3)
Cl1	O11	1.417(4)
Cl1	O12	1.418(3)
Cl1	O13	1.442(3)
Cl1	O14	1.417(4)
Cl2	O21	1.385(5)
Cl2	O22	1.411(4)
Cl2	O23	1.419(4)
Cl2	O24	1.332(6)
Cl3	O31A	1.252(12)
Cl3	O32A	1.557(19)
Cl3	O33A	1.463(8)
Cl3	O34A	1.493(12)
Cl3	O31B	1.494(13)
Cl3	O32B	1.19(2)
Cl3	O33B	1.406(14)
Cl3	O34B	1.217(14)
O2	C1	1.284(4)
O3	C1	1.250(5)
O4	C5	1.367(5)
N11	C111	1.346(5)
N11	C115	1.349(5)
N12	C121	1.331(5)
N12	C125	1.342(5)
N13	C131	1.342(5)
N13	C135	1.343(5)
N14	C116	1.478(5)

Atom	Atom	Length/Å
C5	C6	1.369(6)
C7	C6	1.382(6)
C111	C112	1.371(7)
C112	C113	1.367(8)
C113	C114	1.370(8)
C114	C115	1.381(6)
C115	C116	1.501(6)
C121	C122	1.368(6)
C122	C123	1.384(6)
C123	C124	1.383(6)
C124	C125	1.381(6)
C125	C126	1.494(6)
C131	C132	1.372(7)
C132	C133	1.380(7)
C133	C134	1.370(7)
C134	C135	1.380(6)
C135	C136	1.493(6)
C211	C212	1.368(7)
C212	C213	1.366(8)
C213	C214	1.364(8)
C214	C215	1.385(7)
C215	C216	1.494(7)
C221	C222	1.358(7)
C222	C223	1.383(8)
C223	C224	1.372(7)
C224	C225	1.378(6)
C225	C226	1.500(6)

Atom	Atom	Length/Å	Atom	Atom	Length/Å
N14	C126	1.494(5)	C231	C232	1.369(7)
N14	C136	1.486(5)	C232	C233	1.374(8)
N21	C211	1.333(5)	C233	C234	1.340(8)
N21	C215	1.352(5)	C234	C235	1.382(7)
N22	C221	1.349(5)	C235	C236	1.502(7)

Table 28. Bond angles for $\left[\{Fe(TPA)\}_2O(4\text{-hydroxybenzoato})\right](ClO_4)_3$

Atom	Atom	Atom2	Angle/°	Atom	Atom	Atom	Angle/°
O1	Fe1	O2	99.99(11)	C211	N21	C215	119.5(4)
O1	Fe1	N11	93.58(13)	Fe2	N22	C221	123.3(3)
O1	Fe1	N12	173.17(11)	Fe2	N22	C225	117.9(3)
O1	Fe1	N13	95.26(12)	C221	N22	C225	118.5(4)
O1	Fe1	N14	94.77(11)	Fe2	N23	C231	124.5(3)
O2	Fe1	N11	98.35(12)	Fe2	N23	C235	117.2(3)
O2	Fe1	N12	86.63(11)	C231	N23	C235	118.2(4)
O2	Fe1	N13	106.42(12)	Fe2	N24	C216	106.5(3)
O2	Fe1	N14	164.35(12)	Fe2	N24	C226	109.7(2)
N11	Fe1	N12	87.07(12)	Fe2	N24	C236	106.3(3)
N11	Fe1	N13	151.76(12)	C216	N24	C226	111.7(4)
N11	Fe1	N14	75.41(12)	C216	N24	C236	111.8(3)
N12	Fe1	N13	81.15(12)	C226	N24	C236	110.6(4)
N12	Fe1	N14	78.80(12)	O2	C1	O3	123.8(3)
N13	Fe1	N14	77.16(12)	O2	C1	C2	117.9(4)
O1	Fe2	O3	98.23(11)	O3	C1	C2	118.3(3)
O1	Fe2	N21	105.28(12)	C1	C2	C3	121.3(4)
O1	Fe2	N22	97.08(12)	C1	C2	C7	119.9(4)
O1	Fe2	N23	102.67(13)	C3	C2	C7	118.8(4)

Atom	Atom	Atom2	Angle/[°]	Atom	Atom	Atom	Angle/[°]
O1	Fe2	N24	175.67(13)	C2	C3	C4	120.3(4)
O3	Fe2	N21	86.95(13)	C3	C4	C5	120.2(4)
O3	Fe2	N22	163.67(12)	O4	C5	C4	115.8(4)
O3	Fe2	N23	92.05(13)	O4	C5	C6	123.8(4)
O3	Fe2	N24	86.04(12)	C4	C5	C6	120.3(4)
N21	Fe2	N22	83.59(13)	C5	C6	C7	119.7(4)
N21	Fe2	N23	151.88(13)	C2	C7	C6	120.7(4)
N21	Fe2	N24	75.52(13)	N11	C111	C112	122.4(5)
N22	Fe2	N23	90.07(13)	C111	C112	C113	118.7(5)
N22	Fe2	N24	78.73(13)	C112	C113	C114	120.1(5)
N23	Fe2	N24	76.38(14)	C113	C114	C115	118.9(5)
O11	Cl1	O12	110.1(3)	N11	C115	C114	121.6(4)
O11	Cl1	O13	108.9(3)	N11	C115	C116	114.8(4)
O11	Cl1	O14	109.2(3)	C114	C115	C116	123.6(4)
O12	Cl1	O13	108.8(2)	N14	C116	C115	110.0(3)
O12	Cl1	O14	110.4(3)	N12	C121	C122	123.8(4)
O13	Cl1	O14	109.4(2)	C121	C122	C123	118.4(4)
O21	Cl2	O22	107.6(3)	C122	C123	C124	118.4(4)
O21	Cl2	O23	108.0(4)	C123	C124	C125	119.6(4)
O21	Cl2	O24	110.9(6)	N12	C125	C124	121.5(4)
O22	Cl2	O23	110.3(2)	N12	C125	C126	117.5(3)
O22	Cl2	O24	110.2(4)	C124	C125	C126	120.9(3)
O23	Cl2	O24	109.8(4)	N14	C126	C125	114.4(3)
O31A	Cl3	O32A	120.1(10)	N13	C131	C132	122.1(4)
O31A	Cl3	O33A	116.7(11)	C131	C132	C133	118.1(5)
O31A	Cl3	O34A	114.0(11)	C132	C133	C134	120.1(5)
O32A	Cl3	O33A	104.4(7)	C133	C134	C135	119.1(5)

Atom	Atom	Atom2	Angle/[°]	Atom	Atom	Atom	Angle/[°]
O32A	Cl3	O34A	103.4(8)	N13	C135	C134	120.9(4)
O33A	Cl3	O34A	94.5(8)	N13	C135	C136	116.0(4)
O31B	Cl3	O32B	100.6(13)	C134	C135	C136	123.0(4)
O31B	Cl3	O33B	100.6(12)	N14	C136	C135	109.9(3)
O31B	Cl3	O34B	102.0(11)	N21	C211	C212	122.7(5)
O32B	Cl3	O33B	101.9(18)	C211	C212	C213	118.3(5)
O32B	Cl3	O34B	135(2)	C212	C213	C214	119.8(5)
O33B	Cl3	O34B	111.8(17)	C213	C214	C215	120.2(5)
Fe1	O1	Fe2	129.86(14)	N21	C215	C214	119.6(5)
Fe1	O2	C1	127.8(2)	N21	C215	C216	115.8(4)
Fe2	O3	C1	132.3(2)	C214	C215	C216	124.6(4)
Fe1	N11	C111	126.1(3)	N24	C216	C215	109.3(3)
Fe1	N11	C115	115.2(3)	N22	C221	C222	123.2(5)
C111	N11	C115	118.4(4)	C221	C222	C223	117.6(5)
Fe1	N12	C121	127.2(3)	C222	C223	C224	120.2(5)
Fe1	N12	C125	113.6(3)	C223	C224	C225	118.9(4)
C121	N12	C125	118.1(3)	N22	C225	C224	121.6(4)
Fe1	N13	C131	125.8(3)	N22	C225	C226	117.2(4)
Fe1	N13	C135	114.5(3)	C224	C225	C226	121.2(4)
C131	N13	C135	119.6(4)	N24	C226	C225	115.7(3)
Fe1	N14	C116	105.7(2)	N23	C231	C232	123.2(5)
Fe1	N14	C126	110.8(2)	C231	C232	C233	117.5(6)
Fe1	N14	C136	106.0(2)	C232	C233	C234	120.4(5)
C116	N14	C126	110.4(3)	C233	C234	C235	119.8(5)
C116	N14	C136	112.3(3)	N23	C235	C234	120.8(5)
C126	N14	C136	111.4(3)	N23	C235	C236	115.4(4)
Fe2	N21	C211	123.8(3)	C234	C235	C236	123.8(4)

Atom	Atom	Atom2	Angle/$^{\circ}$	Atom	Atom	Atom	Angle/$^{\circ}$
Fe2	N21	C215	116.6(3)	N24	C236	C235	110.2(3)

Table 29. Hydrogen atom coordinates ($\text{\AA} \times 10^4$) and isotropic displacement parameters ($\text{\AA}^2 \times 10^3$) for $[\{Fe(TPA)\}_2O(4\text{-hydroxybenzoato})](ClO_4)_3$

Atom	x	y	z	U(eq)
H111	5666.65	6438.47	7495.67	71
H112	5687.27	7744.96	7829.44	88
H113	6513.5	8084.99	8872.4	99
H114	7292.42	7111.38	9568.41	80
H121	4457.81	4494.29	7305.01	62
H122	3121.73	3963.58	7559.69	75
H123	3121.33	3638.59	8662.96	86
H124	4461.93	3926.42	9467.09	74
H131	6255.51	3068.3	7369	63
H132	6408.69	1750.9	7687.47	86
H133	7070.25	1452.44	8785.75	100
H134	7534.04	2470.46	9534.23	86
H211	8440.33	6631.49	8332.12	70
H212	8713.99	7976.15	8442.02	90
H213	9017.36	8682.9	7545.75	105
H214	9064.27	8027.08	6575.24	97
H221	9639.72	4910.4	8676.37	73
H222	11176.5	5004.54	9225.84	97
H223	12318.9	5334.72	8621.72	93
H224	11867.6	5636.55	7507.84	75
H231	8327.92	3426.88	7491.48	77
H232	8473.07	2268.21	6927.72	99

H233	8901.61	2356.6	5904.82	104
H234	9087.15	3569.06	5459.21	94
H3	4577.22	4802.3	6152.71	61
H4	3672.31	6758.13	4311.37	130
H6	5214.07	6954.73	4912.79	80
H7	6359.96	6490.21	5781.68	72
H4A	3473.32	5222.93	5243.39	72
H11A	8070.61	5496.41	9285.37	66
H12A	6130.03	4330.06	9723.26	61
H13A	7559.2	3923.47	9765.01	62
H21A	8158.36	6428.87	6003.38	77
H22A	10419.5	6092.07	6616.3	90
H23A	9245.64	5057.79	5633.94	80
H11B	7407.38	5607.63	9795.25	66
H12B	5877.26	5211.48	9504.87	61
H13B	8198.45	4184.7	9270.26	62
H21B	9210.02	6687.73	6025.57	77
H22B	10401.3	5173.94	6478.96	90
H23B	8186.01	5191.53	5682.44	80

Table 30. Partial atomic occupancy for $\{Fe(TPA)\}_2O(4\text{-hydroxybenzoato})](ClO_4)_3$

Atom	Occupancy	Atom	Occupancy	Atom	Occupancy
O32A	0.5	O31B	0.5	O34A	0.5
O33A	0.5	O32B	0.5	O31A	0.5
O33B	0.5	O34B	0.5		

3.3.4. [{Fe(TPA)}₂O(4-methoxybenzoato)](ClO₄)₃

Figure 58 shows the asymmetric unit of [{Fe(TPA)}₂O(4-methoxybenzoato)](ClO₄)₃. The cationic portion of [{Fe(TPA)}₂O(4-methoxybenzoato)](ClO₄)₃ is shown in **Figure 59**. Crystallographic details for [{Fe(TPA)}₂O(4-methoxybenzoato)](ClO₄)₃ are listed in **Table 31**. Fractional atomic coordinates, anisotropic displacement parameters, bond lengths and bond angles involving the non-hydrogen atoms and hydrogen atom coordinates and atomic occupancies for the disordered atoms are listed in **Table 32**, **Table 33**, **Table 34**, **Table 35**, **Table 36** and **Table 37**, respectively.

Figure 60 shows the 4-methoxybenzoate numbering scheme. C1 is bonded to O2 and O3. O2 and O3 coordinate to the Fe1 and Fe2, respectively. The O1 is the bridging oxygen for the Fe1-O1-Fe2 unit in the dimer. O4 bonds to C5 and to the methyl carbon of the methoxy group (C8). All three perchlorate ions are disordered. Two perchlorates are disordered about the Cl1-O11 axis and the Cl3-O13 axis and are modeled with two sets of oxygen atoms with occupancies of 0.60 and 0.40. The third perchlorate is disordered about the Cl2-O21 axis and is modeled with two sets of oxygen atoms with occupancies of 0.63 and 0.37.

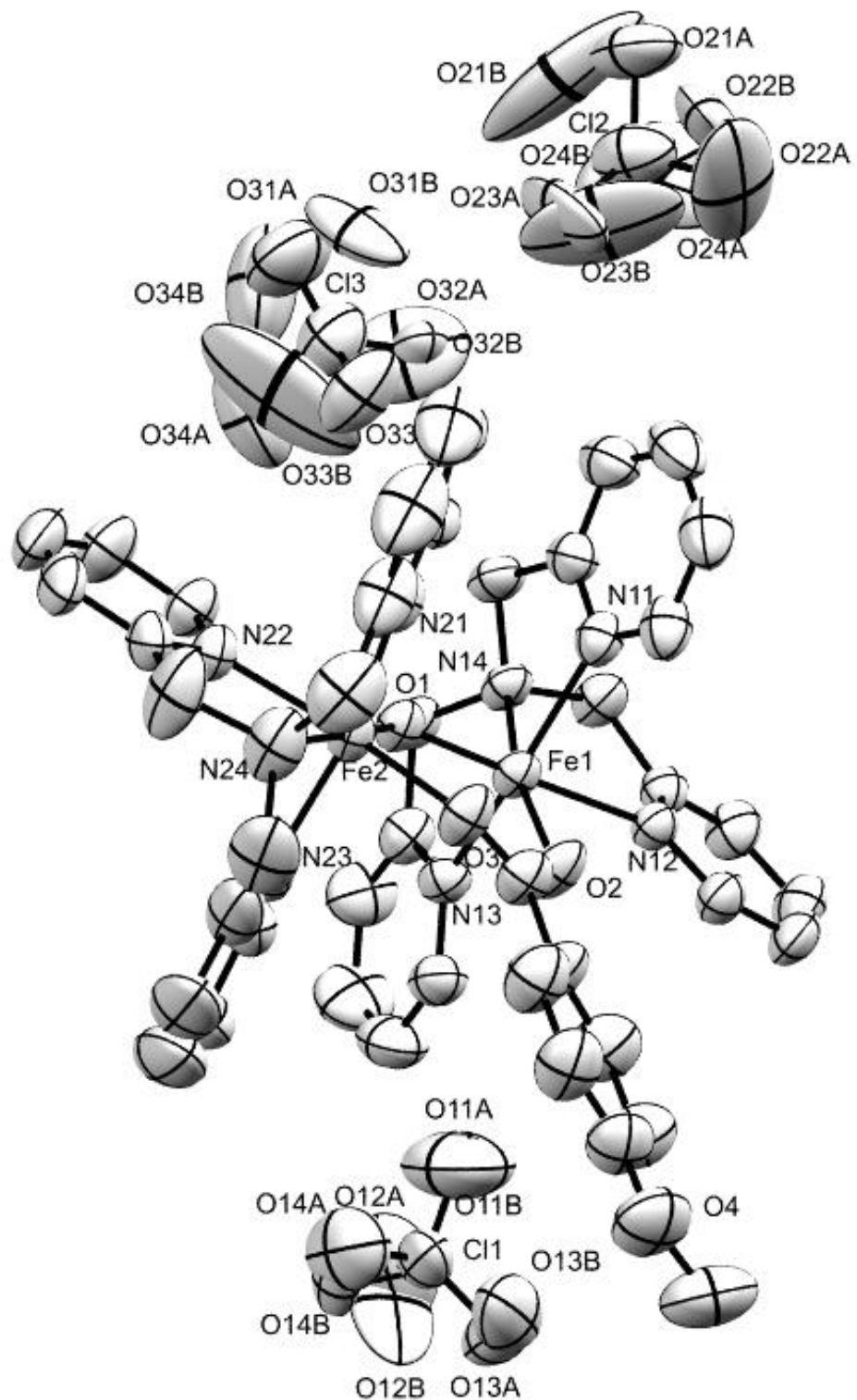


Figure 58. A view of the asymmetric unit of $[\{Fe(TPA)\}_2O(4\text{-methoxybenzoato})](ClO_4)_3$.

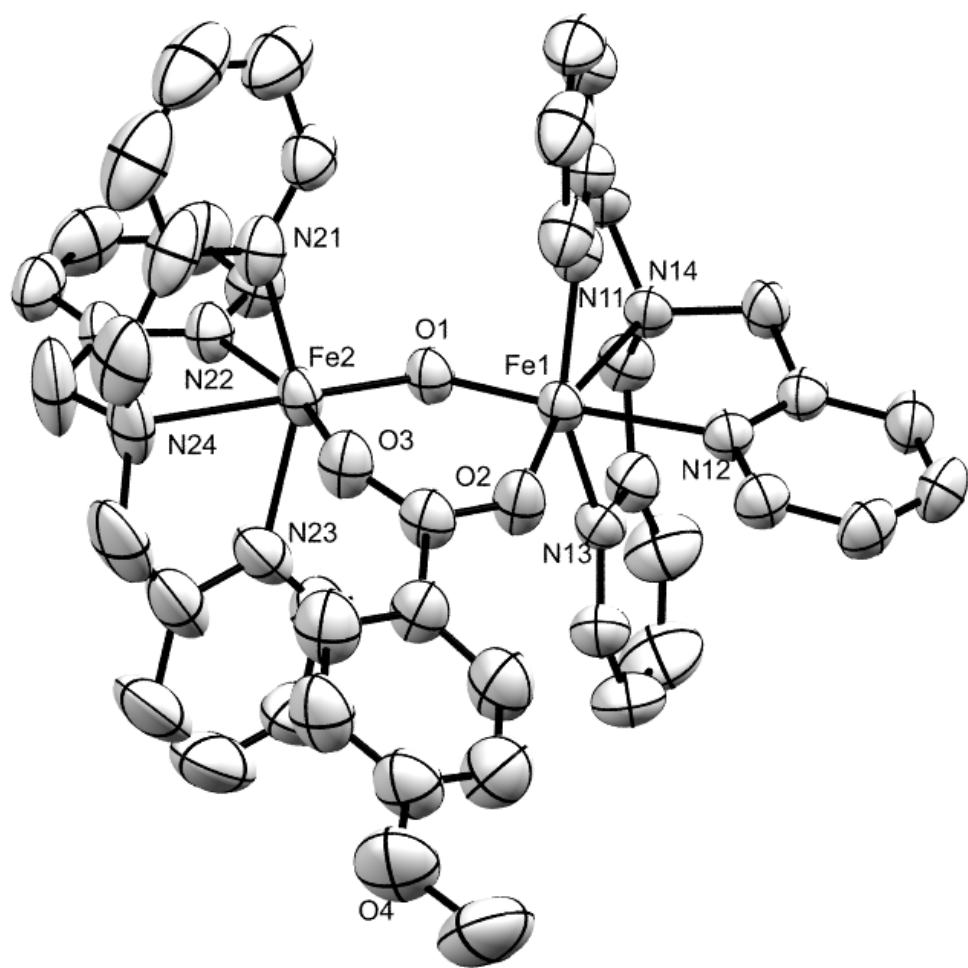


Figure 59. A view of the cationic portion of $\left[\{Fe\text{-}(TPA)\}_2O(4\text{-methoxybenzoato})\right](ClO_4)_3$. Hydrogen atoms are omitted.

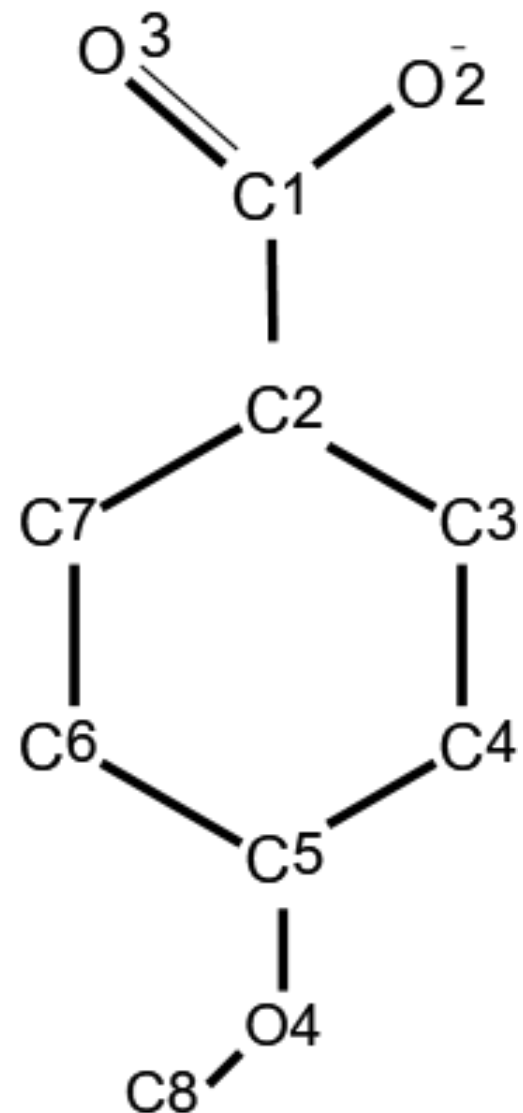


Figure 60. Numbering scheme for 4-methoxybenzoate.

Table 31. Crystallographic data for $\left[\{Fe(TPA)\}_2O(4\text{-methoxybenzoato})\right](ClO_4)_3$

Crystallographic data	
Empirical formula	C ₄₄ H ₄₄ Cl ₃ Fe ₂ N ₈ O ₁₆
Formula weight	1158.92
Temperature/K	298
Crystal system	monoclinic
Space group	P2 ₁ /c
a/Å	14.3467(9)
b/Å	17.1627(13)
c/Å	20.3281(11)
α/°	90
β/°	100.781(6)
γ/°	90
Volume/Å ³	4917.0(6)
Z	4
ρ _{calc} /g cm ⁻³	1.566
μ/mm ⁻¹	0.832
F(000)	2380
Crystal size/mm ³	6.2 × 5.2 × 4.6
Radiation	MoKα ($\lambda = 0.71073$)
2θ range for data collection/°	5.558 to 53
Index ranges	-18 ≤ h ≤ 12, -21 ≤ k ≤ 13, -23 ≤ l ≤ 25

Crystallographic data	
Reflections collected	19784
Independent reflections	10168 [$R_{\text{int}} = 0.0225$, $R_{\text{sigma}} = 0.0352$]
Data/restraints/parameters	10168/0/772
Goodness-of-fit on F^2	1.083
Final R indexes [$\geq 2\sigma$ (I)]	$R_1 = 0.0608$, $wR_2 = 0.1632$
Final R indexes [all data]	$R_1 = 0.0885$, $wR_2 = 0.1912$
Largest diff. peak/hole / e Å ⁻³	0.51/-0.59

Table 32. Fractional atomic coordinates ($\times 10^4$) and equivalent Isotropic displacement parameters ($\text{\AA}^2 \times 10^3$) for $[\{\text{Fe}(TPA)\}_2\text{O}(4\text{-methoxybenzoato})](\text{ClO}_4)_3$

Atom	x	y	z	U(eq)
Fe1	8305.4(4)	4642.4(3)	1993.5(2)	38.98(16)
Fe2	6539.9(4)	5032.1(4)	2735.5(3)	44.46(18)
Cl1	8979.2(9)	1572(1)	3940.3(7)	75.5(4)
Cl2	7176.1(14)	9385.9(12)	895.6(8)	95.2(5)
Cl3	5401.3(12)	6624.6(12)	-44.1(9)	90.6(5)
O1	7074.0(18)	4804.6(17)	2035.1(12)	43.8(6)
O2	8833(2)	4517(2)	2957.8(13)	58.1(8)
O3	7731(2)	5049(2)	3457.2(14)	56.5(8)
O4	10439(4)	3580(3)	5966(2)	102.5(15)
O11A	8959(18)	2272(14)	3683(13)	178(9)
O12A	8835(13)	1076(12)	3357(5)	150(7)
O13A	9824(17)	1362(15)	4350(15)	104(7)
O14A	8197(15)	1665(17)	4263(11)	132(8)

Atom	x	y	z	U(eq)
O21A	6838(9)	10102(7)	663(6)	118(4)
O22A	8050(13)	9661(18)	1337(8)	247(13)
O23A	6713(11)	8974(8)	1316(8)	152(7)
O24A	7720(20)	8967(15)	592(19)	230(20)
O31A	4757(8)	7036(10)	-313(6)	132(4)
O32A	6237(7)	6556(8)	-331(6)	90(4)
O33A	5706(6)	6676(7)	673(4)	103(3)
O34A	4996(9)	5803(8)	-103(7)	145(4)
O11B	9044(17)	2264(18)	3590(10)	99(9)
O12B	8940(20)	865(11)	3590(30)	217(18)
O13B	9800(40)	1640(30)	4500(30)	130(15)
O14B	8208(15)	1390(20)	4258(11)	78(7)
O21B	6330(20)	9630(30)	489(9)	300(30)
O22B	7689(16)	9871(13)	973(16)	209(14)
O23B	7050(30)	9060(20)	1427(8)	240(20)
O24B	7439(15)	8953(14)	387(6)	201(11)
O31B	5220(14)	7522(7)	-139(9)	131(7)
O32B	6160(20)	6492(18)	-330(12)	175(15)
O33B	5060(30)	6333(18)	366(19)	320(20)
O34B	4713(13)	6487(17)	-725(14)	187(10)
N11	8553(2)	5834(2)	1800.2(18)	49.6(8)
N12	9758(2)	4431(2)	1825.8(15)	42.3(7)
N13	8129(3)	3439(2)	1702.7(19)	45.3(8)
N14	8093(2)	4703(2)	904.3(15)	43.1(7)
N21	6445(2)	6265(2)	2754.8(18)	56.3(9)
N22	5117(2)	5087(2)	2208.1(17)	47.9(8)

Atom	x	y	z	U(eq)
N23	6263(3)	3903(3)	3089(2)	66.3(11)
N24	5750(3)	5268(3)	3570.3(19)	74.0(13)
C1	8480(3)	4677(3)	3475.6(19)	50.8(10)
C2	8994(3)	4375(3)	4131(2)	59.0(12)
C3	9705(4)	3849(4)	4156(3)	82.3(17)
C4	10213(5)	3555(4)	4766(3)	88.6(18)
C5	9974(4)	3804(4)	5340(3)	78.6(16)
C6	9227(4)	4328(4)	5338(3)	82.2(17)
C7	8731(4)	4606(4)	4725(3)	78.9(16)
C8	11229(6)	3100(5)	5980(4)	123(3)
C111	9010(3)	6340(3)	2247(3)	62.0(12)
C112	9035(4)	7124(3)	2103(3)	75.8(15)
C113	8576(4)	7390(3)	1495(4)	78.8(17)
C114	8121(4)	6862(3)	1026(3)	70.2(14)
C115	8124(3)	6089(3)	1195(2)	53(1)
C116	7627(3)	5467(3)	728(2)	52.1(10)
C121	10527(3)	4262(3)	2294(2)	50.8(10)
C122	11360(3)	4008(3)	2138(2)	60.6(12)
C123	11410(3)	3907(3)	1475(3)	64.6(13)
C124	10630(3)	4080(3)	983(2)	56.9(11)
C125	9831(3)	4362(2)	1178(2)	44.4(9)
C126	9014(3)	4666(3)	667(2)	51.2(10)
C131	8380(3)	2821(3)	2097(2)	59.1(11)
C132	8256(4)	2078(3)	1866(3)	80.1(16)
C133	7878(5)	1965(4)	1202(4)	98(2)
C134	7630(4)	2591(3)	785(3)	78.7(16)

Atom	x	y	z	U(eq)
C135	7758(3)	3329(3)	1045(2)	53(1)
C136	7458(3)	4048(3)	652(2)	50.9(10)
C211	6540(3)	6732(3)	2254(3)	63.1(12)
C212	6416(4)	7529(4)	2267(4)	91(2)
C213	6203(5)	7847(4)	2827(5)	106(3)
C214	6084(5)	7377(5)	3351(4)	108(3)
C215	6205(4)	6586(4)	3313(3)	77.7(17)
C216	6121(5)	6025(4)	3856(3)	91(2)
C221	4879(3)	5019(3)	1540(2)	56.7(11)
C222	3969(4)	5110(4)	1201(3)	76.3(15)
C223	3272(4)	5259(4)	1569(3)	81.6(17)
C224	3506(3)	5333(3)	2245(3)	68.6(14)
C225	4438(3)	5241(3)	2555(2)	55.2(11)
C226	4718(4)	5305(5)	3299(3)	99(2)
C231	6368(4)	3240(4)	2762(4)	78.4(16)
C232	6262(5)	2525(4)	3036(5)	113(3)
C233	6004(6)	2491(6)	3649(6)	138(4)
C234	5881(6)	3141(6)	3971(4)	119(3)
C235	6015(4)	3871(5)	3694(3)	88(2)
C236	5979(5)	4615(5)	4051(3)	97(2)

Table 33. Anisotropic displacement parameters ($\text{\AA}^2 \times 10^3$) for $[\{Fe(TPA)\}_2O(4\text{-methoxybenzoato})](ClO_4)_3$

Atom	U₁₁	U₂₂	U₃₃	U₂₃	U₁₃	U₁₂
Fe1	37.1(3)	51.5(3)	28.1(3)	0.2(2)	5.2(2)	3.3(2)
Fe2	38.3(3)	65.2(4)	30.7(3)	-1.3(3)	8.6(2)	-1.1(3)
Cl1	57.9(7)	92.6(10)	78.3(9)	31.6(8)	19.0(6)	-4.9(7)

Atom	U₁₁	U₂₂	U₃₃	U₂₃	U₁₃	U₁₂
Cl2	109.6(13)	109.0(13)	75.6(10)	27.2(9)	39.6(9)	37.7(11)
Cl3	81.2(10)	114.5(13)	77.7(9)	-3.2(9)	19.1(8)	13.9(10)
O1	38.9(13)	60.4(17)	31.6(12)	-0.8(12)	5.5(10)	1.8(12)
O2	48.1(16)	91(2)	33.4(14)	-0.4(14)	3.8(12)	15.8(16)
O3	47.7(16)	85(2)	34.7(14)	-7.6(14)	1.6(12)	6.4(15)
O4	103(3)	129(4)	67(2)	22(3)	-5(2)	11(3)
O11A	211(19)	128(16)	198(19)	62(13)	45(14)	57(13)
O12A	182(13)	211(16)	67(7)	-27(7)	52(6)	-48(11)
O13A	74(9)	128(16)	107(13)	39(11)	9(9)	23(10)
O14A	117(10)	160(19)	137(11)	32(10)	68(8)	24(9)
O21A	129(10)	123(8)	107(9)	63(7)	35(7)	53(6)
O22A	157(13)	440(30)	106(9)	114(14)	-73(9)	-111(17)
O23A	160(10)	114(9)	216(17)	70(9)	125(11)	-2(7)
O24A	210(20)	148(19)	390(50)	140(20)	240(30)	128(18)
O31A	111(8)	166(12)	106(8)	29(8)	-13(6)	25(8)
O32A	63(5)	118(9)	89(8)	55(7)	14(4)	14(5)
O33A	86(5)	176(10)	44(3)	-17(4)	0(3)	31(6)
O34A	169(10)	148(10)	133(9)	-42(8)	67(8)	-73(8)
O11B	105(12)	130(20)	64(9)	78(10)	13(8)	-21(12)
O12B	146(19)	36(9)	490(50)	-79(15)	110(30)	-2(8)
O13B	110(20)	140(30)	120(20)	30(20)	-34(17)	-40(20)
O14B	51(8)	129(19)	55(8)	24(8)	13(6)	-26(10)
O21B	220(30)	650(70)	43(7)	50(20)	27(13)	290(40)
O22B	140(17)	159(17)	290(30)	140(20)	-49(18)	-93(14)
O23B	380(50)	300(40)	31(6)	46(11)	21(13)	170(30)
O24B	270(20)	260(20)	67(6)	-46(9)	18(8)	112(16)

Atom	U₁₁	U₂₂	U₃₃	U₂₃	U₁₃	U₁₂
O31B	211(17)	46(6)	171(15)	4(7)	128(14)	17(8)
O32B	240(30)	200(30)	104(16)	-25(15)	79(17)	100(20)
O33B	580(70)	210(30)	280(40)	30(30)	330(40)	-70(40)
O34B	101(12)	230(20)	230(30)	-70(20)	36(14)	-44(14)
N11	41.1(17)	54(2)	55(2)	-3.6(17)	10.4(15)	4.1(15)
N12	38.5(16)	49.7(19)	38.0(16)	2.3(14)	5.3(13)	2.8(14)
N13	48.1(18)	50(2)	38.3(17)	3.0(15)	9.1(14)	3.9(15)
N14	40.1(16)	57(2)	31.8(15)	6.4(14)	5.7(13)	7.9(15)
N21	44.6(18)	73(3)	51(2)	-16.7(19)	8.1(16)	-0.5(18)
N22	38.7(16)	60(2)	45.8(18)	-4.1(16)	9.1(14)	-1.4(15)
N23	50(2)	89(3)	60(2)	27(2)	11.6(18)	-8(2)
N24	61(2)	126(4)	40(2)	-3(2)	23.8(18)	8(2)
C1	54(2)	66(3)	30.0(18)	-4.8(18)	2.5(16)	2(2)
C2	61(3)	79(3)	35(2)	-3(2)	1.6(18)	12(2)
C3	90(4)	104(5)	54(3)	-2(3)	15(3)	13(3)
C4	101(5)	97(5)	66(3)	-4(3)	10(3)	19(4)
C5	79(4)	100(4)	55(3)	10(3)	6(3)	0(3)
C6	79(4)	121(5)	47(3)	0(3)	11(3)	0(4)
C7	72(3)	105(5)	58(3)	-4(3)	7(3)	5(3)
C8	147(7)	106(6)	107(6)	21(5)	-1(5)	45(5)
C111	50(2)	62(3)	75(3)	-17(3)	16(2)	-2(2)
C112	57(3)	65(3)	109(5)	-21(3)	23(3)	-8(2)
C113	71(3)	46(3)	128(5)	7(3)	42(4)	0(3)
C114	66(3)	62(3)	91(4)	20(3)	35(3)	14(3)
C115	48(2)	53(3)	62(3)	7(2)	21(2)	6.6(19)
C116	52(2)	60(3)	44(2)	14.9(19)	8.3(18)	13(2)

Atom	U₁₁	U₂₂	U₃₃	U₂₃	U₁₃	U₁₂
C121	42(2)	62(3)	46(2)	3(2)	2.5(17)	2.4(19)
C122	38(2)	73(3)	67(3)	5(2)	0.2(19)	11(2)
C123	43(2)	73(3)	79(3)	1(3)	15(2)	15(2)
C124	51(2)	67(3)	57(2)	-2(2)	21(2)	10(2)
C125	42.0(19)	45(2)	47(2)	-0.9(18)	10.5(16)	0.0(17)
C126	46(2)	74(3)	35.2(19)	5.6(19)	11.7(16)	11(2)
C131	59(3)	60(3)	58(3)	13(2)	12(2)	8(2)
C132	95(4)	52(3)	96(4)	14(3)	22(3)	10(3)
C133	123(6)	53(3)	117(5)	-20(4)	17(4)	5(3)
C134	96(4)	63(3)	70(3)	-18(3)	-1(3)	2(3)
C135	53(2)	59(3)	46(2)	-6(2)	6.9(19)	3(2)
C136	51(2)	62(3)	36.7(19)	-4.4(18)	1.1(17)	4(2)
C211	51(2)	60(3)	81(3)	-6(3)	19(2)	-3(2)
C212	57(3)	67(4)	148(6)	-2(4)	19(4)	-1(3)
C213	82(4)	68(4)	165(8)	-41(5)	16(5)	3(3)
C214	89(5)	117(6)	114(6)	-65(5)	7(4)	15(4)
C215	62(3)	95(4)	75(3)	-46(3)	10(3)	8(3)
C216	97(4)	135(6)	43(3)	-26(3)	18(3)	20(4)
C221	52(2)	69(3)	47(2)	-7(2)	1.7(19)	3(2)
C222	59(3)	100(4)	61(3)	-5(3)	-11(2)	6(3)
C223	46(3)	89(4)	100(5)	3(3)	-12(3)	9(3)
C224	39(2)	72(3)	98(4)	1(3)	21(2)	4(2)
C225	41(2)	64(3)	64(3)	2(2)	20(2)	-3.0(19)
C226	54(3)	191(8)	60(3)	-7(4)	31(3)	11(4)
C231	58(3)	74(4)	106(4)	16(3)	23(3)	-4(3)
C232	80(4)	84(5)	180(8)	50(5)	37(5)	1(4)

Atom	U₁₁	U₂₂	U₃₃	U₂₃	U₁₃	U₁₂
C233	99(6)	127(7)	197(11)	99(8)	49(6)	8(5)
C234	94(5)	152(8)	117(6)	82(6)	36(4)	-4(5)
C235	59(3)	138(6)	69(3)	42(4)	19(3)	-4(3)
C236	91(4)	160(7)	44(3)	25(4)	26(3)	-7(4)

Table 34. Bond lengths for $[\{Fe(TPA)\}_2O(4\text{-methoxybenzoato})](ClO_4)_3$

Atom	Atom	Length/Å	Atom	Atom	Length/Å
Fe1	O1	1.806(3)	N14	C136	1.477(5)
Fe1	O2	1.977(3)	N21	C211	1.323(6)
Fe1	N11	2.125(4)	N21	C215	1.362(6)
Fe1	N12	2.204(3)	N22	C221	1.342(6)
Fe1	N13	2.151(4)	N22	C225	1.331(5)
Fe1	N14	2.180(3)	N23	C231	1.340(8)
Fe2	O1	1.782(3)	N23	C235	1.344(7)
Fe2	O3	2.033(3)	N24	C216	1.481(8)
Fe2	N21	2.122(4)	N24	C226	1.482(7)
Fe2	N22	2.123(3)	N24	C236	1.483(8)
Fe2	N23	2.130(4)	C1	C2	1.489(6)
Fe2	N24	2.246(4)	C2	C3	1.356(8)
Cl1	O11A	1.31(2)	C2	C7	1.390(7)
Cl1	O12A	1.442(13)	C3	C4	1.409(8)
Cl1	O13A	1.38(2)	C4	C5	1.347(8)
Cl1	O14A	1.41(2)	C5	C6	1.399(9)
Cl1	O11B	1.40(2)	C6	C7	1.398(8)
Cl1	O12B	1.41(2)	C111	C112	1.379(8)
Cl1	O13B	1.48(5)	C112	C113	1.366(9)
Cl1	O14B	1.42(2)	C113	C114	1.386(8)

Atom	Atom	Length/Å
Cl2	O21A	1.372(10)
Cl2	O22A	1.476(13)
Cl2	O23A	1.372(9)
Cl2	O24A	1.297(19)
Cl2	O21B	1.40(2)
Cl2	O22B	1.102(17)
Cl2	O23B	1.26(2)
Cl2	O24B	1.382(13)
Cl3	O31A	1.209(11)
Cl3	O32A	1.433(11)
Cl3	O33A	1.444(7)
Cl3	O34A	1.522(11)
Cl3	O31B	1.567(11)
Cl3	O32B	1.34(3)
Cl3	O33B	1.157(18)
Cl3	O34B	1.56(2)
O2	C1	1.280(5)
O3	C1	1.246(5)
O4	C5	1.376(6)
O4	C8	1.398(9)
N11	C111	1.337(6)
N11	C115	1.342(6)
N12	C121	1.347(5)
N12	C125	1.346(5)
N13	C131	1.338(6)
N13	C135	1.357(6)

Atom	Atom	Length/Å
C114	C115	1.371(7)
C115	C116	1.516(7)
C121	C122	1.365(6)
C122	C123	1.374(7)
C123	C124	1.386(7)
C124	C125	1.369(6)
C125	C126	1.506(5)
C131	C132	1.359(8)
C132	C133	1.372(9)
C133	C134	1.374(9)
C134	C135	1.371(7)
C135	C136	1.490(6)
C211	C212	1.379(8)
C212	C213	1.349(10)
C213	C214	1.370(11)
C214	C215	1.374(10)
C215	C216	1.486(9)
C221	C222	1.367(7)
C222	C223	1.380(8)
C223	C224	1.358(9)
C224	C225	1.377(6)
C225	C226	1.496(7)
C231	C232	1.366(9)
C232	C233	1.367(13)
C233	C234	1.322(13)
C234	C235	1.401(10)

Atom	Atom	Length/Å
N14	C116	1.485(5)
N14	C126	1.490(5)

Atom	Atom	Length/Å
C235	C236	1.474(10)

Table 35. Bond angles for $[\{Fe(TPA)\}_2O(4\text{-methoxybenzoato})](ClO_4)_3$

Atom	Atom	Atom2	Angle/ $^{\circ}$	Atom	Atom	Atom	Angle/ $^{\circ}$
O1	Fe1	O2	99.62(12)	Fe1	N14	C136	106.1(2)
O1	Fe1	N11	93.39(13)	C116	N14	C126	110.2(3)
O1	Fe1	N12	173.85(12)	C116	N14	C136	111.5(3)
O1	Fe1	N13	95.45(14)	C126	N14	C136	112.5(3)
O1	Fe1	N14	95.04(11)	Fe2	N21	C211	125.0(3)
O2	Fe1	N11	103.97(15)	Fe2	N21	C215	116.4(4)
O2	Fe1	N12	86.41(12)	C211	N21	C215	118.4(5)
O2	Fe1	N13	99.90(15)	Fe2	N22	C221	123.1(3)
O2	Fe1	N14	165.28(12)	Fe2	N22	C225	118.1(3)
N11	Fe1	N12	86.23(13)	C221	N22	C225	118.7(4)
N11	Fe1	N13	152.73(14)	Fe2	N23	C231	124.1(4)
N11	Fe1	N14	76.27(13)	Fe2	N23	C235	116.3(5)
N12	Fe1	N13	82.27(14)	C231	N23	C235	119.5(6)
N12	Fe1	N14	78.90(12)	Fe2	N24	C216	105.1(3)
N13	Fe1	N14	77.28(14)	Fe2	N24	C226	109.7(3)
O1	Fe2	O3	98.68(12)	Fe2	N24	C236	106.3(4)
O1	Fe2	N21	105.79(14)	C216	N24	C226	111.6(5)
O1	Fe2	N22	97.05(12)	C216	N24	C236	112.7(5)
O1	Fe2	N23	101.84(16)	C226	N24	C236	111.1(5)
O1	Fe2	N24	174.96(15)	O2	C1	O3	123.9(4)
O3	Fe2	N21	91.17(14)	O2	C1	C2	117.0(4)

Atom	Atom	Atom2	Angle/[°]	Atom	Atom	Atom	Angle/[°]
O3	Fe2	N22	164.27(13)	O3	C1	C2	119.1(4)
O3	Fe2	N23	87.39(15)	C1	C2	C3	120.6(4)
O3	Fe2	N24	85.80(14)	C1	C2	C7	120.6(5)
N21	Fe2	N22	84.59(14)	C3	C2	C7	118.8(5)
N21	Fe2	N23	152.22(16)	C2	C3	C4	122.2(5)
N21	Fe2	N24	76.29(18)	C3	C4	C5	118.4(6)
N22	Fe2	N23	89.34(15)	O4	C5	C6	114.9(5)
N22	Fe2	N24	78.48(15)	C4	C5	O4	123.8(6)
N23	Fe2	N24	75.94(19)	C4	C5	C6	121.4(5)
O11A	Cl1	O12A	102.9(13)	C5	C6	C7	119.0(5)
O11A	Cl1	O13A	115.6(17)	C2	C7	C6	120.1(6)
O11A	Cl1	O14A	97.0(18)	N11	C111	C112	121.2(5)
O12A	Cl1	O13A	108.4(12)	C111	C112	C113	119.4(5)
O12A	Cl1	O14A	116.4(12)	C112	C113	C114	119.4(5)
O13A	Cl1	O14A	115.6(15)	C113	C114	C115	118.7(5)
O11B	Cl1	O12B	118(2)	N11	C115	C114	121.7(5)
O11B	Cl1	O13B	102(2)	N11	C115	C116	115.3(4)
O11B	Cl1	O14B	123.6(19)	C114	C115	C116	123.1(5)
O12B	Cl1	O13B	114(2)	N14	C116	C115	109.4(3)
O12B	Cl1	O14B	94(2)	N12	C121	C122	122.8(4)
O13B	Cl1	O14B	104(2)	C121	C122	C123	118.5(4)
O21A	Cl2	O22A	97.4(13)	C122	C123	C124	119.8(4)
O21A	Cl2	O23A	119.6(9)	C123	C124	C125	118.4(4)
O21A	Cl2	O24A	122.5(12)	N12	C125	C124	122.4(4)
O22A	Cl2	O23A	104.0(9)	N12	C125	C126	116.8(3)
O22A	Cl2	O24A	87.1(19)	C124	C125	C126	120.7(4)
O23A	Cl2	O24A	114.5(12)	N14	C126	C125	114.5(3)

Atom	Atom	Atom2	Angle/[°]	Atom	Atom	Atom	Angle/[°]
O21B	Cl2	O22B	110(2)	N13	C131	C132	122.3(5)
O21B	Cl2	O23B	113(2)	C131	C132	C133	118.3(5)
O21B	Cl2	O24B	92.6(13)	C132	C133	C134	120.4(6)
O22B	Cl2	O23B	114(2)	C133	C134	C135	119.0(5)
O22B	Cl2	O24B	104(2)	N13	C135	C134	120.5(5)
O23B	Cl2	O24B	120.7(18)	N13	C135	C136	115.8(4)
O31A	Cl3	O32A	119.4(7)	C134	C135	C136	123.7(4)
O31A	Cl3	O33A	118.8(8)	N14	C136	C135	110.3(3)
O31A	Cl3	O34A	104.9(9)	N21	C211	C212	123.6(6)
O32A	Cl3	O33A	107.3(6)	C211	C212	C213	117.9(7)
O32A	Cl3	O34A	103.2(7)	C212	C213	C214	119.9(7)
O33A	Cl3	O34A	100.1(7)	C213	C214	C215	120.2(7)
O31B	Cl3	O32B	104.0(15)	N21	C215	C214	120.0(7)
O31B	Cl3	O33B	115.5(18)	N21	C215	C216	115.2(5)
O31B	Cl3	O34B	88.7(12)	C214	C215	C216	124.7(6)
O32B	Cl3	O33B	136(2)	N24	C216	C215	110.5(4)
O32B	Cl3	O34B	91.0(15)	N22	C221	C222	122.6(5)
O33B	Cl3	O34B	107(3)	C221	C222	C223	118.0(5)
Fe1	O1	Fe2	129.93(15)	C222	C223	C224	119.9(5)
Fe1	O2	C1	130.9(3)	C223	C224	C225	119.1(5)
Fe2	O3	C1	128.2(3)	N22	C225	C224	121.7(5)
C8	O4	C5	115.7(6)	N22	C225	C226	117.8(4)
Fe1	N11	C111	125.3(3)	C224	C225	C226	120.5(4)
Fe1	N11	C115	114.8(3)	N24	C226	C225	115.7(4)
C111	N11	C115	119.6(4)	N23	C231	C232	121.9(7)
Fe1	N12	C121	126.8(3)	C231	C232	C233	118.7(9)
Fe1	N12	C125	114.5(2)	C232	C233	C234	119.9(8)

Atom	Atom	Atom2	Angle/$^{\circ}$	Atom	Atom	Atom	Angle/$^{\circ}$
C121	N12	C125	118.0(3)	C233	C234	C235	120.9(8)
Fe1	N13	C131	126.3(3)	N23	C235	C234	118.9(8)
Fe1	N13	C135	114.1(3)	N23	C235	C236	117.1(6)
C131	N13	C135	119.5(4)	C234	C235	C236	123.8(7)
Fe1	N14	C116	105.0(2)	N24	C236	C235	110.7(5)
Fe1	N14	C126	111.2(2)				

Table 36. Hydrogen atom coordinates ($\text{\AA} \times 10^4$) and isotropic displacement parameters ($\text{\AA}^2 \times 10^3$) for $[\{\text{Fe}(TPA)\}_2\text{O}(4\text{-methoxybenzoato})](\text{ClO}_4)_3$

Atom	x	y	z	U(eq)
H111	9316.77	6159.98	2663.14	74
H112	9360.79	7468.9	2417.4	91
H113	8568.25	7919.02	1396.47	95
H114	7820.7	7029.96	604.27	84
H121	10488.3	4321.85	2743.1	61
H122	11882.2	3904.71	2472.72	73
H123	11965.6	3723	1356.52	78
H124	10649.7	4007.13	532.94	68
H131	8649.83	2902.32	2544.38	71
H132	8423.02	1656.46	2151.65	96
H133	7788.32	1461.54	1032.65	118
H134	7379.79	2515.88	333.41	94
H211	6699.2	6511.32	1871.94	76
H212	6476.77	7836.52	1900.95	109
H213	6138.05	8383.87	2858.7	127
H214	5919.74	7595.38	3732.01	130
H221	5352.39	4905.13	1298.5	68

Atom	x	y	z	U(eq)
H222	3823.97	5073.87	736.74	92
H223	2642.59	5307.69	1354.49	98
H224	3041.97	5443.59	2495.71	82
H231	6516.91	3266.6	2336.7	94
H232	6364.02	2071.7	2809.41	136
H233	5915.14	2010.8	3840.03	166
H234	5702.82	3114.19	4387.55	143
H3	9862.7	3676.22	3757.1	99
H4	10702.5	3198.3	4771.64	106
H6	9063.35	4490.2	5737.98	99
H7	8223.51	4945.8	4715.25	95
H13	8140(120)	3500(90)	1550(80)	270(70)
H8A	11041.9	2635.82	5727.02	185
H11A	6964.05	5437.61	766.34	62
H12A	9171.2	5185.12	533.13	61
H13A	7476.27	3957.56	183.23	61
H21A	6737.88	5949.08	4138.88	109
H22A	4476.76	5794.05	3438.37	119
H23A	6587.54	4710.47	4339.13	116
H8B	11490.8	2963.27	6435.46	185
H11B	7658.19	5598.31	268.1	62
H12B	8936.09	4335.75	273.76	61
H13B	6811.05	4178.63	686.64	61
H21B	5696.25	6235.63	4131.24	109
H22B	4409.5	4888.38	3500.16	119
H23B	5501.34	4583.59	4330.08	116

Atom	x	y	z	U(eq)
H8C	11698.8	3372.32	5788.64	185

Table 37. Partial atomic occupancy for $[\{Fe(TPA)\}_2O(4\text{-methoxybenzoato})](ClO_4)_3$

Atom	Occupancy
O11A	0.63(3)
O12A	0.63(3)
O13A	0.63(3)
O14A	0.63(3)
O21A	0.6
O22A	0.6
O23A	0.6
O24A	0.4

Atom	Occupancy
O31A	0.6
O32A	0.6
O33A	0.6
O34A	0.6
O11B	0.37(3)
O12B	0.37(3)
O13B	0.37(3)
O14B	0.37(3)

Atom	Occupancy
O21B	0.4
O22B	0.4
O23B	0.4
O24B	0.6
O31B	0.4
O32B	0.4
O33B	0.4
O34B	0.4

3.3.5. $[\{\text{Fe}(TPA)\}_2\text{O}(\text{4-fluorobenzoato})](\text{ClO}_4)_3$

Figure 61 shows the asymmetric unit of $[\{\text{Fe}(TPA)\}_2\text{O}(\text{4-fluorobenzoato})](\text{ClO}_4)_3$. The cationic portion of $[\{\text{Fe}(TPA)\}_2\text{O}(\text{4-fluorobenzoato})](\text{ClO}_4)_3$ is shown in **Figure 62**. Crystallographic details for $[\{\text{Fe}(TPA)\}_2\text{O}(\text{4-fluorobenzoato})](\text{ClO}_4)_3$ are listed in **Table 38**. Fractional atomic coordinates, anisotropic displacement parameters, bond lengths and bond angles involving the non-hydrogen atoms and hydrogen atom coordinates and atomic occupancies for the disordered atoms are listed in **Table 39**, **Table 40**, **Table 41**, **Table 42**, **Table 43** and **Table 44**, respectively.

Figure 63 shows the fluorobenzoate numbering scheme. C1 is bonded to O2 and O3. O2 and O3 coordinate to the Fe1 and Fe2, respectively. O1 is the bridging oxygen for the Fe1-O1-Fe2 unit in the dimer. F1 coordinates to C5. Two of the three perchlorates are disordered. The perchlorate disordered about Cl2-O21 is modeled with two set of oxygen atoms with occupancies of 0.60 and 0.40. The perchlorate disordered about Cl3-O31 is modeled with two set of oxygen atoms with occupancies of 0.70 and 0.30. The remaining perchlorate ion is labeled Cl1, O11, O12, O13 and O14.

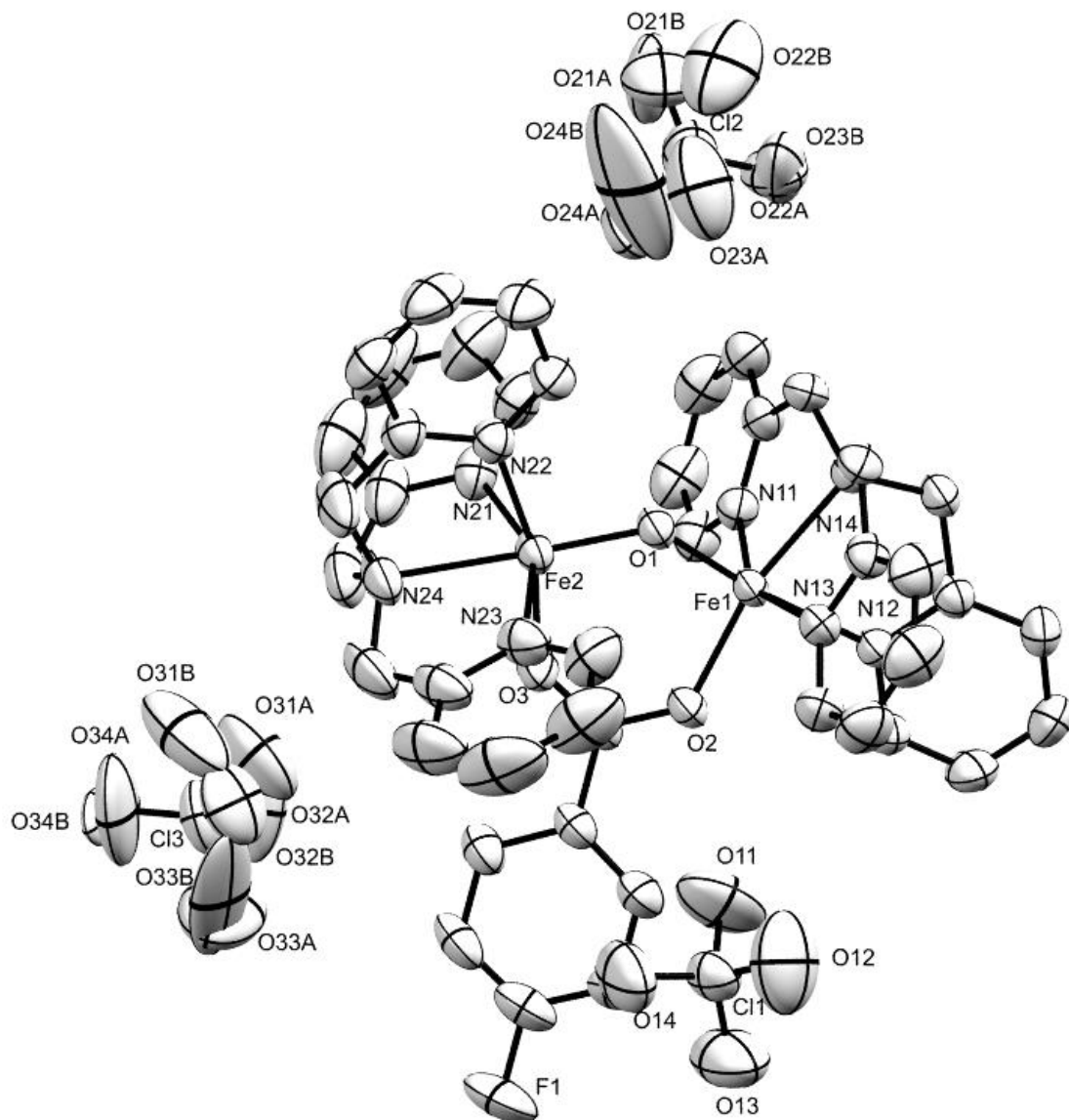


Figure 61. A view of the asymmetric unit of $[\{Fe\text{-}(TPA)\}_2\text{O}(4\text{-fluorobenzoato})](\text{ClO}_4)_3$.

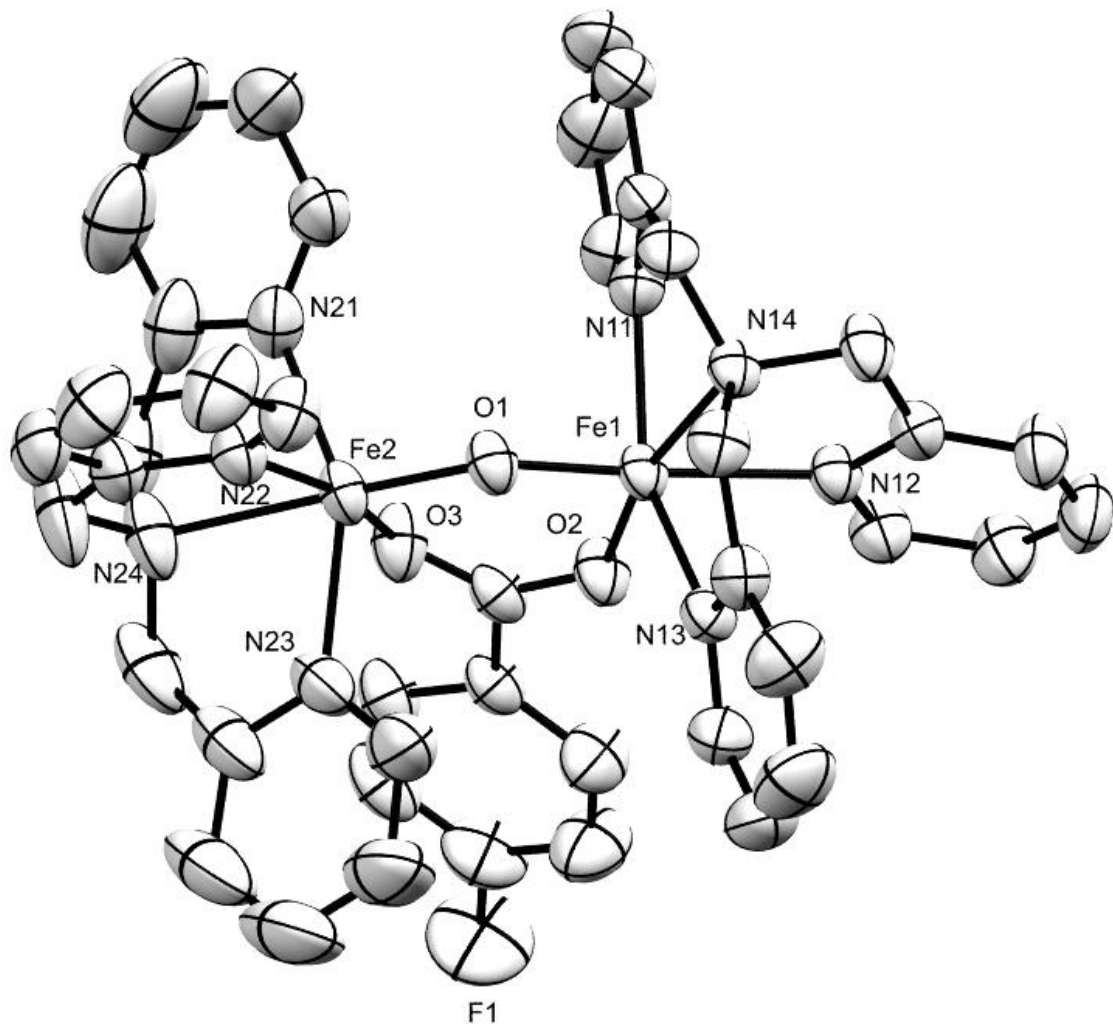


Figure 62. A view of the cationic portion of $\{Fe(TPA)\}_2O(4\text{-fluorobenzoato})](ClO_4)_3$. Hydrogen atoms are omitted.

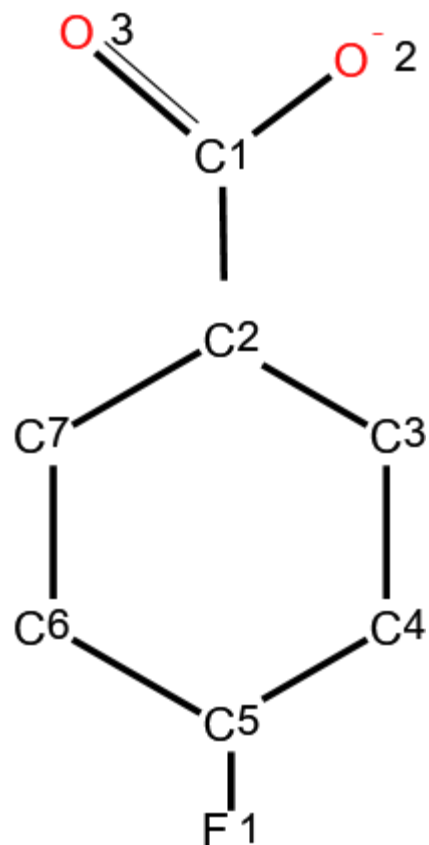


Figure 63. Numbering scheme for 4-fluorobenzoate.

Table 38. Crystallographic data for $[\{Fe\text{-}(TPA)\}_2O(4\text{-fluorobenzoato})](ClO_4)_3$

Crystallographic data	
Empirical formula	C ₄₃ H ₄₀ Cl ₃ FFe ₂ N ₈ O ₁₅
Formula weight	1145.88
Temperature/K	298
Crystal system	monoclinic
Space group	P2 ₁ /c
a/Å	14.3982(9)
b/Å	17.1863(11)
c/Å	20.1075(10)
α/°	90
β/°	101.877(5)
γ/°	90
Volume/Å ³	4869.1(5)
Z	4
ρ _{calc} /g cm ⁻³	1.563
μ/mm ⁻¹	0.840
F(000)	2344
Crystal size/mm ³	0.5 × 0.27 × 0.2
Radiation	MoKα ($\lambda = 0.71073$)
2θ range for data collection/°	5.172 to 53
Index ranges	-18 ≤ h ≤ 18, -21 ≤ k ≤ 21, -25 ≤ l ≤ 9

 Crystallographic data

Reflections collected	21571
Independent reflections	10056 [$R_{\text{int}} = 0.0222$, $R_{\text{sigma}} = 0.0300$]
Data/restraints/parameters	10056/0/721
Goodness-of-fit on F^2	1.016
Final R indexes [$I \geq 2\sigma (I)$]	$R_1 = 0.0450$, $wR_2 = 0.1118$
Final R indexes [all data]	$R_1 = 0.0685$, $wR_2 = 0.1302$
Largest diff. peak/hole / e Å ⁻³	0.78/-0.67

Table 39. Fractional atomic coordinates ($\times 10^4$) and equivalent isotropic displacement parameters ($\text{\AA}^2 \times 10^3$) for $[\{\text{Fe}(TPA)\}_2\text{O}(4\text{-fluorobenzoato})](\text{ClO}_4)_3$

Atom	x	y	z	U(eq)
Fe1	1672.7(3)	5421.8(2)	8010.6(2)	35.11(11)
Fe2	3414.0(3)	5014.6(3)	7260.8(2)	40.12(12)
Cl1	1078.5(6)	8529.8(6)	6156.2(5)	63.3(2)
Cl2	4573.4(9)	3342.6(9)	10026.0(7)	91.9(4)
Cl3	2780.7(8)	4389.6(7)	4045.1(5)	75.0(3)
F1	-409(2)	6555.0(19)	3996.1(11)	115.5(11)
O1	2893.0(13)	5243.7(12)	7967.4(9)	40.7(4)
O2	1135.8(14)	5598.1(13)	7029.9(9)	47.8(5)
O3	2204.5(15)	5030.9(14)	6529.3(10)	52.0(5)
O11	1074(3)	7818(2)	6480.3(19)	131.2(15)
O12	1219(3)	9111(3)	6676(2)	147.2(17)
O13	202(3)	8635(3)	5715(2)	136.3(16)
O14	1815(2)	8548(3)	5799.5(18)	116.5(13)
O21A	5176(5)	2909(7)	10302(4)	164(4)

Atom	x	y	z	U(eq)
O22A	3751(5)	3405(7)	10273(5)	87(3)
O23A	4979(6)	4155(5)	10067(4)	170(3)
O24A	4274(4)	3298(4)	9295(2)	124(2)
O31A	2445(9)	3888(9)	4523(5)	142(5)
O32A	3257(6)	4982(5)	4403(3)	106(2)
O33A	1998(7)	4735(9)	3609(4)	206(6)
O34A	3184(10)	4016(8)	3650(5)	157(5)
O21B	4725(11)	2428(5)	10098(7)	97(5)
O22B	5300(8)	3435(8)	10785(8)	113(4)
O23B	3810(20)	3458(19)	10351(15)	144(13)
O24B	5190(20)	3580(15)	9733(11)	255(16)
O31B	3767(13)	4401(17)	4511(7)	165(9)
O32B	2070(17)	4052(13)	4263(14)	130(11)
O33B	2560(30)	5113(8)	3796(19)	231(18)
O34B	3191(11)	3944(12)	3509(7)	65(4)
N11	1408.6(17)	4225.5(14)	8166.1(12)	42.5(5)
N12	238.2(16)	5640.8(14)	8189.6(11)	38.5(5)
N13	1898.8(17)	6602.4(14)	8351.1(11)	40.9(5)
N14	1916.6(16)	5309.0(14)	9114.8(10)	37.6(5)
N21	3479.8(18)	3782.2(16)	7214.4(14)	51.4(6)
N22	4839.8(17)	4949.3(15)	7795.1(12)	44.3(6)
N23	3707.9(19)	6148.7(19)	6928.6(15)	59.5(7)
N24	4174(2)	4781(2)	6413.0(13)	63.9(8)
C1	1469(2)	5427.0(18)	6509.3(13)	41.2(6)
C2	954(2)	5722.0(18)	5839.6(13)	43.4(7)
C3	252(3)	6267(2)	5801.0(16)	60.9(9)
C4	-209(3)	6559(3)	5183.1(19)	77.0(12)

Atom	x	y	z	U(eq)
C5	50(3)	6273(3)	4611.8(17)	71.9(11)
C6	727(3)	5730(2)	4625.3(15)	63.6(10)
C7	1190(2)	5445(2)	5245.0(14)	51.9(8)
C111	952(2)	3730(2)	7692.2(17)	53.7(8)
C112	927(3)	2946(2)	7802(2)	69.1(10)
C113	1383(3)	2649(2)	8418(2)	68.5(10)
C114	1836(2)	3154(2)	8910.6(19)	58.9(9)
C115	1837(2)	3940.8(18)	8772.5(15)	45.6(7)
C116	2348(2)	4532.5(18)	9267.5(14)	46.6(7)
C121	-537(2)	5833.2(19)	7729.0(15)	47.3(7)
C122	-1340(2)	6120(2)	7903.8(17)	60.5(9)
C123	-1340(3)	6250(2)	8577.3(19)	67.4(10)
C124	-555(2)	6035(2)	9060.9(16)	55.6(8)
C125	204(2)	5711.3(17)	8854.4(14)	41.1(6)
C126	1010(2)	5363(2)	9357.9(14)	49.0(8)
C131	1673(2)	7246.3(19)	7971.0(16)	52.7(8)
C132	1853(3)	7974(2)	8229(2)	68.6(10)
C133	2267(3)	8057(2)	8907(2)	78.8(12)
C134	2484(3)	7410(2)	9300.8(19)	67.1(10)
C135	2307(2)	6684.8(18)	9011.5(15)	45.0(7)
C136	2581(2)	5942.0(18)	9391.3(14)	46.3(7)
C211	3420(2)	3309(2)	7730(2)	60.4(9)
C212	3545(3)	2518(3)	7704(3)	86.9(14)
C213	3734(4)	2205(3)	7126(4)	107.1(19)
C214	3821(4)	2681(3)	6600(3)	101.3(17)
C215	3691(3)	3473(3)	6645(2)	70.0(11)
C216	3766(3)	4051(3)	6099.6(19)	82.0(13)

Atom	x	y	z	U(eq)
C221	5093(2)	5032(2)	8469.1(16)	55.0(8)
C222	6016(3)	4978(2)	8808(2)	74.1(11)
C223	6706(3)	4847(3)	8435(2)	75.9(12)
C224	6456(2)	4756(2)	7750(2)	64.3(10)
C225	5509(2)	4805(2)	7439.9(17)	49.8(7)
C226	5207(3)	4693(3)	6687(2)	89.4(15)
C231	3631(3)	6799(2)	7283(2)	73.4(11)
C232	3768(3)	7522(3)	7026(3)	104.7(18)
C233	4036(4)	7572(4)	6411(4)	127(3)
C234	4150(4)	6911(4)	6064(3)	105.0(19)
C235	3963(3)	6199(3)	6325.1(19)	71.5(11)
C236	3974(3)	5457(3)	5943.8(18)	82.9(14)

Table 40. Anisotropic displacement parameters ($\text{\AA}^2 \times 10^3$) for $[\{\text{Fe}(TPA)\}_2\text{O}(4\text{-fluorobenzoato})](\text{ClO}_4)_3$

Atom	U₁₁	U₂₂	U₃₃	U₂₃	U₁₃	U₁₂
Fe1	36.9(2)	44.5(2)	24.99(18)	1.11(16)	8.91(15)	1.82(17)
Fe2	35.7(2)	55.5(3)	31.2(2)	-0.79(17)	11.87(16)	-2.36(19)
Cl1	56.9(5)	73.8(6)	61.5(5)	18.4(4)	17.5(4)	-4.2(4)
Cl2	76.6(7)	119.5(11)	84.2(8)	-9.6(7)	27.4(6)	8.4(7)
Cl3	82.7(7)	87.1(7)	63.3(5)	-29.1(5)	33.7(5)	-24.6(6)
F1	145(3)	149(3)	40.5(12)	27.0(14)	-7.5(14)	25(2)
O1	37.6(10)	55.8(12)	29.8(9)	-0.6(8)	9.1(8)	0.2(9)
O2	46.7(11)	69.4(14)	28.0(9)	3.5(9)	9.3(8)	8.1(10)
O3	41.2(11)	78.7(16)	35.1(10)	-8.3(10)	5.7(9)	7.1(11)
O11	180(4)	107(3)	100(3)	51(2)	16(3)	-12(3)
O12	156(4)	140(4)	160(4)	-63(3)	68(3)	-38(3)
O13	82(2)	216(5)	107(3)	53(3)	9(2)	26(3)

Atom	U₁₁	U₂₂	U₃₃	U₂₃	U₁₃	U₁₂
O14	87(2)	185(4)	89(2)	24(2)	45.6(19)	6(2)
O21A	104(5)	280(12)	101(5)	52(7)	4(4)	64(7)
O22A	56(3)	121(8)	83(5)	29(4)	8(3)	15(4)
O23A	170(7)	195(8)	163(7)	-59(6)	80(6)	-89(6)
O24A	115(4)	200(6)	56(3)	-19(3)	12(3)	37(4)
O31A	165(11)	184(10)	86(4)	10(4)	47(5)	-62(7)
O32A	129(6)	108(5)	81(4)	-43(4)	19(4)	-36(4)
O33A	156(8)	322(16)	106(6)	-54(8)	-55(6)	82(9)
O34A	237(10)	113(6)	164(9)	-64(6)	143(8)	-17(6)
O21B	141(11)	39(5)	144(11)	-28(5)	103(10)	-15(6)
O22B	71(7)	133(11)	133(11)	-35(9)	20(7)	-22(7)
O23B	240(30)	101(18)	122(17)	25(13)	116(17)	76(17)
O24B	390(40)	260(30)	167(18)	-107(18)	200(20)	-230(30)
O31B	120(13)	300(30)	68(8)	18(13)	4(8)	-78(15)
O32B	119(16)	93(12)	220(30)	-47(16)	130(20)	-49(11)
O33B	390(40)	41(7)	360(40)	45(14)	300(40)	73(15)
O34B	75(7)	82(8)	38(4)	-37(5)	9(5)	23(6)
N11	41.0(12)	44.9(14)	42.9(13)	-1.6(11)	11.3(10)	2.4(11)
N12	36.3(12)	47.3(14)	32.0(11)	0.7(10)	7.4(9)	2.6(10)
N13	43.8(13)	44.3(14)	35.8(12)	3.2(10)	11.1(10)	2.4(11)
N14	37.4(12)	48.8(14)	26.6(10)	3.2(10)	6.7(9)	4.2(10)
N21	43.5(14)	56.2(17)	56.9(15)	-12.7(13)	16.2(12)	-2.0(12)
N22	38.9(12)	52.0(15)	42.6(13)	-0.4(11)	10(1)	-0.4(11)
N23	48.1(15)	73(2)	60.2(17)	22.2(15)	16.7(13)	-3.4(14)
N24	49.6(15)	109(3)	36.9(13)	-2.1(15)	18.6(12)	-0.5(16)
C1	42.8(15)	50.1(17)	31.0(13)	-2.1(12)	8.3(11)	-8.3(14)
C2	46.7(16)	53.8(18)	29.8(13)	-0.4(12)	8.2(12)	-7.5(14)

Atom	U₁₁	U₂₂	U₃₃	U₂₃	U₁₃	U₁₂
C3	76(2)	71(2)	34.8(15)	0.1(15)	8.3(15)	12.3(19)
C4	93(3)	81(3)	52(2)	12.3(19)	4(2)	27(2)
C5	88(3)	87(3)	35.8(17)	13.3(17)	1.8(18)	-5(2)
C6	71(2)	92(3)	28.8(15)	-3.2(16)	12.0(15)	-17(2)
C7	48.8(17)	72(2)	35.7(14)	-6.2(14)	10.0(13)	-8.1(16)
C111	48.3(17)	57(2)	54.6(18)	-10.1(15)	8.1(15)	-2.3(16)
C112	55(2)	56(2)	96(3)	-17(2)	15(2)	-9.0(18)
C113	63(2)	45(2)	104(3)	6(2)	32(2)	-4.6(18)
C114	56(2)	57(2)	69(2)	16.4(17)	24.5(17)	4.7(17)
C115	43.2(16)	48.7(17)	48.3(16)	8.9(14)	17.7(13)	1.7(14)
C116	48.2(16)	54.2(18)	36.8(14)	10.0(13)	7.3(13)	8.9(15)
C121	41.9(16)	58.6(19)	39.6(15)	3.8(14)	4.2(12)	2.1(14)
C122	42.9(17)	80(3)	55.9(19)	13.5(18)	3.0(15)	13.1(17)
C123	50.6(19)	85(3)	71(2)	9(2)	24.0(17)	25.1(19)
C124	51.4(18)	73(2)	46.6(17)	-1.5(16)	20.6(15)	10.2(17)
C125	40.8(15)	45.4(16)	38.4(14)	0.3(12)	11.4(12)	-1.3(13)
C126	44.6(16)	72(2)	32.5(14)	6.3(14)	13.0(12)	8.5(15)
C131	58.7(19)	51.6(19)	49.3(17)	9.1(15)	14.5(15)	5.6(16)
C132	74(2)	48(2)	85(3)	12.8(19)	21(2)	8.1(19)
C133	85(3)	50(2)	98(3)	-15(2)	13(2)	2(2)
C134	74(2)	59(2)	63(2)	-16.3(18)	0.0(19)	0.6(19)
C135	41.8(15)	50.8(18)	42.1(15)	-4.8(13)	7.7(13)	-0.8(14)
C136	45.8(16)	57.4(19)	32.6(13)	-4.5(13)	0.9(12)	2.2(14)
C211	51.0(19)	55(2)	80(2)	-2.0(18)	26.1(18)	-2.2(16)
C212	59(2)	59(3)	147(5)	2(3)	32(3)	-6(2)
C213	81(3)	63(3)	177(6)	-41(4)	25(4)	-2(3)
C214	90(3)	95(4)	122(4)	-60(3)	27(3)	4(3)

Atom	U₁₁	U₂₂	U₃₃	U₂₃	U₁₃	U₁₂
C215	55(2)	85(3)	71(2)	-35(2)	15.4(18)	2(2)
C216	76(3)	122(4)	50(2)	-31(2)	17.5(19)	12(3)
C221	51.8(18)	67(2)	44.1(17)	-7.8(15)	4.9(14)	8.6(16)
C222	60(2)	92(3)	61(2)	-12(2)	-9.7(19)	16(2)
C223	46(2)	85(3)	88(3)	-1(2)	-7(2)	12.2(19)
C224	40.2(17)	71(2)	83(3)	0(2)	16.8(18)	6.8(16)
C225	40.1(16)	55.7(19)	56.8(18)	2.6(15)	17.7(14)	-0.8(14)
C226	44.1(19)	172(5)	58(2)	-5(3)	25.6(17)	8(2)
C231	57(2)	62(2)	106(3)	13(2)	27(2)	-0.8(19)
C232	80(3)	66(3)	173(6)	36(3)	39(3)	-4(2)
C233	84(4)	111(5)	188(7)	89(5)	36(4)	-2(4)
C234	78(3)	137(5)	103(4)	68(4)	25(3)	-7(3)
C235	50.3(19)	107(3)	58(2)	34(2)	12.3(17)	-5(2)
C236	73(3)	137(4)	42.2(19)	19(2)	21.1(18)	-12(3)

Table 41. Bond lengths for $[\{Fe(TPA)\}_2O(4\text{-fluorobenzoato})](ClO_4)_3$

Atom	Atom	Length/Å	Atom	Atom	Length/Å
Fe1	O1	1.8031(19)	N21	C215	1.352(4)
Fe1	O2	1.9877(18)	N22	C221	1.337(4)
Fe1	N11	2.126(3)	N22	C225	1.336(4)
Fe1	N12	2.201(2)	N23	C231	1.342(5)
Fe1	N13	2.145(2)	N23	C235	1.341(5)
Fe1	N14	2.184(2)	N24	C216	1.471(5)
Fe2	O1	1.7819(19)	N24	C226	1.484(5)
Fe2	O3	2.035(2)	N24	C236	1.487(5)
Fe2	N21	2.123(3)	C1	C2	1.486(4)
Fe2	N22	2.115(2)	C2	C3	1.368(5)

Atom	Atom	Length/Å
Fe2	N23	2.131(3)
Fe2	N24	2.243(3)
Cl1	O11	1.387(3)
Cl1	O12	1.430(4)
Cl1	O13	1.397(4)
Cl1	O14	1.398(3)
Cl2	O21A	1.191(7)
Cl2	O22A	1.380(9)
Cl2	O23A	1.509(8)
Cl2	O24A	1.446(5)
Cl2	O21B	1.589(10)
Cl2	O22B	1.671(15)
Cl2	O23B	1.41(3)
Cl2	O24B	1.226(17)
Cl3	O31A	1.445(11)
Cl3	O32A	1.350(5)
Cl3	O33A	1.409(8)
Cl3	O34A	1.253(10)
Cl3	O31B	1.531(16)
Cl3	O32B	1.326(18)
Cl3	O33B	1.353(17)
Cl3	O34B	1.537(16)
F1	C5	1.367(4)
O2	C1	1.272(3)
O3	C1	1.253(4)
N11	C111	1.345(4)
N11	C115	1.340(4)

Atom	Atom	Length/Å
C2	C7	1.392(4)
C3	C4	1.377(5)
C4	C5	1.370(6)
C5	C6	1.345(6)
C6	C7	1.377(5)
C111	C112	1.367(5)
C112	C113	1.374(6)
C113	C114	1.376(5)
C114	C115	1.381(5)
C115	C116	1.505(4)
C121	C122	1.368(4)
C122	C123	1.373(5)
C123	C124	1.381(5)
C124	C125	1.365(4)
C125	C126	1.499(4)
C131	C132	1.359(5)
C132	C133	1.378(6)
C133	C134	1.365(6)
C134	C135	1.376(5)
C135	C136	1.498(4)
C211	C212	1.373(5)
C212	C213	1.357(8)
C213	C214	1.363(8)
C214	C215	1.380(7)
C215	C216	1.500(6)
C221	C222	1.366(5)
C222	C223	1.381(6)

Atom	Atom	Length/Å	Atom	Atom	Length/Å
N12	C121	1.337(4)	C223	C224	1.360(6)
N12	C125	1.353(3)	C224	C225	1.379(5)
N13	C131	1.346(4)	C225	C226	1.499(5)
N13	C135	1.344(4)	C231	C232	1.376(6)
N14	C116	1.477(4)	C232	C233	1.372(9)
N14	C126	1.488(4)	C233	C234	1.360(9)
N14	C136	1.480(4)	C234	C235	1.380(7)
N21	C211	1.335(4)	C235	C236	1.490(6)

Table 42. Bond angles for $[\{Fe(TPA)\}_2O(4\text{-fluorobenzoato})](ClO_4)_3$

Atom	Atom	Atom	Angle/°	Atom	Atom	Atom	Angle/°
O1	Fe1	O2	99.32(8)	C126	N14	C136	112.0(2)
O1	Fe1	N11	92.78(9)	Fe2	N21	C211	124.3(2)
O1	Fe1	N12	173.49(8)	Fe2	N21	C215	116.7(3)
O1	Fe1	N13	95.19(9)	C211	N21	C215	118.7(3)
O1	Fe1	N14	94.56(8)	Fe2	N22	C221	122.9(2)
O2	Fe1	N11	104.40(9)	Fe2	N22	C225	118.0(2)
O2	Fe1	N12	87.12(8)	C221	N22	C225	119.1(3)
O2	Fe1	N13	100.08(9)	Fe2	N23	C231	123.5(3)
O2	Fe1	N14	166.05(8)	Fe2	N23	C235	116.9(3)
N11	Fe1	N12	86.51(9)	C231	N23	C235	119.6(4)
N11	Fe1	N13	152.63(9)	Fe2	N24	C216	105.3(2)
N11	Fe1	N14	76.16(9)	Fe2	N24	C226	110.2(2)
N12	Fe1	N13	82.64(9)	Fe2	N24	C236	106.4(2)
N12	Fe1	N14	78.98(8)	C216	N24	C226	110.7(4)
N13	Fe1	N14	77.13(9)	C216	N24	C236	112.7(3)
O1	Fe2	O3	97.77(8)	C226	N24	C236	111.3(3)

Atom	Atom	Atom	Angle/[°]	Atom	Atom	Atom	Angle/[°]
O1	Fe2	N21	106.58(10)	O2	C1	O3	123.9(3)
O1	Fe2	N22	97.50(9)	O2	C1	C2	117.7(3)
O1	Fe2	N23	101.03(11)	O3	C1	C2	118.4(3)
O1	Fe2	N24	175.35(10)	C1	C2	C3	120.6(3)
O3	Fe2	N21	91.22(10)	C1	C2	C7	119.8(3)
O3	Fe2	N22	164.69(9)	C3	C2	C7	119.6(3)
O3	Fe2	N23	87.51(10)	C2	C3	C4	120.9(3)
O3	Fe2	N24	86.09(9)	C3	C4	C5	117.5(4)
N21	Fe2	N22	85.52(10)	F1	C5	C4	117.9(4)
N21	Fe2	N23	152.27(11)	F1	C5	C6	118.5(4)
N21	Fe2	N24	75.82(12)	C4	C5	C6	123.6(3)
N22	Fe2	N23	88.46(10)	C5	C6	C7	118.6(3)
N22	Fe2	N24	78.60(10)	C2	C7	C6	119.8(3)
N23	Fe2	N24	76.46(13)	N11	C111	C112	122.3(3)
O11	Cl1	O12	106.7(3)	C111	C112	C113	119.2(4)
O11	Cl1	O13	108.7(3)	C112	C113	C114	118.9(3)
O11	Cl1	O14	109.8(3)	C113	C114	C115	119.5(3)
O12	Cl1	O13	110.3(3)	N11	C115	C114	121.4(3)
O12	Cl1	O14	110.5(3)	N11	C115	C116	115.2(3)
O13	Cl1	O14	110.7(2)	C114	C115	C116	123.3(3)
O21A	Cl2	O22A	118.6(6)	N14	C116	C115	110.2(2)
O21A	Cl2	O23A	108.5(7)	N12	C121	C122	122.7(3)
O21A	Cl2	O24A	118.4(5)	C121	C122	C123	118.9(3)
O22A	Cl2	O23A	105.0(6)	C122	C123	C124	119.0(3)
O22A	Cl2	O24A	105.8(5)	C123	C124	C125	119.0(3)
O23A	Cl2	O24A	97.8(4)	N12	C125	C124	122.1(3)
O21B	Cl2	O22B	87.8(7)	N12	C125	C126	116.8(2)

Atom	Atom	Atom	Angle/[°]	Atom	Atom	Atom	Angle/[°]
O21B	Cl2	O23B	101.7(14)	C124	C125	C126	121.0(3)
O21B	Cl2	O24B	105.9(15)	N14	C126	C125	114.4(2)
O22B	Cl2	O23B	88.0(13)	N13	C131	C132	122.4(3)
O22B	Cl2	O24B	91.7(14)	C131	C132	C133	118.9(4)
O23B	Cl2	O24B	152(2)	C132	C133	C134	119.4(4)
O31A	Cl3	O32A	107.3(6)	C133	C134	C135	119.5(3)
O31A	Cl3	O33A	109.4(7)	N13	C135	C134	121.2(3)
O31A	Cl3	O34A	112.3(9)	N13	C135	C136	115.4(3)
O32A	Cl3	O33A	105.5(6)	C134	C135	C136	123.3(3)
O32A	Cl3	O34A	118.2(7)	N14	C136	C135	110.6(2)
O33A	Cl3	O34A	103.7(7)	N21	C211	C212	122.9(4)
O31B	Cl3	O32B	119.0(14)	C211	C212	C213	118.5(5)
O31B	Cl3	O33B	109.4(19)	C212	C213	C214	119.5(5)
O31B	Cl3	O34B	89.6(10)	C213	C214	C215	120.4(5)
O32B	Cl3	O33B	112.7(16)	N21	C215	C214	120.0(5)
O32B	Cl3	O34B	116.6(13)	N21	C215	C216	114.9(4)
O33B	Cl3	O34B	107.0(13)	C214	C215	C216	125.0(4)
Fe1	O1	Fe2	130.56(10)	N24	C216	C215	109.5(3)
Fe1	O2	C1	130.22(19)	N22	C221	C222	122.2(3)
Fe2	O3	C1	128.52(18)	C221	C222	C223	118.3(4)
Fe1	N11	C111	125.8(2)	C222	C223	C224	120.0(3)
Fe1	N11	C115	115.1(2)	C223	C224	C225	118.8(4)
C111	N11	C115	118.7(3)	N22	C225	C224	121.6(3)
Fe1	N12	C121	127.34(19)	N22	C225	C226	118.2(3)
Fe1	N12	C125	113.79(17)	C224	C225	C226	120.2(3)
C121	N12	C125	117.9(2)	N24	C226	C225	115.0(3)
Fe1	N13	C131	126.4(2)	N23	C231	C232	121.2(5)

Atom	Atom	Atom	Angle/$^{\circ}$	Atom	Atom	Atom	Angle/$^{\circ}$
Fe1	N13	C135	114.94(19)	C231	C232	C233	118.9(6)
C131	N13	C135	118.7(3)	C232	C233	C234	119.8(5)
Fe1	N14	C116	105.32(16)	C233	C234	C235	119.4(5)
Fe1	N14	C126	111.11(16)	N23	C235	C234	120.9(5)
Fe1	N14	C136	105.85(16)	N23	C235	C236	116.4(4)
C116	N14	C126	110.3(2)	C234	C235	C236	122.6(4)
C116	N14	C136	112.0(2)	N24	C236	C235	111.3(3)

Table 43. Hydrogen atom coordinates ($\text{\AA} \times 10^4$) and isotropic displacement parameters ($\text{\AA}^2 \times 10^3$) for $[\{Fe(TPA)\}_2O(4\text{-fluorobenzoato})](ClO_4)_3$

Atom	x	y	z	U(eq)
H3	84.72	6442.79	6197.64	73
H4	-679.19	6935.82	5154.76	92
H6	878.41	5550.84	4224.32	76
H7	1658.67	5068.03	5266.39	62
H111	641.21	3927.37	7274.86	64
H112	605.55	2617.3	7464.66	83
H113	1385.48	2116.79	8500.01	82
H114	2140.44	2966.1	9333.3	71
H121	-529.37	5769.77	7270.76	57
H122	-1877.7	6224.16	7571.68	73
H123	-1860.6	6479.85	8706.02	81
H124	-543.59	6110.52	9520.52	67
H131	1383.46	7190.95	7515.4	63
H132	1698.86	8409.05	7953.08	82
H133	2396.83	8549.99	9094.06	95
H134	2749.57	7457.75	9761.32	80

Atom	x	y	z	U(eq)
H211	3287.64	3523.79	8125.02	72
H212	3501.07	2204.26	8072.64	104
H213	3803.56	1670.05	7089.34	128
H214	3968.21	2470.8	6208.46	122
H221	4624.86	5130.38	8715.41	66
H222	6175.04	5028.45	9278.73	89
H223	7341.04	4821.33	8652.66	91
H224	6914.58	4662.22	7494.66	77
H231	3482.83	6759.9	7710.77	88
H232	3680.33	7970.14	7265.25	126
H233	4139.45	8055.33	6231.67	152
H234	4352.31	6938.81	5653.79	126
H11A	2312.51	4382.51	9726.74	56
H12A	1115.79	5673.1	9769.52	59
H13A	3220.42	5797.74	9355.08	56
H21A	4165.81	3843.42	5808.53	98
H22A	5543.11	5065.76	6461.52	107
H23A	3363.89	5384.41	5639.05	99
H11B	3011.67	4550.54	9238.44	56
H12B	828.66	4844.46	9474.08	59
H13B	2575.47	6018.09	9868.45	56
H21B	3141.45	4149.95	5822.39	98
H22B	5398.07	4176.63	6573.18	107
H23B	4455.39	5486.22	5670.85	99

Table 44. Partial atomic occupancy for $\{\text{Fe}(TPA)\}_2\text{O}(4\text{-fluorobenzoato})](\text{ClO}_4)_3$

Atom	Occupancy	Atom	Occupancy	Atom	Occupancy
O21A	0.7	O32A	0.7	O23B	0.3
O22A	0.7	O33A	0.7	O24B	0.3
O23A	0.7	O34A	0.7	O31B	0.3
O24A	0.7	O21B	0.3	O32B	0.3
O31A	0.7	O22B	0.3	O33B	0.3
				O34B	0.3

3.3.6 $[\text{Fe}_2(\text{TPA})_2\text{O}(3,5\text{-dimethylbenzoato})](\text{ClO}_4)_3 \bullet 0.5\text{H}_2\text{O}$

Figure 64 shows the asymmetric unit of $[\text{Fe}_2(\text{TPA})_2\text{O}(3,5\text{-dimethylbenzoato})](\text{ClO}_4)_3 \bullet 0.5\text{H}_2\text{O}$. The cationic portion of the $[\text{Fe}_2(\text{TPA})_2\text{O}(3,5\text{-dimethylbenzoato})](\text{ClO}_4)_3 \bullet 0.5\text{H}_2\text{O}$ is shown in **Figure 65**. Crystallographic details for $[\text{Fe}_2(\text{TPA})_2\text{O}(3,5\text{-dimethylbenzoato})](\text{ClO}_4)_3 \bullet 0.5\text{H}_2\text{O}$ are listed in **Table 45**. Fractional atomic coordinates, anisotropic displacement parameters, bond lengths and bond angles involving the non-hydrogen atoms and hydrogen atom coordinates are and atomic occupancies for the disordered atoms listed in **Table 46**, **Table 47**, **Table 48**, **Table 49**, **Table 50**, **Table 51**, respectively.

Crystals of $[\text{Fe}_2(\text{TPA})_2\text{O}(3,5\text{-dimethylbenzoato})](\text{ClO}_4)_3$ were obtained from two different synthetic procedures. The fact that these crystals are the same material is confirmed by identical cell constants (within experimental error). The best structure is reported here.

The asymmetric unit of $[\text{Fe}_2(\text{TPA})_2\text{O}(3,5\text{-dimethylbenzoato})](\text{ClO}_4)_3$ is comprised of two $[\text{Fe}_2(\text{TPA})_2\text{O}(3,5\text{-dimethylbenzoato})](\text{ClO}_4)_3$ and one H_2O . In each unit of $[\text{Fe}_2(\text{TPA})_2\text{O}(3,5\text{-dimethylbenzoato})](\text{ClO}_4)_3$, O1 is the bridging oxygen for Fe1-

O1-Fe2 unit in the diiron complex. **Figure 66** shows the 3,5-dimethyl benzoate numbering scheme. C1 is bonded to O2 and O3. O2 and O3 coordinate to the Fe1 and Fe2, respectively. C8 and C9 are bonded to C4 and C6, respectively. Two perchlorates are disordered and modeled with two sets of oxygens. The Cl2 perchlorate is disordered about the Cl2-O24 axis and modeled with occupancies of 0.38 and 0.62. The Cl3 perchlorate is disordered about the Cl3-O33 axis and modeled with occupancies of 0.46 and 0.54.

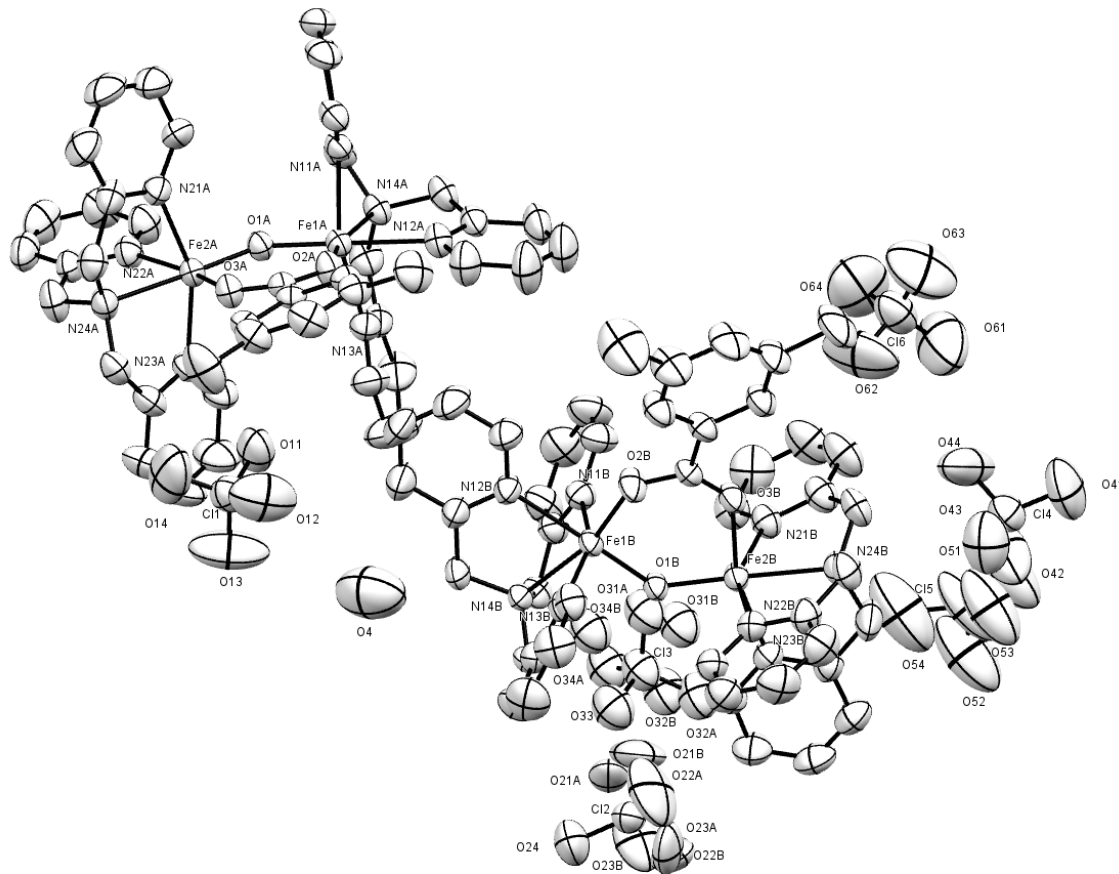


Figure 64. A view of the asymmetric unit of $[Fe(TPA)_2O(3,5\text{-dimethylbenzoato})](ClO_4)_3 \bullet 0.5H_2O$.

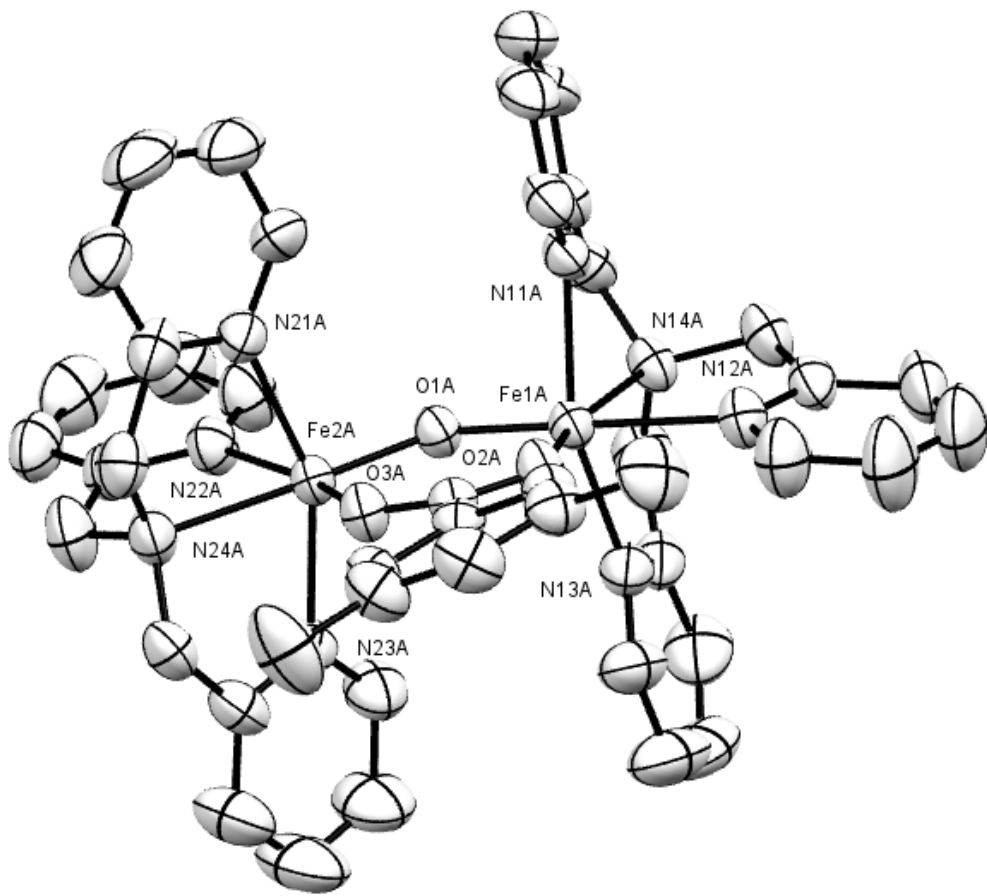


Figure 65. A view of the cationic portion of $[Fe_2(TPA)_2O(3,5\text{-dimethylbenzoato})](ClO_4)_3 \bullet 0.5H_2O$. Hydrogen atoms are omitted.

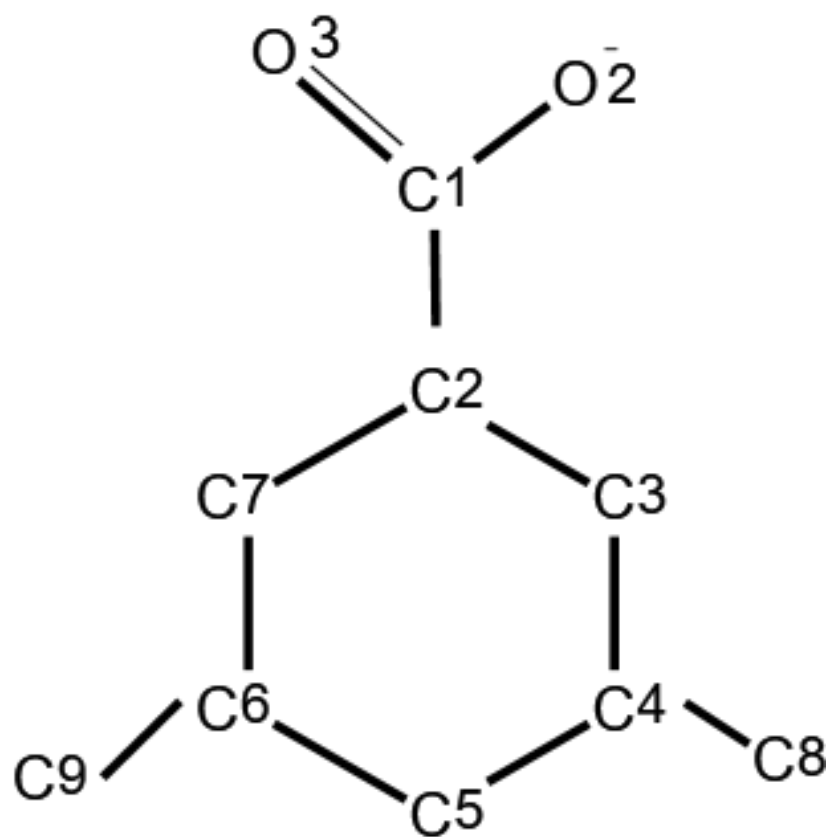


Figure 66. Numbering scheme for 3,5-dimethylbenzoate.

Table 45. Crystallographic data for $[Fe(TPA)_2O(3,5\text{-dimethylbenzoato})](ClO_4)_3 \cdot 0.5H_2O$

Crystallographic data	
Empirical formula	C ₉₀ H ₉₃ Cl ₆ Fe ₄ N ₁₆ O ₃₁
Formula weight	2330.90
Temperature/K	298
Crystal system	triclinic
Space group	P-1
a/Å	13.3609(6)
b/Å	19.0514(8)
c/Å	22.0575(9)
α/°	89.662(3)
β/°	74.095(4)
γ/°	84.089(4)
Volume/Å ³	5369.5(4)
Z	2
ρ _{calc} /g cm ⁻³	1.442
μ/mm ⁻¹	0.761
F(000)	2398
Crystal size/mm ³	4.5 × 2.4 × 1.2
Radiation	MoKα ($\lambda = 0.71073$)
2θ range for data collection/°	5.612 to 50.5

 Crystallographic data

Index ranges	-16 ≤ h ≤ 15, -22 ≤ k ≤ 21, -26 ≤ l ≤ 26
Reflections collected	31311
Independent reflections	19409 [R _{int} = 0.0276, R _{sigma} = 0.0527]
Data/restraints/parameters	19409/3/1334
Goodness-of-fit on F ²	1.053
Final R indexes [I≥2σ (I)]	R ₁ = 0.0728, wR ₂ = 0.2136
Final R indexes [all data]	R ₁ = 0.1037, wR ₂ = 0.2582
Largest diff. peak/hole / e Å ⁻³	1.82/-0.70

Table 46. Fractional atomic coordinates ($\times 10^4$) and equivalent isotropic displacement parameters ($\text{\AA}^2 \times 10^3$) for [Fe(TPA)₂O(3,5-dimethylbenzoato)](ClO₄)₃•0.5H₂O.

Atom	x	y	z	U(eq)
Fe1A	10820.3(4)	7791.3(3)	1826.5(2)	38.23(14)
Fe2A	10097.3(4)	7524.9(3)	553.1(2)	38.75(14)
Fe1B	6114.3(4)	7154.3(3)	5484.1(2)	38.09(14)
Fe2B	6092.9(4)	6952.3(3)	6961.9(2)	39.43(14)
Cl1	5679.1(11)	7447.2(8)	1939.9(7)	76.3(4)
Cl2	2664.8(9)	5412.0(6)	6821.1(5)	62.7(3)
Cl3	7349.7(11)	4165.9(7)	6004.5(7)	74.3(4)
Cl4	8084(2)	5436.4(13)	8987.5(16)	159.8(11)
Cl5	6155.4(11)	8628.5(7)	9483.4(6)	73.6(3)
Cl6	9857.3(12)	8754.3(10)	7516.5(8)	95.1(5)
O4	4055(6)	7436(5)	3720(5)	193(3)
O11	6725(3)	7414(3)	1965.6(19)	95.0(12)

Atom	x	y	z	U(eq)
O12	5044(4)	7982(3)	2359(3)	146(2)
O13	5271(5)	6833(3)	2091(4)	175(3)
O14	5681(4)	7631(4)	1325(3)	158(2)
O24	2080(3)	5325(3)	6394.4(17)	105.8(14)
O33	6323(3)	4286(3)	5947(2)	104.1(13)
O41	9013(9)	5452(5)	9043(9)	393(8)
O42	7893(9)	4788(5)	9105(7)	281(5)
O43	7869(10)	5426(6)	8385(6)	288(5)
O44	7445(7)	5986(4)	9287(4)	202(3)
O51	6428(5)	8957(3)	9975(2)	140(2)
O52	6203(6)	7909(3)	9527(3)	161(3)
O53	5158(4)	8881(3)	9481(3)	136(2)
O54	6818(5)	8773(3)	8911(3)	174(3)
O61	9994(7)	9412(3)	7675(4)	206(3)
O62	9979(7)	8250(4)	8002(4)	204(4)
O63	8916(4)	8716(4)	7385(4)	192(3)
O64	10625(5)	8500(4)	6992(3)	189(3)
O1A	10960.8(19)	7442.0(13)	1043.6(11)	41.1(6)
O2A	9482(2)	8403.1(14)	1970.5(12)	49.3(7)
O3A	8946(2)	8224.8(14)	1115.6(12)	45.6(6)
O21A	3662(4)	5255(9)	6406(4)	87(5)
O22A	2381(14)	6109(4)	7044(8)	180(6)
O23A	2586(11)	4955(7)	7326(5)	166(7)
O31A	7735(13)	4788(7)	5946(11)	136(6)
O32A	7231(12)	3893(7)	6612(5)	140(4)
O34A	7962(11)	3622(8)	5595(7)	120(4)

Atom	x	y	z	U(eq)
O1B	5972(2)	6692.7(12)	6210.6(11)	39.8(6)
O2B	6250(3)	8112.8(13)	5772.4(13)	56.8(8)
O3B	6471(2)	7962.0(13)	6732.7(12)	49.1(7)
O21B	3536(8)	5794(8)	6669(7)	144(5)
O22B	1890(7)	5628(11)	7373(4)	102(6)
O23B	3069(16)	4716(3)	6879(10)	132(7)
O31B	7628(17)	4766(10)	6261(10)	184(7)
O32B	7739(12)	3628(10)	6235(13)	177(6)
O34B	8019(8)	4154(9)	5349(5)	128(4)
N11A	11895(2)	8545.9(16)	1501.2(15)	42.5(7)
N12A	10779(3)	8110.3(18)	2799.3(15)	49.9(8)
N13A	10342(3)	6859.5(18)	2292.7(16)	50.8(8)
N14A	12298(3)	7265.0(16)	1924.3(15)	44.3(7)
N21A	10581(3)	8427.7(17)	-1.5(15)	48.2(8)
N22A	11075(3)	6926.3(18)	-244.0(15)	50.7(8)
N23A	9179(3)	6677.3(17)	799.3(16)	50.5(8)
N24A	9085(3)	7604.9(18)	-102.3(15)	50.3(8)
N11B	7682(3)	6672.4(17)	5072.1(15)	48.2(8)
N12B	6419(3)	7605.6(16)	4535.7(14)	46.8(8)
N13B	4482(3)	7327.0(16)	5546.4(14)	43.6(7)
N14B	5867(3)	6279.8(15)	4923.4(13)	40.4(7)
N21B	7689(3)	6676.0(18)	6924.6(16)	52.1(8)
N22B	5695(3)	6026.8(17)	7462.3(15)	47.3(8)
N23B	4539(3)	7412.1(17)	7424.4(15)	48.3(8)
N24B	6197(3)	7268.7(18)	7914.3(15)	52.7(9)
C1A	8847(3)	8529.5(18)	1632.2(16)	37.1(8)

Atom	x	y	z	U(eq)
C2A	7954(3)	9078.9(17)	1875.1(17)	37.0(8)
C3A	7930(3)	9527.1(19)	2374.3(18)	43.4(9)
C4A	7087(3)	10034(2)	2610(2)	53.5(11)
C5A	6277(4)	10082(2)	2324(2)	64.3(12)
C6A	6290(3)	9650(2)	1819(2)	59.0(11)
C7A	7130(3)	9149(2)	1600.8(19)	46.3(9)
C8A	7045(5)	10510(3)	3157(3)	79.8(15)
C9A	5395(5)	9712(4)	1526(3)	100(2)
C1B	6384(3)	8346.3(19)	6281.0(17)	40.3(8)
C2B	6429(3)	9113(2)	6333.9(19)	46.1(9)
C3B	6095(4)	9570(2)	5922(2)	59.8(12)
C4B	6129(5)	10288(2)	5968(3)	77.6(15)
C5B	6507(5)	10541(3)	6435(3)	81.1(16)
C6B	6876(4)	10099(2)	6847(2)	67.2(13)
C7B	6815(4)	9383(2)	6799(2)	54.6(11)
C8B	5774(8)	10779(3)	5516(4)	140(3)
C9B	7342(6)	10390(3)	7337(3)	107(2)
C111	11658(4)	9239(2)	1438(2)	53.4(10)
C112	12387(4)	9664(2)	1120(2)	65.5(13)
C113	13401(4)	9362(3)	865(2)	68.1(13)
C114	13664(4)	8656(3)	950(2)	61.7(12)
C115	12890(3)	8258(2)	1268.5(18)	47.0(9)
C116	13092(3)	7479(2)	1354(2)	51.6(10)
C121	9958(4)	8455(3)	3221(2)	73.0(14)
C122	9940(6)	8553(4)	3840(3)	98(2)
C123	10784(6)	8294(4)	4031(3)	95.1(19)

Atom	x	y	z	U(eq)
C124	11634(5)	7938(3)	3610(2)	72.1(14)
C125	11611(4)	7855(2)	2990.8(19)	49.6(10)
C126	12536(4)	7499(2)	2509(2)	57.0(11)
C131	9341(4)	6748(3)	2582(2)	66.7(13)
C132	9091(5)	6133(3)	2872(3)	88.6(18)
C133	9871(6)	5621(3)	2875(3)	89.9(18)
C134	10897(5)	5722(2)	2595(3)	76.4(15)
C135	11119(4)	6353(2)	2294.1(19)	54.2(11)
C136	12195(4)	6504(2)	1919(2)	56.1(11)
C211	11462(4)	8717(2)	-27(2)	60.0(12)
C212	11751(5)	9283(3)	-395(2)	78.6(16)
C213	11134(5)	9543(3)	-759(3)	89.8(19)
C214	10239(5)	9245(3)	-744(2)	78.6(15)
C215	9963(4)	8688(2)	-350.8(19)	55.8(11)
C216	8964(4)	8359(2)	-271(2)	61.3(12)
C221	12050(4)	6655(3)	-280(2)	66.7(13)
C222	12688(4)	6313(3)	-824(3)	79.5(15)
C223	12303(5)	6235(3)	-1321(3)	82.7(17)
C224	11301(5)	6507(3)	-1291(2)	68.7(14)
C225	10700(4)	6854(2)	-737.9(19)	52.9(10)
C226	9567(4)	7139(3)	-669(2)	70.6(14)
C231	9432(4)	6121(2)	1121(2)	65.7(13)
C232	8777(5)	5590(3)	1296(3)	93.3(19)
C233	7857(6)	5656(3)	1123(4)	110(2)
C234	7617(5)	6213(3)	782(3)	86.7(17)
C235	8285(4)	6725(2)	621(2)	56.9(11)

Atom	x	y	z	U(eq)
C236	8079(3)	7359(2)	259(2)	57.0(11)
C311	8570(4)	6966(3)	5018(2)	65.9(13)
C312	9539(4)	6603(3)	4745(3)	83.2(16)
C313	9584(4)	5925(3)	4534(3)	86.1(17)
C314	8672(4)	5633(3)	4580(3)	73.0(14)
C315	7733(3)	6012(2)	4855.8(19)	48.5(10)
C316	6701(3)	5719(2)	4952.6(19)	48.7(10)
C321	6780(4)	8230(2)	4372(2)	63.2(12)
C322	7000(5)	8457(3)	3761(2)	81.2(17)
C323	6869(5)	8035(3)	3311(2)	89.0(19)
C324	6544(5)	7381(3)	3465(2)	75.1(15)
C325	6311(4)	7181(2)	4084.6(18)	52.6(10)
C326	5907(4)	6488(2)	4266.0(18)	56.6(11)
C331	3856(4)	7926(2)	5721(2)	58.3(11)
C332	2808(4)	7975(3)	5794(3)	77.7(15)
C333	2378(4)	7383(4)	5681(3)	87.7(17)
C334	3004(4)	6762(3)	5497(3)	71.0(13)
C335	4061(3)	6749(2)	5430.2(18)	49.4(10)
C336	4812(3)	6090(2)	5260.7(19)	48.3(10)
C411	8369(4)	6250(2)	6471(2)	64.1(12)
C412	9417(5)	6127(3)	6443(3)	88.4(18)
C413	9767(5)	6444(4)	6895(4)	98(2)
C414	9083(5)	6866(3)	7355(3)	89.6(18)
C415	8047(4)	6977(2)	7363(2)	59.6(11)
C416	7272(4)	7459(3)	7838(2)	63.1(12)
C421	5424(4)	5462(2)	7207(2)	57.2(11)

Atom	x	y	z	U(eq)
C422	5146(4)	4877(3)	7547(3)	73.2(14)
C423	5126(4)	4876(3)	8174(3)	72.8(14)
C424	5397(4)	5451(3)	8440(2)	66.1(13)
C425	5671(3)	6029(2)	8075.4(19)	51.4(10)
C426	5963(5)	6663(3)	8349(2)	81.6(17)
C431	3696(3)	7339(2)	7225(2)	53.8(10)
C432	2727(4)	7651(3)	7532(2)	69.8(13)
C433	2611(4)	8047(3)	8065(3)	82.2(16)
C434	3463(4)	8120(3)	8288(2)	77.8(15)
C435	4432(4)	7797(2)	7953(2)	57.1(11)
C436	5407(4)	7880(3)	8134(2)	63.9(12)

Table 47. Anisotropic displacement parameters ($\text{\AA}^2 \times 10^3$) for $[\text{Fe}(\text{TPA})_2\text{O}(3,5\text{-dimethylbenzoato})](\text{ClO}_4)_3 \bullet 0.5\text{H}_2\text{O}$.

Atom	U₁₁	U₂₂	U₃₃	U₂₃	U₁₃	U₁₂
Fe1A	40.2(3)	38.4(3)	39.6(3)	0.2(2)	-16.6(2)	-4.9(2)
Fe2A	41.8(3)	41.7(3)	35.2(3)	-2.0(2)	-13.8(2)	-6.7(2)
Fe1B	51.9(3)	31.6(3)	34.0(3)	-2.48(19)	-15.1(2)	-9.9(2)
Fe2B	49.2(3)	36.8(3)	36.3(3)	-0.3(2)	-17.7(2)	-6.7(2)
Cl1	65.6(8)	84.9(9)	82.2(9)	11.2(7)	-25.1(7)	-12.4(7)
Cl2	58.8(7)	72.7(8)	56.0(6)	-5.5(5)	-9.2(5)	-21.6(6)
Cl3	78.3(9)	65.0(8)	87.6(9)	3.3(6)	-38.8(8)	-1.1(6)
Cl4	149(2)	106.2(16)	257(3)	-87.5(18)	-128(2)	41.0(14)
Cl5	78.2(9)	70.4(8)	75.3(8)	-7.9(6)	-25.1(7)	-10.7(7)
Cl6	67.6(9)	111.5(13)	107.6(12)	-25.5(10)	-26.0(9)	-8.9(8)
O4	136(6)	193(7)	266(10)	45(7)	-73(6)	-38(5)
O11	69(2)	139(4)	82(3)	-2(2)	-30(2)	-10(2)

Atom	U₁₁	U₂₂	U₃₃	U₂₃	U₁₃	U₁₂
O12	87(3)	118(4)	203(6)	-36(4)	3(4)	8(3)
O13	129(5)	74(3)	308(9)	29(4)	-26(5)	-36(3)
O14	113(4)	267(8)	112(4)	37(4)	-62(3)	-11(4)
O24	119(4)	135(4)	78(3)	-15(2)	-42(3)	-34(3)
O33	78(2)	131(4)	115(3)	-4(3)	-42(2)	-15(2)
O41	232(7)	204(8)	830(30)	-170(12)	-326(12)	63(5)
O42	303(11)	130(5)	427(13)	-63(7)	-135(10)	-6(5)
O43	296(11)	281(10)	277(7)	-146(6)	-110(8)	111(9)
O44	254(7)	160(5)	222(6)	-84(5)	-154(6)	85(5)
O51	149(5)	169(5)	112(4)	-62(3)	-59(3)	8(4)
O52	257(7)	73(3)	203(6)	21(3)	-152(6)	-12(4)
O53	119(4)	165(5)	123(4)	-21(3)	-50(3)	42(4)
O54	188(6)	198(6)	111(4)	-61(4)	45(4)	-129(5)
O61	229(8)	115(5)	286(9)	-60(5)	-83(7)	-40(5)
O62	305(10)	176(6)	186(7)	66(5)	-146(7)	-60(6)
O63	90(4)	180(6)	338(10)	42(6)	-106(5)	-32(4)
O64	123(5)	250(8)	158(6)	-51(6)	14(4)	7(5)
O1A	39.4(14)	46.7(15)	40.0(13)	-2.3(11)	-15.5(11)	-3.7(11)
O2A	48.5(16)	54.0(17)	48.4(15)	-8.1(12)	-21.9(13)	5.3(13)
O3A	46.1(15)	49.9(16)	43.1(14)	-6.5(12)	-18.0(12)	1.5(12)
O21A	42(5)	144(13)	72(7)	2(7)	-3(5)	-35(6)
O22A	273(18)	122(9)	177(13)	-67(9)	-115(13)	-19(10)
O23A	201(14)	235(15)	112(8)	112(9)	-83(9)	-153(12)
O31A	106(8)	58(5)	267(18)	41(6)	-86(9)	-22(5)
O32A	146(9)	163(10)	97(5)	45(5)	-31(5)	36(7)
O34A	127(7)	111(7)	124(6)	-28(7)	-55(6)	27(6)

Atom	U₁₁	U₂₂	U₃₃	U₂₃	U₁₃	U₁₂
O1B	55.0(16)	32.9(13)	36.4(13)	0.5(10)	-19.0(12)	-9.5(11)
O2B	96(2)	33.7(15)	50.4(16)	-2.1(12)	-33.6(16)	-15.1(14)
O3B	68.5(19)	38.8(15)	50.3(16)	1.4(12)	-30.3(14)	-14.7(13)
O21B	121(8)	162(11)	174(11)	65(9)	-54(7)	-102(8)
O22B	92(9)	164(16)	43(6)	-24(7)	-9(5)	1(9)
O23B	187(17)	66(8)	160(15)	-33(9)	-92(14)	31(9)
O31B	185(12)	150(8)	249(14)	-100(10)	-104(11)	-37(8)
O32B	125(9)	138(7)	236(13)	105(11)	-17(9)	34(7)
O34B	85(4)	194(12)	111(6)	1(5)	-34(4)	-31(6)
N11A	43.6(18)	42.2(19)	47.5(18)	1.3(14)	-20.7(15)	-8.6(14)
N12A	56(2)	51(2)	45.9(18)	-3.6(15)	-20.4(17)	-3.2(16)
N13A	61(2)	46(2)	49.3(19)	3.6(15)	-18.1(17)	-12.8(17)
N14A	46.5(19)	41.6(18)	50.4(18)	-1.4(14)	-23.5(16)	-2.6(14)
N21A	58(2)	49(2)	40.9(17)	4.8(14)	-16.1(16)	-10.4(16)
N22A	55(2)	52(2)	45.0(19)	-8.3(15)	-14.1(16)	-4.7(17)
N23A	59(2)	43.7(19)	53(2)	0.1(15)	-20.5(17)	-12.5(16)
N24A	51(2)	60(2)	43.9(18)	-4.2(15)	-19.6(16)	-6.4(17)
N11B	51(2)	44.6(19)	48.0(18)	-1.0(14)	-11.0(16)	-9.4(15)
N12B	64(2)	41.2(18)	37.6(17)	6.0(13)	-15.7(16)	-12.2(16)
N13B	56(2)	36.9(18)	39.4(16)	0.0(13)	-16.9(15)	-3.2(15)
N14B	53.1(19)	35.7(17)	33.8(15)	-1.7(12)	-11.6(14)	-12.5(14)
N21B	55(2)	51(2)	56(2)	0.6(16)	-24.9(18)	-1.8(17)
N22B	52(2)	46.5(19)	45.5(18)	6.2(14)	-16.2(16)	-6.2(15)
N23B	51(2)	51(2)	43.0(18)	-1.3(14)	-13.0(16)	-7.2(16)
N24B	70(2)	54(2)	42.0(18)	0.5(15)	-24.9(17)	-13.1(18)
C1A	37(2)	36.2(19)	37.3(19)	3.7(15)	-8.6(16)	-6.4(15)

Atom	U₁₁	U₂₂	U₃₃	U₂₃	U₁₃	U₁₂
C2A	37.7(19)	28.5(18)	44(2)	3.4(14)	-8.9(16)	-5.9(15)
C3A	44(2)	40(2)	46(2)	2.8(16)	-10.6(18)	-8.4(17)
C4A	57(3)	42(2)	58(3)	-4.5(18)	-10(2)	-4.4(19)
C5A	51(3)	51(3)	86(3)	-10(2)	-16(3)	9(2)
C6A	47(2)	54(3)	79(3)	-4(2)	-24(2)	3(2)
C7A	45(2)	41(2)	56(2)	1.2(17)	-17.9(19)	-6.4(17)
C8A	92(4)	64(3)	78(3)	-25(3)	-17(3)	-1(3)
C9A	68(4)	112(5)	133(5)	-28(4)	-58(4)	23(3)
C1B	44(2)	36(2)	43(2)	-5.6(16)	-15.7(17)	-7.1(16)
C2B	51(2)	36(2)	55(2)	-4.9(17)	-21(2)	-7.5(17)
C3B	78(3)	41(2)	71(3)	-2(2)	-38(3)	-6(2)
C4B	104(4)	41(3)	102(4)	8(2)	-53(4)	-5(3)
C5B	115(5)	36(3)	105(4)	-4(2)	-46(4)	-18(3)
C6B	98(4)	46(3)	69(3)	-9(2)	-36(3)	-26(3)
C7B	72(3)	43(2)	58(3)	-1.6(18)	-30(2)	-14(2)
C8B	219(10)	57(4)	187(8)	27(4)	-133(8)	-6(5)
C9B	161(7)	74(4)	112(5)	-17(3)	-70(5)	-44(4)
C111	59(3)	48(3)	62(3)	-1.3(19)	-30(2)	-11(2)
C112	82(4)	48(3)	81(3)	13(2)	-41(3)	-26(2)
C113	68(3)	76(3)	71(3)	22(3)	-28(3)	-37(3)
C114	49(3)	75(3)	67(3)	8(2)	-19(2)	-24(2)
C115	46(2)	56(3)	46(2)	2.0(18)	-23.5(19)	-11.0(19)
C116	38(2)	58(3)	60(3)	-1.6(19)	-15(2)	-6.0(19)
C121	73(3)	88(4)	56(3)	-15(2)	-22(3)	12(3)
C122	105(5)	132(6)	55(3)	-32(3)	-27(3)	13(4)
C123	113(5)	126(5)	53(3)	-16(3)	-36(3)	-6(4)

Atom	U₁₁	U₂₂	U₃₃	U₂₃	U₁₃	U₁₂
C124	91(4)	82(4)	59(3)	1(2)	-44(3)	-11(3)
C125	63(3)	45(2)	50(2)	2.1(17)	-26(2)	-13(2)
C126	61(3)	58(3)	63(3)	-2(2)	-36(2)	-4(2)
C131	63(3)	64(3)	69(3)	7(2)	-7(2)	-20(2)
C132	95(4)	73(4)	87(4)	13(3)	3(3)	-34(3)
C133	122(5)	58(3)	83(4)	20(3)	-10(4)	-30(4)
C134	109(5)	43(3)	83(4)	11(2)	-34(3)	-9(3)
C135	80(3)	39(2)	51(2)	2.9(17)	-27(2)	-12(2)
C136	66(3)	40(2)	65(3)	-0.7(19)	-24(2)	1(2)
C211	63(3)	69(3)	47(2)	3(2)	-8(2)	-23(2)
C212	100(4)	70(3)	66(3)	7(3)	-11(3)	-39(3)
C213	121(5)	71(4)	74(4)	31(3)	-12(4)	-35(4)
C214	102(4)	74(4)	65(3)	26(3)	-30(3)	-12(3)
C215	69(3)	53(3)	44(2)	2.3(18)	-16(2)	-2(2)
C216	67(3)	69(3)	55(3)	13(2)	-28(2)	-4(2)
C221	61(3)	76(3)	60(3)	-18(2)	-16(2)	3(2)
C222	65(3)	84(4)	77(4)	-22(3)	-4(3)	8(3)
C223	95(4)	76(4)	61(3)	-24(3)	0(3)	5(3)
C224	95(4)	67(3)	43(2)	-9(2)	-16(3)	-10(3)
C225	67(3)	49(2)	42(2)	-5.5(17)	-13(2)	-11(2)
C226	80(4)	83(4)	54(3)	-18(2)	-30(3)	-3(3)
C231	81(3)	49(3)	75(3)	6(2)	-31(3)	-16(2)
C232	108(5)	58(3)	127(5)	24(3)	-46(4)	-32(3)
C233	105(5)	79(4)	165(7)	25(4)	-52(5)	-51(4)
C234	71(4)	75(4)	126(5)	6(3)	-39(4)	-30(3)
C235	52(3)	57(3)	68(3)	-8(2)	-22(2)	-15(2)

Atom	U₁₁	U₂₂	U₃₃	U₂₃	U₁₃	U₁₂
C236	51(3)	65(3)	63(3)	-4(2)	-27(2)	-9(2)
C311	63(3)	59(3)	77(3)	-3(2)	-14(3)	-21(2)
C312	47(3)	100(5)	100(4)	2(3)	-13(3)	-19(3)
C313	54(3)	97(5)	95(4)	-17(3)	-5(3)	4(3)
C314	58(3)	74(3)	83(3)	-26(3)	-14(3)	-3(3)
C315	50(2)	47(2)	48(2)	-5.5(17)	-12.4(19)	-7.1(19)
C316	58(3)	37(2)	50(2)	-9.8(16)	-13(2)	-2.8(18)
C321	85(3)	52(3)	55(3)	8(2)	-19(2)	-20(2)
C322	118(5)	64(3)	61(3)	22(2)	-15(3)	-33(3)
C323	129(5)	94(4)	45(3)	25(3)	-18(3)	-41(4)
C324	106(4)	76(3)	44(2)	5(2)	-19(3)	-24(3)
C325	67(3)	53(3)	39(2)	3.2(17)	-14(2)	-14(2)
C326	83(3)	57(3)	37(2)	-4.1(17)	-22(2)	-22(2)
C331	67(3)	54(3)	58(3)	-1(2)	-26(2)	2(2)
C332	69(3)	72(4)	88(4)	-5(3)	-23(3)	13(3)
C333	51(3)	106(5)	106(5)	2(4)	-28(3)	6(3)
C334	54(3)	80(4)	86(4)	0(3)	-27(3)	-18(3)
C335	54(3)	54(3)	42(2)	3.2(17)	-16.2(19)	-11(2)
C336	54(2)	44(2)	51(2)	-0.7(17)	-17(2)	-18.2(19)
C411	66(3)	56(3)	72(3)	-3(2)	-28(3)	7(2)
C412	76(4)	81(4)	101(4)	-10(3)	-25(3)	25(3)
C413	62(4)	107(5)	137(6)	-8(4)	-53(4)	9(3)
C414	76(4)	96(4)	113(5)	-12(4)	-57(4)	1(3)
C415	65(3)	52(3)	72(3)	1(2)	-36(3)	-5(2)
C416	69(3)	67(3)	67(3)	-9(2)	-40(3)	-8(2)
C421	72(3)	45(2)	59(3)	1.3(19)	-24(2)	-13(2)

Atom	U₁₁	U₂₂	U₃₃	U₂₃	U₁₃	U₁₂
C422	91(4)	51(3)	81(4)	9(2)	-22(3)	-25(3)
C423	76(3)	60(3)	80(4)	27(3)	-13(3)	-17(3)
C424	64(3)	72(3)	59(3)	23(2)	-12(2)	-3(2)
C425	53(3)	55(3)	47(2)	9.6(18)	-17(2)	-5(2)
C426	135(5)	77(4)	47(3)	13(2)	-42(3)	-32(3)
C431	52(3)	61(3)	52(2)	6.6(19)	-18(2)	-9(2)
C432	54(3)	82(4)	73(3)	8(3)	-19(3)	-5(3)
C433	57(3)	90(4)	87(4)	-9(3)	-3(3)	6(3)
C434	75(4)	83(4)	64(3)	-21(3)	-3(3)	4(3)
C435	62(3)	60(3)	46(2)	-9.5(19)	-10(2)	-3(2)
C436	78(3)	64(3)	50(2)	-20(2)	-19(2)	-5(2)

Table 48. Bond lengths for [Fe(TPA)₂O(3,5-dimethylbenzoato)](ClO₄)₃•0.5H₂O.

Atom	Atom	Length/Å	Atom	Atom	Length/Å
Fe1A	O1A	1.809(2)	N21B	C415	1.345(6)
Fe1A	O2A	1.980(3)	N22B	C421	1.344(5)
Fe1A	N11A	2.119(3)	N22B	C425	1.344(5)
Fe1A	N12A	2.218(3)	N23B	C431	1.337(5)
Fe1A	N13A	2.114(3)	N23B	C435	1.346(5)
Fe1A	N14A	2.186(3)	N24B	C416	1.483(6)
Fe2A	O1A	1.781(2)	N24B	C426	1.498(6)
Fe2A	O3A	2.058(3)	N24B	C436	1.477(6)
Fe2A	N21A	2.155(3)	C1A	C2A	1.485(5)
Fe2A	N22A	2.135(3)	C2A	C3A	1.389(5)
Fe2A	N23A	2.107(3)	C2A	C7A	1.390(5)
Fe2A	N24A	2.229(3)	C3A	C4A	1.390(6)
Fe1B	O1B	1.796(2)	C4A	C5A	1.388(6)

Atom	Atom	Length/Å
Fe1B	O2B	1.979(3)
Fe1B	N11B	2.151(3)
Fe1B	N12B	2.206(3)
Fe1B	N13B	2.139(3)
Fe1B	N14B	2.186(3)
Fe2B	O1B	1.786(2)
Fe2B	O3B	2.064(3)
Fe2B	N21B	2.122(4)
Fe2B	N22B	2.111(3)
Fe2B	N23B	2.143(3)
Fe2B	N24B	2.233(3)
Cl1	O11	1.410(4)
Cl1	O12	1.419(5)
Cl1	O13	1.344(5)
Cl1	O14	1.398(5)
Cl2	O24	1.398(3)
Cl2	O21A	1.398(3)
Cl2	O22A	1.398(3)
Cl2	O23A	1.397(3)
Cl2	O21B	1.398(3)
Cl2	O22B	1.398(3)
Cl2	O23B	1.398(3)
Cl3	O33	1.407(4)
Cl3	O31A	1.331(13)
Cl3	O32A	1.409(9)
Cl3	O34A	1.412(11)
Cl3	O31B	1.406(13)

Atom	Atom	Length/Å
C4A	C8A	1.500(6)
C5A	C6A	1.384(7)
C6A	C7A	1.375(6)
C6A	C9A	1.503(7)
C1B	C2B	1.474(5)
C2B	C3B	1.385(6)
C2B	C7B	1.391(6)
C3B	C4B	1.379(6)
C4B	C5B	1.374(7)
C4B	C8B	1.500(8)
C5B	C6B	1.390(7)
C6B	C7B	1.380(6)
C6B	C9B	1.520(7)
C111	C112	1.370(6)
C112	C113	1.383(7)
C113	C114	1.380(7)
C114	C115	1.377(6)
C115	C116	1.500(6)
C121	C122	1.371(7)
C122	C123	1.355(8)
C123	C124	1.372(8)
C124	C125	1.385(6)
C125	C126	1.494(6)
C131	C132	1.359(7)
C132	C133	1.354(8)
C133	C134	1.373(8)
C134	C135	1.388(6)

Atom	Atom	Length/Å
Cl3	O32B	1.268(12)
Cl3	O34B	1.476(10)
Cl4	O41	1.284(9)
Cl4	O42	1.298(10)
Cl4	O43	1.436(11)
Cl4	O44	1.333(6)
Cl5	O51	1.405(5)
Cl5	O52	1.371(5)
Cl5	O53	1.371(5)
Cl5	O54	1.374(5)
Cl6	O61	1.347(6)
Cl6	O62	1.465(6)
Cl6	O63	1.375(6)
Cl6	O64	1.372(6)
O2A	C1A	1.280(4)
O3A	C1A	1.250(4)
O2B	C1B	1.273(4)
O3B	C1B	1.257(4)
N11A	C111	1.341(5)
N11A	C115	1.346(5)
N12A	C121	1.341(6)
N12A	C125	1.340(5)
N13A	C131	1.352(6)
N13A	C135	1.344(6)
N14A	C116	1.491(5)
N14A	C126	1.491(5)
N14A	C136	1.470(5)

Atom	Atom	Length/Å
C135	C136	1.505(6)
C211	C212	1.370(6)
C212	C213	1.356(8)
C213	C214	1.368(8)
C214	C215	1.383(6)
C215	C216	1.499(7)
C221	C222	1.387(6)
C222	C223	1.348(8)
C223	C224	1.369(8)
C224	C225	1.390(6)
C225	C226	1.523(7)
C231	C232	1.390(7)
C232	C233	1.378(9)
C233	C234	1.359(9)
C234	C235	1.368(7)
C235	C236	1.487(6)
C311	C312	1.382(7)
C312	C313	1.365(8)
C313	C314	1.371(7)
C314	C315	1.365(6)
C315	C316	1.502(6)
C321	C322	1.374(6)
C322	C323	1.342(7)
C323	C324	1.373(7)
C324	C325	1.377(6)
C325	C326	1.488(6)
C331	C332	1.360(7)

Atom	Atom	Length/Å	Atom	Atom	Length/Å
N21A	C211	1.338(6)	C332	C333	1.371(8)
N21A	C215	1.334(5)	C333	C334	1.370(8)
N22A	C221	1.333(6)	C334	C335	1.376(6)
N22A	C225	1.331(5)	C335	C336	1.504(6)
N23A	C231	1.338(6)	C411	C412	1.380(7)
N23A	C235	1.351(5)	C412	C413	1.378(8)
N24A	C216	1.486(6)	C413	C414	1.365(9)
N24A	C226	1.489(5)	C414	C415	1.374(7)
N24A	C236	1.483(5)	C415	C416	1.496(7)
N11B	C311	1.340(6)	C421	C422	1.367(6)
N11B	C315	1.337(5)	C422	C423	1.376(7)
N12B	C321	1.341(5)	C423	C424	1.372(7)
N12B	C325	1.333(5)	C424	C425	1.380(6)
N13B	C331	1.335(5)	C425	C426	1.488(7)
N13B	C335	1.344(5)	C431	C432	1.362(6)
N14B	C316	1.478(5)	C432	C433	1.365(8)
N14B	C326	1.489(5)	C433	C434	1.378(8)
N14B	C336	1.483(5)	C434	C435	1.386(7)
N21B	C411	1.358(6)	C435	C436	1.487(7)

Table 49. Bond angles for [Fe(TPA)₂O(3,5-dimethylbenzoato)](ClO₄)₃•0.5H₂O.

Atom	Atom	Atom	Angle/°	Atom	Atom	Atom	Angle/°
O1A	Fe1A	O2A	100.72(11)	Fe1B	N13B	C331	126.7(3)
O1A	Fe1A	N11A	93.71(12)	Fe1B	N13B	C335	114.4(3)
O1A	Fe1A	N12A	173.17(12)	C331	N13B	C335	118.8(4)
O1A	Fe1A	N13A	95.03(12)	Fe1B	N14B	C316	104.4(2)
O1A	Fe1A	N14A	95.85(12)	Fe1B	N14B	C326	111.9(2)

Atom	Atom	Atom	Angle/[°]	Atom	Atom	Atom	Angle/[°]
O2A	Fe1A	N11A	100.12(12)	Fe1B	N14B	C336	104.4(2)
O2A	Fe1A	N12A	85.68(12)	C316	N14B	C326	112.8(3)
O2A	Fe1A	N13A	102.49(13)	C316	N14B	C336	112.1(3)
O2A	Fe1A	N14A	163.28(12)	C326	N14B	C336	110.7(3)
N11A	Fe1A	N12A	87.46(13)	Fe2B	N21B	C411	124.1(3)
N11A	Fe1A	N13A	153.75(13)	Fe2B	N21B	C415	116.9(3)
N11A	Fe1A	N14A	76.44(12)	C411	N21B	C415	118.9(4)
N12A	Fe1A	N13A	81.15(13)	Fe2B	N22B	C421	123.4(3)
N12A	Fe1A	N14A	77.86(12)	Fe2B	N22B	C425	117.0(3)
N13A	Fe1A	N14A	78.07(13)	C421	N22B	C425	119.5(4)
O1A	Fe2A	O3A	98.09(11)	Fe2B	N23B	C431	124.6(3)
O1A	Fe2A	N21A	102.62(12)	Fe2B	N23B	C435	116.0(3)
O1A	Fe2A	N22A	98.26(13)	C431	N23B	C435	119.3(4)
O1A	Fe2A	N23A	104.64(13)	Fe2B	N24B	C416	107.3(3)
O1A	Fe2A	N24A	177.02(12)	Fe2B	N24B	C426	108.9(3)
O3A	Fe2A	N21A	85.64(12)	Fe2B	N24B	C436	106.8(3)
O3A	Fe2A	N22A	162.47(12)	C416	N24B	C426	111.6(4)
O3A	Fe2A	N23A	92.10(12)	C416	N24B	C436	111.5(3)
O3A	Fe2A	N24A	84.76(11)	C426	N24B	C436	110.6(4)
N21A	Fe2A	N22A	84.65(13)	O2A	C1A	C2A	116.9(3)
N21A	Fe2A	N23A	152.70(14)	O3A	C1A	O2A	123.8(3)
N21A	Fe2A	N24A	76.66(13)	O3A	C1A	C2A	119.3(3)
N22A	Fe2A	N23A	89.87(13)	C1A	C2A	C3A	120.9(3)
N22A	Fe2A	N24A	78.81(13)	C1A	C2A	C7A	119.9(3)
N23A	Fe2A	N24A	76.04(13)	C3A	C2A	C7A	119.3(3)
O1B	Fe1B	O2B	99.93(11)	C2A	C3A	C4A	121.0(4)
O1B	Fe1B	N11B	93.79(12)	C3A	C4A	C5A	117.8(4)

Atom	Atom	Atom	Angle/[°]	Atom	Atom	Atom	Angle/[°]
O1B	Fe1B	N12B	172.90(12)	C3A	C4A	C8A	121.3(4)
O1B	Fe1B	N13B	96.37(12)	C5A	C4A	C8A	120.9(4)
O1B	Fe1B	N14B	97.04(11)	C4A	C5A	C6A	122.3(4)
O2B	Fe1B	N11B	106.27(13)	C5A	C6A	C7A	118.6(4)
O2B	Fe1B	N12B	85.36(12)	C5A	C6A	C9A	120.9(4)
O2B	Fe1B	N13B	96.54(13)	C7A	C6A	C9A	120.5(4)
O2B	Fe1B	N14B	162.30(11)	C2A	C7A	C6A	121.0(4)
N11B	Fe1B	N12B	80.10(13)	O2B	C1B	O3B	123.7(3)
N11B	Fe1B	N13B	153.00(12)	O2B	C1B	C2B	117.1(3)
N11B	Fe1B	N14B	77.43(12)	O3B	C1B	C2B	119.2(3)
N12B	Fe1B	N13B	87.67(12)	C1B	C2B	C3B	120.7(4)
N12B	Fe1B	N14B	78.18(11)	C1B	C2B	C7B	120.1(4)
N13B	Fe1B	N14B	76.53(12)	C3B	C2B	C7B	119.3(4)
O1B	Fe2B	O3B	97.45(10)	C2B	C3B	C4B	121.2(4)
O1B	Fe2B	N21B	105.40(13)	C3B	C4B	C5B	118.3(4)
O1B	Fe2B	N22B	99.28(12)	C3B	C4B	C8B	120.8(5)
O1B	Fe2B	N23B	102.24(13)	C5B	C4B	C8B	120.9(5)
O1B	Fe2B	N24B	178.33(13)	C4B	C5B	C6B	122.3(4)
O3B	Fe2B	N21B	87.44(13)	C5B	C6B	C7B	118.3(4)
O3B	Fe2B	N22B	163.15(12)	C5B	C6B	C9B	121.2(4)
O3B	Fe2B	N23B	87.50(12)	C7B	C6B	C9B	120.5(5)
O3B	Fe2B	N24B	83.50(11)	C2B	C7B	C6B	120.6(4)
N21B	Fe2B	N22B	89.99(13)	N11A	C111	C112	122.4(4)
N21B	Fe2B	N23B	152.31(13)	C111	C112	C113	118.1(4)
N21B	Fe2B	N24B	75.98(14)	C112	C113	C114	120.0(4)
N22B	Fe2B	N23B	87.07(13)	C113	C114	C115	118.8(5)
N22B	Fe2B	N24B	79.72(13)	N11A	C115	C114	121.3(4)

Atom	Atom	Atom	Angle/[°]	Atom	Atom	Atom	Angle/[°]
N23B	Fe2B	N24B	76.40(13)	N11A	C115	C116	116.3(3)
O11	Cl1	O12	110.6(3)	C114	C115	C116	122.4(4)
O11	Cl1	O13	112.2(4)	N14A	C116	C115	109.1(3)
O11	Cl1	O14	106.6(3)	N12A	C121	C122	122.4(5)
O12	Cl1	O13	108.2(4)	C121	C122	C123	118.8(6)
O12	Cl1	O14	108.1(4)	C122	C123	C124	120.0(5)
O13	Cl1	O14	111.0(5)	C123	C124	C125	118.8(5)
O24	Cl2	O21A	98.1(5)	N12A	C125	C124	121.4(4)
O24	Cl2	O22A	104.8(5)	N12A	C125	C126	117.8(3)
O24	Cl2	O23A	119.4(5)	C124	C125	C126	120.7(4)
O24	Cl2	O21B	121.6(5)	N14A	C126	C125	114.1(3)
O24	Cl2	O22B	102.4(5)	N13A	C131	C132	122.0(5)
O24	Cl2	O23B	101.4(7)	C131	C132	C133	118.7(6)
O21A	Cl2	O22A	117.1(12)	C132	C133	C134	120.7(5)
O21A	Cl2	O23A	107.3(9)	C133	C134	C135	118.8(5)
O22A	Cl2	O23A	110.2(8)	N13A	C135	C134	120.2(5)
O21B	Cl2	O22B	115.9(11)	N13A	C135	C136	115.5(3)
O21B	Cl2	O23B	104.9(11)	C134	C135	C136	124.2(5)
O22B	Cl2	O23B	109.5(10)	N14A	C136	C135	111.0(3)
O33	Cl3	O31A	106.9(7)	N21A	C211	C212	122.2(5)
O33	Cl3	O32A	104.6(6)	C211	C212	C213	118.5(5)
O33	Cl3	O34A	112.8(5)	C212	C213	C214	119.9(5)
O33	Cl3	O31B	110.7(9)	C213	C214	C215	119.5(5)
O33	Cl3	O32B	126.6(8)	N21A	C215	C214	120.3(5)
O33	Cl3	O34B	104.3(5)	N21A	C215	C216	116.3(4)
O31A	Cl3	O32A	112.3(11)	C214	C215	C216	123.3(4)
O31A	Cl3	O34A	115.5(10)	N24A	C216	C215	111.2(4)

Atom	Atom	Atom	Angle/[°]	Atom	Atom	Atom	Angle/[°]
O32A	Cl3	O34A	104.4(9)	N22A	C221	C222	121.6(5)
O31B	Cl3	O32B	107.5(16)	C221	C222	C223	119.2(5)
O31B	Cl3	O34B	101.9(10)	C222	C223	C224	120.0(5)
O32B	Cl3	O34B	102.8(14)	C223	C224	C225	118.4(5)
O41	Cl4	O42	104.0(8)	N22A	C225	C224	121.8(5)
O41	Cl4	O43	122.3(11)	N22A	C225	C226	117.6(4)
O41	Cl4	O44	111.2(6)	C224	C225	C226	120.6(4)
O42	Cl4	O43	93.9(7)	N24A	C226	C225	114.3(4)
O42	Cl4	O44	122.7(8)	N23A	C231	C232	121.4(5)
O43	Cl4	O44	103.1(5)	C231	C232	C233	117.4(5)
O51	Cl5	O52	113.2(4)	C232	C233	C234	120.9(5)
O51	Cl5	O53	109.8(3)	C233	C234	C235	119.6(6)
O51	Cl5	O54	110.4(4)	N23A	C235	C234	120.3(5)
O52	Cl5	O53	108.3(4)	N23A	C235	C236	116.2(4)
O52	Cl5	O54	107.1(4)	C234	C235	C236	123.5(5)
O53	Cl5	O54	107.8(4)	N24A	C236	C235	109.8(4)
O61	Cl6	O62	111.4(5)	N11B	C311	C312	121.6(5)
O61	Cl6	O63	113.0(5)	C311	C312	C313	118.7(5)
O61	Cl6	O64	111.3(5)	C312	C313	C314	119.3(5)
O62	Cl6	O63	110.4(5)	C313	C314	C315	119.8(5)
O62	Cl6	O64	103.4(5)	N11B	C315	C314	121.4(4)
O63	Cl6	O64	106.8(5)	N11B	C315	C316	115.5(3)
Fe1A	O1A	Fe2A	131.21(14)	C314	C315	C316	123.1(4)
Fe1A	O2A	C1A	132.2(2)	N14B	C316	C315	111.1(3)
Fe2A	O3A	C1A	133.5(2)	N12B	C321	C322	122.3(5)
Fe1B	O1B	Fe2B	131.97(14)	C321	C322	C323	119.0(5)
Fe1B	O2B	C1B	132.5(2)	C322	C323	C324	119.5(5)

Atom	Atom	Atom	Angle/[°]	Atom	Atom	Atom	Angle/[°]
Fe2B	O3B	C1B	131.9(2)	C323	C324	C325	119.4(5)
Fe1A	N11A	C111	126.6(3)	N12B	C325	C324	121.2(4)
Fe1A	N11A	C115	113.5(3)	N12B	C325	C326	118.6(3)
C111	N11A	C115	119.4(3)	C324	C325	C326	120.2(4)
Fe1A	N12A	C121	125.7(3)	N14B	C326	C325	114.8(3)
Fe1A	N12A	C125	115.2(3)	N13B	C331	C332	122.8(5)
C121	N12A	C125	118.6(4)	C331	C332	C333	118.4(5)
Fe1A	N13A	C131	125.3(3)	C332	C333	C334	120.0(5)
Fe1A	N13A	C135	115.3(3)	C333	C334	C335	118.8(5)
C131	N13A	C135	119.5(4)	N13B	C335	C334	121.3(4)
Fe1A	N14A	C116	103.8(2)	N13B	C335	C336	115.3(4)
Fe1A	N14A	C126	112.1(2)	C334	C335	C336	123.3(4)
Fe1A	N14A	C136	105.9(2)	N14B	C336	C335	109.6(3)
C116	N14A	C126	110.4(3)	N21B	C411	C412	121.8(5)
C116	N14A	C136	112.3(3)	C411	C412	C413	118.3(5)
C126	N14A	C136	112.0(3)	C412	C413	C414	120.0(5)
Fe2A	N21A	C211	124.0(3)	C413	C414	C415	119.7(6)
Fe2A	N21A	C215	116.4(3)	N21B	C415	C414	121.3(5)
C211	N21A	C215	119.6(4)	N21B	C415	C416	116.6(4)
Fe2A	N22A	C221	123.2(3)	C414	C415	C416	122.0(5)
Fe2A	N22A	C225	117.7(3)	N24B	C416	C415	110.4(4)
C221	N22A	C225	119.0(4)	N22B	C421	C422	122.1(4)
Fe2A	N23A	C231	123.6(3)	C421	C422	C423	118.5(5)
Fe2A	N23A	C235	116.1(3)	C422	C423	C424	119.8(4)
C231	N23A	C235	120.3(4)	C423	C424	C425	119.3(5)
Fe2A	N24A	C216	106.9(3)	N22B	C425	C424	120.8(4)
Fe2A	N24A	C226	110.3(3)	N22B	C425	C426	118.5(4)

Atom	Atom	Atom	Angle/[°]	Atom	Atom	Atom	Angle/[°]
Fe2A	N24A	C236	105.4(2)	C424	C425	C426	120.7(4)
C216	N24A	C226	111.8(4)	N24B	C426	C425	115.7(4)
C216	N24A	C236	112.3(3)	N23B	C431	C432	122.3(4)
C226	N24A	C236	109.9(4)	C431	C432	C433	118.9(5)
Fe1B	N11B	C311	126.7(3)	C432	C433	C434	120.1(5)
Fe1B	N11B	C315	114.1(3)	C433	C434	C435	118.5(5)
C311	N11B	C315	119.2(4)	N23B	C435	C434	120.9(5)
Fe1B	N12B	C321	125.9(3)	N23B	C435	C436	116.5(4)
Fe1B	N12B	C325	115.3(2)	C434	C435	C436	122.5(4)
C321	N12B	C325	118.5(3)	N24B	C436	C435	111.3(3)

Table 50. Hydrogen atom coordinates ($\text{\AA} \times 10^4$) and isotropic displacement parameters ($\text{\AA}^2 \times 10^3$) for $[\text{Fe}(\text{TPA})_2\text{O}(3,5\text{-dimethylbenzoato})](\text{ClO}_4)_3 \bullet 0.5\text{H}_2\text{O}$.

Atom	x	y	z	U(eq)
H111	10975.6	9437.86	1616.23	64
H112	12203.6	10142.6	1076.74	79
H113	13907.6	9635.04	635.56	82
H114	14350.5	8453.43	796.09	74
H121	9380.18	8634.03	3089.19	88
H122	9358.99	8792.27	4122.37	118
H123	10786.3	8357.55	4448.57	114
H124	12214.3	7756.67	3738.24	87
H131	8808.21	7103.04	2583.28	80
H132	8396.62	6065.65	3065.27	106
H133	9710.93	5195.98	3068.15	108
H134	11433.2	5374.6	2606.55	92
H211	11893	8527.04	213.08	72
H212	12356.2	9484.77	-396.35	94

Atom	x	y	z	U(eq)
H213	11320	9922.5	-1017.7	108
H214	9818.82	9416.97	-996.9	94
H221	12309.3	6696.47	66.91	80
H222	13373.1	6138.7	-844.61	95
H223	12717.7	5997.32	-1684.7	99
H224	11028.2	6461.22	-1632.4	82
H231	10060.4	6088.87	1229.55	79
H232	8952.85	5204.24	1521.39	112
H233	7393.7	5315.74	1241.23	133
H234	7002.39	6246.32	657.89	104
H311	8534.35	7426.46	5166.74	79
H312	10148.7	6815.87	4706.85	100
H313	10227.2	5664.59	4361.21	103
H314	8691.44	5177.85	4423.13	88
H321	6884.48	8520.06	4681.66	76
H322	7236.75	8897.48	3662.15	97
H323	6998.11	8184.57	2896.67	107
H324	6480.82	7074.82	3153.38	90
H331	4150.82	8327.42	5795.7	70
H332	2391.61	8399.74	5916.95	93
H333	1662.22	7401.71	5729.43	105
H334	2720.32	6357.85	5419.72	85
H411	8121.5	6035.58	6171.16	77
H412	9874.65	5837.2	6127.59	106
H413	10469.7	6370.18	6886.56	118
H414	9317.15	7077.36	7662.7	108
H421	5425.93	5469.84	6784.93	69

Atom	x	y	z	U(eq)
H422	4974.42	4487.81	7359.3	88
H423	4930.26	4485.85	8417.21	87
H424	5395.66	5451.52	8862.24	79
H431	3773.82	7065.57	6863.84	65
H432	2154.15	7595.63	7380.97	84
H433	1955.74	8267.62	8278.09	99
H434	3389.31	8381.12	8655.54	93
H3A	8486.67	9487.74	2553.82	52
H4A	4497.69	7092.17	3548.8	290
H5A	5705.59	10416.5	2477.87	77
H7A	7145.68	8852.31	1264.26	56
H11A	13047.4	7222.91	985.2	62
H12A	13070.6	7821.71	2394.62	68
H13A	12714.3	6253.52	2096.33	67
H21A	8413.45	8614.08	57.05	74
H22A	9532.32	7401.94	-1041.9	85
H23A	7681.87	7243.78	-27.77	68
H31A	6762.26	5360.29	4630.21	58
H32A	6345.43	6126.15	3978.12	68
H33A	4842.82	5839.76	5640.5	58
H41A	7436.68	7425.93	8239.46	76
H42A	6573.68	6523.62	8496.11	98
H43A	5690.95	8306.81	7951.76	77
H3B	5843.19	9389.9	5607.84	72
H4B	4294.89	7796.29	3527.14	290
H5B	6515.97	11025.9	6476.5	97
H7B	7034.56	9079.34	7079.7	66

Atom	x	y	z	U(eq)
H11B	13789.2	7367.69	1403.79	62
H12B	12821	7091.46	2696.02	68
H13B	12323.9	6335.99	1487.53	67
H21B	8760.47	8394.58	-660.96	74
H22B	9156.21	6744.05	-649.37	85
H23B	7669.78	7731.05	546.99	68
H31B	6516.37	5497.3	5359.87	58
H32B	5206.9	6504.3	4214.01	68
H33B	4571.28	5781.55	4994.19	58
H41B	7314.59	7943.03	7700.96	76
H42B	5395.48	6827.28	8714.62	98
H43B	5244.82	7929.41	8588.78	77
H8AA	6976.44	10993.1	3034.43	120
H9AA	5658.96	9758.55	1078.28	151
H8AB	7677.39	10414.1	3283.39	120
H9AB	4921.25	10120.3	1699.9	151
H8AC	6455.81	10427.6	3502.47	120
H9AC	5032.53	9297.47	1612.18	151
H8BA	6373.84	10914.6	5203.6	209
H9BA	7330.56	10053.2	7663.12	160
H8BB	5377.76	11192	5742.02	209
H9BB	6938.59	10822.6	7516.07	160
H8BC	5345.02	10545.2	5314.51	209
H9BC	8051.29	10479	7139.9	160

Table 51. Partial atomic occupancy for $[Fe(TPA)_2O(3,5\text{-dimethylbenzoato})](ClO_4)_3 \bullet 0.5H_2O$.

Atom	Occupancy	Atom	Occupancy	Atom	Occupancy
O21A	0.383(13)	O32A	0.538(11)	O23B	0.383(13)
O22A	0.617(13)	O34A	0.462(11)	O31B	0.538(11)
O23A	0.617(13)	O21B	0.617(13)	O32B	0.462(11)
O31A	0.462(11)	O22B	0.383(13)	O34B	0.538(11)

3.3.7 $[\{Fe(TPA)\}_2O(3,5\text{-dihydroxybenzoato})](ClO_4)_3 \bullet CH_3CN$

Figure 67 shows the asymmetric unit of $[\{Fe(TPA)\}_2O(3,5\text{-dihydroxybenzoato})](ClO_4)_3 \bullet CH_3CN$. The cationic portion of $[\{Fe(TPA)\}_2O(3,5\text{-dihydroxybenzoato})](ClO_4)_3 \bullet CH_3CN$ is shown in **Figure 68**. Crystallographic details for $[\{Fe(TPA)\}_2O(3,5\text{-dihydroxybenzoato})](ClO_4)_3 \bullet CH_3CN$ are listed in **Table 52**. Fractional atomic coordinates, anisotropic displacement parameters, bond lengths and bond angles involving the non-hydrogen atoms and hydrogen atom coordinates are listed in **Table 53**, **Table 54**, **Table 55**, **Table 56** and **Table 57**, respectively. **Table 58** lists the atom occupancies for the disordered perchlorate.

Crystals of $[\{Fe(TPA)\}_2O(3,5\text{-dihydroxybenzoato})](ClO_4)_3$ were obtained from two different synthetic procedures. The fact that these crystals are the same material is confirmed by identical cell constants (within experimental error). The best structure is reported here.

O1 is the bridging oxygen of the Fe1-O1-Fe2 unit in the diiron complex. **Figure 69** shows the 3,5-dihydroxybenzoate numbering scheme. C1 is bonded to O2 and O3. O2 and O3 coordinate to the Fe1 and Fe2, respectively. O4 and O5 are bonded to C4 and C6, respectively. One of the perchlorates is disordered and modeled with two orientations half occupied. O4 and O5 of the dihydroxybenzoate are hydrogen bonded to

two perchlorates O14 and O31, respectively. The other perchlorates are labeled C11, O11, O12, O13 and O14, and Cl3, O31, O32, O33 and O34, respectively. The acetonitrile is labeled N1, C8 and C9.

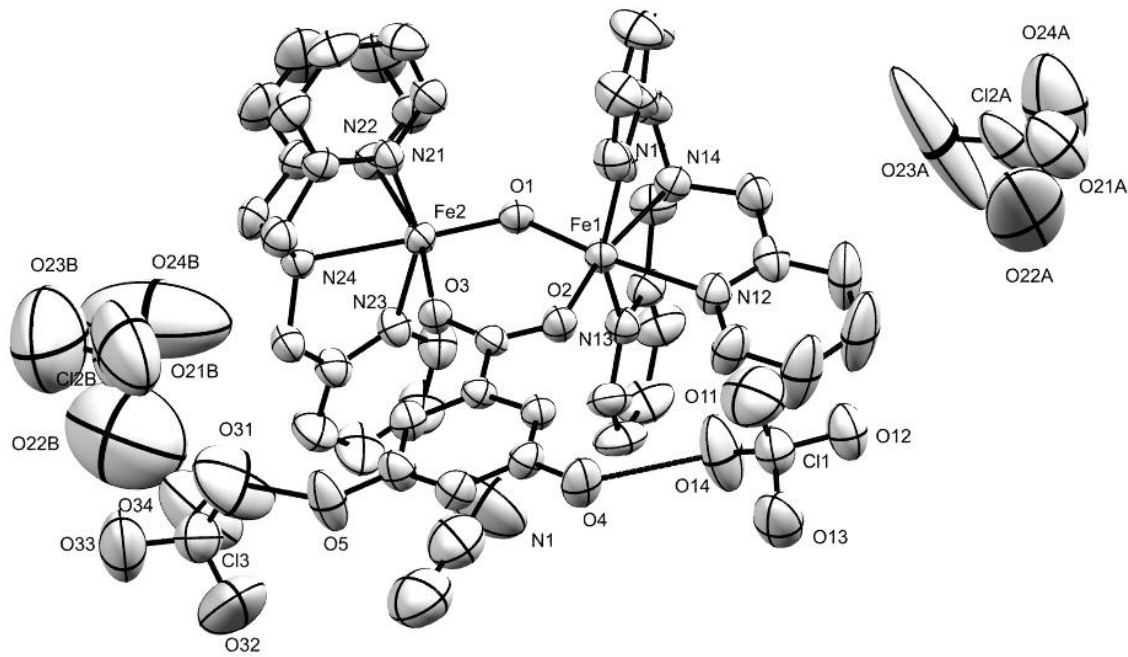


Figure 67. A view of the asymmetric unit of $[\{Fe(TPA)\}_2O(3,5\text{-dihydroxybenzoato})](ClO_4)_3 \bullet CH_3CN$.

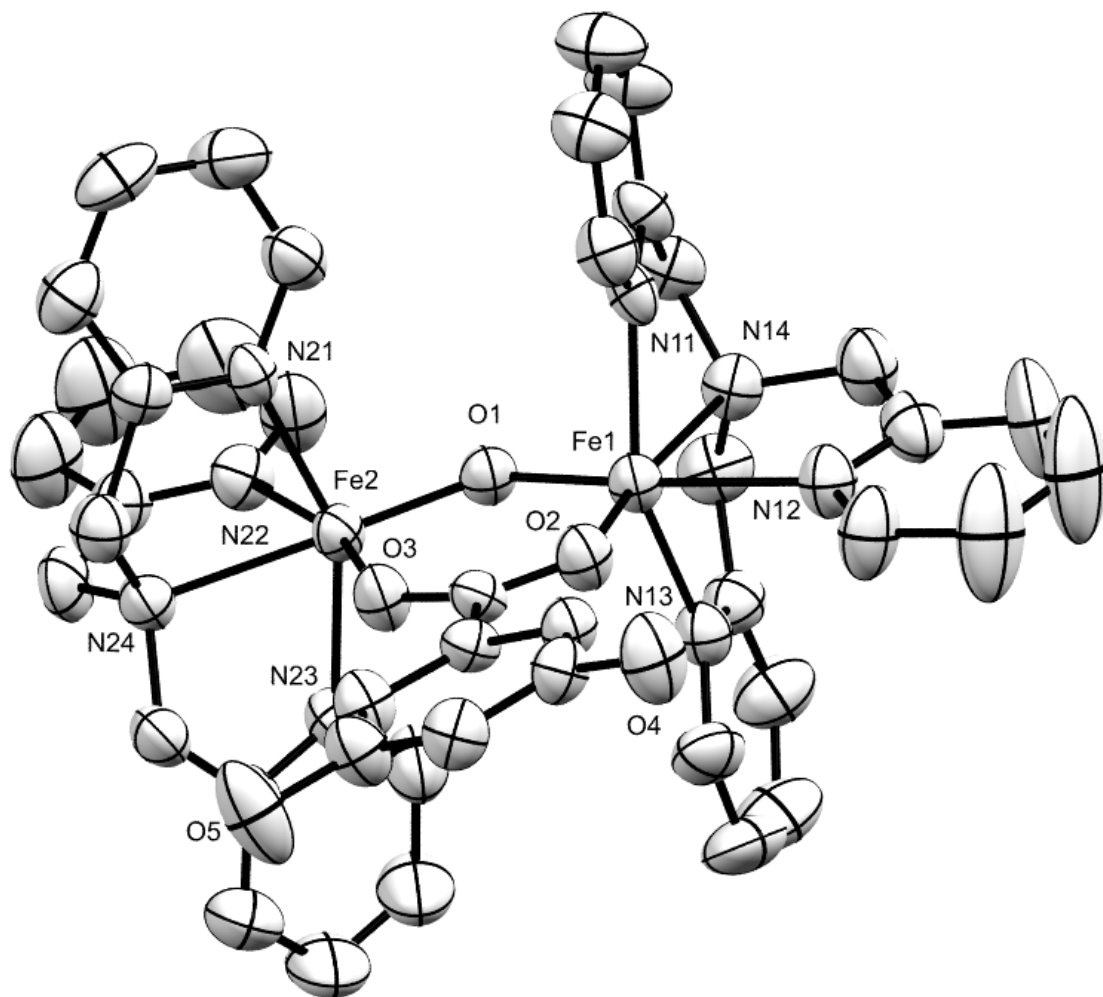


Figure 68. A view of the cationic portion of $\left[\{Fe(TPA)\}_2O(3,5\text{-dihydroxybenzoato})\right](ClO_4)_3 \cdot CH_3CN$. Hydrogen atoms are omitted.

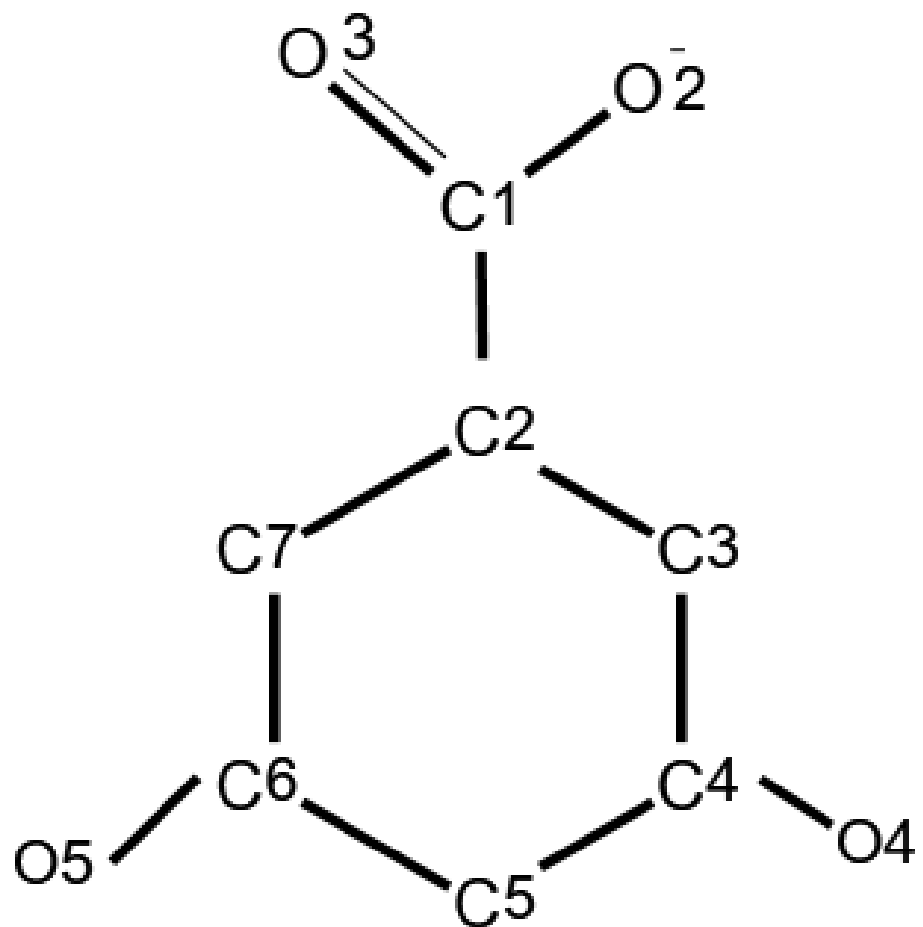


Figure 69. Numbering scheme for dihydroxybenzoate.

Table 52. Crystallographic data for $[\{Fe(TPA)\}_2O(3,5\text{-dihydroxybenzoato})](ClO_4)_3 \bullet CH_3CN$

Crystallographic data	
Empirical formula	C ₄₅ H ₄₄ Cl ₃ Fe ₂ N ₉ O ₁₇
Formula weight	1200.94
Temperature/K	298
Crystal system	monoclinic
Space group	P2 ₁ /n
a/Å	13.1877(11)
b/Å	22.2892(12)
c/Å	19.7183(13)
α/°	90
β/°	95.193(7)
γ/°	90
Volume/Å ³	5772.3(7)
Z	4
ρ _{calc} /g cm ⁻³	1.382
μ/mm ⁻¹	0.713
F(000)	2464
Crystal size/mm ³	6.7 × 4.7 × 2.7
Radiation	MoKα ($\lambda = 0.71073$)
2θ range for data collection/°	5.862 to 47.996

Crystallographic data

Index ranges	-15 ≤ h ≤ 10, -25 ≤ k ≤ 22, -13 ≤ l ≤ 22
Reflections collected	18889
Independent reflections	9021 [R _{int} = 0.0384, R _{sigma} = 0.0555]
Data/restraints/parameters	9021/4/733
Goodness-of-fit on F ²	1.145
Final R indexes [I≥2σ (I)]	R ₁ = 0.0834, wR ₂ = 0.2161
Final R indexes [all data]	R ₁ = 0.1174, wR ₂ = 0.2543
Largest diff. peak/hole / e Å ⁻³	1.11/-0.45

Table 53. Fractional atomic coordinates ($\times 10^4$) and equivalent isotropic displacement parameters ($\text{\AA}^2 \times 10^3$) for $\{[\text{Fe}(TPA)]_2\text{O(3,5-dihydroxybenzoato)}\}(\text{ClO}_4)_3 \bullet \text{CH}_3\text{CN}$.

Atom	x	y	z	U(eq)
Fe1	3452.2(7)	6007.4(4)	6762.4(4)	38.6(3)
Fe2	2460.3(7)	7154.4(4)	5887.2(5)	37.8(3)
Cl1	2190.5(18)	2949.1(9)	6103.5(11)	66.5(6)
Cl3	1395(2)	6777.4(12)	2419.3(14)	89.3(8)
Cl2A	5977(7)	4428(3)	9921(3)	122(3)
Cl2B	2956(4)	9133(3)	3451(3)	87.2(17)
O1	3150(3)	6790.6(18)	6594(2)	40.5(10)
O2	2657(4)	5619.9(18)	5977(2)	45.9(11)
O3	1999(4)	6393.7(19)	5353(2)	45.8(11)
O4	969(5)	3811(2)	4775(3)	68.2(16)
O5	152(6)	5413(3)	3269(3)	87(2)
O11	2874(5)	2766(3)	6670(3)	81.3(18)

Atom	x	y	z	U(eq)
O12	2140(7)	2500(3)	5602(4)	108(3)
O13	2504(7)	3501(3)	5844(4)	123(3)
O14	1198(7)	3011(5)	6323(5)	145(4)
O31	899(12)	6582(6)	2975(6)	197(6)
O32	1833(16)	6303(7)	2145(7)	279(10)
O33	727(9)	7061(4)	1913(5)	151(4)
O34	2097(9)	7201(6)	2694(5)	179(5)
O21A	5727(18)	3925(9)	10127(10)	141(8)
O22A	6250(50)	4024(12)	9570(20)	360(30)
O23A	5950(40)	5028(15)	9583(13)	400(40)
O24A	6670(20)	4551(12)	10458(15)	230(15)
O21B	2247(14)	8805(9)	3537(9)	124(6)
O22B	3493(19)	8789(14)	2960(15)	201(12)
O23B	2880(30)	9661(13)	3227(18)	270(20)
O24B	3300(40)	9246(15)	3940(20)	300(30)
N1	3984(14)	5766(9)	4350(8)	186(7)
N11	2366(4)	5904(2)	7497(3)	41.1(13)
N12	3990(5)	5107(2)	7104(3)	50.8(14)
N13	4975(4)	6082(2)	6470(3)	45.5(13)
N14	4337(4)	6216(2)	7738(3)	45.1(13)
N21	946(4)	7234(2)	6211(3)	40.6(12)
N22	2656(5)	8065(2)	6232(3)	48.1(14)
N23	3558(4)	7318(3)	5174(3)	47.2(14)
N24	1600(4)	7648(2)	5021(3)	44.3(13)
C1	2115(5)	5844(3)	5466(3)	39.1(15)
C2	1581(5)	5415(3)	4965(3)	37.7(14)
C3	1535(5)	4806(3)	5123(3)	42.7(15)

Atom	x	y	z	U(eq)
C4	1030(5)	4416(3)	4662(3)	44.2(16)
C5	585(5)	4624(3)	4036(4)	50.5(17)
C6	626(6)	5227(3)	3886(4)	54.5(18)
C7	1109(5)	5630(3)	4354(4)	48.4(17)
C8	3581(11)	5605(7)	3872(9)	117(4)
C9	3042(12)	5355(8)	3241(8)	141(5)
C111	1459(5)	5619(3)	7386(4)	51.3(17)
C112	746(6)	5642(4)	7862(4)	63(2)
C113	965(7)	5961(4)	8459(4)	76(3)
C114	1896(7)	6249(4)	8581(4)	66(2)
C115	2593(6)	6215(3)	8083(3)	48.1(17)
C116	3606(6)	6534(3)	8143(4)	52.7(18)
C121	3819(7)	4586(3)	6760(5)	68(2)
C122	4211(10)	4051(4)	6996(7)	115(5)
C123	4778(11)	4045(4)	7643(8)	134(6)
C124	4962(9)	4563(4)	7984(6)	98(4)
C125	4560(6)	5083(4)	7703(4)	56.3(19)
C126	4736(7)	5664(3)	8103(4)	63(2)
C131	5297(7)	5898(3)	5870(4)	61(2)
C132	6264(7)	6005(4)	5717(5)	75(3)
C133	6939(7)	6306(4)	6178(6)	84(3)
C134	6610(6)	6484(4)	6783(5)	70(2)
C135	5615(6)	6379(3)	6922(4)	50.7(17)
C136	5171(6)	6611(4)	7550(4)	57.5(19)
C211	731(7)	7165(3)	6862(4)	57(2)
C212	-233(7)	7270(4)	7058(5)	71(2)
C213	-967(6)	7484(4)	6593(5)	68(2)

Atom	x	y	z	U(eq)
C214	-739(6)	7570(4)	5922(4)	61(2)
C215	231(5)	7435(3)	5750(3)	45.2(16)
C216	504(6)	7474(3)	5021(4)	53.2(18)
C221	3128(7)	8228(4)	6841(4)	67(2)
C222	3108(9)	8801(4)	7079(6)	93(3)
C223	2632(10)	9241(4)	6660(6)	106(4)
C224	2184(8)	9081(4)	6025(5)	83(3)
C225	2202(6)	8485(3)	5820(4)	52.5(18)
C226	1734(7)	8308(3)	5120(4)	56.7(19)
C231	4577(6)	7297(4)	5341(5)	64(2)
C232	5249(7)	7364(5)	4845(5)	87(3)
C233	4877(8)	7468(5)	4188(6)	94(3)
C234	3841(7)	7493(4)	4015(5)	76(3)
C235	3193(6)	7424(3)	4525(4)	52.5(18)
C236	2055(6)	7446(3)	4389(3)	51.7(17)

Table 54. Anisotropic displacement parameters ($\text{\AA}^2 \times 10^3$) for $[\{Fe(TPA)\}_2O(3,5\text{-dihydroxybenzoato})](ClO_4)_3 \bullet CH_3CN$.

Atom	U₁₁	U₂₂	U₃₃	U₂₃	U₁₃	U₁₂
Fe1	45.0(6)	33.1(5)	36.5(5)	-2.7(4)	-3.0(4)	0.0(4)
Fe2	46.1(6)	30.3(5)	36.8(5)	-0.3(4)	2.0(4)	0.1(4)
Cl1	74.5(14)	59.4(12)	63.2(12)	8.1(9)	-7.1(10)	-4.4(10)
Cl3	107(2)	77.8(16)	84.9(17)	6.3(13)	16.1(15)	5.4(15)
Cl2A	175(7)	120(5)	68(3)	-1(3)	-13(4)	-61(5)
Cl2B	61(3)	101(4)	97(4)	25(3)	-7(3)	-19(3)
O1	47(3)	35(2)	38(2)	-5.5(18)	-1.6(19)	1(2)
O2	61(3)	32(2)	43(3)	-3.2(19)	-5(2)	2(2)
O3	60(3)	35(2)	39(2)	-2.7(19)	-7(2)	-1(2)

Atom	U₁₁	U₂₂	U₃₃	U₂₃	U₁₃	U₁₂
O4	93(4)	32(3)	75(4)	-4(2)	-15(3)	-11(3)
O5	129(6)	61(4)	62(4)	11(3)	-42(4)	-29(4)
O11	87(4)	79(4)	73(4)	14(3)	-21(3)	-10(3)
O12	149(7)	88(5)	81(5)	-10(4)	-26(5)	1(5)
O13	170(8)	75(5)	113(6)	42(4)	-51(6)	-41(5)
O14	90(6)	205(11)	139(8)	-15(7)	9(5)	27(6)
O31	276(15)	178(11)	143(9)	29(8)	60(10)	-94(11)
O32	410(30)	241(15)	181(12)	-55(11)	-2(14)	216(17)
O33	208(11)	108(7)	124(7)	19(5)	-48(7)	26(7)
O34	147(9)	264(14)	123(8)	3(8)	1(7)	-102(10)
O21A	190(20)	128(14)	103(13)	18(11)	5(13)	-60(14)
O22A	750(110)	89(17)	230(30)	-50(20)	-40(40)	100(30)
O23A	770(90)	250(20)	128(19)	120(20)	-140(30)	-310(40)
O24A	250(30)	180(20)	240(30)	20(20)	-140(20)	-50(20)
O21B	109(13)	149(15)	107(12)	37(11)	-35(10)	-14(12)
O22B	137(19)	260(30)	210(30)	-90(20)	6(18)	-10(20)
O23B	370(50)	170(30)	280(40)	140(30)	110(30)	40(30)
O24B	420(50)	200(30)	310(40)	-160(30)	280(40)	-180(30)
N1	202(16)	247(19)	107(10)	-21(11)	5(10)	-54(14)
N11	42(3)	45(3)	33(3)	3(2)	-13(2)	-5(3)
N12	54(4)	40(3)	57(4)	2(3)	-5(3)	0(3)
N13	49(3)	42(3)	44(3)	-2(2)	-3(3)	-1(3)
N14	47(3)	41(3)	46(3)	-6(2)	-4(3)	-3(3)
N21	47(3)	39(3)	35(3)	2(2)	-3(2)	1(2)
N22	55(4)	37(3)	52(3)	-2(3)	4(3)	-7(3)
N23	49(3)	47(3)	46(3)	6(3)	3(3)	-5(3)
N24	52(3)	42(3)	39(3)	1(2)	3(3)	0(3)

Atom	U₁₁	U₂₂	U₃₃	U₂₃	U₁₃	U₁₂
C1	45(4)	40(4)	33(3)	1(3)	7(3)	-1(3)
C2	45(4)	33(3)	36(3)	-4(3)	5(3)	-5(3)
C3	48(4)	39(3)	40(4)	0(3)	1(3)	1(3)
C4	45(4)	33(3)	54(4)	-4(3)	0(3)	-2(3)
C5	46(4)	46(4)	57(4)	-9(3)	-9(3)	-8(3)
C6	67(5)	50(4)	44(4)	-2(3)	-8(4)	-9(4)
C7	55(4)	38(4)	51(4)	-1(3)	-3(3)	-9(3)
C8	98(10)	134(12)	121(12)	-1(9)	26(9)	20(8)
C9	125(12)	173(15)	126(12)	-22(11)	15(10)	28(11)
C111	48(4)	53(4)	51(4)	1(3)	-10(3)	-6(3)
C112	53(5)	74(5)	63(5)	-2(4)	3(4)	-16(4)
C113	66(6)	102(7)	61(5)	-6(5)	21(4)	-15(5)
C114	70(6)	78(6)	52(5)	-14(4)	11(4)	-15(4)
C115	54(4)	51(4)	38(4)	-2(3)	-6(3)	-5(3)
C116	62(5)	51(4)	44(4)	-15(3)	0(3)	-14(4)
C121	75(6)	37(4)	87(6)	-6(4)	-19(5)	6(4)
C122	129(10)	37(5)	165(12)	-7(6)	-64(9)	-3(5)
C123	168(13)	41(5)	177(13)	14(7)	-74(11)	13(7)
C124	112(8)	59(6)	111(8)	26(5)	-51(7)	2(5)
C125	49(4)	63(5)	57(5)	13(4)	0(4)	-3(4)
C126	71(5)	58(5)	55(5)	2(4)	-13(4)	7(4)
C131	72(5)	54(4)	57(5)	-13(4)	16(4)	8(4)
C132	67(6)	82(6)	81(6)	-13(5)	37(5)	9(5)
C133	52(5)	89(7)	115(8)	-13(6)	34(5)	-8(5)
C134	53(5)	72(5)	86(6)	-15(5)	12(4)	-5(4)
C135	48(4)	48(4)	57(4)	0(3)	6(3)	-1(3)
C136	49(4)	61(5)	62(5)	-12(4)	1(4)	-14(4)

Atom	U₁₁	U₂₂	U₃₃	U₂₃	U₁₃	U₁₂
C211	79(6)	50(4)	43(4)	2(3)	3(4)	3(4)
C212	57(5)	97(7)	60(5)	-12(5)	18(4)	3(5)
C213	39(4)	73(5)	95(7)	-21(5)	20(4)	-3(4)
C214	48(4)	61(5)	72(5)	-7(4)	-1(4)	2(4)
C215	47(4)	41(4)	47(4)	-6(3)	-1(3)	-1(3)
C216	53(4)	54(4)	51(4)	2(3)	-3(3)	1(4)
C221	88(6)	52(4)	57(5)	-12(4)	-12(4)	10(4)
C222	128(9)	60(6)	87(7)	-29(5)	-13(6)	-14(6)
C223	151(11)	48(5)	113(9)	-27(6)	-22(8)	-5(6)
C224	115(8)	37(4)	93(7)	-11(4)	-7(6)	9(5)
C225	63(5)	38(4)	58(4)	2(3)	10(4)	0(3)
C226	82(6)	30(3)	58(5)	10(3)	2(4)	7(4)
C231	56(5)	64(5)	71(5)	16(4)	-2(4)	1(4)
C232	62(6)	106(8)	97(8)	34(6)	32(5)	9(5)
C233	74(7)	126(9)	90(7)	40(7)	42(6)	11(6)
C234	79(6)	91(7)	60(5)	18(5)	23(5)	5(5)
C235	65(5)	47(4)	46(4)	8(3)	11(4)	-2(4)
C236	62(5)	51(4)	42(4)	8(3)	4(3)	2(4)

Table 55. Bond lengths for [{Fe(TPA)}₂O(3,5-dihydroxybenzoato)](ClO₄)₃•CH₃CN.

Atom	Atom	Length/Å
Fe1	O1	1.814(4)
Fe1	O2	1.987(4)
Fe1	N11	2.140(6)
Fe1	N12	2.212(6)
Fe1	N13	2.145(6)
Fe1	N14	2.207(5)

Atom	Atom	Length/Å
N22	C221	1.351(9)
N22	C225	1.346(9)
N23	C231	1.356(10)
N23	C235	1.345(9)
N24	C216	1.496(9)
N24	C226	1.491(8)

Atom	Atom	Length/Å
Fe2	O1	1.789(4)
Fe2	O3	2.059(4)
Fe2	N21	2.158(6)
Fe2	N22	2.149(5)
Fe2	N23	2.139(6)
Fe2	N24	2.251(5)
Cl1	O11	1.430(6)
Cl1	O12	1.405(7)
Cl1	O13	1.408(7)
Cl1	O14	1.423(9)
Cl3	O31	1.396(10)
Cl3	O32	1.342(11)
Cl3	O33	1.418(9)
Cl3	O34	1.396(10)
Cl2A	O21A	1.248(19)
Cl2A	O22A	1.22(3)
Cl2A	O23A	1.49(3)
Cl2A	O24A	1.36(2)
Cl2B	O21B	1.211(19)
Cl2B	O22B	1.47(3)
Cl2B	O23B	1.26(3)
Cl2B	O24B	1.05(5)
O2	C1	1.283(7)
O3	C1	1.253(7)
O4	C4	1.372(8)
O5	C6	1.380(9)
O21A	O22A	1.38(5)

Atom	Atom	Length/Å
N24	C236	1.500(9)
C1	C2	1.502(9)
C2	C3	1.396(9)
C2	C7	1.390(9)
C3	C4	1.385(9)
C4	C5	1.395(10)
C5	C6	1.380(10)
C6	C7	1.398(10)
C8	C9	1.49(2)
C111	C112	1.388(11)
C112	C113	1.383(12)
C113	C114	1.388(12)
C114	C115	1.408(11)
C115	C116	1.507(10)
C121	C122	1.365(12)
C122	C123	1.418(16)
C123	C124	1.347(15)
C124	C125	1.371(11)
C125	C126	1.522(11)
C131	C132	1.358(12)
C132	C133	1.386(13)
C133	C134	1.364(12)
C134	C135	1.385(11)
C135	C136	1.508(10)
C211	C212	1.382(12)
C212	C213	1.358(12)
C213	C214	1.397(12)

Atom	Atom	Length/Å	Atom	Atom	Length/Å
O24B	O23B	1.73(6)	C214	C215	1.386(10)
N1	C8	1.099(18)	C215	C216	1.517(10)
N11	C111	1.355(9)	C221	C222	1.362(12)
N11	C115	1.356(8)	C222	C223	1.395(15)
N12	C121	1.354(9)	C223	C224	1.381(14)
N12	C125	1.343(9)	C224	C225	1.388(10)
N13	C131	1.356(9)	C225	C226	1.513(10)
N13	C135	1.346(9)	C231	C232	1.386(12)
N14	C116	1.486(9)	C232	C233	1.364(14)
N14	C126	1.497(9)	C233	C234	1.378(14)
N14	C136	1.482(9)	C234	C235	1.387(11)
N21	C211	1.349(9)	C235	C236	1.502(11)
N21	C215	1.326(8)			

Table 56. Bond angles for $\{Fe(TPA)\}_2O(3,5\text{-dihydroxybenzoato})](ClO_4)_3 \bullet CH_3CN$.

Atom	Atom	Atom	Angle/°	Atom	Atom	Atom	Angle/°
O1	Fe1	O2	100.61(18)	C211	N21	C215	119.5(6)
O1	Fe1	N11	94.5(2)	Fe2	N22	C221	124.6(5)
O1	Fe1	N12	170.8(2)	Fe2	N22	C225	115.6(5)
O1	Fe1	N13	94.1(2)	C221	N22	C225	119.6(6)
O1	Fe1	N14	92.67(19)	Fe2	N23	C231	123.3(5)
O2	Fe1	N11	98.19(19)	Fe2	N23	C235	116.7(5)
O2	Fe1	N12	88.6(2)	C231	N23	C235	119.9(7)
O2	Fe1	N13	105.4(2)	Fe2	N24	C216	107.1(4)
O2	Fe1	N14	166.08(19)	Fe2	N24	C226	109.7(4)
N11	Fe1	N12	85.0(2)	Fe2	N24	C236	105.8(4)
N11	Fe1	N13	152.9(2)	C216	N24	C226	111.1(6)

Atom	Atom	Atom	Angle/^o	Atom	Atom	Atom	Angle/^o
N11	Fe1	N14	76.5(2)	C216	N24	C236	112.3(5)
N12	Fe1	N13	82.5(2)	C226	N24	C236	110.7(5)
N12	Fe1	N14	78.2(2)	O2	C1	O3	124.8(6)
N13	Fe1	N14	77.5(2)	O2	C1	C2	117.7(5)
O1	Fe2	O3	97.54(18)	O3	C1	C2	117.6(6)
O1	Fe2	N21	103.0(2)	C1	C2	C3	119.9(6)
O1	Fe2	N22	98.2(2)	C1	C2	C7	119.9(5)
O1	Fe2	N23	105.3(2)	C3	C2	C7	120.2(6)
O1	Fe2	N24	177.62(19)	C2	C3	C4	119.5(6)
O3	Fe2	N21	88.9(2)	O4	C4	C3	122.9(6)
O3	Fe2	N22	164.1(2)	O4	C4	C5	116.3(6)
O3	Fe2	N23	89.4(2)	C3	C4	C5	120.7(6)
O3	Fe2	N24	84.81(19)	C4	C5	C6	119.5(6)
N21	Fe2	N22	85.2(2)	O5	C6	C5	117.3(6)
N21	Fe2	N23	151.6(2)	O5	C6	C7	122.1(6)
N21	Fe2	N24	76.6(2)	C5	C6	C7	120.5(7)
N22	Fe2	N23	88.7(2)	C2	C7	C6	119.6(6)
N22	Fe2	N24	79.4(2)	N1	C8	C9	177(2)
N23	Fe2	N24	75.1(2)	N11	C111	C112	121.0(7)
O11	Cl1	O12	109.5(4)	C111	C112	C113	119.5(8)
O11	Cl1	O13	110.3(4)	C112	C113	C114	119.9(8)
O11	Cl1	O14	108.8(5)	C113	C114	C115	118.5(7)
O12	Cl1	O13	111.3(5)	N11	C115	C114	120.9(7)
O12	Cl1	O14	107.3(6)	N11	C115	C116	115.7(6)
O13	Cl1	O14	109.5(7)	C114	C115	C116	123.3(6)
O31	Cl3	O32	108.7(11)	N14	C116	C115	110.2(5)
O31	Cl3	O33	112.7(9)	N12	C121	C122	122.5(8)

Atom	Atom	Atom	Angle/[°]	Atom	Atom	Atom	Angle/[°]
O31	Cl3	O34	104.4(7)	C121	C122	C123	117.9(9)
O32	Cl3	O33	109.2(8)	C122	C123	C124	119.9(9)
O32	Cl3	O34	113.2(12)	C123	C124	C125	118.5(9)
O33	Cl3	O34	108.6(7)	N12	C125	C124	123.7(8)
O21A	Cl2A	O22A	68(2)	N12	C125	C126	117.9(6)
O21A	Cl2A	O23A	162(2)	C124	C125	C126	118.4(8)
O21A	Cl2A	O24A	96.0(16)	N14	C126	C125	114.9(6)
O22A	Cl2A	O23A	114(3)	N13	C131	C132	121.0(8)
O22A	Cl2A	O24A	112(3)	C131	C132	C133	120.0(8)
O23A	Cl2A	O24A	99.1(17)	C134	C133	C132	118.5(8)
O21B	Cl2B	O22B	101.6(16)	C133	C134	C135	120.4(8)
O21B	Cl2B	O23B	125(2)	N13	C135	C134	120.0(7)
O21B	Cl2B	O24B	107.2(17)	N13	C135	C136	116.5(6)
O22B	Cl2B	O23B	107(2)	C134	C135	C136	123.4(7)
O22B	Cl2B	O24B	122(3)	N14	C136	C135	110.8(6)
O23B	Cl2B	O24B	96(3)	N21	C211	C212	121.7(8)
Fe1	O1	Fe2	131.8(2)	C211	C212	C213	119.2(8)
Fe1	O2	C1	131.3(4)	C212	C213	C214	119.2(7)
Fe2	O3	C1	133.6(4)	C213	C214	C215	118.9(8)
Cl2A	O21A	O22A	54.9(12)	N21	C215	C214	121.4(7)
Cl2A	O22A	O21A	57(2)	N21	C215	C216	117.0(6)
Cl2B	O23B	O24B	37.2(11)	C214	C215	C216	121.5(7)
Cl2B	O24B	O23B	46(3)	N24	C216	C215	109.0(6)
Fe1	N11	C111	125.2(5)	N22	C221	C222	122.4(8)
Fe1	N11	C115	114.3(4)	C221	C222	C223	118.5(9)
C111	N11	C115	120.1(6)	C222	C223	C224	119.2(8)
Fe1	N12	C121	126.2(5)	C223	C224	C225	119.6(9)

Atom	Atom	Atom	Angle/[°]	Atom	Atom	Atom	Angle/[°]
Fe1	N12	C125	116.3(5)	N22	C225	C224	120.6(8)
C121	N12	C125	117.5(6)	N22	C225	C226	119.5(6)
Fe1	N13	C131	125.8(5)	C224	C225	C226	119.9(7)
Fe1	N13	C135	114.0(4)	N24	C226	C225	114.2(5)
C131	N13	C135	120.0(6)	N23	C231	C232	120.5(8)
Fe1	N14	C116	104.6(4)	C231	C232	C233	119.3(9)
Fe1	N14	C126	112.4(4)	C232	C233	C234	120.4(9)
Fe1	N14	C136	104.7(4)	C233	C234	C235	118.5(9)
C116	N14	C126	110.5(6)	N23	C235	C234	121.2(8)
C116	N14	C136	112.6(5)	N23	C235	C236	116.2(6)
C126	N14	C136	111.7(6)	C234	C235	C236	122.6(7)
Fe2	N21	C211	123.5(5)	N24	C236	C235	109.2(6)
Fe2	N21	C215	116.4(4)				

Table 57. Hydrogen atom coordinates ($\text{\AA} \times 10^4$) and isotropic displacement parameters ($\text{\AA}^2 \times 10^3$) for $\{[\text{Fe}(TPA)\}_2\text{O}(3,5\text{-dihydroxybenzoato})]\text{ClO}_4)_3 \bullet \text{CH}_3\text{CN}$.

Atom	x	y	z	U(eq)
H3	1841.22	4663.38	5535.05	51
H4	1127.42	3739.94	5178.63	102
H5	344.55	5752.65	3184.22	131
H7	1113.56	6037.95	4256.75	58
H111	1311.84	5403.58	6985.32	62
H112	124.94	5445.18	7779.97	76
H113	488.47	5981.56	8778.95	91
H114	2055.29	6460.75	8983.47	79
H121	3418.85	4593.2	6346.38	82
H122	4110.06	3701.79	6741.52	138
H123	5022.6	3684.6	7829.96	161

Atom	x	y	z	U(eq)
H124	5351.86	4567.08	8401.63	117
H131	4848.03	5695.73	5558.69	73
H132	6472.7	5876.66	5303.45	90
H133	7601.53	6383.88	6077.5	100
H134	7057.36	6677.08	7103.2	84
H211	1244.16	7043.05	7187.77	69
H212	-377.67	7195.56	7503.61	85
H213	-1612.5	7571.31	6719.91	82
H214	-1230.3	7716.36	5595.24	73
H221	3479.67	7937.56	7108.07	80
H222	3404.7	8896.61	7511.29	111
H223	2615.33	9637.02	6805.9	127
H224	1873.86	9370.2	5736.54	99
H231	4827.62	7237.69	5792.23	77
H232	5947.78	7337.22	4959.45	104
H233	5323.82	7523.71	3854.86	113
H234	3583.01	7554.38	3565.78	91
H5A	263.87	4357.45	3723.84	61
H11A	3515.93	6942.69	7980.76	63
H12A	4418.17	5628.55	8525.55	75
H13A	5700.5	6628.41	7925.12	69
H21A	390.52	7089.04	4796.96	64
H22A	1074.31	8500.49	5038.76	68
H23A	1866.65	7723.08	4019.28	62
H11B	3874.63	6547.9	8617.62	63
H12B	5462.37	5712.41	8218.43	75
H13B	4912.07	7013.6	7466.68	69

Atom	x	y	z	U(eq)
H21B	77.42	7769.93	4772.94	64
H22B	2161.87	8458.53	4782.86	68
H23B	1796.14	7052.08	4256.22	62
H9A	2704.1	4989.4	3346.33	212
H9B	3524.98	5273.43	2916.38	212
H9C	2548.46	5639.49	3051.71	212

Table 58. Partial atomic occupancy for $\left[\{Fe(TPA)\}_2O(3,5\text{-dihydroxybenzoato})\right](ClO_4)_3 \cdot CH_3CN$.

Atom	Occupancy
Cl2A	0.5
Cl2B	0.5

Atom	Occupancy
O21A	0.5
O22A	0.5
O23A	0.5
O24A	0.5

Atom	Occupancy
O21B	0.5
O22B	0.5
O23B	0.5
O24B	0.5

CHAPTER IV

Discussion

4.1 Syntheses Discussion

The main ligand used in all of these syntheses is TPA which was prepared in the form where all 3 pyridine rings are protonated TPA•3HClO₄ because this is a crystalline form and is therefore easy to measure and store. The deprotonated form of TPA is an oil.

The primary goal of this study was to synthesize (μ -sulfido)(μ -carboxylato) diiron(III)TPA complexes. During the attempted synthesis of (μ -sulfido)(μ -OAc) diiron(III)TPA (in section 2.3.2.1) and (μ -sulfido)(μ -OBz)diiron(III)TPA (in section 2.3.2.2), instead of the desired sulfido-bridged complexes, the oxido-bridged $[\text{Fe}_2(\text{TPA})_2\text{O}(\text{OAc})](\text{ClO}_4)_3$ was formed, which has been previously synthesized and characterized.²⁵ A possible reason is that iron is oxophilic. During the reaction, iron bonds to water in the reaction mixture. Many of the reagents are hydrates and methanol is hygroscopic.

The synthesis of $[\{\text{Fe}(\text{TPA})\text{Br}\}_2\text{O}](\text{ClO}_4)_2 \cdot \text{H}_2\text{O}$ in section 2.3.4.7 lead to the expected product. Though the structure has been reported by in Mathew Mullaney's M. S. thesis⁴³ the structure needed to be repeated due to a lack of documentation.

All attempts to make singly-bridged (μ -oxido)(carboxylato)₂ diiron(III)TPA complexes were unsuccessful. Instead, dibridged complexes formed. The bent (μ -oxido) (μ -carboxylato) diiron(III)TPA unit is likely to be more thermodynamically stable. In the previously reported $[\{\text{Fe}(\text{TPA})(4\text{-nitrobenzoato})\}_2\text{O}]^{2+}$, the linear complex converted to a bent (μ -oxido)(μ -carboxylato) diiron(III)TPA strucuture in solution.

During the attempted synthesis of (μ -oxido)(μ -carboxylato) diiron(III)TPA complexes, five systems produced the expected crystalline product and their X-ray structures are reported in section 3.3 and discussed in 4.4. Two systems produced crystalline product, but the X-ray structure proved unexpected results.

The attempted synthesis of $[\text{Fe}_2(\text{TPA})_2\text{O}(3,5\text{-dibromobenzoato})(\text{ClO}_4)_3]$ (in section 2.3.5.5) and the attempted synthesis of $[\text{Fe}_2(\text{TPA})_2\text{O}(4\text{-pyridinecarboxylato})(\text{ClO}_4)_3]$ (in section 2.3.5.9) resulted in two different polymorphs of $[\{\text{Fe}(\text{TPA})\}_2\text{O}(\text{OAc})](\text{ClO}_4)_3 \cdot \text{H}_2\text{O}$. These are differentiated by the position of three perchlorate ions around the $[\{\text{Fe}(\text{TPA})\}_2\text{O}(\text{OAc})]^{3+}$ and the position of water.

In several cases, upon attempted recrystallization of a modified benzoate complex, $[\{\text{Fe}(\text{TPA})\}_2\text{O}(\text{OAc})](\text{ClO}_4)_3$ resulted. Since the iron centers of these TPA complexes are highly reactive, it is possible that during recrystallization, the solvent was hydrolyzed producing acetate. The hydrolysis of acetonitrile by Fe(III)TPA complexes in the presence of water has been reported previously.⁴⁴ Or ethyl acetate (the vapor diffusion of ethyl acetate is used to produce crystals) might have hydrolyzed. When we compare some of the proton NMR spectra before recrystallization there clearly was no evidence for the presence of the acetate group—no acetate peak around 14 ppm.

Small, roughly spherical, counter ions like perchlorate are convenient tools for synthesis due to their ability to produce a well-packed crystalline lattice. In most of the X-ray structures in this study, the perchlorates are disordered.

4.2 ^1H NMR Spectroscopy Discussion

The main reason for measuring the ^1H NMR spectra is to determine whether the solid-state structure persists in solution, particularly with respect to the μ -carboxylate. It is always difficult to predict the symmetry and orientation of oxido-bridged diiron(III)TPA complexes without X-ray crystallography. Fortunately, ^1H NMR is another useful tool in determining the symmetry of these complexes. The chemical shifts of all of the complexes (**1-13**) are listed in **Table 3** along with the proposed peak assignments. The assignments are based on previously reported (μ -oxido)diiron(III)TPA complexes.^{24,25,42}

To date, there are two main TPA orientations which are observed in (μ -oxido) diiron(III) TPA complexes by X-ray crystallography. One is symmetric TPA orientation where both tertiary amine nitrogens are *cis* to the oxido bridge and the other is asymmetric TPA orientation with the tertiary amine of one TPA *cis* to the oxido-bridge and the other tertiary amine nitrogen is *trans* to the oxido-bridge.²⁵ These orientations were confirmed and explained in section 4.1.

The ^1H NMR spectrum for the singly bridged $[\{\text{Fe}(\text{TPA})\text{Br}\}_2\text{O}](\text{ClO}_4)_2 \cdot \text{H}_2\text{O}$ (**1**) is shown in **Figure 33**. **Figures 34-45** show the ^1H NMR spectra for 1,3-carboxylato bridged diiron(III) TPA complexes (**2-13**). All of the spectra of dinuclear oxido-bridged diiron(III) TPA complexes show ^1H NMR features in the 0-40 ppm region, which indicates relatively strong antiferromagnetic coupling between the two iron centers.²⁹ The NMR spectrum for $[\{\text{Fe}(\text{TPA})\text{Br}\}_2\text{O}](\text{ClO}_4)_2 \cdot \text{H}_2\text{O}$ (**1**) is quite different than the other complexes.

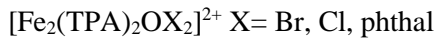
$[\{\text{Fe}(\text{TPA})\text{Cl}\}_2\text{O}](\text{ClO}_4)_2$, and $[\{\text{Fe}(\text{TPA})\}_2\text{O}(\text{phthal})](\text{ClO}_4)_2 \bullet \text{CH}_3\text{OH} \bullet \text{H}_2\text{O}$ have symmetric TPA orientations in solution and this orientation was confirmed to be present in the solid-state.^{29,24} $[\{\text{Fe}(\text{TPA})\text{Cl}\}_2\text{O}](\text{ClO}_4)_2$ is linear and $[\{\text{Fe}(\text{TPA})\}_2\text{O}(\text{phthal})](\text{ClO}_4)_2 \bullet \text{CH}_3\text{OH} \bullet \text{H}_2\text{O}$ has a Fe-O-Fe bond angle of 143.4° . For complexes with symmetric TPA orientations, their ^1H NMR spectra can be separated into three groupings of signals in the following regions: 6-9 ppm, 10-18 ppm and 20-40 ppm.

Table 59 compares the NMR data of $[\{\text{Fe}(\text{TPA})\text{Br}\}_2\text{O}](\text{ClO}_4)_2 \bullet \text{H}_2\text{O}$ with previously reported symmetric structures. All of these spectra have a very similar number of peaks in each respective region with characteristic peak intensities. There is a pair of peaks of relative intensities 4:2 in the 6-8 ppm region. These peaks are assigned to the pyridine 4-protons; these can be assigned to four 4-H's of the four TPA rings *cis* to the oxido bridge and two 4-H's of the two TPA rings *trans* to the oxido bridge, respectively. These peaks are sharp and least paramagnetically shifted due to the act that 4-H's are farthest from the diiron center.

In the 10-18 ppm region there are four characteristic peaks with relative intensity 4:4:2:2 which can be seen in all of these symmetric complexes. These peaks are assigned to the pyridine 3,5-protons. The pair of peaks around 11 and 12 ppm have less intensity corresponding to protons arising from rings that are *trans* to the oxido bridge. The reason the 3,5-H's that are *trans* to the oxido-bridge give different signals is that they are in different environments which is related to the relative distance from Fe. **Figure 70** identifies the different environments of the 3,5 protons of pyridine *trans* to the oxido-bridge in a linear complex by the “*” sign. A second pair of peaks can be observed around the (15-16) and (17-18) ppm region and has more intensity corresponding to

protons 4:4 and arises from rings *cis* to the oxido bridge. The most paramagnetically shifted peak around 18 ppm is due to the four 5-H's that are closer to the diiron core.

Table 59. Comparison and assignments of ^1H NMR chemical shifts for symmetric (μ -oxido)diiron(III)TPA



X	Br	Br ²⁹	Cl ²⁹	phthal ²⁴	Assignment
Chemical Shifts (ppm)	7.1	6.7	7.1	6.9	4-H
	7.6	7.4	7.5	8.1	4-H
	11.2	11.1	11.5	12.1	3,5-H
	12.8	12.6	12.9	13.3	3,5-H
	15.9	16.7	16.7	16.2	3,5-H
	18.0	17.9	17.7	17.2	3,5-H
	20.9	21	20	19	6-H or CH ₂
	24.3				6-H or CH ₂
	29.3	29	29		6-H or CH ₂
	34.6	34	33	32	6-H or CH ₂
				8.8	(phthal)
				8.0	(phthal)

The other peak is due to 3-H's that are farther from the diiron core. **Figure 70** identifies 3,5-H protons of pyridine *cis* to oxido-bridge that are farther from the diiron core with an “a” sign and those that are closer to the diiron core with a “b”.

Finally, the 18-40 ppm region has two broad features of comparable intensity assignable to the 6-H protons and CH₂ protons of TPA.²⁴ The additional pair of peaks of $[\{\text{Fe}(\text{TPA})\text{Br}\}_2\text{O}](\text{ClO}_4)_2 \cdot \text{H}_2\text{O}$ in the 20.9 ppm and 24.3 ppm can be assigned to the CH₂ protons. The pattern of ^1H NMR peaks and intensities confirms that

$[\{\text{Fe}(\text{TPA})\text{Br}\}_2\text{O}](\text{ClO}_4)_2 \cdot \text{H}_2\text{O}$ has retained a symmetric TPA environment in solution, as seen by X-ray crystallography in section 3.3.1.

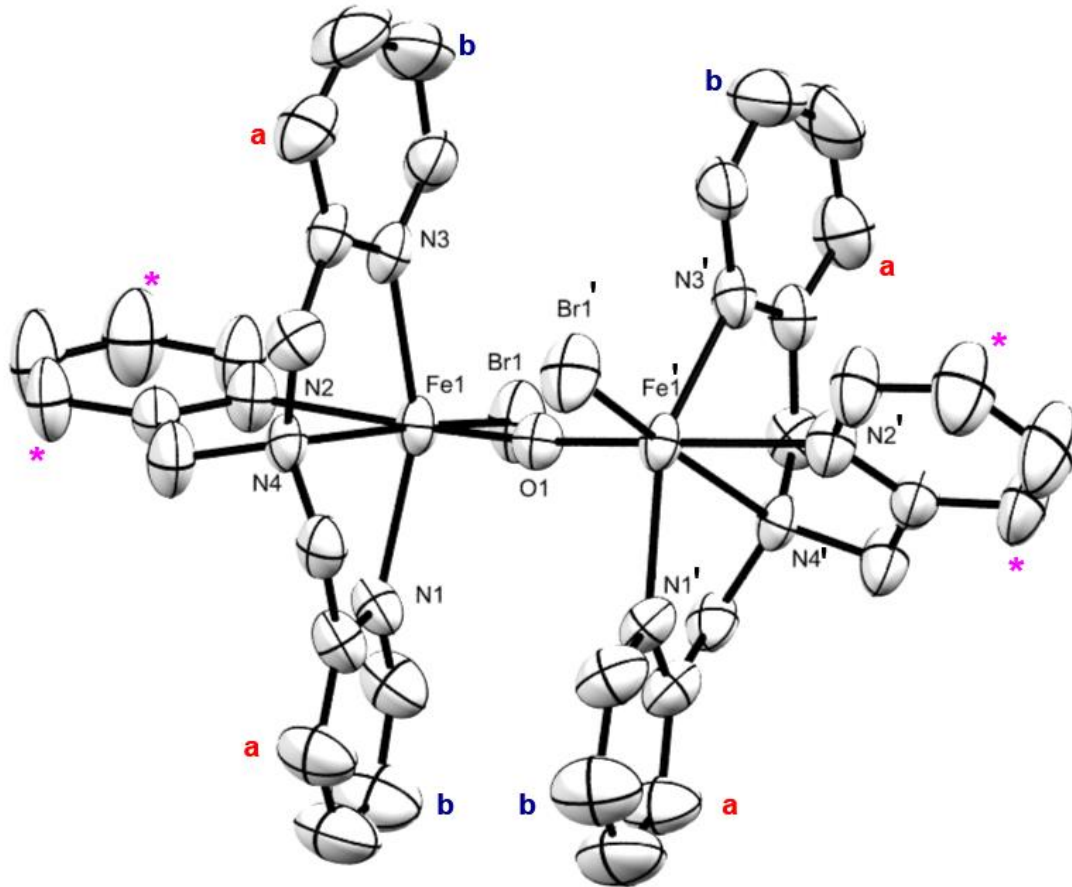


Figure 70. Different environment of 3,5-H's in symmetric TPA orientation.

Table 60 compares the ^1H NMR features of $[\{\text{Fe}(\text{TPA})\}_2\text{O}(\text{OAc})](\text{ClO}_4)_3 \cdot \text{H}_2\text{O}$ (**2,3**), $[\{\text{Fe}(\text{TPA})\}_2\text{O}(4\text{-hydroxybenzoato})](\text{ClO}_4)_3$ (**4**), $[\{\text{Fe}(\text{TPA})\}_2\text{O}(4\text{-methoxybenzoato})](\text{ClO}_4)_3$ (**5**), $[\{\text{Fe}(\text{TPA})\}_2\text{O}(4\text{-fluorobenzoato})](\text{ClO}_4)_3$ (**6**), $[\{\text{Fe}(\text{TPA})\}_2\text{O}(3,5\text{-dimethylbenzoato})](\text{ClO}_4)_3 \cdot 0.5\text{H}_2\text{O}$ (**8**) and $[\{\text{Fe}(\text{TPA})\}_2\text{O}(3,5\text{-dihydroxybenzoato})](\text{ClO}_4) \cdot \text{CH}_3\text{CN}$ (**9**) with the features of previously reported asymmetric TPA bearing bent (μ -oxido)diiron(III) complexes, such as $[\text{Fe}_2(\text{TPA})_2\text{O}(4\text{-methylbenzoato})](\text{ClO}_4)_3 \cdot 2\text{CH}_3\text{CN}$ and $[\text{Fe}_2(\text{TPA})_2\text{O}(4\text{-chlorobenzoato})](\text{ClO}_4)_3 \cdot 4\text{CH}_3\text{OH}$.⁴² The ^1H NMR

spectra of all these complexes are typical for asymmetric TPA orientation in solution, which suggests that the solid state structures persist in solution.

Table 60. Comparison and assignment of 1H NMR chemical shifts for bent oxido-bridged dinuclear complexes.

OAc	4-OH	4-OCH ₃	4-F	3,5-CH ₃	3,5-OH	4-Cl ^{42a}	4-CH ₃ ^{42b}	Assignment
6.4	6.5	6.4	6.4	6.4	6.4			4-H
6.5						6.5	6.5	4-H
6.9	7.0	7.0	7.0	7.0	7.0	6.9	6.9	4-H
7.9	7.8	7.9	8.0	7.9	7.7	8.0	8.0	4-H
11.1	11.1	11.1	11.3		7.9	11.1	11.0	3,5-H
12.3	12.2	12.1	12.3	10.9	11.1	12.2	12.2	3,5-H
12.6	12.6	12.6	12.7	12.2	12.2	12.7	12.6	3,5-H
16.5	16.4	16.4	16.5	12.6	12.7	16.5	16.5	3,5-H
17.4	17.3	17.3	17.3	16.5	16.5	17.4	17.4	3,5-H
20.0	20.3	20.1	20.5	17.3	17.4	20.5	20.0	6-H/CH ₂
23.7	23.3	23.2	23.2	20.2	20.4	23.5	23.0	6-H/CH ₂
32.1	31.4	31.7	31.5	23.3	23.5	32.0	32.0	6-H/CH ₂
35.9	36.2	36.2	36.6	32.2	31.9	37.0	36.5	6-H/CH ₂
				36.3	37.0			6-H/CH ₂
				40.4				6-H/CH ₂
13.9 (OAc)		4.3 (OCH ₃)					4.2 (CH ₃)	
				1.2 (CH ₃)				
	8.2	8.3	8.7			9.1	8.8	

In most bent oxido-bridged diiron(III) TPA complexes, the TPA ligands have an asymmetric orientation. Similar to the symmetric orientation, the ¹H NMR features can be separated into three main groups. The complex set of peaks in the 6-9 ppm region with relative intensities of 2:1:3 correspond to the *para* protons of the pyridine ring (4-H). These peaks are the sharpest and least paramagnetically-shifted due to the fact that 4-H's are farthest away from the diiron center. In the 10-18 ppm region there are four characteristic peaks with relative intensities of 2:1:1:1 corresponding to the *meta* protons of the pyridine ring (3,5-H), which are an intermediate distance from the diiron core. There is another set of four broad peaks in the 20-40 ppm range, corresponding to the *ortho* protons of the pyridine ring (6-H) or the CH₂ protons, which are closest to the diiron core.^{24,25}

The ¹H NMR of [{Fe(TPA)}₂O(OAc)](ClO₄)₃•H₂O shows the typical features of asymmetric TPA orientation and exhibits one additional peak at 13.9 ppm which corresponds to the CH₃ of the acetate group.

The ¹H NMR of [{Fe(TPA)}₂O(4-hydroxybenzoato)](ClO₄)₃ shows the typical features of asymmetric TPA orientation and exhibits one additional peak at 8.2 ppm which corresponds to the *meta* protons of the 4-hydroxybenzoate.

The ¹H NMR of [{Fe(TPA)}₂O(4-methoxybenzoato)](ClO₄)₃ shows the typical features of asymmetric TPA orientation and exhibits a peak at 8.3 ppm which corresponds to the *meta* protons of the 4-methoxybenzoate. Additionally, there is a peak at 4.3 ppm which corresponds to the three protons from the methoxy group.

The ^1H NMR of $[\{\text{Fe}(\text{TPA})\}_2\text{O}(4\text{-fluorobenzoato})](\text{ClO}_4)_3$ shows the typical features of asymmetric TPA orientation and exhibits one additional peak at 8.7 which corresponds to the *meta* protons of the 4-fluorobenzoate.

The ^1H NMR of $[\{\text{Fe}(\text{TPA})\}_2\text{O}(3,5\text{-dimethylbenzoato})](\text{ClO}_4)_3 \bullet 0.5\text{H}_2\text{O}$ shows the typical features of asymmetric TPA orientation and exhibits a peak at 6.2 ppm which corresponds to the *para* proton of the 3,5-dimethylbenzoate. Additionally, there is a peak with a higher intensity at 1.2 ppm which corresponds to the protons of the methyl groups.

The ^1H NMR of $[\{\text{Fe}(\text{TPA})\}_2\text{O}(3,5\text{-dihydroxybenzoato})](\text{ClO}_4) \bullet \text{CH}_3\text{CN}$ shows the typical features of asymmetric TPA orientation and exhibits one additional peak at 5.4 ppm which corresponds to the *para* proton of the 3,5-hydroxybenzoate.

4.3 Electronic Spectroscopy Discussion

Different concentrations of the compounds were used to measure important spectral features. Electronic spectra of (μ -oxido)(μ -carboxylato)diiron(III)TPA complexes are sensitive to variations of the structural features such as charge, basicity, and bite angle of the additional bridging ligand.²⁴ Except for linear $[\{\text{Fe}(\text{TPA})\text{Br}\}_2\text{O}] (\text{ClO}_4)_2 \bullet \text{H}_2\text{O}$ (**1**) which has features in the near UV, the bent diiron carboxylate complexes (complex **2-13**) also have additional features in the visible to near infrared region. The spectra of all bent diiron carboxylate complexes show similar features despite variations in the bridging component. The spectra of (**2-13**) do not have any strong absorptions in the visible region, but there are very strong absorption bands in the near UV region and this can be noted by the differences in extinction coefficient values

in these regions.⁴⁵ All of the electronic spectra have two artifacts caused by the instrument around 485 nm and 650 nm.

TPA is a weak field ligand. Consequently, diiron(III)TPA complexes are high spin. Thus d-d transitions are spin forbidden and therefore weak. The ground state term symbol for weak field octahedral Fe(III) is $^6A_{1g}$ and there is no hexet excited state. A single spin flip gives rise to quartet states.

For oxido-bridged diiron(III) systems the electronic structure is often approximated as isolated octahedral Fe(III) centers acting independently. This is only an approximation since the two Fe(III) centers are antiferromagnetically coupled. Nevertheless, it is common practice. The d^5 Tanabe-Sugano diagram for high spin shows three transitions: lowest energy $^6A_{1g} \rightarrow ^4T_{1g}$, mid energy $^6A_{1g} \rightarrow ^4T_{2g}$ and highest energy $^6A_{1g} \rightarrow ^4A_{1g}, ^4E_g$.⁴⁶ According to the Tanabe-Sugano diagram, it can be seen that for the three transitions the energy of the $^6A_{1g} \rightarrow ^4A_{1g}, ^4E_g$ transition is independent of the ligand field strength.⁴⁶ This transition is caused by a spin flip of an electron in the e_g orbital.¹²

In these (μ -oxido)diiron(III)TPA complexes, the lowest energy $^6A_{1g} \rightarrow ^4T_{1g}$ transition usually occurs in the near IR at 1000 nm and its energy depends primarily on the charge of the bridging ligand.²⁴ Solomon *et al.* assigned a transition in the 550-700 nm region as $^6A_{1g} \rightarrow ^4T_{2g}$.⁴⁷ The 490-503 nm region contains the third highest energy $^6A_{1g} \rightarrow ^4A_{1g}, ^4E_g$ d-d transition. However, all of these d-d transitions are very weak.

(μ -Oxido)diiron(III)TPA complexes show a broad range of additional comparatively high intensity features due to oxo-Fe(III) charge transfer transitions in the near UV to visible region. These charge transfer transitions are largely dependent on the

Fe-O-Fe bond angle and when the Fe-O-Fe bond angle increases, the angle dependent features are blue-shifted. Blue-shifts arise from increased π bonding between the iron and bridging oxygen when the Fe-O-Fe angle becomes larger. This lowers the Lewis acidity of the iron centers and at the same time lowers the basicity of the bridging oxide. As a result, the energy gap increases between the oxide *p* orbitals and acceptor *d* orbitals in iron centers.²⁴

Table 1 reports the absorption data for the complexes **1-13** of the current study. Additionally, **Table 61** shows a comparison of several of the oxido-bridged diiron(III)TPA complexes with other previously reported oxido-bridged diiron(III)TPA complexes. When comparing the spectral features, the linear complexes have notably fewer features than the bent oxido complexes. $[\{\text{Fe}(\text{TPA})\text{Br}\}_2\text{O}](\text{ClO}_4)_2 \cdot \text{H}_2\text{O}$ (**1**) exhibits just a very few features in the near UV region. In contrast, (μ -oxido)diiron(III)TPA complexes exhibit a number of features in a broad range from the near UV to the far visible region (250-715 nm).

All complexes' (**1-13**) spectra have their highest intensity peak in the 250-270 nm region. $\pi-\pi^*$ pyridine ring transitions of TPA likely contribute to this particular peak. Additionally, bridging benzoates may also contribute in this region. As seen in **Figure 71**, in 4-substituted benzoates the benzoate rings have intense transitions that occur in the 250-270 nm region. The near UV features for di *meta*-substituted benzoate ligands are shown in **Figure 72**. There are 2-3 strong peaks in the 250-270 nm region.

$[\{\text{Fe}(\text{TPA})\text{Br}\}_2\text{O}](\text{ClO}_4)_2 \cdot \text{H}_2\text{O}$ (**1**) exhibits two other features at 304 nm and 396 nm. Previously reported linear dibromo and dichloro diiron(III)TPA have similar features yet the band at 274 nm is not included in the reported data. All these features

can be assigned as Br⁻ to Fe(III) LMCT transitions.⁴⁸ This is supported by extinction coefficients that are larger than 10 mM⁻¹cm⁻¹ especially when compared to the visible region peak intensities of (μ -oxido)(μ -carboxylato)diiron(III)TPA complexes which have low (0.07-3.71 mM⁻¹cm⁻¹) extinction coefficients.

From this point onward, the additional features of the **2-13** (μ -oxido) (μ -carboxylato)diiron(III)TPA electronic spectra will be discussed. In addition to the highest energy peak around 250-270 nm, there are two peaks in the near UV region of 300-400 nm in all of these spectra of **2-13**. The 300-400 nm region is known as the oxo dimer region and these transitions depend on the Fe-O-Fe angle and the strength of the Fe-O bond hence these can be assigned as oxo-to-Fe(III) charge-transfer transitions.¹² Additional transitions from the bridging benzoate also have features in this region.

Table 61. Comparison of the absorption bands of the oxido-bridged diiron complexes with some previously reported complexes.

(Wavelength in nm, the parentheses are ε in $\text{mM}^{-1}\text{cm}^{-1}$)

Br⁴⁸	Cl^{42a}	Br	OAc²⁵	OAc	4-OCH₃	4-CH₃^{42b}	3,5-CH₃	malH²⁴	4-F	4-Cl^{42c}	3,5-OH
		274 (19.95)		270 (13.5)	270 (35.81)		271 (17.61)		271 (16.26)	330 (sh)	272 (19.27)
320 (13.8)	328 (9.2)	304 (sh)	332 (10)	330 (9.75)	322 (17.19)	325 (sh)	323 (10.91)	330(12)	333 (12.10)		306 (sh)
378 (15)	374 (6.85)	396 (10.04)	366 (sh)	366 (sh)	364 (11.48)	340 (sh)	350 (sh)	360(6.8)	365 (sh)	372 (sh)	362 (8.60)
			425 (sh)	420 (sh)	435 (sh)	380 (9.1)	416 (sh)	425(sh)	422 (sh)		421 (sh)
			458 (1.2)	460 (1.01)	449 (sh)	460 (1.8)	458 (0.997)	460(1.21)	459 (1.14)	462 (1)	457 (1.29)
			492 (1.0)	489 (0.871)	490 (sh)	490 (1.5)	502 (0.737)	490(1.05)	494 (0.97)	498 (sh)	490 (1.034)
			504 (0.94)	498 (sh)		503(sh)		506(0.97)			

Br⁴⁸	Cl^{42a}	Br	OAc²⁵	OAc	4-OCH₃	4-CH₃^{42b}	3,5-CH₃	malH²⁴	4-F	4-Cl^{42c}	3,5-OH
			530 (sh)	535 (sh)	534(sh)	535(sh)	530(sh)	530(sh)	525 (sh)	520 (sh)	524 (sh)
			700 (0.14)	699 (0.135)	677 (0.237)	680 (0.39)	699 (0.13)	694 (0.18)	698 (0.149)	702 (0.13)	683 (0.065)

24. [Fe₂(TPA)₂O(maleate)](ClO₄)₃•2acetone
 25. [Fe₂(TPA)₂O(OAc)](ClO₄)₃•H₂O•acetone
 42a. [{Fe(TPA)Cl}₂O](ClO₄)₂
 42b. [Fe₂(TPA)₂O(4-methylbenzoato)](ClO₄)₃•2CH₃CN
 42c. [Fe₂(TPA)₂O(4-chlorobenzoato)](ClO₄)₃•4CH₃OH
 48. [{Fe(TPA)Br}₂O](ClO₄)₂•H₂O

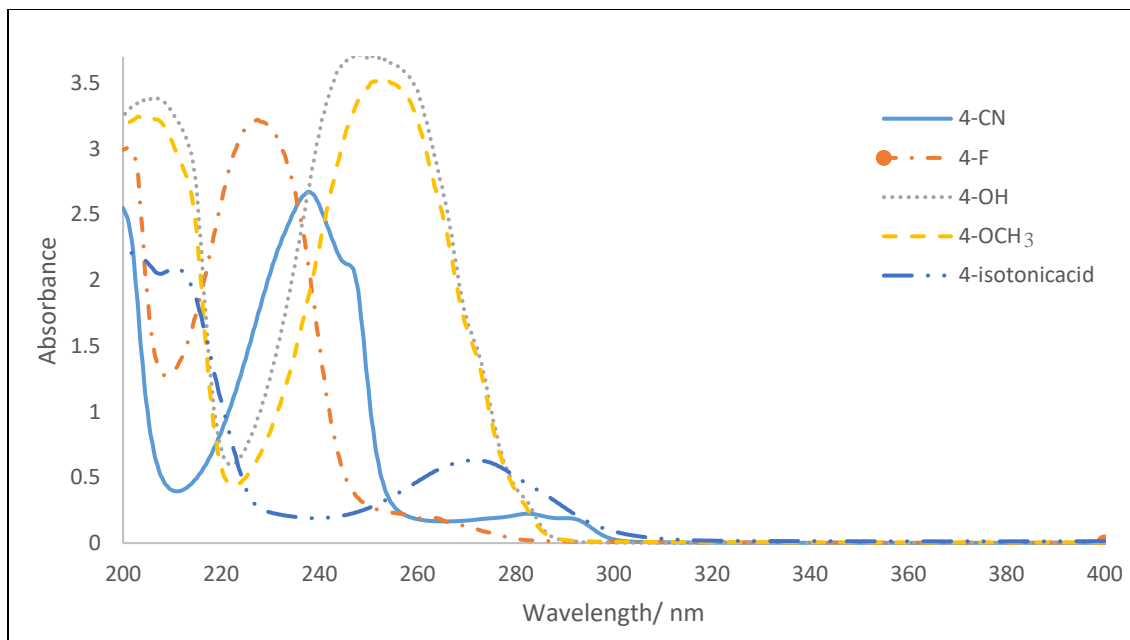


Figure 71. Near-UV features for *para* substituted-benzoate ligands.

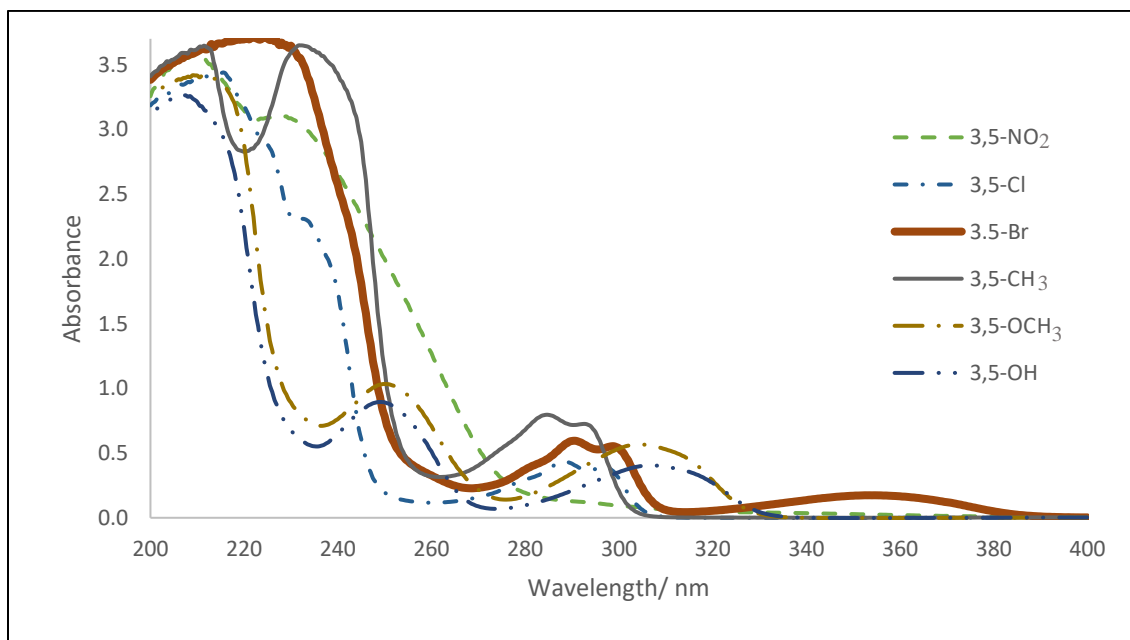


Figure 72. Near-UV features for *meta* disubstituted-benzoate ligands.

Figure 71 shows there are peaks in the 290-295 nm region and also the tails of high intensity features in the 250-270 nm region may contribute to the features observed 300-400 nm in **2-7**. **Figure 72** shows there are peaks in the 285-370 nm region from the di *meta*-substituted benzoic acids and these features must contribute to the 300-400 nm features that can be seen in **8-13**.

A pair of absorption bands around 415-460 nm and 460-490 nm with a 5-10 fold lower extinction coefficient ($0.7\text{--}3.7 \text{ mM}^{-1}\text{cm}^{-1}$) than those on the 300-400 nm region are also observed in all of the (μ -oxido)(μ -carboxylato)diiron(III)TPA complex spectra. This feature can also be assigned as oxo-to-Fe(III) charge-transfer. These bands are also associated with transitions inherent in bent oxido-bridged TPA complexes and these also depend on the Fe-O-Fe angle.

The 490-508 nm feature is largely independent of the Fe-O-Fe bond angle. **Table 62** lists some of the Fe-O-Fe bond angles for (1,3- μ -carboxylato)(μ -oxido)diiron(III) TPA complexes and the position of the 490 nm feature. The graph in **Figure 73** shows how this 490 nm feature is largely independent of the Fe-O-Fe bond angle with the complexes **3-6**, and **8-9** from the current study. However this graph has a slight slope because this feature is superimposed on an oxo-to-Fe(III) LMCT and one of the artifacts lies in this region. Therefore this feature around 490 nm can be assigned to the $^6\text{A}_1 \rightarrow ^4\text{A}_1, ^4\text{E}$ d-d transition.²⁴ The shoulder at 530 nm is due to forbidden oxo-to-Fe(III) charge transfer in dibridged complexes.¹²

Table 62. Comparison of Fe-O-Fe angle vs 490 nm feature.

Bridging carboxylate ligand	Fe-O-Fe bond angle/ $^\circ$	Wavelength/nm
4-ethylbenzoate ^{42d}	128.90	501

Bridging carboxylate ligand	Fe-O-Fe bond angle/ $^{\circ}$	Wavelength/nm
OAc ⁴⁰	129.70	492
OAc	129.82	489
4-hydroxybenzoate	129.86	487
4-methoxybenzoate	129.93	490
4-fluorobenzoate	130.56	494
4-methylbenzoate ^{42b}	131.10	490
3,5-dimethylbenzoate	131.59	493
3,5-dihydroxybenzoate	131.70	490

- 42b. $[\text{Fe}_2(\text{TPA})_2\text{O}(4\text{-methylbenzoato})](\text{ClO}_4)_3 \cdot 2\text{CH}_3\text{CN}$
 42d. $[\text{Fe}_2(\text{TPA})_2\text{O}(4\text{-ethylbenzoato})](\text{ClO}_4)_3 \cdot \text{CH}_3\text{CN} \cdot \text{CH}_3\text{COOC}_2\text{H}_5$

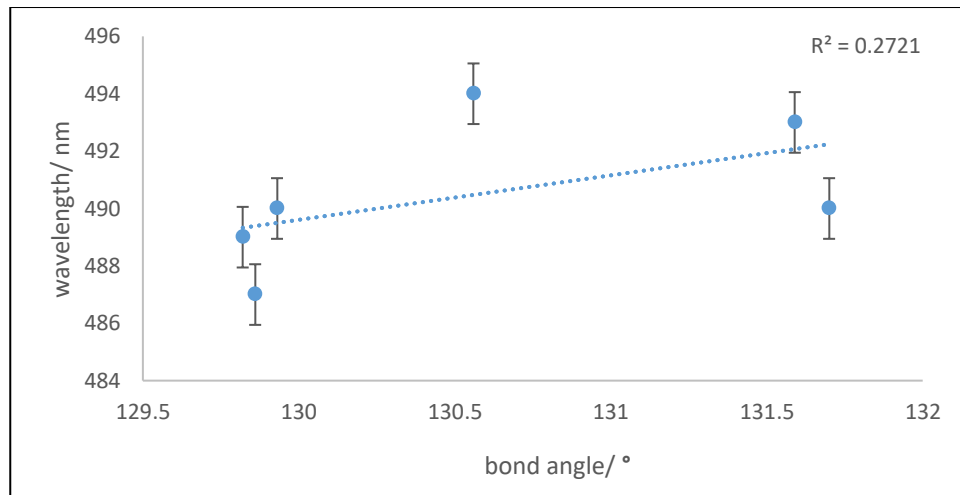


Figure 73. Graph of Fe-O-Fe bond angle vs 490 nm feature.

Lastly, all (μ -1,3 carboxylato)(μ -oxido)diiron(III)TPA complexes have features in the 550-700 nm region which are Fe-O-Fe angle dependent. Therefore, these features are due to forbidden oxo-to-Fe(III) charge transfer transitions. These gain intensity from the higher energy LMCT bands. This transition usually obscures the ${}^6\text{A}_{1g} \rightarrow {}^4\text{T}_{2g}$

transition.²⁴ The presence of features in the 400-700 nm region for **2-13** indicates the presence of a bent oxido-bridge. The lack of features in the 400-700 nm region indicates a linear oxido-bridge.²⁴

4.4 X-ray Crystallography Discussion

4.4.1 Oxido-bridged diiron(III) complexes with symmetric TPA orientation

$[\{\text{Fe}(\text{TPA})\text{Br}\}_2\text{O}](\text{ClO}_4)_2 \cdot \text{H}_2\text{O}$ was made for the first time by graduate student Matthew Mullaney at Duquesne University in 1996,⁴³ but the data were lost. In order to publish the details of the structure, the compound was resynthesized, and X-ray data were recollected. $[\{\text{Fe}(\text{TPA})\text{Br}\}_2\text{O}](\text{ClO}_4)_2 \cdot \text{H}_2\text{O}$ affords an oxido-bridged diiron core with symmetric TPA orientation, see **Figures 74 and 75** (these previously appeared as **Figure 49 and 50**). **Table 63** compares the structural features of $[\{\text{Fe}(\text{TPA})\text{Br}\}_2\text{O}](\text{ClO}_4)_2 \cdot \text{H}_2\text{O}$ to several linear oxido bridged complexes.

$[\{\text{Fe}(\text{TPA})\text{Br}\}_2\text{O}](\text{ClO}_4)_2 \cdot \text{H}_2\text{O}$ is quite similar to $[\{\text{Fe}(\text{TPA})\text{Cl}\}_2\text{O}](\text{ClO}_4)_2$,⁴⁴ $[\{\text{Fe}(\text{TPA})(\text{NCO})\}_2\text{O}](\text{ClO}_4)_2 \cdot 2\text{CH}_3\text{OH}$,⁴² and $[\{\text{Fe}(\text{TPA})(\text{NCS})\}_2\text{O}](\text{ClO}_4)_2$ ²⁶ and these are linear. All these dimers are symmetric with their bridging oxides sitting on special positions. Except for $[\{\text{Fe}(\text{TPA})(\text{NCS})\}_2\text{O}](\text{ClO}_4)_2$ where the bridging oxide sits on a center of symmetry, the structures have a two-fold symmetry axis containing the bridging oxide. Therefore, the asymmetric unit contains half of the cation.

In all these complexes the iron centers are pseudo-octahedral. Each iron is bonded to four nitrogens of TPA, the bridging oxide, and either Br/ Cl/ NCO/ NCS. One of the pyridine nitrogen atoms (N2) is *trans* to the oxido bridge and the tertiary amine is *cis* to the oxido bridge. Two of the pyridyl nitrogen atoms (N1 and N3) are mutually

trans to each other. Each Br/Cl/NCO/NCS atom is *trans* to the tertiary amine nitrogen and *cis* to the bridging oxide. The halides/pseudo-halides are *anti*.

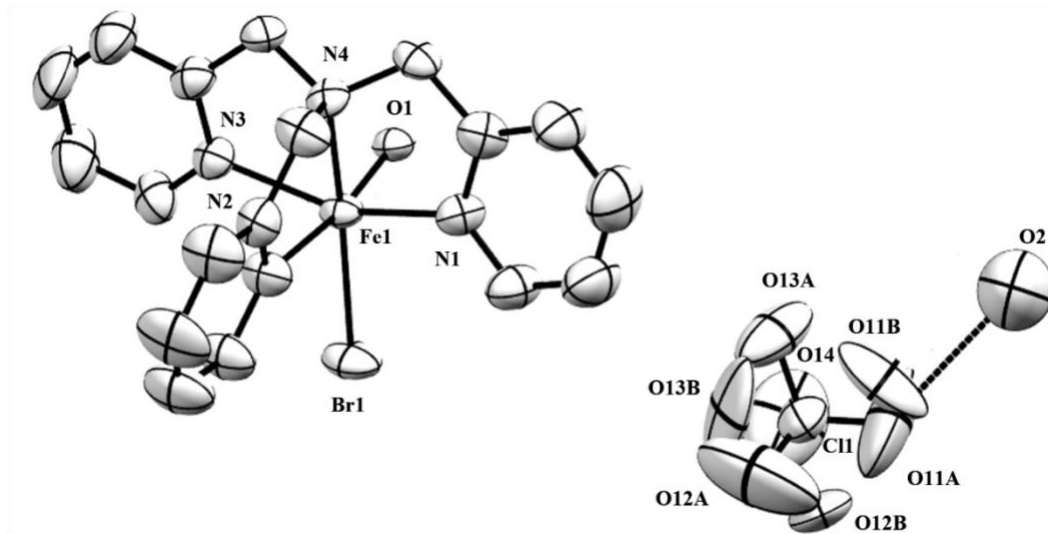


Figure 74. A view of the asymmetric unit of $[\{Fe(TPA)Br\}_2O](ClO_4)_2 \bullet H_2O$.

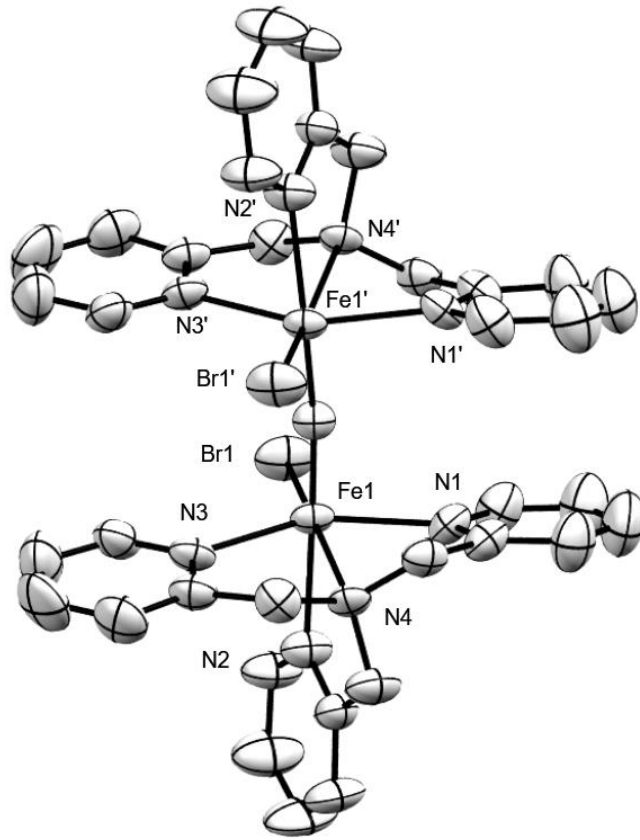


Figure 75. A view of the cationic portion of $[\{Fe(TPA)Br\}_2O](ClO_4)_2 \cdot H_2O$. Hydrogen atoms are omitted.

In $[\{Fe(TPA)Br\}_2O](ClO_4)_2 \cdot H_2O$ the Fe-N_{py} (N2) distance *trans* to the oxido bridge is longer (2.237(7) Å) than the other two Fe-N_{py} bonds that are mutually *trans* (average 2.144(7) Å). This demonstrates the strong *trans* influence of the oxide compared to the pyridine nitrogen. The Fe-N_{amine} distance (2.220(6) Å) is significantly longer than the average Fe-N_{pyr} distance (2.175(7) Å). The Fe-O bond length is 1.7844(11) Å. Comparing $[\{Fe(TPA)Br\}_2O](ClO_4)_2 \cdot H_2O$ to $[\{Fe(TPA)Cl\}_2O](ClO_4)_2$ ⁴⁴, $[\{Fe(TPA)(NCO)\}_2O](ClO_4)_2 \cdot 2CH_3OH$ ²⁶ and $[\{Fe(TPA)(NCS)\}_2O](ClO_4)_2$ ²⁶ the average Fe-N_{pyr} distances for these four complexes are (excluding the N_{pyr} *trans* to the oxido bridge) 2.144(7), 2.143(7), 2.152(3) and 2.147(3) Å, which are all within 3σ. For

the Fe-O distances, the first two are quite similar ($1.7844(11)$ Å and $1.785(1)$ Å, respectively) and the other two are similar to each other ($1.7925(6)$ Å and $1.7921(4)$ Å).

Clearly the Fe-O bond distance for $[\{\text{Fe}(\text{TPA})\text{Br}\}_2\text{O}] (\text{ClO}_4)_2 \bullet \text{H}_2\text{O}$ is significantly shorter than $[\{\text{Fe}(\text{TPA})(\text{NCO})\}_2\text{O}] (\text{ClO}_4)_2 \bullet 2\text{CH}_3\text{OH}$ ²⁶ and $[\{\text{Fe}(\text{TPA})(\text{NCS})\}_2\text{O}] (\text{ClO}_4)_2$.²⁶ This indicates that $[\{\text{Fe}(\text{TPA})\text{Br}\}_2\text{O}] (\text{ClO}_4)_2 \bullet \text{H}_2\text{O}$ has the strongest Fe-oxido bond while $[\{\text{Fe}(\text{TPA})(\text{NCO})\}_2\text{O}] (\text{ClO}_4)_2 \bullet 2\text{CH}_3\text{OH}$ has the weakest Fe-oxido bond.

One can compare the $[\{\text{Fe}(\text{TPA})\text{Br}\}_2\text{O}] (\text{ClO}_4)_2 \bullet \text{H}_2\text{O}$ complex with the linear yet asymmetric TPA complexes: $[\{\text{Fe}(\text{TPA})(\text{N}_3)\}_2\text{O}] (\text{ClO}_4)_2 \bullet \text{CH}_3\text{CN}$ ²⁶ and $[\{\text{Fe}(\text{TPA})\text{F}\}_2\text{O}] (\text{ClO}_4)_2 \bullet 0.5\text{CH}_3\text{OH}$.⁴⁸ In these asymmetric complexes the two iron centers are distinct. At one site a pyridine is *trans* to the oxide bridge while the tertiary amine is *trans* to the oxide bridge at the other site. The appropriate comparison is $[\{\text{Fe}(\text{TPA})\text{Br}\}_2\text{O}] (\text{ClO}_4)_2 \bullet \text{H}_2\text{O}$ to the analogous iron site (Fe1) of $[\{\text{Fe}(\text{TPA})(\text{N}_3)\}_2\text{O}] (\text{ClO}_4)_2 \bullet \text{CH}_3\text{CN}$; that is, the iron with the pyridine nitrogen *trans* to the oxido bridge.

Table 63. Comparison of relevant distances and angles of some symmetrical oxido-bridged dinuclear Fe(III)-TPA and the mononuclear $[Fe(TPA)Br_2]^+$.

	X = Br	X = Cl ⁴⁴	X = NCO ²⁶	X = NCS ²⁶	X = N ₃ ²⁶	X = Br (monomer) ²⁶
∠Fe1-O-Fe2	174.6(5)	174.7(5)	169.0(2)	180	173.9(2)	
Fe1-----Fe2	3.565(4)	3.565(2)				
Fe-O	1.7844(11)	1.785(1)	1.7925(6)	1.7921(4)	1.807(4)	
Fe-N _{3°}	2.220(6)	2.227(6)	2.219(3)	2.208(3)	2.232(5)	2.207(5)
Fe-N _{py}	2.160(7)	2.158(7)	2.166(3)	2.151(3)	2.170(5)	2.133(5)
	2.127(7)	2.127(7)	2.137(3)	2.142(3)	2.152(4)	2.121(5)
Fe-N _{trans}	2.237(7)	2.245(6)	2.231(3)	2.213(2)	2.230(5)	2.222(6)
Fe-X	2.4477(13)	2.298(2)	1.993(3)	2.046(3)	1.969(5)	2.389(1)
						2.449(1)*
Fe'-X					2.023(5)	
Fe'-O					1.788(4)	
Fe'-N _{3°}					2.264(5)	
Fe'-N _{py}					2.175(5)	

	X = Br	X = Cl ⁴⁴	X = NCO ²⁶	X = NCS ²⁶	X = N ₃ ²⁶	X = Br (monomer) ²⁶
					2.146(5)	
Fe'-N _{cis}					2.203(5)	

a : distances corresponding to Fe1

b : distances corresponding to Fe2

N_{py}: distances of pyridyl N which are mutually
trans

* : the Fe-Br distance *trans* to pyridine

N_{trans} : pyridyl N distance *trans* to the oxido
bridge (and *trans* to bromide for the
monomer)

The Fe-N_{3°} bond of [{Fe(TPA)Br}₂O](ClO₄)₂•H₂O is (2.220(6)) Å and the corresponding distances in [{Fe(TPA)(N₃)₂O](ClO₄)₂•CH₃CN and [{Fe(TPA)F}₂O](ClO₄)₂•0.5CH₃OH (2.232(5) Å and 2.247(5) Å, respectively) are significantly longer than the Fe-N_{py} bonds. The Fe-O (1.7844(11) Å) of the bromide dimer is comparable to the other complexes (1.807(4) Å and 1.799(4) Å).

If we compare the average Fe-N_{pyr} distances that are mutually *trans* in [{Fe(TPA)Br}₂O](ClO₄)₂•H₂O (2.244(7) Å) to the monomeric complex [Fe(TPA)Br₂](ClO₄)₂ (2.127(5) Å) the latter is considerably shorter. Similarly, for the N_{3°} and Cl⁻ systems, where both dimeric and monomeric forms have been structurally characterized,^{26,48} the mutually *trans* Fe-N_{pyr} bond distances for the dimers are 2.270(7) Å and 2.238(4) Å and for the monomers those values are 2.130(6) Å and 2.130(4) Å, respectively. The oxido bridged complexes have longer Fe-N_{pyr} distances than the monomers. This major difference in bond distances is due to the presence of the bridging oxide. If we designate the Fe-O vector as the z-axis, then the p_z orbital of oxide interacts in a σ fashion with the iron d_{z²} orbital, and the d_{x²-y²} orbital remains to interact with the

tertiary amine, the halide *trans* to it and the mutually *trans* pyridine nitrogens in a σ fashion. If we designate the Fe-Br vector as the x-axis, then this orients the metal d_{xz} orbital for π interaction with both the oxide and the bromide. Since oxide is a stronger π donor than bromide, the presence of oxide will weaken the ability of bromide to donate to the metal in π manner. Evidence for this is found in the much longer Fe-Br distance for the dimer as compared to the monomer ($2.4411(13)$ Å verses $2.389(1)$ Å, respectively). This is also referred to as the *cis* effect of the oxide.

4.4.2. Oxido-bridged diiron(III) complexes with asymmetric TPA orientation

Seven bent-oxido complexes, two polymorphic $[\{\text{Fe}(\text{TPA})\}_2\text{O}(\text{OAc})](\text{ClO}_4)_3 \cdot \text{H}_2\text{O}$ (**2,3**), $[\{\text{Fe}(\text{TPA})\}_2\text{O}(4\text{-hydroxybenzoato})](\text{ClO}_4)_3$ (**4**), $[\{\text{Fe}(\text{TPA})\}_2\text{O}(4\text{-methoxybenzoato})](\text{ClO}_4)_3$ (**5**), $[\{\text{Fe}(\text{TPA})\}_2\text{O}(4\text{-fluorobenzoato})](\text{ClO}_4)_3$ (**6**), $[\text{Fe}_2(\text{TPA})_2\text{O}(3,5\text{-dimethylbenzoato})](\text{ClO}_4)_3 \cdot 0.5\text{H}_2\text{O}$ (**8**) and $[\{\text{Fe}(\text{TPA})\}_2\text{O}(3,5\text{-dihydroxybenzoato})](\text{ClO}_4)_3 \cdot \text{CH}_3\text{CN}$ (**9**) were synthesized and their crystal structures were determined. All of these (μ -oxido)(μ -carboxylato)diiron(III)TPA complexes contain distinct iron centers with the tertiary amine *trans* to the oxido-bridge on Fe2 while the pyridine nitrogen is *trans* to the oxido-bridge on Fe1. Each iron is connected to four nitrogen atoms of TPA, the bridging oxide, and a bridging carboxylate oxygen, hence the iron centers are pseudo-octahedral.

For Fe1, the bridging oxide is *trans* to the pyridine nitrogen (N12) and for Fe2, it is *trans* to the tertiary amine nitrogen (N24). This orientation makes the Fe-O_{COOR} *trans* to the tertiary amine on Fe1, while it is *trans* to the pyridine nitrogen for Fe2. Also, for both iron centers this Fe-O_{COOR} bond is *cis* to the oxido bridge. For each iron center

there are two pyridine nitrogens that are mutually *trans* (N11 and N13 for Fe1, and N21 and N23 for Fe2). Similar to the Fe-O_{COOR} bonds, these mutually *trans* pyridines are also *cis* to the oxido bridge. **Table 64** lists selected pertinent bond lengths and angles of these seven structures. **Table 65** lists several previously reported bent oxido-bridged diiron(III)TPA complexes that also have an asymmetric diiron(III)TPA core. In all of these complexes, the bonds *trans* to the bridging oxide (Fe-N_{pyr} on Fe1 and Fe-N_{3°} of Fe2) are the longest iron ligand bonds for each iron. This indicates that oxide has the strongest *trans* influence. After the longest Fe-N_{pyr} bond, which is *trans* to the oxide, for the two polymorphic [{Fe(TPA)}₂O(OAc)][ClO₄]₃•H₂O (**2,3**) complexes the second longest Fe-N_{pyr} bond is Fe2-N22 which is *trans* to the carboxylate bridge. For the remaining five complexes, the second longest Fe-N_{pyr} is one that is *trans* to another pyridine.

The complexes all have two different tertiary amine distances: the Fe2-N_{3°} bond which is *trans* to the bridging oxide is longer than the Fe1-N_{3°} bond which is *trans* to the carboxylate oxygen. This indicates that oxide has a stronger *trans* influence than carboxylate. This is reinforced by comparing the Fe-N_{pyr} distances that are *trans* to the oxido bridge and those that are *trans* to the carboxylate oxygen. Oxide is more basic and a stronger σ and π donor to the metal center. In asymmetric (μ -oxido)(μ -carboxylato) diiron(III)TPA complexes, the shortest metal ligand bond distances are always for the Fe-O_{bridge}. When comparing the Fe-N distances that are *trans* to the carboxylate, the Fe-N_{3°} on Fe1 is longer than Fe-N_{pyr} on Fe2.

Table 64. Comparison of pertinent bond distances and angles of (μ -oxido)(μ -carboxylato)diiron(III)TPA complexes.

(All bond lengths are in Å, and all angles are in deg.).

	OAc(2)	OAc(3)	L4	L5	L6	L8		L9
Fe-O-Fe	129.95(12)	129.82(19)	129.86(14)	129.93(15)	130.56(10)	131.21(14)	131.97(14)	131.8(2)
Fe-O _{bridge}	1.800(2) ^a	1.810(3) ^a	1.801(3) ^a	1.806(3) ^a	1.8031(19) ^a	1.809(2) ^a	1.796(2) ^a	1.814(4) ^a
	1.777(2) ^b	1.777(3) ^b	1.790(2) ^b	1.782(3) ^b	1.7819(19) ^b	1.781(2) ^b	1.786(2) ^b	1.789(4) ^b
Fe-O _{COOR}	1.949(3) ^{a,d}	1.968(4) ^{a,d}	1.986(2) ^{a,d}	1.977(3) ^{a,d}	1.987(18) ^{a,d}	1.980(3) ^{a,d}	1.979(3) ^{a,d}	1.988(5) ^{a,d}
	2.017(2) ^b	2.031(4) ^b	2.023(3) ^b	2.033(3) ^b	2.035(2) ^b	2.058(3) ^b	2.064(3) ^b	2.059(4) ^b
Fe-N _{3°}	2.186(3) ^{a,e}	2.196(4) ^{a,e}	2.187(3) ^{a,e}	2.180(3) ^{a,e}	2.184(2) ^{a,e}	2.186(3) ^{a,e}	2.186(3) ^{a,e}	2.205(6) ^{a,e}
	2.237(3) ^{b,c}	2.243(4) ^{b,c}	2.237(3) ^{b,c}	2.246(4) ^{b,c}	2.243(3) ^{b,c}	2.229(3) ^{b,c}	2.233(3) ^{b,c}	2.251(6) ^{b,c}
Fe-N _{pyr}	2.125(3) ^a	2.133(5) ^a	2.140(3) ^a	2.125(4) ^a	2.126(3) ^a	2.119(3) ^a	2.151(3) ^a	2.140(6) ^a
	2.213(3) ^{a,c}	2.214(4) ^{a,c}	2.218(3) ^{a,c}	2.204(3) ^{a,c}	2.201(2) ^{a,c}	2.218(3) ^{a,c}	2.206(3) ^{a,c}	2.212(6) ^{a,c}
	2.129(3) ^a	2.135(5) ^a	2.158(3) ^a	2.151(4) ^a	2.145(2) ^a	2.114(3) ^a	2.139(3) ^a	2.144(6) ^a
	2.135(3) ^b	2.146(5) ^b	2.138(3) ^b	2.122(4) ^b	2.123(3) ^b	2.155(3) ^b	2.122(4) ^b	2.158(6) ^b
	2.139(3) ^{b,e}	2.147(4) ^{b,e}	2.123(3) ^{b,e}	2.123(3) ^{b,e}	2.115(2) ^{b,e}	2.135(3) ^{b,e}	2.111(3) ^{b,e}	2.148(6) ^{b,e}
	2.125(3) ^b	2.126(5) ^b	2.117(3) ^b	2.130(4) ^b	2.131(3) ^b	2.107(3) ^b	2.143(3) ^b	2.139(6) ^b

L4 : [{Fe(TPA)}₂O(4-hydroxybenzoato)]
 $(\text{ClO}_4)_3$
L5 : [{Fe(TPA)}₂O(4-methoxybenzoato)]
 $(\text{ClO}_4)_3$
L6 : [{Fe(TPA)}₂O(4-fluorobenzoato)]
 $(\text{ClO}_4)_3$

a : distances corresponding to Fe1
b : distances corresponding to Fe2

L8 : [Fe₂(TPA)₂O(3,5-dimethylbenzoato)]
 $(\text{ClO}_4)_3 \cdot 0.5\text{H}_2\text{O}$
L9 : [{Fe(TPA)}₂O(3,5-dihydroxybenzoato)]
 $(\text{ClO}_4)_3 \cdot \text{CH}_3\text{CN}$

c : atoms *trans* to the oxido bridge
d : atoms *trans* to the tertiary amine
e : atoms *trans* to carboxylate

Table 65. Comparison of pertinent bond distances and angles of previously studied (μ -oxido)(μ -carboxylato)diiron(III)TPA complexes along with linear (μ -oxido)(4-nitrobenzoate)₂diiron(III)TPA complex.
(All bond lengths are in Å, and all angles are in deg.).

	L10	L11	L12	L13	L14	L15	L16
Fe-O-Fe	130.10(4)	128.9(2)	129.1(2)	129.7(3)	131.0(3)	125.4(3)	180
Fe-O _{bridge}	1.807(2) ^a	1.806(4) ^a	1.811(4) ^a	1.804(5) ^a	1.808(6) ^a	1.817(5) ^a	1.783(8)
	1.780(2) ^b	1.793(4) ^b	1.775(4) ^b	1.776(4) ^b	1.779(5) ^b	1.784(5) ^b	
Fe-O _{COOR}	1.983(3) ^{a,d}	1.971(4) ^{a,d}	1.995(4) ^{a,d}	1.985(5) ^{a,d}	1.973(5) ^{a,d}	1.911(6) ^{a,d}	
	2.053(3) ^b	2.040(4) ^b	2.040(4) ^b	2.046(5) ^b	2.034(5) ^b	1.953(6) ^b	
Fe-N _{3°}	2.170(3) ^a	2.175(4) ^a	2.198(5) ^a	2.190(6) ^a	2.187(6) ^a	2.204(7) ^a	2.224(3)
	2.247(3) ^{b,c}	2.234(4) ^{b,c}	2.224(5) ^{b,c}	2.218(6) ^{b,c}	2.239(7) ^{b,c}	2.245(7) ^{b,c}	
Fe-N _{pyr}	2.130(3) ^a	2.143(5) ^a	2.120(5) ^a	2.115(6) ^a	2.140(3) ^a	2.137(7) ^a	2.215(3) ^c

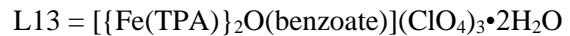
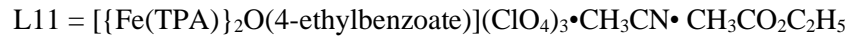
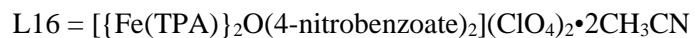
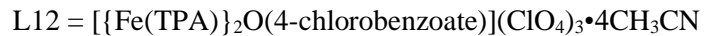
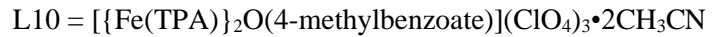
	L10	L11	L12	L13	L14	L15	L16
	2.141(3) ^a	2.144(5) ^a	2.122(6) ^a	2.132(7) ^a	2.209(8) ^a	2.205(6) ^a	2.182(3)
	2.214(3) ^{a,c}	2.223(4) ^{a,c}	2.185(5) ^{a,c}	2.185(6) ^{a,c}	2.143(8) ^{a,c}	2.112(7) ^{a,c}	2.159(3)
	2.124(3) ^b	2.119(4) ^b	2.140(6) ^b	2.131(6) ^b	2.133(9) ^b	2.149(8) ^b	
	2.124(3) ^b	2.119(5) ^b	2.134(5) ^b	2.138(6) ^b	2.103(7) ^b	2.156(8) ^b	
	2.122(3) ^b	2.116(5) ^b	2.138(5) ^b	2.118(6) ^b	2.133(8) ^b	2.158(9) ^b	
Reference	42	42	42	25	24	24	42

a : distances corresponding to Fe1

b : distances corresponding to Fe 2

c : atoms *trans* to the oxido bridge

d : atoms *trans* to the tertiary amine



The Fe-O_{COOR} distance which is *trans* to the pyridine nitrogen is always longer than the Fe-O_{COOR} distance which is *trans* to the tertiary amine nitrogen. Similarly, the Fe1-O1 distance is longer than Fe2-O1 (the latter bond is *trans* to the tertiary amine). Taken together, this demonstrates that the pyridine nitrogen exerts a stronger *trans* influence than the tertiary amine.

The cationic portion of $\left[\{\text{Fe}(\text{TPA})\}_2\text{O}(\text{OAc})\right](\text{ClO}_4)_3 \cdot \text{H}_2\text{O}$ P2₁/c (**2**) polymorph is shown in **Figure 76** (this previously appeared as **Figure 52**). This illustrates the typical asymmetric TPA environment of this complex. The relevant bond angles and distances and crystallographic information are given in section 3.3.2.1.

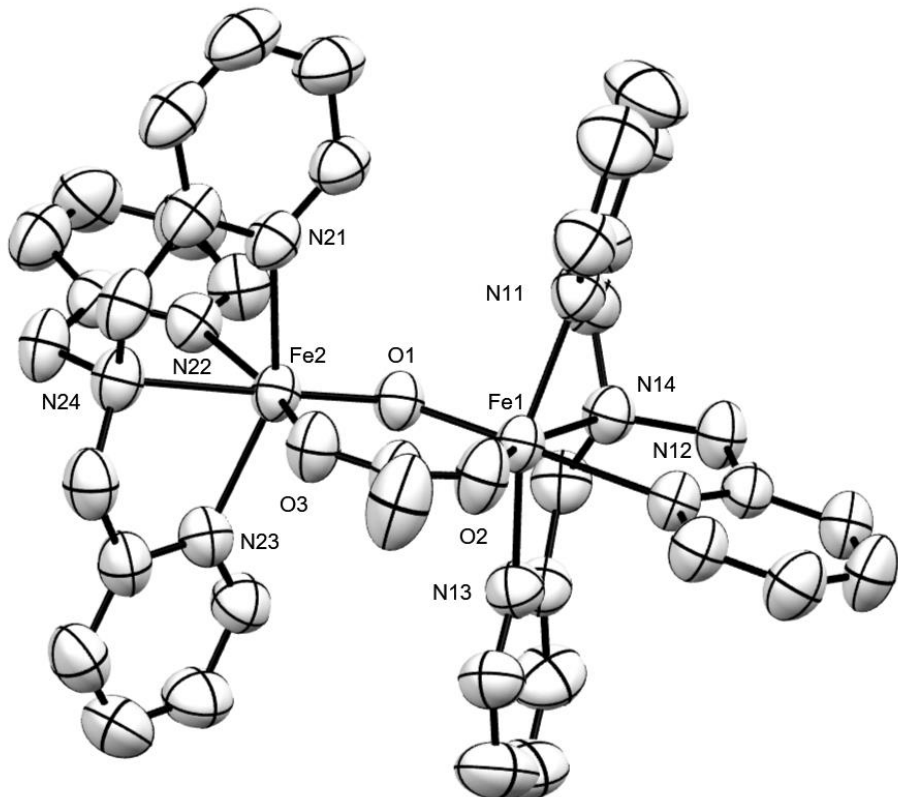


Figure 76. A view of the cationic portion of $\left[\{\text{Fe}(\text{TPA})\}_2\text{O}(\text{OAc})\right](\text{ClO}_4)_3 \cdot \text{H}_2\text{O}$ P2₁/c polymorph. Hydrogen atoms are omitted.

The average Fe-TPA distances on Fe1 and Fe2, excluding the bonds *trans* to the oxido bridge, are 2.145(3) Å and 2.133(3) Å, respectively.

The cationic portion of $\left[\{Fe(TPA)\}_2O(OAc)\right](ClO_4)_3 \cdot H_2O$ P2₁/n (**3**) polymorph is shown in **Figure 77** (this previously appeared as **Figure 54**). This again illustrates the typical asymmetric TPA environment of this complex. The relevant bond angles and distances and crystallographic information are given in section 3.3.2.2. The average Fe-TPA distances on Fe1 and Fe2 excluding the bonds *trans* to the oxido bridge 2.155(5) Å and 2.140(5) Å, respectively.

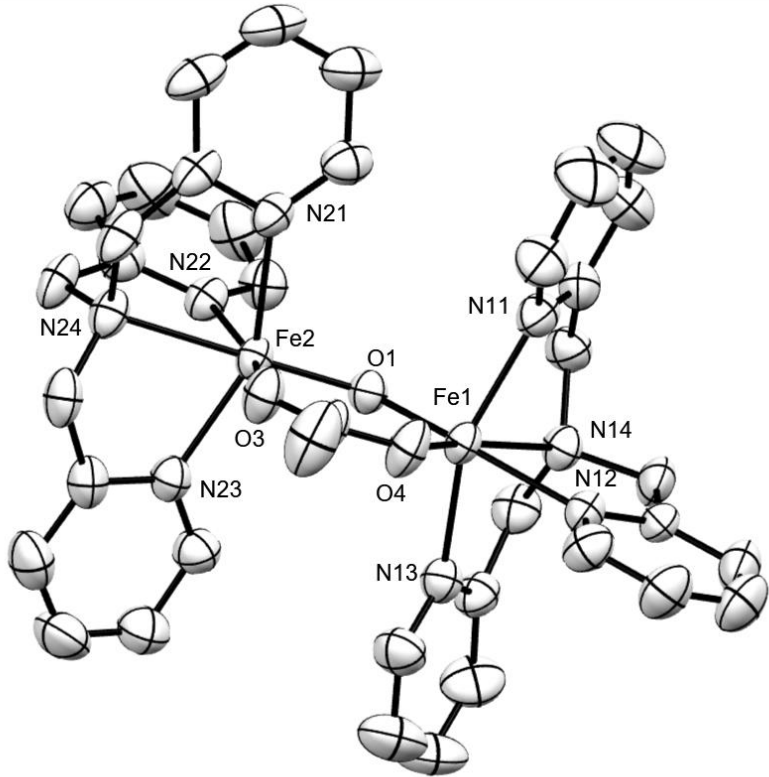


Figure 77. A view of the cationic portion of $\left[\{Fe(TPA)\}_2O(OAc)\right](ClO_4)_3 \cdot H_2O$ P2₁/n polymorph. Hydrogen atoms are omitted.

When we compare the two polymorphic structures, all of the bond lengths and angles are similar, and none are significantly different between the two structures. The differences of the structures **2** and **3** are the differences in the packing of the perchlorates and the water molecule as mentioned previously in the section 3.3.2.

The cationic portion of $\left[\{\text{Fe}(TPA)\}_2\text{O}(4\text{-hydroxybenzoato})\right](\text{ClO}_4)_3$ is shown in **Figure 78** (this previously appeared as **Figure 56**). This again illustrates the typical asymmetric TPA environment of this complex. The relevant bond angles and distances and crystallographic information are given in section 3.3.3. The average Fe-TPA

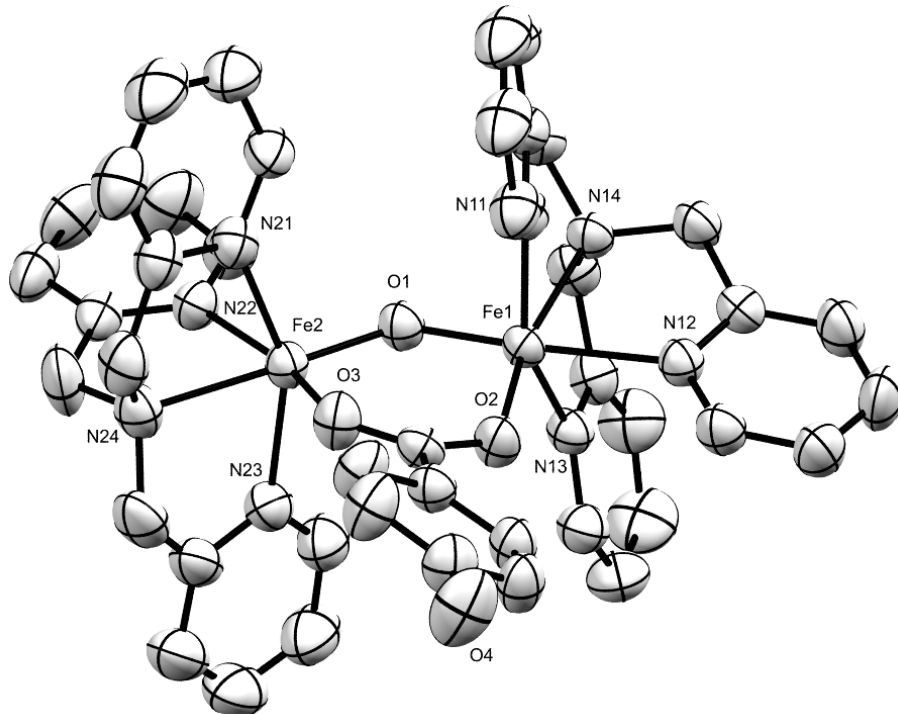


Figure 78. A view of the cationic portion of $\left[\{\text{Fe}(TPA)\}_2\text{O}(4\text{-hydroxybenzoato})\right](\text{ClO}_4)_3$. Hydrogen atoms are omitted.

distances on Fe1 and Fe2, excluding the bonds *trans* to the oxido bridge, are 2.162(3) Å and 2.126(3) Å, respectively.

The cationic portion of $[\{Fe(TPA)\}_2O(4\text{-methoxybenzoato})](ClO_4)_3$ (**5**) is shown in **Figure 79** (this previously appeared as **Figure 59**). This again illustrates the typical asymmetric TPA environment of this complex. The relevant bond angles and distances and crystallographic information are given in section 3.3.4. The average Fe-TPA distances on Fe1 and Fe2, excluding the bonds *trans* to the oxido bridge are 2.152(4) Å and 2.125(4), Å respectively.

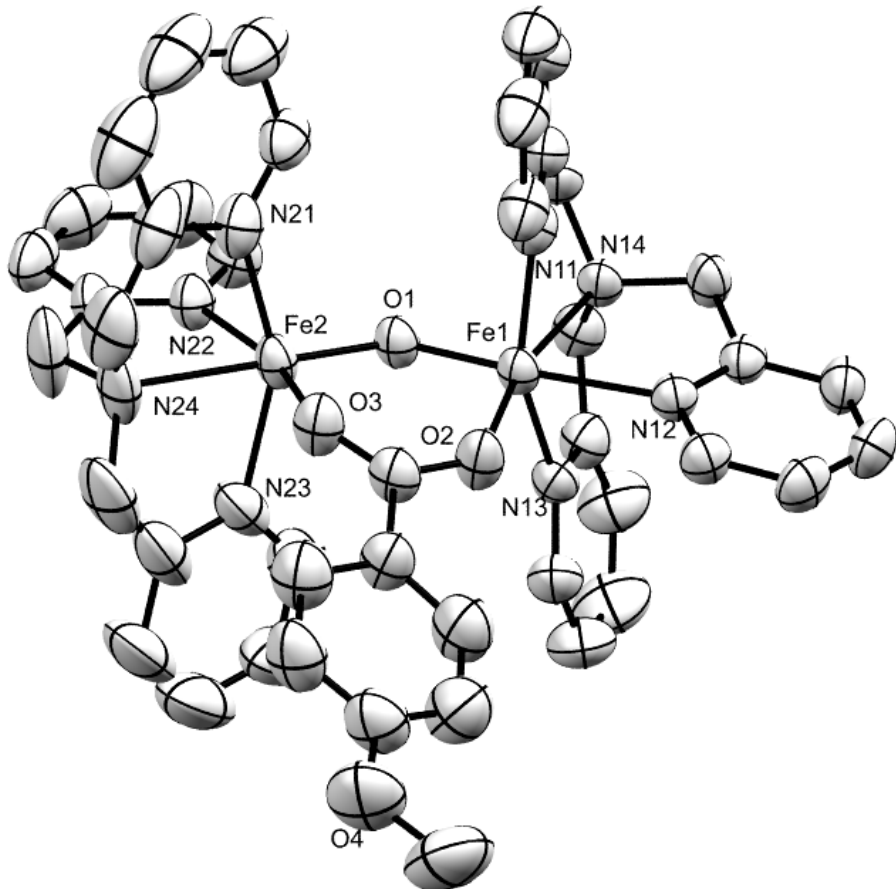


Figure 79. A view of the cationic portion of $[\{Fe(TPA)\}_2O(4\text{-methoxybenzoato})](ClO_4)_3$. Hydrogen atoms are omitted.

The cationic portion of $[\{Fe(TPA)\}_2O(4\text{-fluorobenzoato})](ClO_4)_3$ (**6**) is shown in **Figure 80** (this previously appeared as **Figure 62**). This again illustrates the typical asymmetric TPA environment of this complex. The relevant bond angles and distances and crystallographic information are given in section 3.3.5. The average Fe-TPA distances on Fe1 and Fe2, excluding the bonds *trans* to the oxido bridge, are 2.152(3) Å and 2.123(3) Å, respectively.

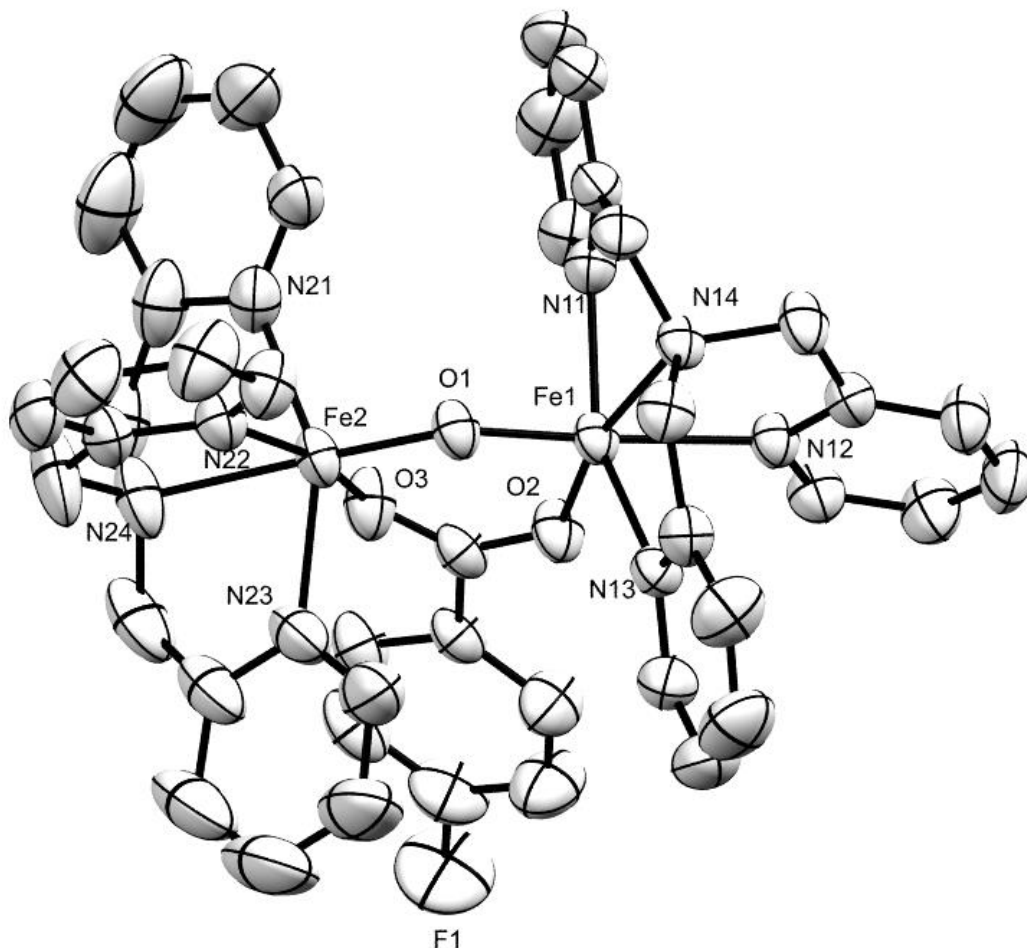


Figure 80. A view of the cationic portion of $[\{Fe(TPA)\}_2O(4\text{-fluorobenzoato})](ClO_4)_3$. Hydrogen atoms are omitted.

The cationic portion of $[Fe_2(TPA)_2O(3,5\text{-dimethylbenzoato})](ClO_4)_3 \bullet 0.5H_2O$ (**8**) is shown in **Figure 81** (this previously appeared as **Figure 65**). This again illustrates the typical asymmetric TPA environment of this complex. The relevant bond angles and distances and crystallographic information are given in section 3.3.6. The asymmetric unit of this complex contains two complete dimeric units. There is only one water molecule per asymmetric unit.

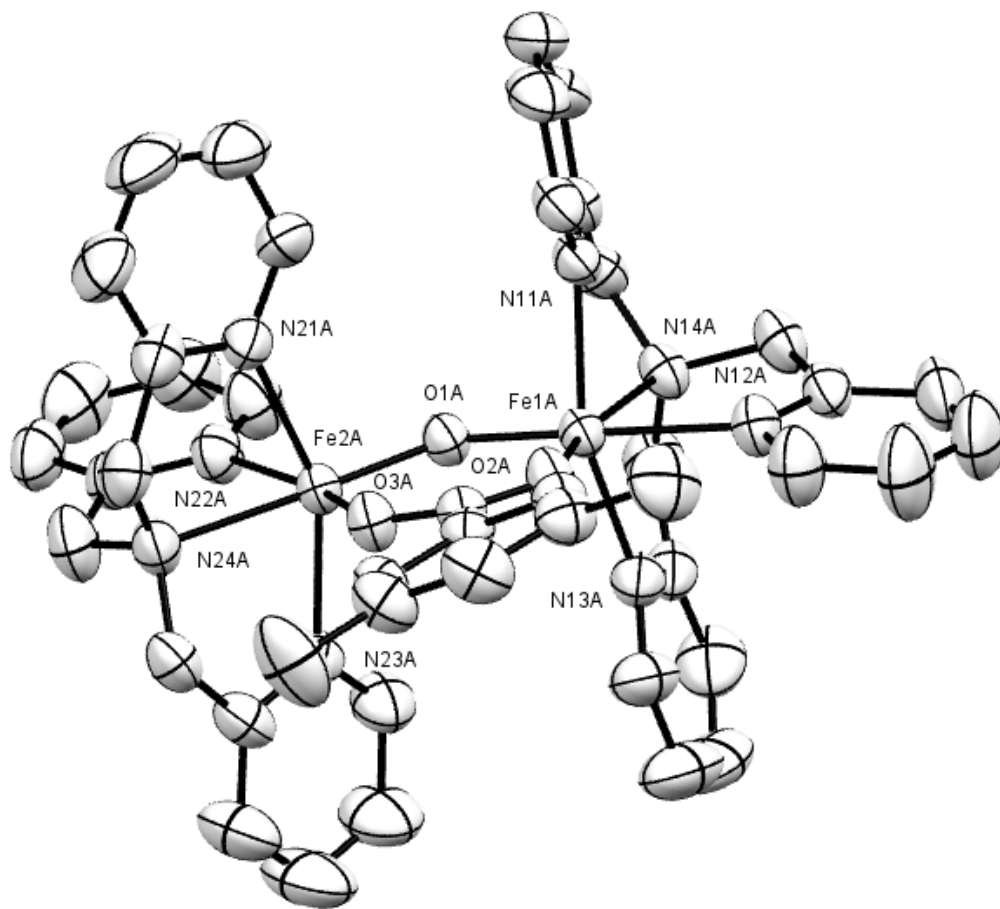


Figure 81. A view of the cationic portion of $[Fe(TPA)_2O(3,5\text{-dimethylbenzoato})](ClO_4)_3 \bullet 0.5H_2O$. Hydrogen atoms are omitted.

The cationic portion of $[\{\text{Fe}(TPA)\}_2\text{O}(3,5\text{-dihydroxybenzoato})](\text{ClO}_4)_3 \bullet \text{CH}_3\text{CN}$ (9) is shown in **Figure 82** (this previously appeared as **Figure 68**). This again illustrates the typical asymmetric TPA environment of this complex. The relevant bond angles and distances and crystallographic information are given in section 3.3.7. The average Fe-TPA distances on Fe1 and Fe2, excluding the bonds *trans* to the oxido bridge, are 2.163(6) Å and 2.148(6) Å, respectively.

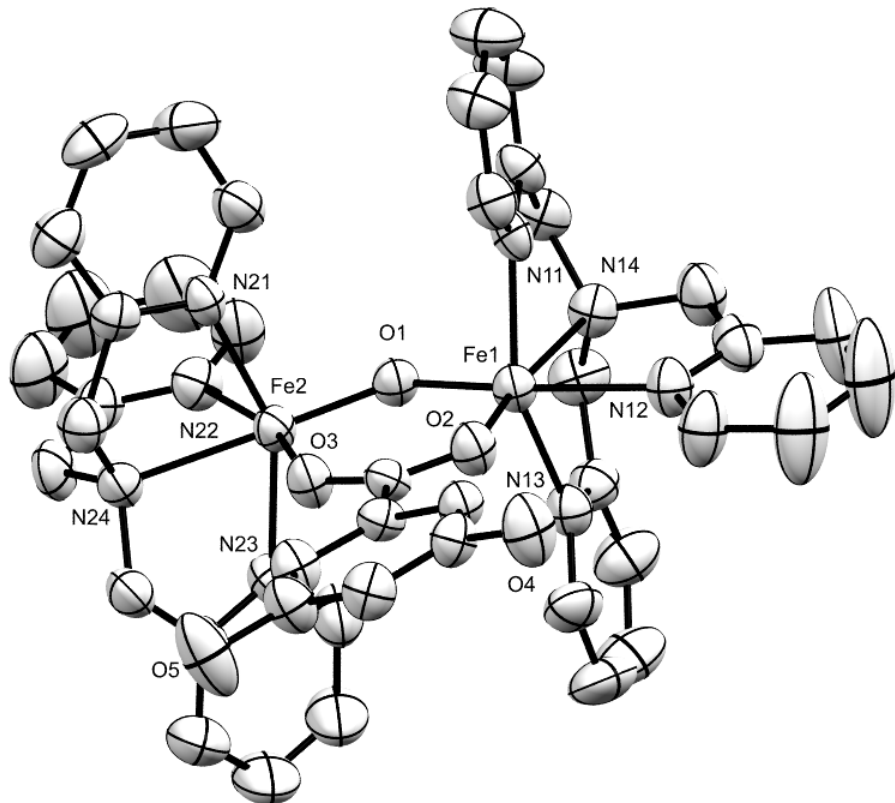


Figure 82. A view of the cationic portion of $[\{\text{Fe}(TPA)\}_2\text{O}(3,5\text{-dihydroxybenzoato})](\text{ClO}_4)_3 \bullet \text{CH}_3\text{CN}$. Hydrogen atoms are omitted.

Table 66 compares selected bond angles and bond lengths for the two polymorphic $[\{\text{Fe}(TPA)\}_2\text{O}(\text{OAc})](\text{ClO}_4)_3 \bullet \text{H}_2\text{O}$ structures of the current study along

with two previously reported $[\{\text{Fe}(TPA)\}_2\text{O}(\text{OAc})]^{3+}$. Since these cations are the same, they have the same general structure as described above. All the Fe-N, Fe-oxido and Fe-O_(OAc) distances are similar within experimental error with minor variations. The average Fe-N bond distances (2.139(3) Å and 2.148(5) Å) for the two polymorphs are very similar and the two previously reported structures have slightly longer Fe-N distances (2.164 (4) Å and 2.161(7) Å). When considering the carboxylate bond distances, the Fe-O_{COOR} bond that is *trans* to the tertiary amine is slightly shorter in the P2₁/c polymorph (complex **2**) in the current study (1.949(3) Å) and the three others have an average of 1.971(2) Å. The Fe-O_{COOR} bond that is *trans* to the pyridine nitrogen is also comparatively shorter for the P2₁/c polymorph (2.017(2) Å) and the three others have an average of 2.041(6) Å. Unlike the other structures studied, in these four complexes the second longest Fe-N_{pyr} bond is the bond *trans* to the carboxylate.

Table 66. The comparison of (μ -oxido)(μ -OAc)diiron(III)TPA polymorphs with previous acetate bridged diiron(III) complexes.

(All bond lengths are in Å, and all angles are in deg.).

	L2	L3	Reference ⁴⁹	Reference ³³
Fe-O-Fe	129.95(12)	129.82(19)	131.26(15)	129.2(2)
Fe-O _{bridge}	1.800(2) ^a	1.810(3) ^a	1.814(3) ^a	1.800(4) ^a
	1.777(2) ^b	1.777(3) ^b	1.778(3) ^b	1.790(5) ^b
Fe-O _{COOR}	1.949(3) ^{a,d}	1.968(4) ^{a,d}	1.974(3) ^{a,d}	1.972(6) ^{a,d}
	2.017(2) ^b	2.031(4) ^b	2.054(3) ^b	2.038(6) ^b
Fe-N _{3°}	2.186(3) ^a	2.196(4) ^a	2.192(3) ^a	2.198(7) ^a
	2.237(3) ^{b,c}	2.243(4) ^{b,c}	2.241(3) ^{b,c}	2.242(6) ^{b,c}
Fe-N _{pyr}	2.125(3) ^a	2.133(5) ^a	2.134(4) ^a	2.128(6) ^a
	2.213(3) ^{a,c}	2.214(4) ^{a,c}	2.192(4) ^{a,c}	2.199(6) ^{a,c}
	2.129(3) ^a	2.135(5) ^a	2.133(4) ^a	2.125(6) ^a

	L2	L3	Reference ⁴⁹	Reference ³³
	2.135(3) ^b	2.146(5) ^b	2.135(4) ^b	2.133(6) ^b
	2.139(3) ^b	2.147(4) ^b	2.156(4) ^b	2.154(6) ^b
	2.125(3) ^b	2.126(5) ^b	2.124(3) ^b	2.105(6) ^b

a : distances corresponding to Fe1
b : distances corresponding to Fe2

c : atoms *trans* to the oxido bridge
d : atoms *trans* to the tertiary amine

L2 = P2₁/c polymorph of [{Fe(TPA)}₂O(OAc)][ClO₄]₃•H₂O
L3= P2₁/n polymorph of [{Fe(TPA)}₂O(OAc)][ClO₄]₃•H₂O

When we compare the previous (μ -oxido)(μ -carboxylato)diiron(III)TPA structures with the current structures, we note that the carbonate bridged Fe(III)-TPA complex exhibits differences in many of its bond lengths and the Fe-O-Fe angle. The carbonate bridged complex has shorter Fe-Ocoor bond distances (1.932(6) Å) while all of the other complexes have an average of 2.00 Å or more. This, in turn, results in a smaller Fe-O-Fe bond angle (125.4(3)° vs an average 130.3(3)°) and longer iron oxido bridge (Fe-O_{bridge}) bond distances (1.800(5) Å vs an average 1.795(3) Å). This is due to the 2- charge of the carbonate compared to 1- for carboxylates. The higher charge of carbonate makes it more basic and a stronger donor to the metal center. The Fe-N bonds in the carbonate are longer than the rest of the complexes (2.170(9) Å vs 2.161(5) Å). These comparatively long Fe-N distances demonstrate the strong *trans* influence of carbonate compared to other carboxylates which have less charge and are hence less basic.

Previously, Harshini Arachchilage studied three (μ -oxido)(μ -modifiedbenzoate) diiron(III)TPA complexes (series 1) with 4-methylbenzoate, 4-ethylbenzoate, and 4-chlorobenzoate.⁴²

The modified benzoic acids used in the current study (4-hydroxybenzoic acid, 4-methoxybenzoic acid, 3,5-dimethylbenzoic acid, 4-fluorobenzoic acid, and 3,5-dihydroxybenzoic acid) have pK_a 's decreasing in the order 4.57, 4.47, 4.34, 4.14 and 3.96, respectively (series 2). Series 1 and series 2 have comparable Fe-O_{bridge} distances. For Fe1, the average Fe-O_{bridge} distances are 1.808(2) Å and 1.805(2) Å, respectively. For Fe2, the average Fe-O_{bridge} distances are 1.783(5) Å and 1.785(2) Å, respectively.

The average Fe-O_{COOR} bond distances for the resultant complexes are (2.005(3) Å, 2.005(3) Å, 2.024(18) Å, 2.020(3) Å, 2.020(5) Å) roughly increasing with the decreasing pK_a . As the pK_a decreases, the basicity of the carboxylate decreases resulting in weaker and therefore longer bonds. Both have similar Fe-O_{COOR} distances within experimental error. In series 1 and series 2 the Fe-O_{COOR} bond distance that are *trans* to the tertiary amine nitrogen are 1.983(7) Å and 1.984(2) Å, respectively. The Fe-O_{COOR} bond distance that are *trans* to the pyridine nitrogen are 2.044(4) Å and 2.042(7) Å, respectively. But these series have different Fe-N_{pyr} (2.148(6) Å and 2.134(5) Å) and Fe-N_{3°} (2.186(3) Å and 2.123(3) Å) distances. These variations in bond distances are not solely dependent on substituent pK_a . Factors like steric effects, H-bonding, and packing may also have an influence.

There is only one structurally characterized (μ -oxido)(modifiedbenzoate)₂ diiron(III)TPA complex: [{Fe(TPA)(4-nitrobenzoato)}₂O](ClO₄)₂ • 2CH₃CN.⁴² It is linear with symmetric TPA orientations. The iron center of [{Fe(TPA)(4-nitrobenzoato)}₂O](ClO₄)₂ • 2CH₃CN is comparable to the iron center with the oxido bridge *trans* to a pyridine and the carboxylate *trans* to tertiary amine (Fe1 site) in our complexes. When compared to that iron center of the bent (μ -oxido)(μ -modified-

benzoate)diiron(III) TPA complexes in this study, $pK_a = 3.42$ and the Fe-O_{COOR} are similar within experimental error. For our complexes, the average Fe-O_{COOR} distance is 1.984(2) Å, while for $[\{\text{Fe}(\text{TPA})(\text{4-nitrobenzoato})\}_2\text{O}](\text{ClO}_4)_2 \cdot 2\text{CH}_3\text{CN}$ it is 1.988(3) Å. The average Fe-O_{bridge} distance in these complexes (1.805(2) Å) is considerably longer than for $[\{\text{Fe}(\text{TPA})(\text{4-nitrobenzoato})\}_2\text{O}](\text{ClO}_4)_2 \cdot 2\text{CH}_3\text{CN}$ (1.7930(8) Å). Also, the Fe-N_{3°} bond (Fe1-N14) *trans* to the carboxylate oxygen is shorter in our complexes (average 2.188(6) Å) than the 4-nitro complex (2.224(3) Å). This indicated that the least basic 4-nitrobenzoate has bound to the iron weakly.

4.4.3. Lewis acidity and Trans influence of modified benzoate ligands

The Lewis acidity of a metal center is known to influence electron and group transfer processes in catalytic reactions.⁵⁰ Consequently it is expected to play an important role in reactions catalyzed by diiron(III)TPA complexes.

The factors affecting Lewis acidity in these complexes are often difficult to isolate.⁴⁸ As supportive evidence in these Fe(III)-TPA oxido bridged dimers, the Fe(III)-ligand bonds are dissimilar. The Fe-Oxide bond is longer for Fe1 and shorter for Fe2. The longer Fe-Oxide bond is associated with pyridine *trans* to the oxido bridge, and with the shorter Fe-carboxylate distance. In Jia Xue's study, she suggested that the Lewis acidity of the iron centers affects the Fe-N_{pyr} bond distances that are mutually *trans*. This, in turn, cancels the *trans* influence of the pyridine nitrogens. However, this does not rule out the *cis* influence of the oxido bridge, yet the effect is considerably smaller when compared to the *trans* influence.

The Fe-N_{pyr} distances that are mutually *trans* (Fe1-N11/ Fe1-N13 for Fe1 and Fe2-N21/ Fe2-N23 for Fe2) in this study are compared to those of previously reported complexes **Table 67**. In some cases, the Fe-N_{pyr} average distance for Fe1 is longer than for Fe2, but this is not universal. Generally, the average Fe-N_{pyr} distances are similar for all of the complexes and are not significantly different at the 3σ level. This suggests that all of the iron centers have similar Lewis acidities.

Since TPA is tetradentate, when coordinated to iron, there are one or two available coordination sites that permits study of the *trans* effect and *trans* influence. These two phenomena are widely used in coordination chemistry. The *trans* effect is the ability of a ligand to facilitate substitution in the position *trans* to itself, and it is a kinetic phenomenon. Thus, the higher the *trans* effect of a particular ligand, the higher the rate substitution of a ligand *trans* to it. In contrast, the *trans* influence is a thermodynamic phenomenon and is the impact that a ligand has on the metal-ligand bond *trans* to it. Thus, *trans* ligands have an influence on bond lengths and stabilities of ligands *trans* to it.⁵¹ Because of *trans* influences, the relative positions of ligands can affect reactions of the metal complexes by weakening certain bonds which enables bonding to an incoming ligand. The remaining part of the discussion is focused on *trans* influences.

Among (μ -oxido)(μ -modifiedbenzoato)diiron(III)TPA complexes the primary difference in the structure details is due to the substituted benzoate. These substituted benzoates have different basicities and the parent acids have different pK_a values. **Table 68** lists some structural features for the complexes and **Table 69** lists some previously reported carboxylate complexes. The basicities of the substituted benzoates in

these (μ -oxido)(μ -modified-benzoato)diiron(III)TPA complexes can affect the Fe-O_{COOR} bond strength. This, in turn, can be related to changes in the bonds *trans* to Fe-O_{COOR}. If one considers these Fe-O_{COOR} bonds to depend solely on the p*K*_a of substituted benzoates, as the p*K*_a decreases, the Fe-O_{COOR} bond strength should decrease, and this bond should be elongated. In turn, this makes the metal center more Lewis acidic, and the Fe1-N_{3°} or Fe-N_{pyr} should be shorter.

To examine any correlation between the basicity of the bridging carboxylate and the relevant iron-carboxylate bond distances, the Fe-O_(COOR) distances were plotted against the p*K*_a values of the acid form of the substituted benzoate for the complexes. Since the two Fe-O_(COOR) bond distances are significantly different, plots for Fe-O_(COOR) vs p*K*_a have been plotted for the two iron centers separately. A plot of the Fe-O_(COOR) bond distances for Fe1 center vs p*K*_a is shown in **Figure 83** for five of the (μ -oxido)(μ -modifiedbenzoato)diiron(III)TPA complexes in this study (where μ - modifiedbenzoato = 4-hydroxybenzoato, 4-methoxybenzoato, 4-fluorobenzoato, 3,5-dimethylbenzoato and 3,5-di-hydroxybenzoato). **Figure 84** is a plot of the Fe1-O_(COOR) bond distance vs p*K*_a of previously reported complexes (μ -modifiedbenzoato = 4-methylbenzoate, 4-ethylbenzoate, 4-chlorobenzoate,⁴² and benzoate²⁵). **Figure 85** combines the data in one plot. From these plots, one can observe that the data follow a similar trend. As p*K*_a decreases, Fe1-O_(COOR) bond distance increases.

A plot of the Fe-O_(COOR) bond distances for Fe2 center vs p*K*_a is shown in **Figure 86** for five of the (μ -oxido)(μ -modifiedbenzoato)diiron(III)TPA complexes in this study (when μ -modifiedbenzoato = 4-hydroxybenzoato, 4-methoxybenzoato, 4-fluorobenzoato, 3,5-dimethylbenzoato and 3,5-di-hydroxybenzoato).

Table 67. Comparison of Fe-pyridine bonds for asymmetric Fe(III)-TPA complexes.
All bond lengths are in Å

Complex	Fe1-N _{pyr} ^a		Average	Fe2-N _{pyr} ^b		Average	Average all	Reference
OAc	2.125(3)	2.129(3)	2.127(3)	2.135(3)	2.125(3)	2.130(3)	2.129(3)	This study
4-hydroxybenzoate	2.140(3)	2.158(3)	2.149(3)	2.138(3)	2.117(3)	2.127(3)	2.138(3)	This study
4-methoxybenzoate	2.125(4)	2.151(4)	2.138(4)	2.122(4)	2.130(4)	2.126(4)	2.132(4)	This study
4-fluorobenzoate	2.126(3)	2.145(2)	2.135(3)	2.123(3)	2.131(3)	2.127(3)	2.131(3)	This study
3,5-dimethylbenzoate	2.135(3)	2.127(3)	2.131(3)	2.139(4)	2.125(3)	2.132(4)	2.132(4)	This study
3,5-dihydroxybenzoate	2.140(6)	2.144(6)	2.142(6)	2.158(6)	2.139(6)	2.148(6)	2.145(6)	This study
4-methylbenzoate	2.130(3)	2.141(3)	2.135(3)	2.124(3)	2.122(3)	2.123(3)	2.129(3)	⁴²
4-ethylbenzoate	2.143(5)	2.144(5)	2.143(5)	2.119(4)	2.119(5)	2.119(5)	2.131(5)	⁴²
4-chlorobenzoate	2.120(5)	2.122(6)	2.121(6)	2.140(6)	2.138(5)	2.139(6)	2.130(6)	⁴²
OAc	2.128(6)	2.125(6)	2.126(6)	2.133(6)	2.105(6)	2.119(6)	2.123(6)	²⁵
OBz	2.132(7)	2.115(6)	2.124(7)	2.131(6)	2.118(6)	2.125(6)	2.125(7)	²⁵
Maleate-H	2.140(3)	2.143(8)	2.142(8)	2.133(9)	2.133(8)	2.133(9)	2.138(9)	²⁴

a. Iron center with pyridine *trans* to oxido bridge

Table 68. Bond lengths (\AA), bond angles ($^{\circ}$) of (μ -oxido)(μ -carboxylato)diiron(III)TPA complexes and pK_a of the acid form of the bridging carboxylates.

	L4	L5	L6	L8		L9
Fe-O-Fe	129.86(14)	129.93(15)	130.56(10)	131.21(14)	131.97(14)	131.8(2)
Fe-O _{COOR}	1.986(2) ^{a,d}	1.977(3) ^{a,d}	1.9877(18) ^{a,d}	1.980(3) ^{a,d}	1.979(3) ^{a,d}	1.988(5) ^{a,d}
	2.023(3) ^{b,c}	2.033(3) ^{b,c}	2.035(2) ^{b,c}	2.058(3) ^{b,c}	2.064(3) ^{b,c}	2.059(4) ^{b,c}
Fe-N _{3°}	2.187(3) ^{a,e}	2.180(3) ^{a,e}	2.184(2) ^{a,e}	2.186(3) ^{a,e}	2.186(3) ^{a,e}	2.205(6) ^{a,e}
Fe-N _{pyr}	2.138(3) ^{b,e}	2.122(4) ^{b,e}	2.123(3) ^{b,e}	2.155(3) ^{b,e}	2.122(4) ^{b,e}	2.148(6) ^{b,e}
C-O _(carboxylate)	1.284(4)	1.280(5)	1.272(3)	1.273(6)	1.272(6)	1.283(8)
	1.250(5)	1.246(5)	1.253(4)	1.247(6)	1.255(6)	1.256(8)
pK_a	4.57	4.47	4.14		4.34	3.96

a.Bonded to Fe1

c.*Trans* to pyridine nitrogen

e.*Trans* to bridging carboxylate

b. Bonded to Fe2

d. *Trans* to tertiary amine

L4 : [{Fe(TPA)}₂O(4-hydroxybenzoato)](ClO₄)₃

L5 : [{Fe(TPA)}₂O(4-methoxybenzoato)](ClO₄)₃

L6 : [{Fe(TPA)}₂O(4-fluorobenzoato)](ClO₄)₃

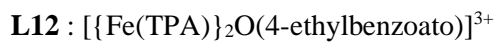
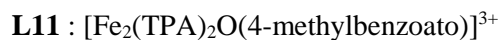
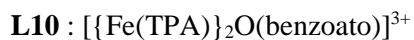
L8 : [Fe₂(TPA)₂O(3,5-dimethylbenzoato)](ClO₄)₃•0.5H₂O

L9 : [{Fe(TPA)}₂O(3,5-dihydroxybenzoato)](ClO₄)₃•CH₃CN

Table 69. Bond lengths and bond angles of relevant (μ -oxido)diiron(III)TPA complexes and pK_a of the acid form of the bridging carboxylates.

	L10 ²⁵	L11 ⁴²	L12 ⁴²	L13 ⁴²
Fe-O-Fe	129.7(3)	130.10(14)	128.9(2)	129.1(2)
Fe-O _{COOR}	1.984(5) ^{a,d}	1.983(3) ^{a,d}	1.971(4) ^{a,d}	1.995(4) ^{a,d}
	2.046(5) ^{b,c}	2.053(3) ^{b,c}	2.040(4) ^{b,c}	2.040(4) ^{b,c}
Fe-N _{3°}	2.190(6) ^{a,e}	2.170(3) ^{a,e}	2.175(4) ^{a,e}	2.198(5) ^{a,e}
Fe-N _{pyr}	2.138(6) ^{b,e}	2.124(3) ^{b,e}	2.116(5) ^{b,e}	2.134(5) ^{b,e}
C-O _(carboxylate)	1.259(9)	1.265(4)	1.281(6)	1.259(7)
	1.280(9)	1.257(4)	1.261(6)	1.275(7)
pK _a	4.21	4.37	4.35	3.97

- a. Atoms on Fe1
- b. Atoms on Fe2
- c. Atoms *trans* to pyridine nitrogen
- d. Atoms *trans* to tertiary amine nitrogen
- e. Atoms *trans* to bridging carboxylate



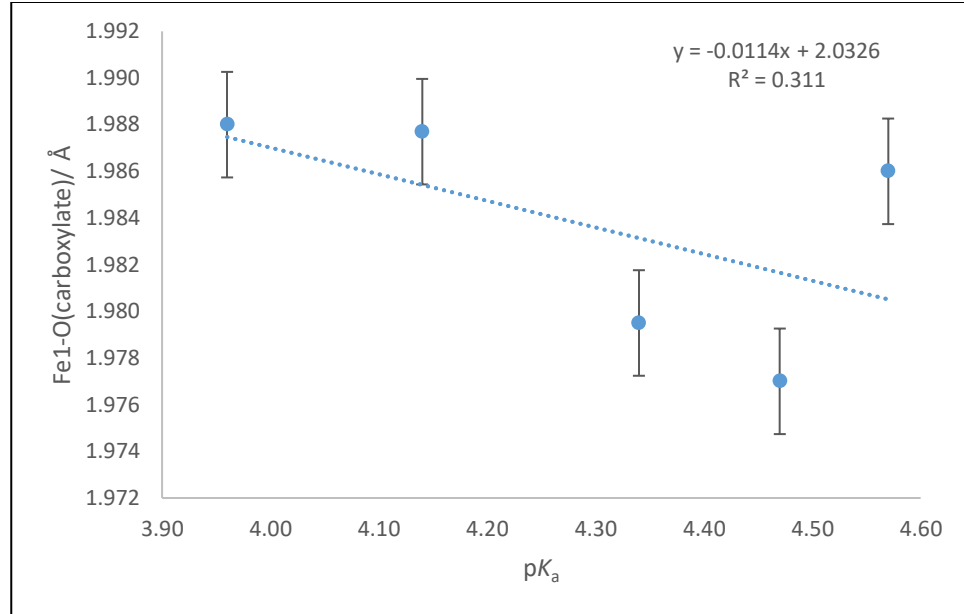


Figure 83. Graph of $Fe\text{-}O(\text{carboxylate})$ vs pK_a in current ($\mu\text{-oxido})(\mu\text{-modified-benzoato})$ diiron(III)TPA structures.

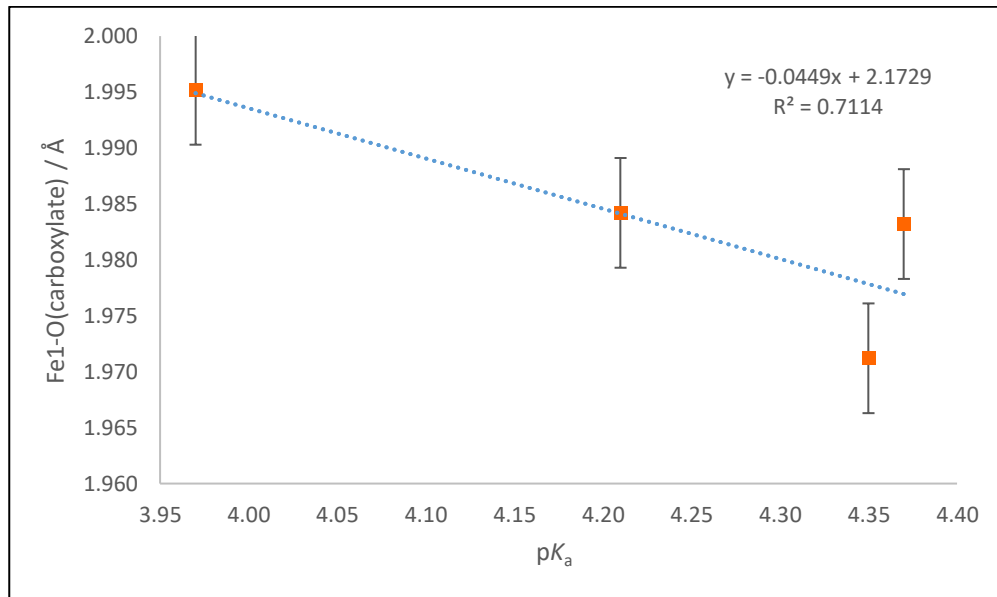


Figure 84. Graph of $Fe\text{-}O(\text{carboxylate})$ vs pK_a for previously reported ($\mu\text{-oxido})(\mu\text{-modified-benzoato})$ diiron(III) TPA complexes.

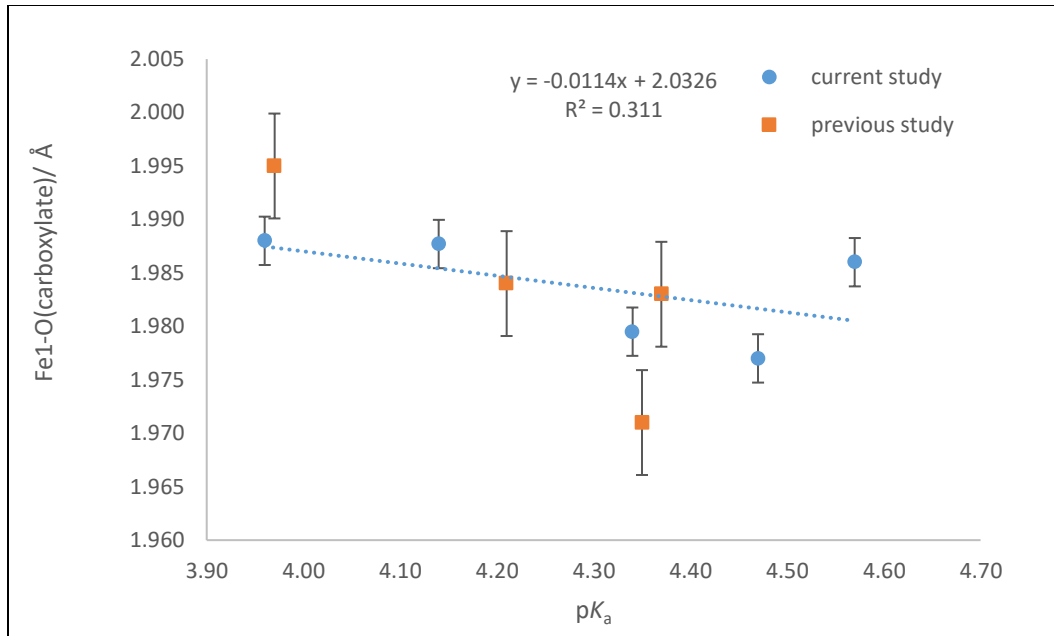


Figure 85. Graph of $\text{Fe}-\text{O}(\text{carboxylate})$ vs pK_a for current and previously reported (μ -oxido)(μ -modified-benzoato)diiron(III) TPA complexes.

Figure 87 is a plot of the $\text{Fe}-\text{O}(\text{COOR})$ bond distance vs pK_a of previously reported complexes (μ -modifiedbenzoato = 4-methylbenzoate, 4-ethylbenzoate, 4-chlorobenzoate,⁴² and benzoate²⁵). In the current study the $\text{Fe}-\text{O}(\text{COOR})$ bond distance increases as pK_a decreases, while in the previously reported complexes this $\text{Fe}-\text{O}(\text{COOR})$ bond distance decreases as pK_a decreases. Therefore

Figure 88 combines the data and show all these data as a single series to obtain the general trend. So, this general pattern agrees with the current study that is the $\text{Fe}-\text{O}(\text{COOR})$ bond distance increases as pK_a decreases.

Overall, the $\text{Fe}-\text{O}(\text{COOR})$ bond distance increases with decreasing pK_a (decreasing basicity of the substituted benzoates) for both Fe1 and Fe2. This is likely due to the fact that the decreasing basicity of the carboxylates causes them to bind to the iron more weakly. Since the two $\text{Fe}-\text{O}(\text{COOR})$ distances are distinct for the two iron centers, it might

be interesting to know what is going on for the C-O distances in these carboxylate ligands.

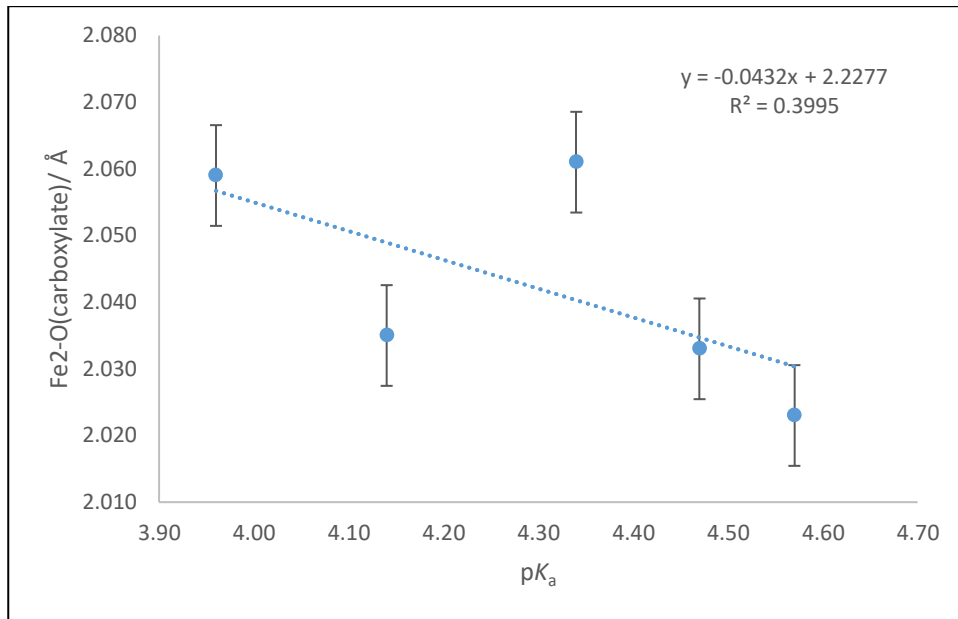


Figure 86. Graph of $\text{Fe}-\text{O}(\text{carboxylate})$ vs $\text{p}K_a$ in current (μ -oxido)(μ -modified-benzoato)diiron(III)TPA structures.

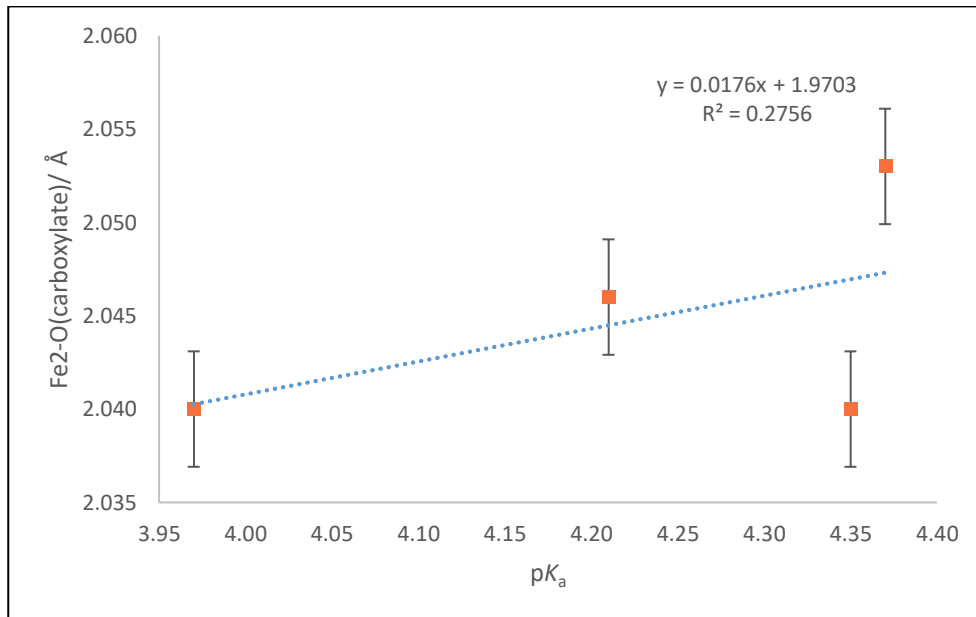


Figure 87. Graph of $\text{Fe}-\text{O}(\text{carboxylate})$ vs $\text{p}K_a$ for previously reported (μ -oxido)(μ -modified-benzoato)diiron(III) TPA complexes.

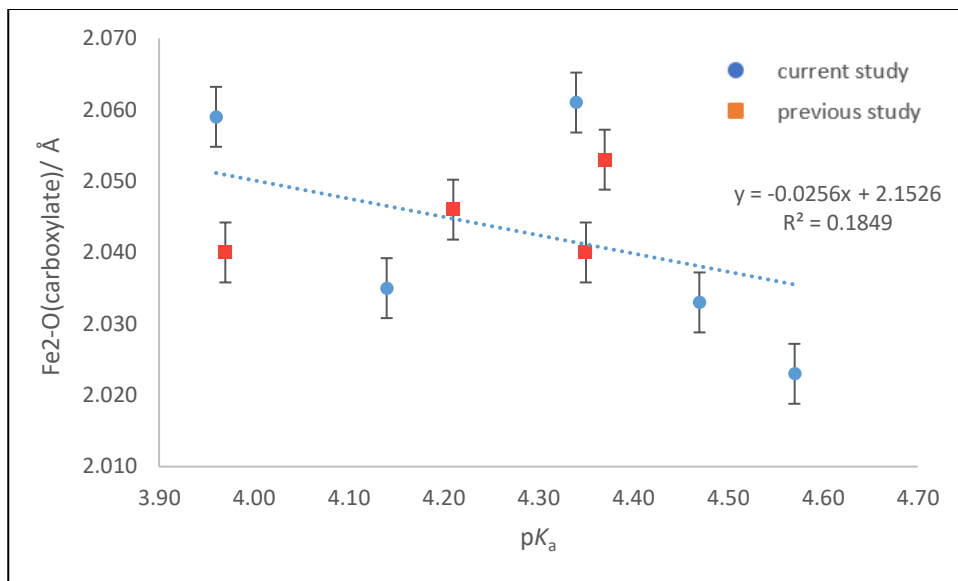


Figure 88. Graph of $\text{Fe}-\text{O}(\text{carboxylate})$ vs pK_a for current and previously reported (μ -oxido)(μ -modified-benzoato)diiron(III) TPA complexes.

The C-O bond distances bound to Fe1 are different from Fe2. Except for the two previously reported complexes with 4-chlorobenzoate⁴² and benzoate,²⁵ the C-O distance for the carboxylate oxygen bound to Fe1 is longer (average C1-O2 = 1.273(3) Å) than the C-O distance for the carboxylate bound to Fe2 (C1-O3 = 1.259(1) Å). The conclusion is that the O-C bond of the O bound to Fe1 has more single bond character and the O-C bond of the O bound to Fe2 has more double bond character. The former is expected to be a better base and will have a stronger bond to Fe1, as is observed.

Apart from the $\text{Fe}-\text{O}_{(\text{carboxylic})}$ bond distances, the bonds *trans* to this carboxylate ($\text{Fe}-\text{N}_3^\circ$ on Fe 1) can also provide some insight to the *trans* influence. A plot of the $\text{Fe}-\text{N}_3^\circ$ bond distances vs pK_a is shown in **Figure 89** for five of the (μ -oxido)(μ -modified-benzoato)diiron(III)TPA complexes in this study (where μ -modifiedbenzoato = 4-hydroxybenzoato, 4-methoxybenzoato, 4-fluorobenzoato, 3,5-dimethylbenzoato and 3,5-di-hydroxybenzoato). **Figure 90** is a plot of the $\text{Fe}-\text{N}_3^\circ$ bond distance vs pK_a of

previously reported complexes (μ -modifiedbenzoato = 4-methylbenzoate, 4-ethylbenzoate, 4-chlorobenzoate,⁴² and benzoate²⁵). **Figure 91** combines the data in one plot. From these plots, one can observe that the data follow a similar trend—as pK_a decreases, $\text{Fe}-\text{N}_3^\circ$ increases. However, the tertiary amine bonds are constrained in these structures since TPA is tethered by the other $\text{Fe}-\text{N}_{\text{pyr}}$ bonds.

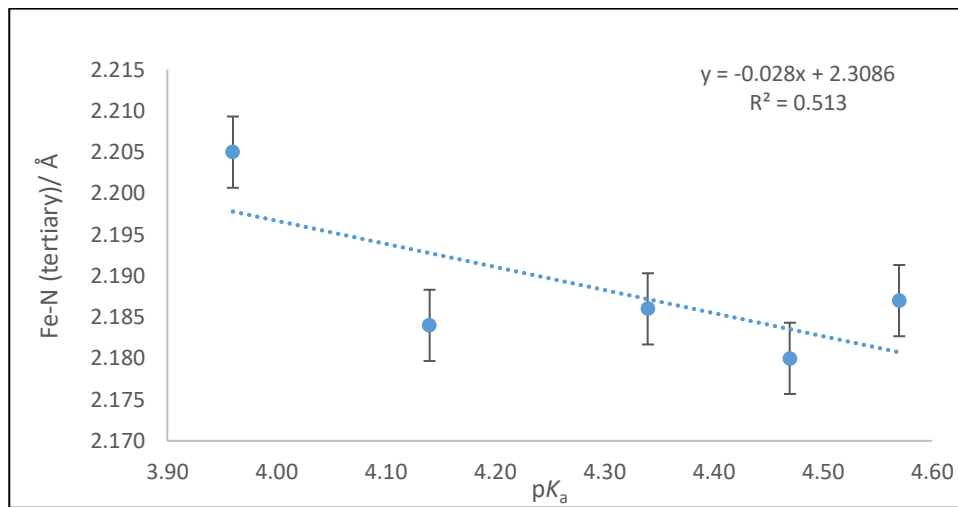


Figure 89. Plot of $\text{Fe1}-\text{N}_3^\circ$ bond distance vs pK_a for $(\mu\text{-oxido})(\mu\text{-modifiedbenzoato})$ diiron(III)TPA of the current study.

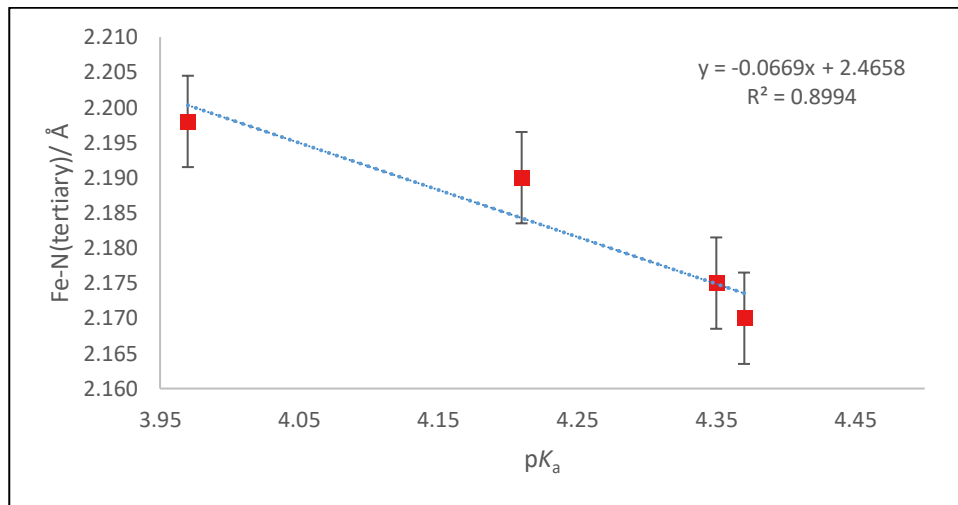


Figure 90. Plot of $\text{Fe1}-\text{N}_3^\circ$ bond distance vs pK_a for previously reported $(\mu\text{-oxido})(\mu\text{-modifiedbenzoato})$ diiron(III) TPA complexes.⁴²

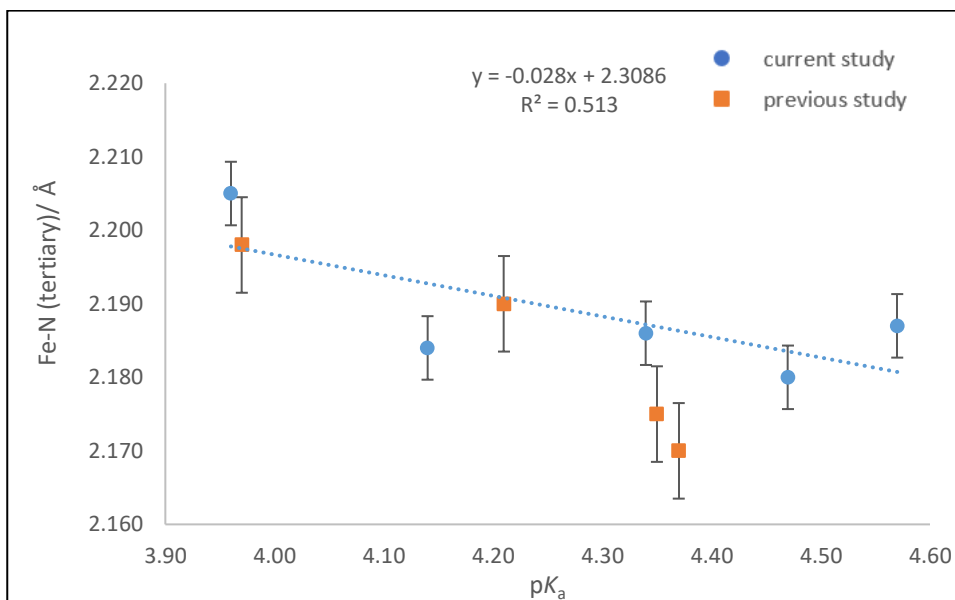


Figure 91. Plot of FeI-N_3° bond distance vs $\text{p}K_a$ for current and previously reported (μ -oxido)(μ -modifiedbenzoato)diiron(III) TPA complexes.

A plot of the Fe-N_{pyr} bond distances vs $\text{p}K_a$ is shown in **Figure 92** for five of the (μ -oxido)(μ -modifiedbenzoato)diiron(III)TPA complexes in this study (where μ -modifiedbenzoato = 4-hydroxybenzoato, 4-methoxybenzoato, 4-fluorobenzoato, 3,5-dimethylbenzoato and 3,5-di-hydroxybenzoato). **Figure 93** is a plot of the Fe-N_{pyr} bond distance vs $\text{p}K_a$ of previously reported complexes (μ -modifiedbenzoato = 4-methylbenzoate, 4-ethylbenzoate, 4-chlorobenzoate,⁴² and benzoate²⁵). **Figure 94** combines the data in one plot. From these plots, one can observe that the data follow a similar trend—as the $\text{p}K_a$ decreases, the Fe-N_{pyr} bonds *trans* to Fe-Ocoor lengthen. Of these complexes [$\{\text{Fe}(\text{TPA})_2\text{O}(3,5\text{-dihydroxybenzoato})\}(\text{ClO}_4)_3$] has the smallest $\text{p}K_a$ of the corresponding acid (3.96) and is expected to have the shortest Fe-N distances. However, it has the longest Fe-N distances ($\text{Fe-N}_3^\circ = 2.205(6)$ Å and $\text{Fe-N}_{\text{pyr}} = 2.148(6)$ Å).

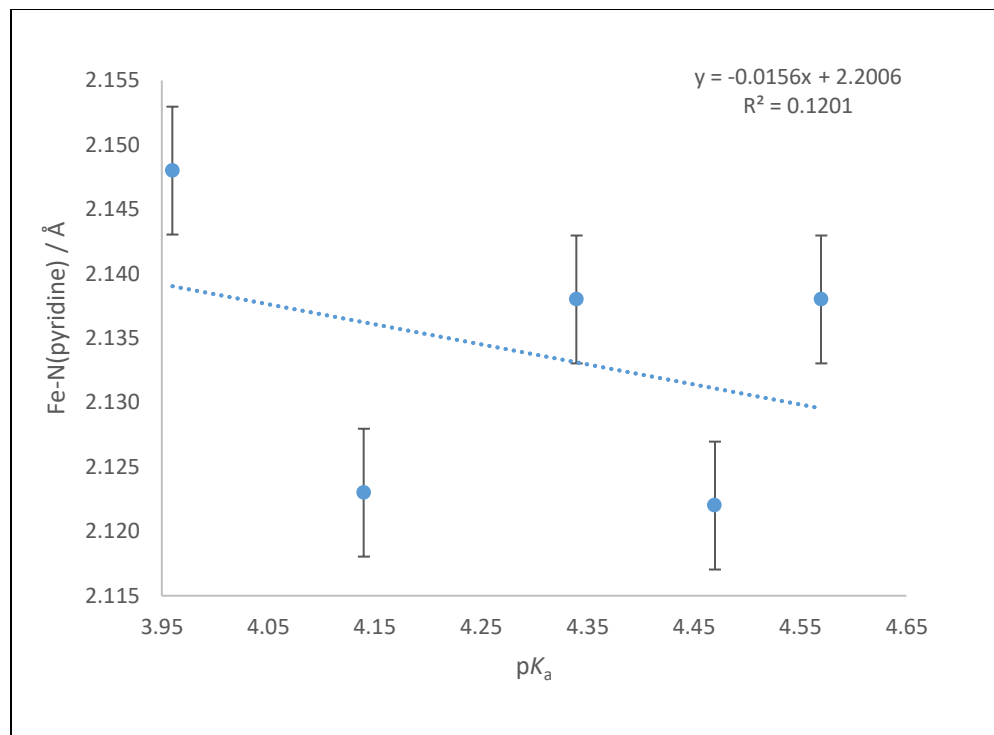


Figure 92. Plot of $Fe\text{-}N_{pyr}$ bond distance vs pK_a for current (μ -oxido)(μ -modified-benzoato)diiron(III) TPA.

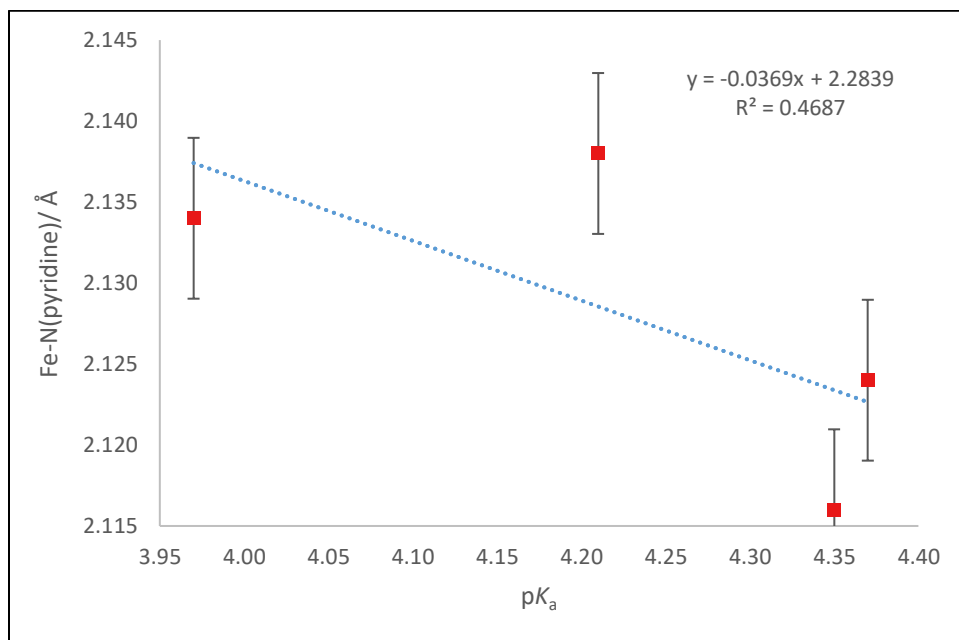


Figure 93. Plot of $Fe\text{-}N_{pyr}$ bond distance vs pK_a for previously reported (μ -oxido) (μ -modifiedbenzoato) diiron(III) TPA complexes.⁴²

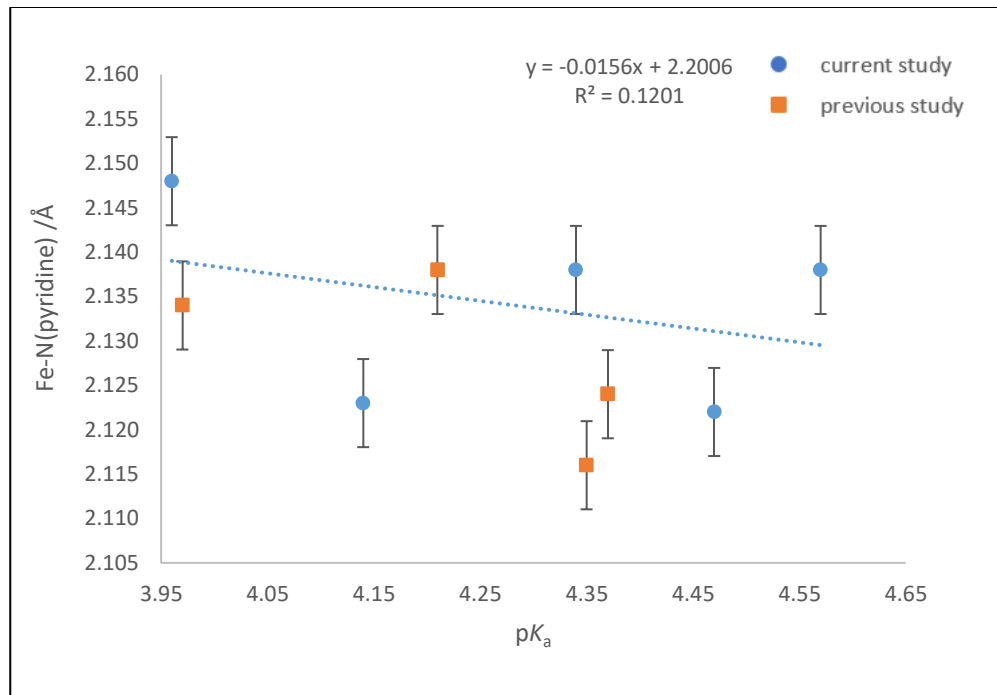


Figure 94. Plot of $\text{Fe1-N}_{\text{pyr}}$ bond distance vs $\text{p}K_{\text{a}}$ for current and previously reported (μ -oxido)(μ -modified-benzoato)diiron(III) TPA complexes.

For all of the iron(III)TPA complexes with benzoates synthesized to date, the singly bridged $[\{\text{Fe}(\text{TPA})\}_2\text{O}(4\text{-nitrobenzoato})_2]^{2+}$ which has the lowest $\text{p}K_{\text{a}}$ (3.42), has the longest Fe-N_{3° distance (2.224(3) Å). $[\{\text{Fe}(\text{TPA})\}_2\text{O}(4\text{-hydroxybenzoato})] (\text{ClO}_4)_3$ has the second smallest $\text{p}K_{\text{a}}$ (3.96) and has the second longest Fe-N_{3° distance (2.205(6) Å). As the bottom line, the expected Fe-N bond shortening with decreasing $\text{p}K_{\text{a}}$ (decreasing basicity of the substituted benzoates) was not observed, and the reverse is true. Therefore, the $\text{p}K_{\text{a}}$ of the substituted benzoic acid itself does not appear to determine the *trans* influence of these carboxylates. Other factors like steric interactions, and orbital synergies are likely to be important.

REFERENCES

- (1) Taylor, K. G.; Konhauser, K. O. Iron in Earth Surface Systems: A Major Player in Chemical and Biological Processes. *Elements* **2011**, *7*, 83–88. DOI:10.2113/gselements.7.2.83.
- (2) Outten, F. W.; Theil, E. C. Iron-Based Redox Switches in Biology. *Antioxid. Redox Signal.* **2009**, *11*, 1029–1046. DOI:10.1089/ars.2008.2296.
- (3) Lippard, S. J. Oxo-Bridged Polyiron Centers in Biology and Chemistry. *Angew. Chemie Int. Ed. English* **1988**, *27*, 344–361. DOI:10.1002/anie.198803441.
- (4) Groves, J. T. Key Elements of the Chemistry of Cytochrome P-450: The Oxygen Rebound Mechanism. *J. Chem. Educ.* **1985**, *62*, 928–931. DOI:10.1021/ed062p928.
- (5) Schwederski, B.; Kaim, W. *Bioinorganic Chemistry : Inorganic Elements in the Chemistry of Life. An Introduction and Guide*, 1st ed.; John Wiley & Sons, Incorporated: Chichester, United Kingdom, 1994.
- (6) Flint, D. H.; Allen, R. M. Iron–Sulfur Proteins with Nonredox Functions. *Chem. Rev.* **1996**, *96*, 2315–2334. DOI:10.1021/cr950041r.
- (7) Hall, D. O.; Rao, K. K.; Cammack, R. The Iron-Sulphur Proteins: Structure, Function and Evolution of a Ubiquitous Group of Proteins. *Sci. Prog.* **1975**, *62*, 285–317. DOI:stable/43420303.
- (8) Rouault, T. A. Mammalian Iron–Sulphur Proteins: Novel Insights into Biogenesis and Function. *Nat. Rev. Mol. Cell Biol.* **2015**, *16*, 45–55. DOI:10.1038/nrm3909.
- (9) Holm, R. H.; Kennepohl, P.; Solomon, E. I. Structural and Functional Aspects of Metal Sites in Biology. *Chem. Rev.* **1996**, *96*, 2239–2314.

- DOI:10.1021/cr9500390.
- (10) Fox, B. G.; Shanklin, J.; Somerville, C.; Münck, E. Stearoyl-acyl Carrier Protein Δ^9 Desaturase from *Ricinus communis* is a Diiron-Oxo Protein. *Proc. Natl. Acad. Sci.* **1993**, *90*, 2486–2490. DOI:10.1073/pnas.90.6.2486.
- (11) Ravi, N.; Prickril, B. C.; Kurtz, D., M., Jr.; Huynh, B. H. Spectroscopic Characterization of ^{57}Fe -Reconstituted Rubrerythrin, a Non-Heme Iron Protein with Structural Analogies to Ribonucleotide Reductase. *Biochemistry* **1993**, *32*, 8487–8491. DOI:10.1021/bi00084a013.
- (12) Kurtz, D. M., Jr. Oxo- and Hydroxo-Bridged Diiron Complexes: A Chemical Perspective on a Biological Unit. *Chem. Rev.* **1990**, *90*, 585–606.
DOI:10.1021/cr00102a002.
- (13) Dutta, S. K.; Werner, R.; Flörke, U.; Mohanta, S.; Nanda, K. K.; Haase, W.; Nag, K. Model Compounds for Iron Proteins. Structures and Magnetic, Spectroscopic, and Redox Properties of $\text{Fe}^{\text{III}}\text{M}^{\text{II}}$ and $[\text{Co}^{\text{III}}\text{Fe}^{\text{III}}]_2\text{O}$ Complexes with (μ -Carboxylato)bis(μ -phenoxo)dimetalate and (μ -Oxo)diiron(III) Cores. *Inorg. Chem.* **1996**, *35*, 2292–2300. DOI:10.1021/ic9508334.
- (14) Armstrong, W. H.; Lippard, S. J. (μ -Oxo)bis(μ -acetato)bis(tri-1-pyrazolylborato) diiron(III), $[(\text{HBpz}_3)\text{FeO}(\text{CH}_3\text{CO}_2)_2\text{Fe}(\text{HBpz}_3)]$: Model for the Binuclear Iron Center of Hemerythrin. *J. Am. Chem. Soc.* **1983**, *105*, 4837–4838.
DOI:10.1021/ja00352a053.
- (15) Hartman, J. A. R.; Rardin, R. L.; Chaudhuri, P.; Pohl, K.; Wieghardt, K.; Nuber, B.; Weiss, J.; Papaefthymiou, G. C.; Frankel, R. B.; Lippard, S. J. Synthesis and Characterization of (μ -Hydroxo)bis(μ -acetato)diiron(II) and (μ -Oxo)bis(μ -

- acetato)diiron(III) 1,4,7-Trimethyl-1,4,7-triazacyclononane Complexes as Models for Binuclear Iron Centers in Biology; Properties of the Mixed Valence Diiron(II,III) Species. *J. Am. Chem. Soc.* **1987**, *109*, 7387–7396.
DOI:10.1021/ja00258a023.
- (16) Stenkamp, R. E.; Sieker, L. C.; Jensen, L. H. Binuclear Iron Complexes in Methemerythrin and Azidomethemerythrin at 2.0 Å Resolution. *J. Am. Chem. Soc.* **1984**, *106*, 618–622. DOI:10.1021/ja00315a027.
- (17) Nordlund, P.; Sjöberg, B.-M.; Eklund, H. Three-dimensional Structure of the Free Radical Protein of Ribonucleotide Reductase. *Nature* **1990**, *345*, 593–598.
DOI:10.1038/345593a0.
- (18) Reichard, P.; Ehrenberg, A. Ribonucleotide Reductase—A Radical Enzyme. *Science*. **1983**, *221*, 514–519. DOI:10.1126/science.6306767.
- (19) Elango, N.; Radhakrishnan, R.; Froland, W. A.; Wallar, B. J.; Earhart, C. A.; Lipscomb, J. D.; Ohlendorf, D. H. Crystal Structure of The Hydroxylase Component of Methane Monooxygenase from *Methylosinus trichosporium* QB3b. *Protein Sci.* **1997**, *6*, 556–568. DOI:10.1002/pro.5560060305.
- (20) Dorfman, J. R.; Girerd, J. J.; Simhon, E. D.; Stack, T. D. P.; Holm, R. H. Synthesis, Structure, and Electronic Features of (μ -Sulfido)bis[$(N,N'$ -ethylenebis(salicylaldiminato))iron(III)], [Fe(salen)]₂S, Containing the Only Authenticated Example of the Fe(III)-Sulfur-Fe(III) Single Bridge. *Inorg. Chem.* **1984**, *23*, 4407–4412. DOI:10.1021/ic00194a002.
- (21) Maroney, M. J.; Scarrow, R. C.; Que, L., Jr.; Roe, A. L.; Lukat, G. S.; Kurtz, D. M., Jr. X-ray Absorption Spectroscopic Studies of the Sulfide Complexes of

- Hemerythrin. *Inorg. Chem.* **1989**, *28*, 1342–1348. DOI:10.1021/ic00306a026.
- (22) Pombeiro, A. J. L. Alkane functionalization: Introduction and Overview. In *Alkane Functionalization*; Pombeiro, A. J. L., Guedes Da Silva, M. F. C., Eds.; John Wiley & Sons, Ltd: New Jersey, USA, 2019; p 01. DOI:10.1002/9781119379256.ch1.
- (23) Murray, K. S. Binuclear Oxo-bridged Iron(iii) Complexes. *Coord. Chem. Rev.* **1974**, *12*, 1–35. DOI:10.1016/S0010-8545(00)80384-7.
- (24) Norman, R. E.; Holz, R. C.; Menage, S.; Que, L., Jr.; O'Connor, C. J.; Zhang, J. H. Structures and Properties of Dibridged (μ -Oxo)diiron(III) Complexes. Effects of the Fe-O-Fe Angle. *Inorg. Chem.* **1990**, *29*, 4629–4637. DOI:10.1021/ic00348a010.
- (25) Norman, R. E.; Yan, S.; Que, L., Jr.; Backes, G.; Ling, J.; Sanders-Loehr, J.; Zhang, J. H.; O'Connor, C. J. (μ -Oxo)(μ -carboxylato)diiron(III) Complexes with Distinct Iron Sites. Consequences of the Inequivalence and Its Relevance to Dinuclear Iron-Oxo Proteins. *J. Am. Chem. Soc.* **1990**, *112*, 1554–1562. DOI:10.1021/ja00160a039.
- (26) Xue, J.; Hangun-Balkir, Y.; Mullaney, M.; Nadir, S.; Lewis, J. C.; Henry-Smith, C.; Jayaratna, N. B.; Kumarihami, C. A. U. K.; Norman, R. E. Syntheses and Structures of $[Fe(TPA)X_2](ClO_4)$ and $\{[Fe(TPA)Y]_2O\}(ClO_4)_2$ Where TPA = Tris-(2-pyridylmethyl)amine, X = N_3 , or Br, and Y = N_3 , Br, NCO, or NCS. *J. J. Chem. Crystallogr.* **2022**, 1–16. DOI:10.1007/s10870-022-00941-5.
- (27) Costas, M.; Chen, K.; Que, L., Jr. Biomimetic Nonheme Iron Catalysts for Alkane Hydroxylation. *Coor. Chem. Rev.* **2000**, *200*-202, 517–544. DOI:10.1016/S0010-

- 8545(00)00320-9.
- (28) Leising, R. A.; Kim, J.; Pérez, M. A.; Que, L., Jr. Alkane Functionalization at (μ -Oxo)diiron(III) Centers. *J. Am. Chem. Soc.* **1993**, *115*, 9524–9530. DOI:10.1021/ja00074a017.
- (29) Kojima, T.; Leising, R. A.; Yan, S.; Que, L., Jr. Alkane Functionalization at Nonheme Iron Centers. Stoichiometric Transfer of Metal-Bound Ligands to Alkane. *J. Am. Chem. Soc.* **1993**, *115*, 11328–11335. DOI:10.1021/ja00077a035.
- (30) Arends, I. W. C. E.; Ingold, K. U.; Wayner, D. D. M. A Mechanistic Probe for Oxygen Activation by Metal Complexes and Hydroperoxides and Its Application to Alkane Functionalization by $[\text{Fe}^{\text{III}}\text{Cl}_2\text{tris}(\text{2-pyridinylmethyl})\text{amine}]^+\text{BF}_4^-$. *J. Am. Chem. Soc.* **1995**, *117*, 4710–4711. DOI:10.1021/ja00121a031.
- (31) Gerber, N. C.; Sligar, S. G. A Role for Asp-251 in Cytochrome P-450_{cam} Oxygen Activation. *J. Biol. Chem.* **1994**, *269*, 4260–4266. DOI:10.1016/S0021-9258(17)41772-8.
- (32) Kitajima, N.; Tamura, N.; Amagai, H.; Fukui, H.; Moro-oka, Y.; Mizutani, Y.; Kitagawa, T.; Mathur, R.; Heerwagh, K.; Reed, C. A.; Randall, C. R.; Que, L., Jr.; Tatsumi, K. Monomeric Carboxylate Ferrous Complexes as Models for the Dioxygen Binding Sites in Non-Heme Iron Proteins. The Reversible Formation and Characterization of μ -Peroxo Diferric Complexes. *J. Am. Chem. Soc.* **1994**, *116*, 9071–9085. DOI:10.1021/ja00099a025.
- (33) Yan, S.; Cox, D. D.; Pearce, L. L.; Juarez-Garcia, C.; Que, L., Jr.; Zhang, J. H.; O'Connor, C. J. A (μ -Oxo)(μ -carboxylato)diiron(III) Complex with Distinct Iron Sites. *Inorg. Chem.* **1989**, *28*, 2507–2509. DOI:10.1021/ic00312a001.

- (34) Armstrong, W. H.; Spool, A.; Papaefthymiou, G. C.; Frankel, R. B.; Lippard, S. J. Assembly and Characterization of an Accurate Model for the Diiron Center in Hemerythrin. *J. Am. Chem. Soc.* **1984**, *106*, 3653–3667. DOI:10.1021/ja00324a041.
- (35) Mimmi, M. C.; Miccichè, F.; Kooijman, H.; Spek, A. L.; Warzeska, S. T.; Bouwman, E. Dinuclear Iron Complexes of the Tridentate Ligand *N,N*-bis(2-ethyl-5-methyl-imidazol-4-ylmethyl)aminopropane (biap). *Inorg. Chimica Acta*. **2002**, *340*, 197–200. DOI:10.1016/S0020-1693(02)01070-8.
- (36) Atkin, C. L.; Thelander, L.; Reichard, P.; Lang, G. Iron and Free Radical in Ribonucleotide Reductase: Exchange of Iron and Mössbauer Spectroscopy of the Protein B2 Subunit of the *Escherichia coli* Enzyme. *J. Biol. Chem.* **1973**, *248*, 7464–7472. DOI:10.1016/S0021-9258(19)43313-9.
- (37) Antanaitis, B. C.; Aisen, P.; Lilenthal, H. R. Physical Characterization of Two-iron Uteroferrin. Evidence for a Spin-coupled Binuclear Iron Cluster. *J. Biol. Chem.* **1983**, *258*, 3166–3172. DOI:10.1016/S0021-9258(18)32844-8.
- (38) Bravin, C.; Badetti, E.; Licini, G.; Zonta, C. Tris(2-pyridylmethyl)amines as Emerging Scaffold in Supramolecular Chemistry. *Coord. Chem. Rev.* **2021**, *427*, 213558. DOI:10.1016/j.ccr.2020.213558.
- (39) Kim, C.; Chen, K.; Kim, J.; Que, L., Jr. Stereospecific Alkane Hydroxylation with H₂O₂ Catalyzed by an Iron(II)–Tris(2-pyridylmethyl)amine Complex. *J. Am. Chem. Soc.* **1997**, *119*, 5964–5965. DOI:10.1021/ja9642572.
- (40) Chandrasekaran, V.; Collier, S. J. Tris(2-pyridylmethyl)amine. In *Handbook of Reagents for Organic Synthesis: Catalytic Oxidation Reagents*; John Wiley &

- Sons, Ltd: Chichester, United Kingdom, 2013; pp 670–676.
- (41) Yan, S.; Que, L., Jr.; Taylor, L. F.; Anderson, O. P. A Model for the Chromophoric Site of Purple Acid Phosphatases. *J. Am. Chem. Soc.* **1988**, *110*, 5222–5224. DOI:10.1021/ja00223a068.
- (42) Arachchilage, H. M. J. Synthesis and Structural Characterization of (μ -Oxo)(μ -modified benzoate)diiron(III)tris(2-pyridylmethyl)amine complexes., M.S. Thesis, Sam Houston State University, 2015.
- (43) Mullaney, M. Structural Characterization of Several Fe(III) Tris(2-pyridylmethyl)amine Complexes., M.S. Thesis, Duquesne University, 1996.
- (44) Hazell, A.; Jensen, K. B.; McKenzie, C. J.; Toftlund, H. Synthesis and Reactivity of (μ -Oxo)diiron(III) Complexes of Tris(2-pyridylmethyl)amine. X-ray Crystal Structures of [tpa(OH)FeOFe(H₂O)tpa](ClO₄)₃ and [tpa(Cl)FeOFe(Cl)tpa](ClO₄)₂. *Inorg. Chem.* **1994**, *33*, 3127–3134. DOI:10.1021/ic00092a019.
- (45) Ariyananda, L. M. Structural and Spectroscopic Studies of Cr(III), Mn(II), Fe(III), Fe(II) and Ni(II) Complexes with Nitrogenous Ligands, M.S. Thesis, University of Louisiana at Monroe, 2003.
- (46) Solomon, E. I.; Bell, C. B., III. Inorganic and Bioinorganic Spectroscopy. In *Physical Inorganic Chemistry: Principles, Methods, and Models*; Bakac, A., Ed.; Wiley: New Jersey, USA, 2010; p 6.
- (47) Reem, R. C.; McCormick, J. M.; Richardson, D. E.; Devlin, F. J.; Stephens, P. J.; Musselman, R. L.; Solomon, E. I. Spectroscopic Studies of the Coupled Binuclear Ferric Active Site in Methemerythrins and Oxyhemerythrin: The Electronic

- Structure of Each Iron Center and the Iron-Oxo and Iron-Peroxide Bonds. *J. Am. Chem. Soc.* **2002**, *111*, 4688–4704. DOI:10.1021/ja00195a024.
- (48) Xue, J. Structural Characterization of Iron(III) Tris(2-pyridylmethyl)amine Complexes with the Formulas $[\text{Fe}(\text{TPA})\text{X}_2](\text{ClO}_4)$ and $[\{\text{Fe}(\text{TPA})\text{X}\}_2\text{O}](\text{ClO}_4)_2$, M.S. Thesis, Duquesne University, 1996.
- (49) Norman, R. E.; Peterson, N. L.; Chang, S. C. μ -Acetato- $O':O'$ - μ -oxo-bis{[tris(2-pyridylmethyl)amine-*N,N',N'',N'''*]iron(III)} Tris(trifluoromethanesulfonate) Dihydrate. *Acta Cryst* **1996**, *C53*, 452–453. DOI:10.1107/S0108270196015016.
- (50) Lionetti, D.; Suseno, S.; Tsui, E. Y.; Lu, L.; Stich, T. A.; Carsch, K. M.; Nielsen, R. J.; Goddard, W. A.; Britt, R. D., III; Agapie, T. Effects of Lewis Acidic Metal Ions (M) on Oxygen-Atom Transfer Reactivity of Heterometallic Mn_3MO_4 Cubane and $\text{Fe}_3\text{MO}(\text{OH})$ and $\text{Mn}_3\text{MO}(\text{OH})$ Clusters. *Inorg. Chem.* **2019**, *58*, 2336–2345.
DOI:10.1021/ACS.INORGCHEM.8B02701/SUPPL_FILE/IC8B02701_SI_001.PDF.
- (51) Cotton, A. F.; Wilkinson, G. *Advanced Inorganic Chemistry*, 5th ed.; John Wiley & Sons, Ltd: New York, 1988. p 1299-1300.

VITA

Codithuwakku Arachchige Upeshka Kawshalya Kumarihami was born in Kandy, Sri Lanka. She attended Mahamaya Girls' College, Kandy and she graduated in 2010. She entered the University of Kelaniya, Sri Lanka and received her B.Sc (Special) Chemistry with honors, in 2017. She worked as a Chemistry teaching assistant at the University of Kelaniya and then as a research assistant in National Institute of Fundamental Studies, Sri Lanka. She entered Sam Houston State University in Spring 2019 to pursue her Master's degree. She worked on synthesis and characterization of iron complexes under the supervision of Professor Richard E. Norman. She plans to join the University of California Santa Barbara to pursue her Ph.D.